Chemistry Department College of Natural Sciences

Addis Ababa University

Bioassay Directed Chemical Study of Antimalarial Substances from *Clerodendrum myricoides* and *Dodonaea angustifolia*

and

Comparative Chemical Studies of *Moringa stenopetala* and *Moringa oleifera*

By: Yadessa Melaku

June 2015

Bioassay Directed Chemical Study of Antimalarial Substances from *Clerodendrum myricoides* and *Dodonaea angustifolia*

and

Comparative Chemical Studies of *Moringa stenopetala* and *Moringa oleifera*

By Yadessa Melaku

A Dissertation Submitted to the Department of Chemistry, College of Natural Sciences, Addis Ababa University In Partial Fulfillment of the Requirements for the Degree of Doctor of Philosophy in Chemistry

June 2015

Addis Ababa, Ethiopia

Chemistry Department College of Natural Sciences Addis Ababa University

Bioassay Directed Chemical Study of Antimalarial Substances from *Clerodendrum myricoides* and *Dodonaea angustifolia*

and

Comparative Chemical Studies of *Moringa stenopetala* and *Moringa oleifera*

By Yadessa Melaku

Approved by:

1. Professor Ermias Dagne _____
   Advisor
2. Professor Dr Yang Ye _____
   External Examiner
3. Dr Tarekegn G/yesus _____
   Examiner
4. Professor Wendimagegn Mamo _____
   Examiner

June 2015

This work was done from September 2010 to May 2015 at the Addis Ababa University, College of Natural Sciences, Chemistry Department under the supervision of Professor Ermias Dagne

Acknowledgements

I am very indebted to express my sincerest gratitude to my advisor, Professor Ermias Dagne, for his kind supervision, invaluable technical support, suggestions, guidance and encouragement at every stage throughout the whole period of my PhD study. I am also indebted to Professor Yalemtsehay Mekonnen and her coworkers for carrying out the anti-plasmodial tests on crude extracts as well as on purified substances. It's my pleasure to thank Professor Wendimagegn Mamo for training me on how to operate the 400 MHz NMR spectrometer and also for his unreserved help, encouragement and constructive comments. I am indebted to Dr Tarekegn G/yesus for providing me with numerous references and a wide array of documents relevant to my work. I also appreciate very much the other members of staff especially Dr. Ashebir Fiseha, Dr. Nigist Asfaw and Dr. Estifanos Ele for constructive comments and suggestions that helped me improve this dissertation. I am also obliged to Dr. Ahmed Mustafa, Head of the Department of Chemistry, for guidance and administrative support.

I am grateful to Dr. Norbert Arnold and Dr. Juergen Schmidt, Leibniz-Institute for Plant Biochemistry, Weinberg 3, 06120 Halle (Saale), Germany, for running the FT-MS and HPLC-MS of the samples. Their contributions for the fruitfulness of this work are immense. I appreciate the support rendered by my co-workers (Yohannes Meaza, Hanna Kassaye, Mesfin Getachew, Minbale Gashu, Zelalem Gizachew, Sisay Awoke and Tirusew Araya) and my friends (Koster Gudu, Abera Gure, Zelalem Abdissa, Gemechu Muleta, and Bedassa Abdissa). I am greatly indebted to my parents, my beloved sisters and brothers for their moral guidance, prayers and timely help in various ways which enabled me to complete this work. I extend my deepest appreciation to my wife Diribe Wakjira, and my daughter Sinam, for their loving support throughout my study period. Last but not least, the Chemistry Department, Addis Ababa University is thanked for giving me the opportunity to pursue PhD studies and Adama Science and Technology University for leave of absence. I am grateful to the International Science Program

(ISP, Sweden) for the support. In closing, I wish to humbly express my deepest feelings to the Almighty God for giving me strength throughout my life.

Abstract

Bioassay Directed Chemical Study of Antimalarial Substances from *Clerodendrum myricoides* and *Dodonaea angustifolia*

and

Comparative Chemical Studies of *Moringa stenopetala* and *Moringa oleifera*

By Yadessa Melaku

Advisor: Professor Ermias Dagne

Human beings have since time immemorial used plants for different purposes including as food, for flavor, cosmetic, dying clothes, and above all as medicine for treating a wide spectrum of diseases. The main aim of this dissertation work is to find rationale for the use of selected plants in combating one of the most challenging diseases in the world, namely, malaria. The selection of the plant materials for the study was based on ethnomedicinal uses. This led to the need for systematic investigation of two plants, *Clerodendrum myricoides* (Lamiaceae) and *Dodonaea angustifolia* (Sapindaceae), which are indigenous medicinal plants traditionally used as remedies against malaria in some parts of Ethiopia. In the course of this study, bioassay guided investigation on the antiplasmodial activities of the leaves of *C. myricoides* resulted in the isolation of two active compounds, namely, *α*-spinasterol (**63**) and sitosterol-3-O-*β*-D-glucoside (**64**), which significantly suppress parasitaemia by 51% and 44% at 40 mg/kg, respectively.

Furthermore, the acetone extract of the leaves of *C. myricoides* afforded verbascoside (**12**), ixoroside (**73**), and compound **71**. To our knowledge there is no report in the literature for compound **71**. Tetracosanoic, behenic, icosanoic, stearic, and palmitic acid were also identified from the leaves of this plant. Investigation of the radical scavenging activities of the above constituents resulted in verbascoside as the most active compound comparable to ascorbic acid.

Bioassay guided fractionation of the ethyl acetate soluble portion of the 80% aqueous MeOH extract of the leaves of *D. angustifolia* afforded three compounds, namely, pinocembrin (**86**), santin (**81**) and 15,16-epoxy-2-hydroxy-3,13(16),14-clerodtriene-18-oic acid (**128**) which exhibited high percent suppression of parasitaemia by 81% at 40 mg/kg, 80% at 50 mg/kg and 70% at 40 mg/kg, respectively. Under similar conditions chloroquine suppressed parasitaemia by 100% at 25 mg/kg. Column chromatographic fractionation of the ethyl acetate soluble portion of the ethanol extract of *D. angustifolia* leaves gave three other compounds in addition to **81**, **86** and **128**, identified as 5,7,4'-trihydroxy-3,6-dimethoxyflavone (**80**), ent-16-hydroxy-labdan-3α,8β-dihydroxy,13(14)-en-15,16-olide (**114**), and 5,6,7-trihydroxy-3,4'-dimethoxyflavone (**125**). To our knowledge compound **125** has not been reported before as a natural product. The extracts and the four flavonoids isolated from the leaves of *D. angustifolia* were tested for their antiradical properties, which led to 5,7,4'-trihydroxy-3,6-dimethoxyflavone (**80**) as the most active compound.

The leaves of two *Moringa* species, *M. stenopetala* which is confined to the horn of Africa namely Ethiopia, Somalia and Kenya and *M. oleifera* originally from the Indian subcontinent but–now cultivated in different parts of the world including Africa, were compared with respect to their main chemical constituents. Different techniques including TLC, HPLC-MS, and UV-Vis spectrophotometry were employed. Our results unambiguously showed significant differences in the chemical profiles of the leaves of the two species. Rutin (**163**) is the only principal flavonoid glycoside of the leaves of *M. stenopetala*, which however is not detected in the leaves of *M. oleifera*. On the other hand *M. oleifera* contains significant amounts of two other glycosides, namely, quercetin-3-O-β-D-glucoside (**159**) and kaempferol-3-O-β-D-glucoside (**161**). These results are significant in distinguishing the two *Moringa* species. Furthermore, a simple high performance thin layer chromatographic method was developed and validated for quantitative analysis of rutin in the leaves of *M. stenopetala*. The level of rutin in the leaves of *M. stenopetala* was found to be 1.9±0.08%. These fingerprinting results can be used not only to differentiate the two species but also to establish presence or absence of adulterants, an issue that is significant in the use and marketing of crude and derived products from *Moringa* leaves.

Further chemical investigation on the leaves of *M. stenopetala* afforded three compounds identified as heptacosanol (**185**), sitosterol-3-O-*β*-D-glucoside (**64**), and inositol dimer (**186**). The seed kernel and husk of *M. stenopetala* was also investigated in this study for the first time. This resulted in the isolation and characterization of stearic acid (**77**), 4-(*α*-L-rhamnopyranosyloxy) benzyl glucosinolate (**164**) and sucrose (**187**) from the seed kernel while the husk furnished allantoin (**191**) and compound **190**. To our knowledge compound **190** was not reported before as natural product. GC-MS analysis of the fatty acids of the oil of *M. stenopetala* afforded oleic acid (52%), stearic acid (9%), palmitic acid (9%), behenic acid (5%), archidic acid (5%), palmitoleic acid (1%) and myristic acid (0.2%). The above flavonoid glycosides displayed pronounced radical scavenging and anti-lipid peroxidation activities.

Key words: Bioassay, *Clerodendrum myricoides*, *Dodonaea angustifolia*, Sapindaceae, Lamiaceae, Antiplasmodial, radical scavenging, pinocembrin, santin, verbascoside, *Moringa*ceae, Fingerprint, HPLC-MS, TLC, UV, *Moringa stenopetala*, *Moringa oleifera*, quality control, radical scavenging

List of Abbreviations

calcd	Calculated	CC	Column Chromatography
COSY	Correlation Spectroscopy	concd	Concentrated
DEPT	Distortionless Enhancement by Polarization Transfer	CQ	Chloroquine
D_4	Day four	DMSO	Dimethyl sulfoxide
DPPH	2,2-diphenyl-1-picrylhydrazyl radical	EtOAc	Ethyl acetate
CID	Collision-Induced Dissociation	ESI	Electro Spray Ionization
FDA	Food and Drug Administration	Fig.	Figure
FT-MS	Fourier Transform Mass Spectrometry	Fr	Fraction
HSQC	Heteronuclear Single Quantum Correlation	Rf	Retardation factor
HPLC	High Performance Liquid Chromatography	MeOH	Methanol
HMBC	Heteronuclear Multiple Bond Correlation	Hz	Hertz
HPTLC	High Performance Thin Layer Chromatography	IC	Inhibitory Concentration
		IR	Infra Red
LC-MS	Liquid Chromatography-Mass Spectrometry	LOD	Limit of Detection
LOD	Limit of Quantification	Lit.	Literature
m/z	Mass to charge ratio	mp	melting point
NMR	Nuclear Magnetic Resonance	*P. berghei*	*Plasmodium berghei*
PTLC	Preparative Thin Layer Chromatography	NC	Negative Control
RBC	Red blood cells	ROS	Reactive Oxygen Species
RSD	Relative Standard Deviation	SEM	Standard Error of Mean

TLC	Thin Layer Chromatography	% Para	Percentage Parasitaemia
% Supp	Percentage Suppression	ppm	parts per million
UV-Vis	Ultraviolet-Visible	*bro.s*	broad singlet
WHO	World Health Organization	*d*	doublet
dd	doublet of doublet	*t*	triplet
m	multiplet	*s*	singlet

Table of Contents

Contents **Page**

List of Tables

List of Schemes

List of Appendices

Table of Contents

Contents **Page**

Part 2: Bioassay Directed Chemical Study of Antimalarial Substances from *Dodonaea angustifolia*

List of Tables

List of Schemes

List of Figures

Appendix

Table of Contents

Contents **Page**

Part 3: Comparative Chemical Studies of *Moringa stenopetala* and *Moringa oleifera*

List of Tables

List of Schemes

List of Figures

List of Appendices

Bioassay Directed Chemical Study of Antimalarial Substances from *Clerodendrum myricoides* and *Dodonaea angustifolia*

and

Comparative Chemical Studies of *Moringa stenopetala* and *Moringa oleifera*

General Introduction

Nature provides a variety of valuable resources for the survival of all living organisms on earth. Plants are vital to mankind, animals, other living things and also to the environment [1]. The association of plants with humans originated with the beginning of life of humans on earth [2]. Eventually human learned to recognize and categorize plants suited for use in meeting the basic necessities of life. Of these necessities, the use of plants as food supply in the world is a known fact. Among the major crops widely used in this regard are wheat, rice, maize or corn, potato, barley, sorghum etc. Shelter, in the form of wood for houses; and clothing, in the form of cotton fibers, are among the most important uses of plant materials , in addition to the use of plants for transportation, construction and as fuel. It is therefore obvious that plants play significant role in human survival and in improving the quality of human life.

The plant kingdom also contributed immensely to human health [3] in particular before the advent of modern drugs. The use of plants in maintaining and boosting health is firmly rooted in the past and is still developing [3-5]. Even now the majority of people in the world use traditional medicine for treating various life threatening diseases. It is assumed that the major part of traditional therapy involves the use of plant extracts or their active principles [2, 6-8]. The medicinal plants have greatest potential for benefitting people, especially those living in countries suffering from poverty, and poor health [1]. Moreover medicinal plants occupy a significant place in modern medicine as a raw material for some important drugs [6, 9]. The current demands for herbal remedies in both developed and developing countries is increasing. In developed countries this may be partly due to the dissatisfaction with conventional medicines while with the developing countries this is due to shortage of pharmaceutical products and the unaffordable prices [10].

Ethiopia is home for about 6,500 species of higher plants making the country one of the most diverse floristic regions in the world [10]. The country possesses a wide range of potentially useful

medicinal plants with 1000 species identified and reported in the Flora of Ethiopia [10]. Many others are not yet identified [10]. Ethiopian plants have shown remarkably effective medicinal values for many ailments that affect people and livestock [11]. The significance of these plants is supported by a report that 70% of the Ethiopian population still rely on traditional medicine to address their health care needs [12]. The most commonly used plants for the prevention and cure of different diseases in Ethiopia include *Artemisia spp*., *Boswellia spp*., *Brucea antidysentrica Cinnamomum cassia*, *Commiphora spp*., *Cyperus bulbosus*, *Echinops spp*., *Embelia schimperi*, *Glinus lotoides*, *Hagenia abyssinica*, *Juniperus procera*, *Myrtus communis*, *Ocimum spp*., *Otostegia spp*., *Phytolacca dodecandra*, [13] etc. In traditional market places and around churches and mosques in particular during religious ceremonies, many medicinal plants are sold side by side with spices and food items.

Nature has proven to be an endless source of abundant diversity of chemical entities with varying biological activities. Plants serve as a vast reservoir of many complex organic compounds, many of which, at least at our current stage of knowledge, appear to have no direct function for the growth and development of the plant [14]. These compounds, now known as secondary metabolites, are produced either as a result of the organism adapting to its surrounding environment or for its own survival and defense against predators [14, 15]. The most important of these bioactive constituents of plants including alkaloids, flavonoids, phenolics, steroids and terpenoids provide some unique and species-specific characteristics to plants. Many types of secondary metabolites derived from plants played a central role in the history of mankind and possess well defined biological functions. This realization has given a new impetus to the scientific study of secondary metabolites. Even though these metabolites have been exploited for thousands of years using various approaches, only a minor proportion has been investigated on the basis of their profiles and content of biologically active constituents.

Several evidences indicate that only few medicinal plants in different parts of the world have been evaluated for their phytochemical content, biological activities [16, 17] and isolation of active principles. Thus, it is exciting for chemists to search for compounds that have the potential to elicit

beneficial pharmacological activities. In this context phytochemical study to identify chemicals that can exhibit biological activities has got great relevance.

Taking into account the above facts, the work undertaken in this dissertation involves three parts. The first two parts [Part 1 and 2] deal with the activity guided antiplasmodial activities of two indigenous medicinal plants, *Clerodendrum myricoides* (Lamiaceae) and *Dodonaea angustifolia* (Sapindaceae), used as remedy against malaria in some parts of Ethiopia. The choice of the two plant species to establish their antimalarial properties is based on their use in traditional medicines for this purpose.

The third part [Part 3] of this dissertation presents brief review of the literature on the biological activities, water clarifying properties and chemistry of the genus *Moringa* and description of comparative chemical study of two *Moringa* species: *Moringa oleifera* of Indian origin, but now widely distributed in many countries of the world including Africa because of its outstanding pharmacological and nutritional properties, and *Moringa stenopetala*, an endemic plant confined to southern Ethiopia, Somalia and northern Kenya and believed to have remarkable potential with respect to pharmacological, nutritional and water clarifying properties just like *M. oleifera.*

Part 1

Bioassay Directed Chemical Study of Antimalarial Substances from *Clerodendrum myricoides*

1.1. Introduction

1.1.1. Brief Review on Chemistry and Pharmacological Properties of the Genus Clerodendrum

Lamiaceae is an important family of flowering plants known for the wealth of species with various medicinal properties [18]. It comprises of about 236 genera and 7,200 species [19]. *Clerodendrum* is among the genera in the family Lamiaceae [20], distributed in the tropical and subtropical regions of the world [21, 22], and mainly found in Africa and Asia [23]. The genus has more than five hundred species [23, 24], which consists of small trees, shrubs and herbs [25]. The genus is well known for its ornamental uses. *Clerodendrum* contains many plant species that are being used in various health care systems for the treatment of a variety of diseases. Previous pharmacological reports showed that some species of the genus exhibit anti-inflammatory [26], anti-microbial [27, 28], antimalarial [29], anthelminthic [30], antiviral and antioxidant activities [20, 22, 25].

Eight species of the genus *Clerodendrum* are recorded in the Flora of Ethiopia, namely, *C. acerbianum*, *C. alatum*, *C. cephalanthum*, *C. johnstonii*, *C. myricoides*, *C. robecchii*, *C. sp*., and *C. umbellatum* [31]. *Clerodendrum myricoides*, locally called *Misrch* in Amharic, also occurs in most African countries including Kenya, Nigeria and South Africa [31, 32]. *C. myricoides* is an open shrub reaching 4 m tall. This indigenous plant is employed for the treatment of various life threatening ailments. Traditionally, root decoction, leaves and bark of *C. myricoides* are used against malaria, diabetes, typhoid, cough, fevers, pneumonia, headache, snake bites and venereal disease [32-35]. In pharmacological studies, the dichloromethane extracts of the leaves of *C. myricoides* demonstrated anti-mutagenic properties against *Salmonella typhimurium* [36]. The leaves of *C. myricoides* are also used against diarrhea, and dysentery [37].

Efforts have been made by various researchers to isolate the chemical constituents from various species of the genus *Clerodendrum*. Research reports available showed the presence of terpeonids, steroids, phenolics, flavonoids and carbohydrates [32, 38]. So far over 60 compounds have been reported from the genus. A complete list of compounds reported so far from the genus along with their classes, plant source, plant part and literature references are given in Table 1.

Table 1: List of compounds from *Clerodendrum* organized by compound class

Cpd class	Cpd name	Str. No	Plant source	Plant part	Ref
Flavonoids	4'-Methyl 5,7-dihydroxyflavone	**1**	*C. t*	LF	[39]
	Apigenin 7-galacturonide	**2**	"	"	
Iridoids	Seratoside A	**3**	*C. s*	"	[25, 39, 40]
	Seratoside B	**4**	"	"	
	7-*β*-Coumaroyl-oxyugadoside	**5**	"	"	
	7-*β*-Cinnamoyl-oxyugadoside	**6**	*C. b*	"	
	Iridoid glucoside	**7**	"	"	
Phenolics	Bunginoside A	**8**	"	"	[39-41]
	3'',4''-di-O-acetylmartynoside	**9**	"	"	
	Acetylmartynoside B	**10**	"	"	
	Acetylmartynoside A	**11**	"	"	
	Verbascoside	**12**	*C. t*	"	
	3''-O-Acetylmartyonside	**13**	*C. b*	"	
	2''-O-Acetylmartynoside	**14**	"	"	
	Martynoside	**15**	"	"	
	Leucosceptoside A	**16**	"	"	
	Trichotomoside	**17**	"	"	
	O-2,3-Di-O-acetyl-*α*-L-rhamnopyranosyl-(1→3)-(4-O-cis-feruloyl)-*β*-D-glucopyranoside	**18**	"	"	
	Isomartynoside	**19**	"	"	
	Isoacteoside	**20**	"	"	
	Darendoside B	**21**	"	"	
	Phlomisethanoside	**22**	"	"	
	Darendoside A	**23**	"	"	
Steroids	Colebrin A	**24**	*C. c*	"	[42]
	Colebrin B	**25**	"	"	
	Colebrin C	**26**	"	"	
	Colebrin D	**27**	"	"	

Table 1 continued

	Colebrin E	**28**	"	"	
	Clerosterol	**29**	*C. q*	"	[42,43]
	β-Sitosterol	**30**	"	"	[42]
	Stigmasterol	**31**	"	"	
	4*α*-Methyl-24-*β*-ethyl-5*α*-cholesta-14,25-dien-3*β*-ol	**32**	*C. i*	LF	[44]
	24*β*-Ethylcholesta-5,9(11),22E-trien-3*β*-ol	**33**	"		
	22-Dehydroclerosterol	**34**	*C. q*	LF	[43]
	22-Dehydroclerosterol 3*β*-O-*β*-D-(6'-O-margaroyl)-glucopyranoside	**35**	"		
	Clerosterol 3*β*-O-*β*-D-glucoside	**36**	*C. c*	LF	[45]
Terpenoids	Bungnate A	**37**	*C. b*	RT	[41]
	Bungnate B	**38**	"	"	
	15-Dehydrocyrtophyllone A	**39**	"	"	
	15-Dehydro-17-hydroxycyrtophyllone A	**40**	"	"	
	12,16-Epoxy-11,14,17-trihydroxy-6-methoxy-17(15→16)-abeo-abieta-5,8,11,13-tetraene-7-one	**41**	"	"	
	Cyrtophyllone A	**42**	"	"	
	Villosin C	**43**	"	"	
	Teuvincenone F	**44**	"	"	
	19-Hydroxyteuvincenone F	**45**	"	"	
	Mandarone E	**46**	"	"	
	12,16-Epoxy-11,14-dihydroxy-6-methoxy 17(15→16)-abeo-abieta-5,8,11,13,15-pentaene-3,7-dione	**47**	"	"	
	12-O-*β*-D-Glucopyranosyl-3,11,16-trihydroxyabieta-8,11,13-triene	**48**	"	"	
	Uncinatone	**49**	"	"	
	Inerme A	**50**	*C. i*	LF	[44]
	Inerme B	**51**	"	"	
	14,15-dihydro-15-*β*-methoxy-3-epicaryoptin	**52**	"	"	
	14,15-dihydro-15-hydroxy-3-epicaryoptin (Epimer)	**53**	"	"	
	15-epimer of 18	**55**	"	"	

Table 1 continued

Mis.	Clerobungin A	**56**	*C. b*	LF	[46]
	Clerobungin B	**57**	"		
	(+)-Rengyolone	**58**	"		
	Cleroindicin E	**59**	"		
	1-Hydroxy-1-(8-palmitoyloxyethyl) cyclohexanone	**60**	*C. t*	''	[47]
	5-O-butyl cleroindin D	**61**	"		
	Lucumin	**62**	*C. g*	LF	[48]

LF: leaf; RT: root; Str No : structure number; cpd: compound; *C. t*: *C. trichotomum*; *C.s*: *C. serratum*; *C. b*: *C. bungei*; *C. c: C. colebrookianum*; *C. q*: *C. quadriloculare*; *C. i*: *C. inerme*; *C. g*: *C. grayi*, Mis.: miscellaneous

The chemical structures of compounds so far reported from the genus *Clerodendrum* are given below.

Flavonoids [39]

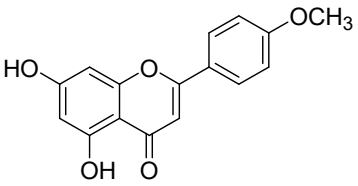

1

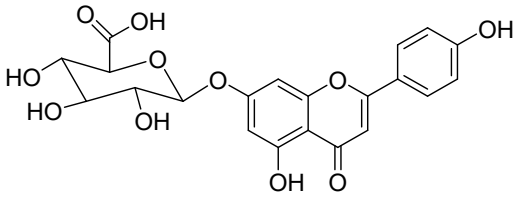

2

Iridoids [25, 40]

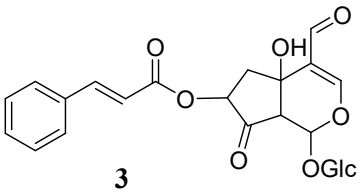

3

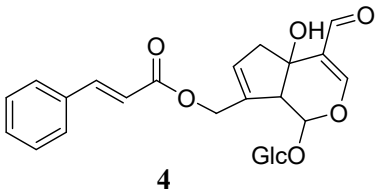

4

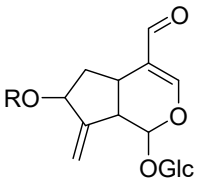

5. R = coumaroyl
6. R = cinnamoyl

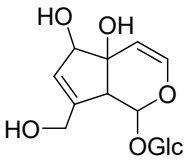

7

Phenolics [39-41]

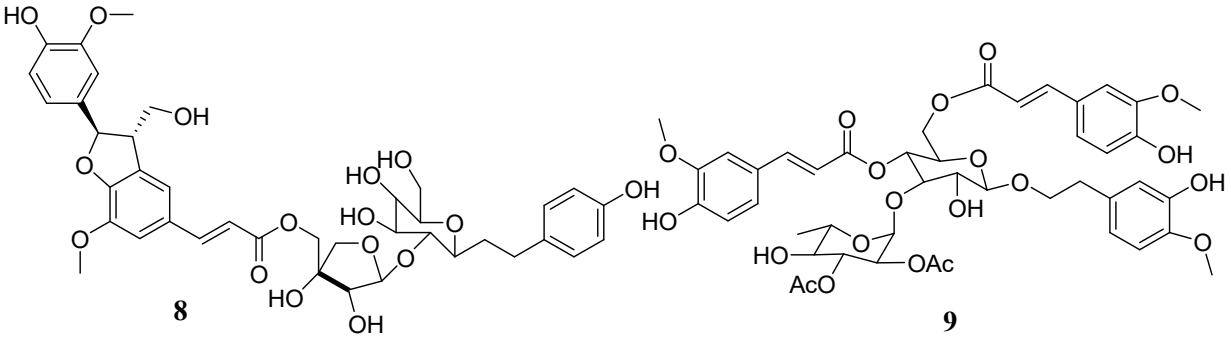

8 **9**

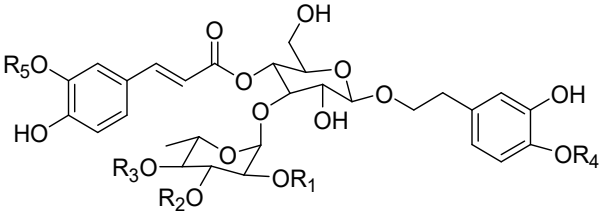

	10	**11**	**12**	**13**	**14**	**15**	**16**	**17**
R1	H	Ac	H	Ac	H	Ac	H	H
R2	Ac	H	H	Ac	Ac	H	H	H
R3	Ac	Ac	H	H	H	H	H	H
R4	Me	Me	H	Me	Me	Me	Me	H
R5	Me	Me	H	Me	Me	Me	Me	Me

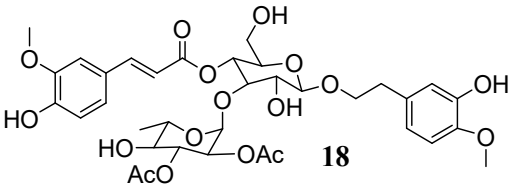

18

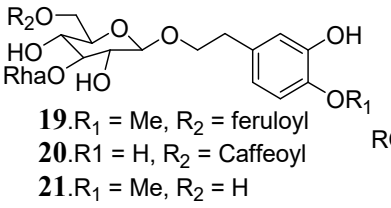

19.R_1 = Me, R_2 = feruloyl
20.R1 = H, R_2 = Caffeoyl
21.R_1 = Me, R_2 = H

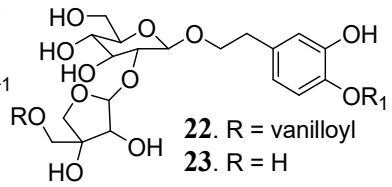

22. R = vanilloyl
23. R = H

Steroids [42-44]

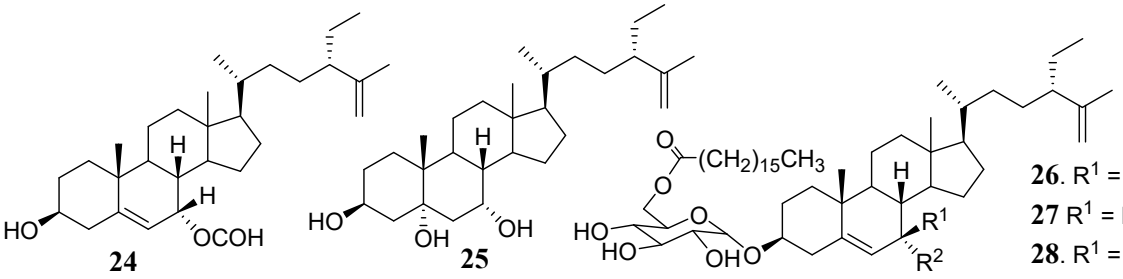

24 **25**

26. R^1 = R^2 = H
27 R^1 = H, R^2 = OH
28. R^1 = OH, R^2 = H

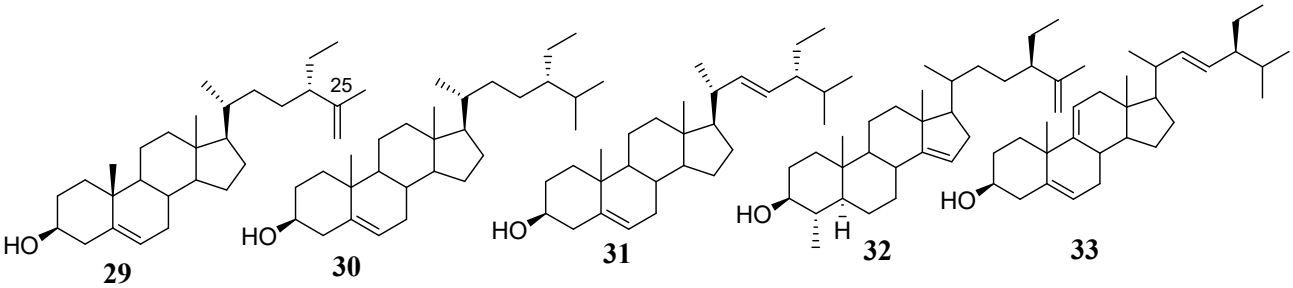

29 **30** **31** **32** **33**

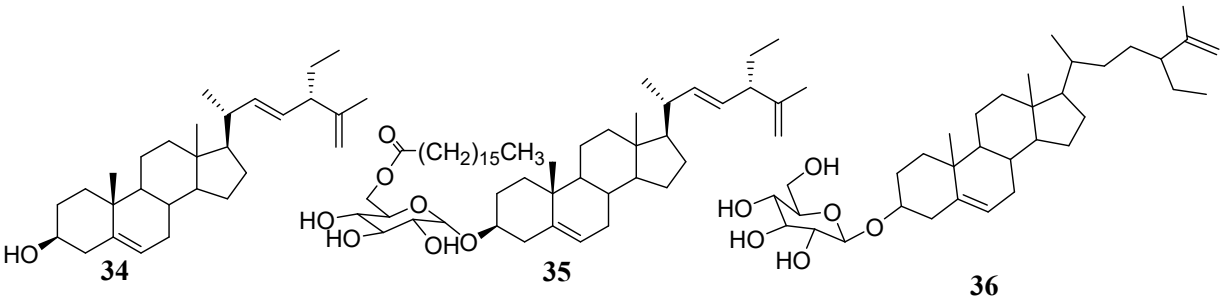

34 **35** **36**

Terpenoids [39, 41, 44]

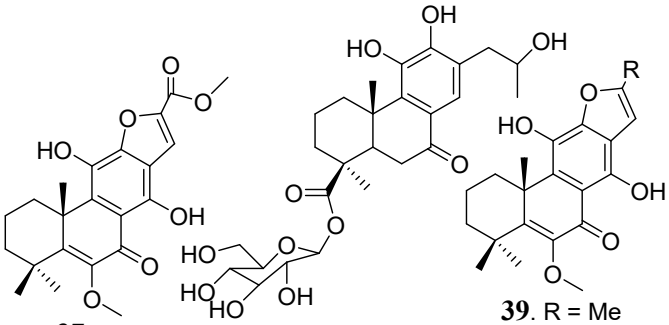

37 **38**

39. R = Me
40. R = CH_2OH

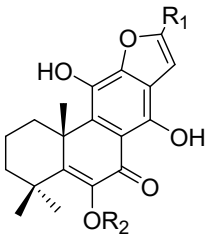

41. $R_1 = CH_2OH$, R_2 = Me
42. $R_1 = R_2$ = Me
43. $R_1 = CH_2OH$, R_2 = H

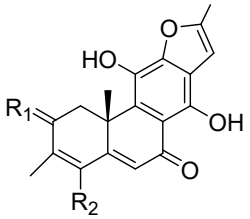

44. R_1 = O, R_2 = Me
45. R_1 = O, $R_2 = CH_2OH$
46. $R_1 = H_2$, $R_2 = CH_3$

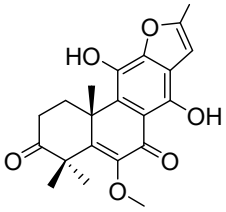

47

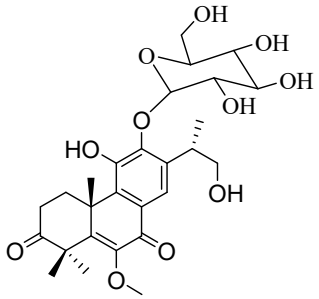

48

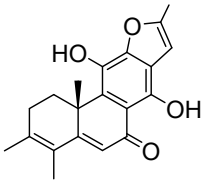

49

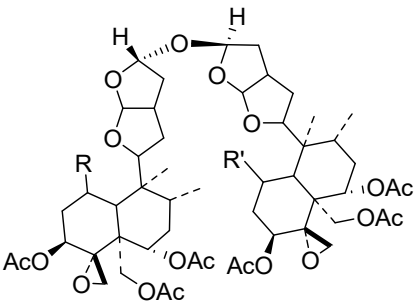

50. R = R' = H
51. R = R' OMe

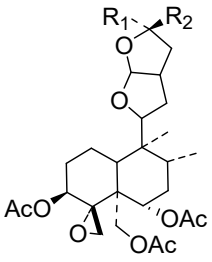

52. R_1 = H, R_2 = OMe
53. R_1 = R_2 = OH

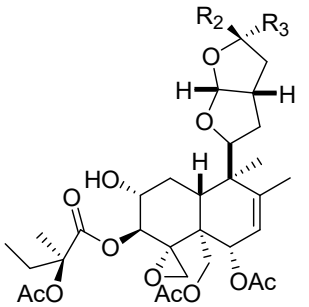

54. R_2= OCH_3, R_3 = H
55. R_2 = H, R_3 = OCH_3

Miscellaneous [46-48]

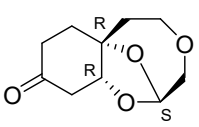

56

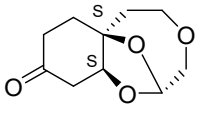

57

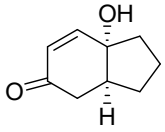

58

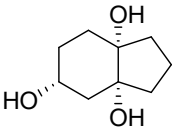

59

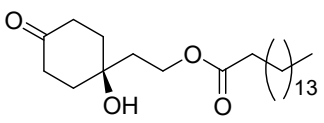

60

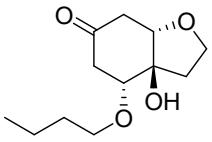

61

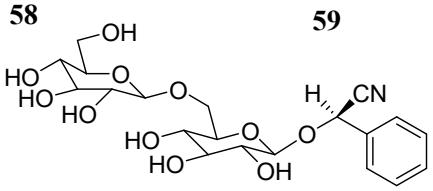

62

Despite the fact that *C. myricoides* is traditionally used for the treatment of various ailments in different parts of the world, there is no prior report on the chemical study of the leaves or other parts of this species. There are reports that deal with the antimalarial activities of some species of the genus [12]; however, there is one unpublished report demonstrating the antiplasmodial potential of the leaves of *C. myricoides* [35]. Indeed two preliminary MSc studies done in the Biology Department of Addis Ababa University [49, 50] clearly established that the ethanol extracts of this plant showed significant antiplasmodial activities. Inspired by this report we set out to undertake bioassay guided isolation of the active compounds from the extracts of *C. myricoides*

1.2. Objectives

The principal objectives of this work are to

- conduct bioassay guided isolation and characterization of compounds responsible for the antiplasmodial activities of the extracts of the leaves of *C. myricoides.*
- identify the compounds responsible for the radical scavenging activities of the extracts

1.3. Results and Discussion

This section describes the activity guided antiplasmodial studies of the leaves of *C. myricoides.* The main achievement of this work is the isolation of two bioactive compounds, namely, *α*-spinasterol (**63**) and sitosterol-3-*O*-*ß*-D-glucopyranoside (**64**) which displayed percent inhibition of parasitaemia by 51% and 44% at 40 mg/kg, respectively. The work was also geared towards the exploration of other chemical constituents of the leaves of this plant. Thus, in this section, the isolation, purification and structure determination of three other compounds, namely, verbascoside (**12**), ixoroside (**76**) and compound **72** is described. To our knowledge there is no report in the literature for compound **72**. In the course of this work five fatty acids, namely, tetracosanoic acid (**77**), behenic acid (**78**), icosanoic acid (**79**), stearic acid (**80**), and palmitic acid (**81**) were identified from the non polar fraction of the acetone extract of the leaves of *C. myricoides*. The radical scavenging activities of the extracts and the pure constituents of the leaves were also investigated.

1.3.1. Characterization of Compounds Isolated from the Leaves of *C. myricoides*

α-Spinasterol (63)

Compound **63** was obtained as a white solid, mp 144-145^{o}C after column chromatography of the acetone extract of the leaves of *C. myricoides* followed by recrystalization from isopropyl alcohol. TLC (hexane:EtOAc, 3:2) gave rise to a spot at Rf = 0.60, visualized after spraying with vanillin/ H_2SO_4 followed by heating with hot air gun. The mass spectrum of compound **63** displayed a molecular ion peak at *m/z* 412 which is compatible with the molecular composition of $C_{29}H_{48}O$. The diagnostic fragments in the mass spectrum at *m/z* 369, 351, 300, and 273 are characterstic of sterols containing two double bonds. Specially important is the fragment at *m/z* 300, which is due to retro Diels-Alder product of sterols with Δ^7 bonds. The IR spectrum showed absorption bands at 3369, 2940, 1609 and 1062 cm^{-1} due to O-H, aliphatic C-H, olefinic C=C and C-O stretching, respectively.

The ^{1}H-NMR spectrum ($CDCl_3$) of compound **63** revealed the presence of six methyls at δ 0.60 (3H, *s*), δ 0.80-0.860 (9H, *m*), δ 0.87 (3H, *d*, *J* = 6.40 Hz) and δ 1.13 (3H, *d*, *J* = 6.80 Hz). Other proton signals integrating for 25 hydrogens were observed in the range δ 2.30 to 1.00. The signal at δ 3.65 (1H, *m,* H-3) corresponding to a proton attached to an oxygenated carbon along with three olefinic proton signals at δ 5.04 (H-23, *dd*, *J* = 8.8 and 15.2 Hz), 5.17 (1H, *m*, H-7) and 5.18 (H-22, *dd*, *J* = 8.4 and 15.2 Hz) support the presence of sterol nucleus with two double bonds. The UV-Vis spectrum of compound **63** displayed absorption maximum at 227 nm demonstrating that the double bonds are isolated.

The proton decoupled ^{13}C-NMR and DEPT-135 spectra ($CDCl_3$) of compound **63** (Table 2) revealed the presence of 29 well resolved carbon signals including six methyl, nine methylene, eleven methine, and three quaternary carbons. The three quaternary carbon signals observed at δ 139.6, 43.3 and 34.2 are due to C-8, C-13 and C-10, respectively. The ^{13}C-NMR spectrum showed signal in the oxygenated region at δ 71.1 assignable to C-3. The presence of two double bonds was evident from the appearance of three olefinic carbon signals attributed to C-7 (δ 117.5), C-22 (δ 129.5) and C-23 (δ 138.1). Particularly noteworthy is the olefinic carbon resonance at δ 117.5 which is characteristics of sterols with Δ^7 bond which rules out the possibility of stigmasterol (**31**) as an option. The proton signal at δ 5.17 (H-7) in the ^{1}H-NMR spectrum of compound **63** supports the above assertion. The ^{13}C-NMR spectral data of compound **63** along with the literature reported for α-spinasterol are given in Table 2 [51].

Table 2: Comparison of the ^{13}C-NMR spectral data of compound **63** with that reported in the literature for α-spinasterol ($CDCl_3$, δ in ppm) [51]

Position	^{13}C-NMR data of **63**	Data reported in the lit. for α-spinasterol	Position	^{13}C-NMR data of **63**	Data reported in the lit. for α-spinasterol
1	37.1	37.1	16	28.5	28.5
2	31.5	31.4	17	55.9	55.8
3	71.0	71.0	18	12.0	12.0
4	38.0	37.9	19	13.0	13.0
5	40.3	40.2	20	40.8	40.8
6	29.6	29.6	21	21.3	21.3
7	117.4	117.4	22	138.2	138.1
8	139.6	139.5	23	129.4	129.4
9	49.4	49.4	24	51.2	51.2
10	34.2	34.2	25	31.8	31.9
11	21.5	21.5	26	21.0	21.0
12	39.4	39.5	27	19.0	19.0
13	43.3	43.2	28	25.4	25.4
14	55.1	55.1	29	12.2	12.2
15	23.0	23.0			

The spectral and physical data of compound **63** are in agreement with the data reported in the literature for α-spinasterol (**63**) (Table 2) [51].

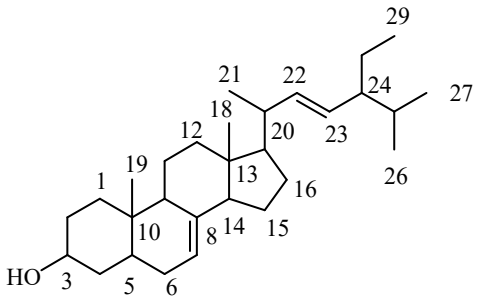

63

α-Spinasterol was previously reported from the twigs of *Samanea saman* [51], *Dillenia indica* [52], stems of *Amaranthus spinosus* [53], fruits of *Luffa cylindrical* [54], aerial part of *Scrophularia takesimensis* [55], flowers of *Stenactis annua* [56] and the seeds of *Nigella sativa* [57]. Pharmacological reports showed that *α*-spinasterol exhibits anti-tumor property in breast, ovarian and cervical cancer cells in a dose-dependent manner [58]. The ability to inhibit inflammations is another key beneficial effect of *α*-spinasterol [59].

Sitosterol-3-O-*β*-D-glucoside (64)

A white solid compound isolated from the acetone extract of the leaves of *C. myricoides*, showed a spot on TLC (Rf = 0.4 (hexane:EtOAc, 1:4)) after spraying with vanillin/H_2SO_4. Compound **64** exhibited $[\alpha]_{589}^{21}$ = -25.0 (c 0.4, MeOH) indicating the presence of chiral center. The IR spectrum showed peaks at 3429, 2918, 1600, and 1063 cm^{-1} due to OH, C-H, C=C and C-O stretching, respectively. The FT-MS data of compound **64** demonstrated the molecular ion peak at *m/z* 599.4293 (calcd 599.8100 for $C_{35}H_{60}O_6Na$) establishing the molecular formula as $C_{35}H_{60}O_6$. This is consistent with the ^{13}C-NMR spectrum which showed resonances for 35 carbon atoms. The peak at *m/z* 203 ($C_6H_{12}O_6Na$) in the mass spectrum witnesses the presence of hexose sugar in the compound. Compound **64** showed no absorption maxima in its UV-Vis spectrum indicating the absence of conjugated chromophore.

Analysis of the ^{1}H-NMR spectrum (DMSO-d6) demonstrated the presence of six methyl signals at *δ* 0.65 (3H, *s*), 0.95 (3H, *s*), 0.90 (3H, *t*, *J* = 6.4 Hz), 0.93 (3H, *d*, *J* = 3.2 Hz), and *δ* 0.80 (6H, *m*). Among these the signals at *δ* 0.65 and 0.95 are due to methyl groups on quaternary carbons. On the other hand signals due to methyl signals on secondary and tertiary carbons were observed at *δ*

0.90 and 0.93, respectively. The olefinic proton signal at δ 5.30 (1H, *bro*. *d*, *J* = 3.2 Hz), and the proton signal on oxygenated carbon at δ 4.47 (1H, *m*) along with the six methyl groups are evident for the presence of sterol with one double bond. The spectrum showed anomeric proton (H-1') signal at δ 4.21 (1H, *d*) with a *J* value of 8.0 Hz establishing the sugar as a β-anomer [60, 61]. Among the sugar protons, those signals situated at δ 3.63 (1H, *m*) and δ 3.45 (1H, *m*) are due to diastereotopic methylene protons on C-5' (δ 61.5) of the glucose moiety as confirmed by HSQC spectral analysis. The remaining proton signals of the glucose moiety at δ 3.12 (1H, *m,* H-5'), 3.47 (1H, *m*, H-2'), 2.89 (1H, *m,* H-3') and 3.06 (1H, *m,* H-4') showed HSQC correlations with the carbon signals at δ 77.4 (C-5'), 77.3 (C-2'), 73.9 (C-3') and 70.5 (C-4'), respectively. The olefinic proton signal at δ 5.30 showed HSQC correlation with C-6 (δ 121.6). Furthermore, the multiplet signals at δ 4.93 and 4.47 integrating for three and one hydrogen, respectively, account for hydrogens on hydroxyl groups of the sugar moiety.

The ^{13}C-NMR spectrum (DMSO-d6) showed thirty five signals (Table 3) where two are due to olefinic carbons, C-5 (δ 140.9) and C-6 (δ 121.8). The signal at δ 77.2 is assigned to C-3. The presence of only one sugar moiety in the compound is verified by the appearance of only one anomeric carbon signal at δ 101.3 along with a set of chemical shifts at δ 77.4, 77.3, 73.9, 70.5 and 61.5. The HMBC correlation observed between the proton signal at δ 4.21 (H-1') with the carbon signal at δ 77.2 (C-3) established the site of attachment of the sugar to the sterol nucleus. The ^{13}C-NMR spectral data of compound **64** were compared with those reported in the literature for sitosterol-3-O-β-D-glucopyranoside with the result given in Table 3.

Table 3: ^{1}H- and ^{13}C-NMR spectral data of compound **64** and the reported ^{13}C-NMR data for sitosterol-3-O-*β*-D-glucoside (DMSO-d6) [62]

Position	NMR data of compound **64**		^{13}C-NMR data reported for sitosterol-3-O-*β*-D-glucoside [62]
	^{1}H-NMR	^{13}C-NMR	^{13}C-NMR
1	1.87 (1H, *m*) and 1.76 (1H, *m*)	36.7	38.0
2	0.98 (1H, *m*) and 1.32 (1H, *m*)	34.0	35.9
3	3.04 (1H, *m*)	77.2	78.0
4	1.97 (1H,*m*) and 1.93 (1H, *m*)	39.7	39.5
5	-	140.9	140.5
6	5.30 (1H, *m*)	121.3	121.5
7	1.80 (1H, *m*) and 1.23 (1H, *m*)	30.0	31.7
8	1.63 (1H, *m*)	28.2	28.2
9	0.92 (1H, *m*)	45.6	45.6
10	-	37.3	36.5
11	1.48 (2H, *m*)	19.5	19.1
12	1.96 (1H, *m*) and 1.40 (1H, *m*)	31.9	32.7
13	-	42.3	42.0
14	1.10 (1H, *m*)	55.9	55.8
15	0.99 (1H, *m*) and 1.53 (1H, *m*)	24.3	24.1
16	1.22 (2H, *m*)	23.0	22.9
17	1.03 (1H, *m*)	56.6	56.4
18	0.95 (3H, *s*)	19.1	18.6

19	0.65 (3H, *s*)	12.5	12.0
20	1.34 (1H, *m*)	29.2	29.7
21	0.80 (3H, *m*)	12.3	11.7
22	2.12 (1H,*m*) and 2.38 (1H,*m*)	36.6	37.0

Table 3 continued

Position	NMR data of compound **64**		^{13}C-NMR data reported for sitosterol-3-O-*β*-D-glucoside [62]
	^{1}H-NMR	^{13}C-NMR	^{13}C-NMR
23	1.77 (1H, *m*) and 1.23 (1H, *m*)	28.3	29.0
24	0.89 (1H, *m*)	50.0	49.4
25	1.89 (1H, *m*)	31.8	31.6
26	0.93 (3H, *d*, *J* = 3.20)	21.0	20.8
27	0.80 (3H, *m*)	20.5	19.6
28	1.14 (2H, *m*)	26.9	26.0
29	0.90 (3H, *t*, *J* = 6.40)	19.4	18.8
1’	4.21 (1H, *d*, *J* = 8.00)	101.3	101.9
2’	3.47 (1H, *m*)	77.3	77.7
3’	2.89 (1H, *m*)	73.9	74.6
4’	3.06 (1H, *m*)	70.5	71.0
5’	3.12 (1H, m)	77.4	77.7
6’	3.63 (1H, *m*) and 3.45 (1H, *m*)	61.5	62.1

Assignments made on the basis of COSY, HSQC and HMBC correlations; *δ* in ppm; Coupling constants are in Hz

The above physical and spectral data of compound **64** are consistent with those reported in the literature for sitosterol-3-O-*β*-D-glucopyranoside (**64**) [62].

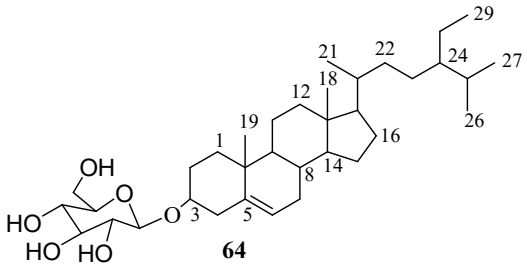

64

Sitosterol-3-O-*β*-D-glucoside (**64**) is an anticancer [63] and antibacterial agent [64] reported from various plant species such as *Solanum melongena* [63], *Moringa peregrina* [64], *Bergenia ligulata* [65], *Mentha suaveolens* [66], *Zilla spinosa* [67], and *Urtica pilulifera* [68].

Verbascoside (12)

Verbascoside (**12**), a phenylethanoid glycoside, is a major constituent in the acetone extract of the leaves of *C. myricoide*s which melted at 147-148ºC (Lit. 145-148ºC) [69]. The compound showed $[\alpha]_{589}^{21}$ = -5.0 (c 0.4, MeOH) indicating the presence of chiral center. TLC, (eluent EtOAc:AcOH, 4:1), showed a single spot at Rf = 0.6 which was visualized as yellow spot with vanillin/H_2SO_4. The UV-Vis spectrum (MeOH) showed absorption maxima at 290 and 329 nm presumably due to $\pi \rightarrow \pi^*$ transition of the phenylethyl and caffeic acid moieties in the compound, respectively. The IR spectrum displayed the presence of hydroxyl and ester carbonyl at 3398 cm^{-1} and 1698 cm^{-1}, respectively. The negative ion mode high resolution FT-MS displayed molecular ion at *m/z* 623.1981 (calcd 623.5794 for $C_{29}H_{35}O_{15}$) which is consistent with the molecular formula $C_{29}H_{36}O_{15}$. Other peaks observed at *m/z* 461.1650 ($C_{20}H_{29}O_{11}$) and 315.1080 ($C_{14}H_{19}O_{11}$) in the mass spectrum are due to sequential loss of the caffeic acid and rhamnose moieties from the parent ion, respectively.

The ^{1}H-NMR (DMSO-d6) spectroscopic data suggested the presence of *trans* double bond at *δ* 7.45 (1H, *d*, *J* = 15.70 Hz) and 6.20 (1H, *d*, *J* = 15.70 Hz), which showed COSY correlation with each other. In the aromatic region, the ^{1}H-NMR spectrum of compound **12** exhibited signals as two different systems, one belonging to the caffeic acid substituent at *δ* 7.02 (1H, *d*, *J* = 1.69 Hz), 6.98

(1H, *dd*, *J* = 8.14, 1.69 Hz), and 6.75 (1H, *d*, *J* = 8.14 Hz) and the other to the 3,4-disubstituted phenylethyl moiety at *δ* 6.63 (1H, *d*, *J* = 8.14 Hz), 6.62 (1H, *bro s*), and 6.49 (1H, *dd*, *J* = 8.14, and 1.48 Hz). The COSY spectrum of compound **12** supports this phenomenon as correlation was observed between the proton signal at *δ* 6.98 with the proton signal at 6.75; and the proton signal at *δ* 6.49 with the signal situated at *δ* 6.62. The anomeric proton and methyl group signals of rhamnose were easily recognized, as they appeared at *δ* 5.01 (1H, *d, J* = 1.3 Hz) and 0.94 (3H, *d*, *J* = 6.24 Hz), respectively, with their corresponding carbon signals in the ^{13}C-NMR spectrum at *δ* 61.1 and 18.6. Contrary to the rhamnosyl group, the coupling constant for the anomeric proton signal of glucose at *δ* 4.35 (1H, *d*, *J* = 7.82 Hz) was in agreement with *β*-configuration [60, 61]. The presence of two anomeric protons in the ^{1}H-NMR spectrum of compound **12** was supported by the appearance of two anomeric carbon signals at *δ* 101.6 (C-1’’’) and 102.7 (C-1’’) in the ^{13}C-NMR spectrum. The signal at *δ* 4.70 (1H, *t*, *J* = 9.60 Hz) is due to methine proton on C-4’’ (*δ* 69.5) which showed HMBC correlation with the carbonyl carbon of caffeic acid substituent establishing the site of attachment of the caffeic acid to the sugar moiety. The signal at *δ* 2.70 (2H, *m*) is a distinctive signal of benzylic protons.

The ^{13}C-NMR spectrum (DMSO-d6) of compound **12** (Table 4) showed carbonyl functional group of an ester at *δ* 166.2 (C-9) which is consistent a strong C=O absorption band at 1698 cm^{-1} in the IR spectrum. The compound exhibited signals due to four oxygenated carbons in the aromatic region at *δ* 148.9 (H-4), 146.0 (H-3), 145.4 (H-3’) and 143.9 (H-4’). The signal of the olefinic carbon (C-7) *β* to the carbonyl was overlapped with the quaternary carbon signal at *δ* 146.0 (C-3). The other carbon signals at *δ* 129.5 and 125.9 are due to C-1’ and C-1, respectively. Six signals due to methine carbons belonging to the aromatic ring were shown at *δ* 121.9, 120.0, 116.7, 116.2, 115.9, 115.0, and 114.0. Eight methine carbon signals of the sugar moieties were observed at *δ* 79.5, 74.9, 72.0, 70.9, 70.8, 69.5 and 69.1. The presence of two sets of methylene carbon signals at *δ* 70.8 (C-8’) and 35.4 (C-7’) were evident for the presence phenylethyl moiety.

The *trans* double bond signals at *δ* 7.45 and 6.20 showed HMBC correlation with the carbonyl carbon which is evident for the presence of an *α*,*β*-unsaturated carbonyl carbon. The HMBC also showed correlations such that the proton signal at *δ* 7.45 correlates with the carbon signals at *δ*

121.9 and 115.0; and the proton signal at δ 6.20 with the carbon signal at δ 125.9. The proton signal observed at δ 6.98 showed HMBC correlation with the carbon signals at δ115.8, and 148.9. Another correlation observed was between the proton signal at δ 7.02 and the carbon signals at δ 121.9, 145.4 and 148.9. Further correlation observed was between the proton signal at δ 6.63 with the carbon signals at δ 129.5 and 143.9; proton signal at δ 6.62 with carbon signal at δ 119.9 ; and the proton signal at δ 6.49 with the carbon signals at δ 143.9 and 116.2. The proton signal at δ 2.70 correlates with the carbon signals at δ 116.2, 119.9, 129.5 and 70.7. The above results were suggestive of fragment **65** and **66**.

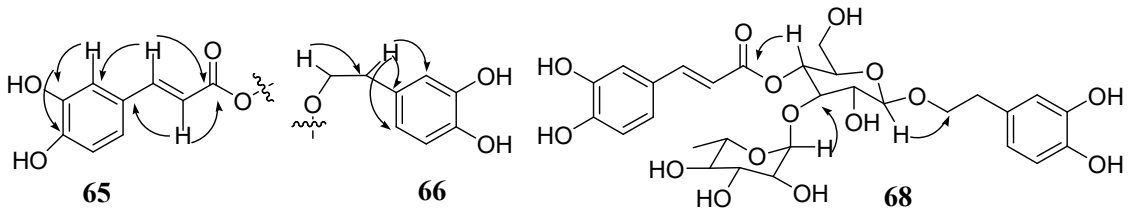

The site of attachment of the aromatic ring containing the phenylethyl group to the anomeric carbon of glucose was established by the appearance of HMBC correlation between the carbon signal at δ 70.8 with the anomeric proton (H-1'') of the glucose moiety. Another key HMBC correlation observed was between the anomeric proton signal of the rhamnose at δ 5.01 with C-3'' (δ 79.5) of glucose indicating that the rhamnopyranose group was attached to glucose through C-3'' (δ 79.5). On the basis of the above spectral studies, the key HMBC correlation is depicted in **68**. The NMR spectral data of compound **12** were compared with those reported in the literature for verbascoside which are given in Table 4.

Table 4: ^{1}H- and ^{13}C-NMR spectral data of compound **12** and the ^{1}H- and ^{13}C-NMR data reported for verbascoside [69]

Position	^{1}H- and ^{13}C-NMR data of **12** (DMSO-d6)		^{1}H- and ^{13}C-NMR data reported for verbascoside [69]	
	^{1}H-NMR	^{13}C-NMR	^{1}H-NMR	^{13}C-NMR
1	-	125.9	-	125.5
2	7.02 (1H, *d*, *J* = 1.69)	115.0	7.02 (1H, *J* = 2.00)	114.7
3	-	146.0	-	145.5
4	-	148.9	-	148.4
5	6.75 (1H, *d*, *J* = 8.14)	115.8	6.76 (1H, *d*, *J* = 8.00)	115.8
6	6.98 (1H, *dd*, *J* = 8.14, 1.69)	121.9	6.97 (1H, *dd*, *J* = 2.00 & 8.00)	121.3
7	7.45 (1H, *d*, *J* = 15.7)	146.0	7.46 (1H, *d*, *J* = 16.00)	145.0
8	6.20 (1H, *d*, *J* = 15.7)	114.1	6.19 (1H, *d*, *J* = 16.00)	113.6
9	-	166.2	-	165.7
1’	-	129.5	-	129.1
2’	6.62 (1H, *bro s*)	116.7	6.63 (1H, *s*, H-2)	116.3
3’	-	145.4	-	145.0
4’	-	143.9	-	143.5
5’	6.63 (1H, *d*, *J* = 8.14)	116.2	6.64 (1H, *dd*, *J* = 8.00)	115.4
6’	6.49 (1H, *dd*, *J* = 8.14 & 1.48).	119.9	6.49 (1H, *dd*, *J* = 2.00 & 8.00)	119.5
7’	2.70 (2H, *m*)	35.4	-	35.5
8’	3.87 (1H, *m*) & 3.68 (1H, *m*)	70.7	-	69.1
1’’	4.35 (1H, *d*, *J* = 7.82)	102.7	4.35 (1H, *d*, *J* = 8.00)	102.3
2’’	3.20 (1H, *m*)	74.9	-	75.0
3’’	3.69 (1H, *m*)	79.5	-	79.5
4’’	4.70 (1H, *d*, *J* = 9.60)	69.5	-	69.6
5’’	3.48 (1H, *m*)	74.9	-	72.1

6''	3.32 (1H, *m*) & 3.39 (1H, *m*)	61.1	-	61.2
1'''	5.01 (1H, *d*, *J* = 1.30)	101.6	5.03 (1H)	101.2
2'''	3.68 (1H, *m*)	70.9	-	70.9
3'''	3.28 (1H, *m*)	70.8	-	70.7
4'''	3.10 (1H, *m*)	72.2	-	71.0
5'''	3.35 (1H, *m*)	69.2	-	69.2
6'''	0.94 (3H, *d*, *J* = 6.00)	18.6	-	18.6

Assignments made on the basis of COSY, HSQC and HMBC correlations; δ in ppm; Coupling constants are in Hz

The spectroscopic data presented above is in good agreement with those reported in the literature for verbascoside (**12**) [69].

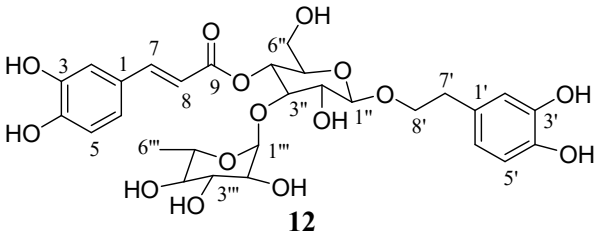

12

Verbascoside was previously isolated from the leaves of olive [70], *Arrabidaea pulchra* [69], *Lantana camara* [71], *Verbascum wiedemonnianum* [72] and *Castilleja tenuiflora* [73]. Pharmacologically, verbascoside exhibited antiviral [69], antitumor [72] and anti-inflammatory [73] properties. Furthermore the ability of verbascoside to prevent the damages caused by reactive oxygen species (ROS) by interfering with initial ROS generating reactions, scavenging the free oxygen molecules required to begin ROS production, and chelating metals that speed up oxidative processes were documented in the literature [74]

Compound 71

Compound **71** was obtained as a solid, mp 178-180°C. TLC, (EtOAc:AcOH, 4:1), showed a pink spot at Rf = 0.4 which was visualized after spraying with vanillin/H_2SO_4. The UV-Vis spectrum displayed absorption maxima at 246 and 313 nm due to π→π* and n→π* transitions, respectively. It is optically active with $[\alpha]_{589}^{21}$ = -147.5 (c 0.4, MeOH). The IR spectral analysis showed peaks at 3369, 1690, 1674, 1631, and 1076 cm^{-1} suggesting the presence of hydroxy, ester carbonyl, aldehyde carbonyl, olefinic C=C, and C-O stretching, respectively. The positive ion mode FT-MS

displayed a molecular peak ion peak at *m/z* 551.2463 (calcd 551.7349 for $C_{26}H_{40}O_{11}Na$) establishing the molecular composition $C_{26}H_{40}O_{11}$.

The ^{1}H-NMR spectrum of **71** (CD_3COCD_3) showed a single singlet at δ 9.31 due to an aldehydic proton. The spectrum disclosed two olefinic proton signals at δ 7.44 (1H, *s*, H-3) and 6.77 (1H, *t, J* = 3.70 Hz, H-3'') . The latter signal showed COSY correlations with the proton signals at δ 1.81 (H-9'') and 2.22 (H-4''). The characteristic proton signal due to an acetal carbinol (H-1) appeared as a doublet at δ 5.99 (1H, *d*, *J* = 2.40 Hz). This signals correlates with the proton signal at δ 2.70 (H-9) in its COSY spectrum. In ^{1}H-NMR spectrum of compound **71**, the anomeric proton signal at δ 4.74 (1H, *d*, *J* = 8.00 Hz, H-1′) and six proton signals at δ 3.24 (1H, *m,* H-2'), 3.33 (1H, *m,* H-4'), 3.46 (2H, *m,* H-3' and 5'), 3.86 (1H, *m,* H-6') and 3.92 (1H, *m,* H-6') are attributed to the glucose moiety. The *J* value of the anomeric proton of the sugar moiety in compound **71** indicated that the glucoside linkage had a β-configuration [75]. The two proton signals at δ 3.86 and 3.92 are due to diastereotopic methylene protons of the glucose moiety in the compound. This was observed clearly from its HSQC spectrum. The signal at δ 3.60 (1H, *m,* H-8'') is due to methylene protons on carbon bearing hydroxyl group. Another signals due to methylene protons were observed at δ 2.22 (2H, *m*, H-4''), 2.08 (1H, *m*, H-7), 1.65 (1H, *m*, H-7), 1.31 (1H, *m*, H-6) and 2.35 (1H, *m,* H-6), 1.56 (1H, *m*, H-5''), 1.28 (1H, *m*, H-5''), and 1.32 (2H, *m*, H-7''). The ^{1}H-NMR spectrum also displayed signals due to methine protons at δ 2.70 (1H, *dd*, *J* = 1.6 and 8.4 Hz, H-9), 1.67 (1H, *m*, H-6'') and 3.08 (1H, *m*, H-5). The presence of two methyl signals on quaternary carbons are evident from the appearance of two peaks at δ 1.81 (3H, *s*, H-9''), and 1.56 (3H, *s*, H-10). The signal due to the third methyl group on tertiary carbon was at δ 0.94 (3H, *d*, *J* = 6.4 Hz, H-10'').

The proton decoupled ^{13}C-NMR spectrum of compound **71** (Table 5) with the aid of DEPT-135 showed the presence of 26 well resolved carbon resonances which corresponds to four quaternary, twelve methine, seven methylene and three methyl groups. The most deshielded signal in ^{13}C-NMR at δ 190.1 is typical of an α,β-unsaturated aldehyde carbonyl (C-11). The presence of four olefinic carbon signals are evident at δ 162.0 (C-3), 142.5 (C-3''), 128.2 (C-2'') and 122.6 (C-4). The compound exhibited signal due to an α,β-unsaturated ester carbonyl at δ 167.6 (C-1''). The characteristic carbon signal of an acetal carbinol is observed at δ 95.6. A series of carbon signals at δ 62.4 (C-6'), 70.9 (C-4'), 73.5 (C-2,), 76.9 (C-5') and 76.9 (C-3') along with the anomeric carbon

signal at δ 99-8 (C-1') is evident for the presence of only one sugar moiety in the compound. The signal of methylene carbon bearing an electronegative oxygen atom was observed at δ 59.9 (C-8''). The signals at δ 20.5 (C-10''), 18.9 (C-10) and 11.5 (C-9'') are ascribed to the three methyl groups in the compound. Furthermore, the carbon signals at δ 49.9, 39.7, 38.8, 35.6, 30.2, 29.4, 29.2, and 25.9 are due to C-9, C-7'', C-7, C-5'', C-5, C-6, C-6'', and C-4'', respectively.

The HMBC spectrum indicated that the aldehydic proton signal at δ 9.31 showed correlations with the carbon signals at δ 162.5 (C-3), 30.2 (C-5) and 49.9 (C-9). The olefinic proton signal at δ 7.44 showed HMBC correlations with the carbon signals at δ 190.1 (C-11), 122.8 (C-4), 95.6 (C-1) and 30.2 (C-5). Another important correlation observed was between the acetal carbionol proton signal at δ 5.99 with the carbon signals at δ 162.5 (C-3), 99.5 (C-1'), and 30.2 (C-5). The proton signal at δ 2.70 (H-9) correlates with C-8, C-5 and C-1 in its HMBC spectrum, indicating the connectivity of C-9 with C-8, C-5 and C-1. Additional evidence for the assignment of the proton signal at δ 2.70 to H-9 was deduced from the COSY spectrum, which revealed coupling between H-9 and H-1. The above spectral analysis along with the HMBC correlation of H-7 with C-5 and C-8 support the presence of an iridoid skeleton shown in **69**. Furthermore the connectivity of the glucose moiety to C-1 of the iridoid skeleton was established based on the HMBC correlation observed between the proton signal at δ 4.75 (H-1') with C-1 as presented in **69**.

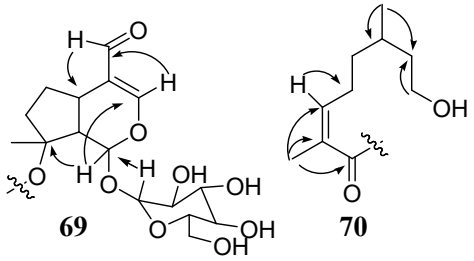

69 **70**

The olefinic proton signal at δ 6.77 correlates with the carbon signal at δ 167.6 which is suggestive of an α,β-unsaturated ester. This is consistent with the IR spectrum of compound **71,** which showed a stretching frequency for an α,β-unsaturated ester at 1690 cm^{-1}. This proton signal also showed HMBC correlation with the carbon signals observed at 25.9 (C-4'') and 11.5 (C-9''). The signal at δ 1.81 (H-9'') showed HMBC correlations with the carbon signals at δ 167.6, 142.5 and 128.2. The proton signal at δ 2.22 (H-4'') correlates with the carbon signals appearing at δ 142.5 (C-3''), 128.2 (C-2'') and 35.6 (C-5''). The doublet at δ 0.94 (H-10'') showed HMBC

connectivity with the carbon resonances appearing at δ 39.7 (C-7''), 35.6 (C-5'') and 29.2 (C-6''). Other HMBC cross peaks observed were between the proton signal at δ 3.60 (H-8'') and the carbon signal at δ 39.7 (C-7''). Based on the above NMR spectral data the presence of fragment structure **70** can be deduced. The observed downfield shift of C-8 (δ 88.6) by 10 ppm in contrast to the signal due to the quaternary carbon bearing hydroxyl group confirms that the hydroxyl group at C-8 is esterified. The ^{1}H- and ^{13}C-NMR spectral data of compound **71** are shown in Table 5.

Table 5: ^{1}H- and ^{13}C-NMR spectral data of compound **71** (CD_3COCD_3, δ in ppm)

Position	^{1}H-NMR (400 MHz)	^{13}C-NMR (100 MHz)	Multiplicity
1	5.99 (1H, *d*, *J* = 2.40 Hz)	95.6	CH
3	7.44 (1H, *s*)	162.0	CH
4	-	122.6	Quaternary
5	3.08 (1H, *m*)	30.2	CH
6	1.31 (1H, *m*) and 2.35 (1H, *m*)	29.4	CH_2
7	2.08 (1H, *m*) and 1.65 (1H, *m*)	38.8	CH_2
8	-	88.6	Quaternary
9	2.70 (1H, *dd*, *J* = 1.60 and 8.40)	49.9	CH_2
10	1.56 (3H, *s*)	18.9	CH_3
11	9.31 (1H, *s*)	190.1	CH
1'	4.74 (1H, *d*, *J* = 8.00)	99.8	CH
2'	3.24 (1H, *m*)	73.5	CH
3'	3.46 (2H, *m*)	76.9	CH
4'	3.33 (1H, *m*)	70.9	CH
5'	3.46 (1H, *m*)	76.9	CH
6'	3.86 (1H, *m*) and 3.92 (1H, *m*)	62.4	CH_2
1''	-	167.6	Quaternary
2''	-	128.2	Quaternary
3''	6.77 (1H, *t*, *J* = 3.70)	142.5	CH
4''	2.22 (2H, *m*)	25.9	CH_2

5''	1.56 (1H, *m*) and 1.28 (1H, *m*)	35.6	CH_2
6''	1.67 (1H, *m*)	29.2	CH
7''	1.32 (2H, *m*)	39.7	CH_2
8''	3.60 (2H, *m*)	59.9	CH_2
9''	1.81 (3H, *s*)	11.5	CH_3
10''	0.94 (3H, *d*, *J* = 6.40)	20.5	CH_3

Assignments made on the basis of COSY, HSQC and HMBC correlations; δ in ppm; Coupling constants are in Hz

Based on the above analysis, the novel structure **71** has been assigned to this compound which was isolated for the first time from the leaves of *C. myricoides*. Determination of the stereochemistry of compound **71** further requires NOE spectral data.

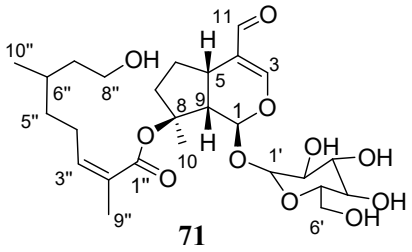

71

Ixoroside (73)

Compound **73** was isolated as a white solid melting at 198-201°C. On TLC, compound **73** was visible as a pink spot at Rf 0.3 (EtOAc:AcOH/4:1) after spraying with vanillin/H_2SO_4. It is optically active with $[\alpha]_{589}^{21}$ = -130.0 (c 0.4, MeOH). The FT-MS demonstrated a molecular ion peak at *m/z* 359.1348 (calcd 359.3484 for $C_{16}H_{23}O_9$) establishing the molecular composition $C_{16}H_{24}O_9$. This finding is supported by the ^{13}C-NMR spectrum, which showed the presence of well resolved resonances of sixteen carbon atoms. An important fragment ion peak was observed in the mass spectrum at *m/z* 197.0819 (molecular formula $C_{10}H_{13}O_4$) corresponding to the aglycone. The UV-Vis spectrum of compound **73** showed absorption maxima at 246 and 313 nm due to $\pi \rightarrow \pi^*$ and $n \rightarrow \pi^*$ transitions, respectively. The IR spectrum of compound **73** exhibited bands due to the stretching of O-H, C-H, C=O (aldehyde carbonyl), C=C, and C-O at 3391, 2922, 1660, 1629, and 1075 cm^{-1}, respectively.

The ^{1}H-NMR spectrum (DMSO-d6) of compound **73** disclosed a signal at δ 9.20 (1H, *s*) attributed to an aldehydic proton. The signal at δ 7.47 (1H, *s*) is characteristic of an olefinic proton (H-3) on a carbon β to a carbonyl. The signals due to an acetal carbinol and an anomeric proton of glucose moiety were observed at δ 5.49 (1H, *d*, *J* = 3.97 Hz) and 4.52 (1H, *d*, *J* = 8.00 Hz), respectively. The coupling constant of the anomeric proton of the glucose established a β configuration [60, 61]. The proton signal of the acetal carbinol (H-1, δ 5.49) showed ^{1}H-^{1}H COSY correlation with H-9 (δ 2.18, 1H, *dd*, *J* = 3.97, 9.00 Hz) indicating that both were situated on adjacent carbon atoms. The signals at δ 3.70 and 3.56 are due to diastereotopic protons (H-6') of the glucose moiety. The presence of one methyl group on a quaternary carbon (δ 78.4) was deduced from the appearance of a singlet signal at δ 1.18 (H-10). The signal due to H-10 showed HMBC correlation with the carbon signal at δ 78.4 establishing the attachment of the methyl group to C-8.

The proton decoupled ^{13}C-NMR spectrum of compound **73** (Table 6) showed a signal at δ 191.2 which is suggestive for the presence of an α,β-unsaturated aldehyde. The olefinic carbon signal at δ 161.7 and 124.5 are assignable to C-3 and C-4 of an iridoid moiety, respectively. The signals arising from the anomeric carbon of the sugar and acetal carbinol were observed at δ 98.7 and 95.1, respectively. The presence of only one sugar moiety is evident from the appearance of only one anomeric carbon signal at δ 98.7 along with series of carbon signals in the oxygenated region at δ 77.7 (C-5'), 77.1 (C-3'), 73.5 (C-2'), 70.5 (C-4') and 61.6 (C-6'). The two methine carbon signals at δ 50.7 and 28.8 are due to C-9 and C-5, respectively. Furthermore, two methylene carbon signals corresponding to C-7 and C-6 were observed at δ 40.7 and 28.7, respectively.

The aldehydic proton signal at δ 9.20 showed HMBC correlation with the signal of the olefinic carbon at δ 124.5. HMBC correlations were also observed between the anomeric proton signal at δ 4.52 (H-1') and the carbon signal of the acetal carbinol at δ 95.1 (C-1) suggesting the attachment of glucose to the iridoid moiety through C-1. Other HMBC correlations observed were between the olefinic proton signal at δ 7.47 (H-3) with the carbon signals at δ 95.1 (C-1) and δ 124.5 (C-4). The proton signal due to the acetal carbinol at δ 5.49 showed HMBC correlations with C-5 (δ 28.8), C-7 (δ 40.7), C-8 (δ 78.4) and C-9 (δ 50.7). The above spectroscopic findings led to the identification of fragment in **72**.

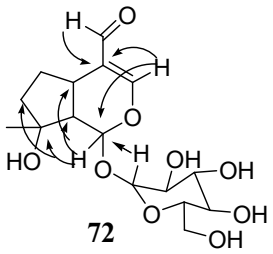

72

The ^{1}H- and ^{13}C-NMR spectral data of compound **73** were compared with the spectral data reported for ixoroside in the literature [61]. A very close agreement was observed between the spectral data as shown in Table 6.

Table 6: ^{1}H- and ^{13}C-NMR spectral data of compound **73** and data reported for ixoroside in the literature [61]

Position	^{1}H- and ^{13}C-NMR data of compound **73** (DMSO)		^{1}H- and ^{13}C-NMR data reported for ixoroside [61]	
	^{1}H-NMR	^{13}C-NMR	^{1}H-NMR	^{13}C-NMR
1	5.49 (1H, *d*, *J* = 3.97)	95.1	5.51 (1H, *br. s*)	96.6
3	7.47 (1H, *s*)	161.7	7.24 (1H, *s*)	163.2
4	-	124.5	-	126.1
5	2.96 (1H, *m*)	28.8	3.07 (*m*)	30.1
6	2.13 (2H, *m*)	28.7	2.19 (1H, *m*) and 1.35 (1H, *m*)	29.7
7	1.55 (1H, *m*) & 2.49 (1H, *m*)	40.7	1.60 (2H, *m*)	41.0
8	-	78.4	-	80.2
9	2.18 (1H, *dd*, *J* = 3.97, 9.00)	50.7	2.15 (1H, *m*)	52.1
10	1.18 (3H, *s*)	22.0	1.20 (3H, *m*)	24.6
11	9.20 (1H, *s*)	191.2	9.10 (1H, *m*)	193.1
1’	4.52 (1H, *d*, *J* = 8.00)	98.7	4.58 (*d*, *J* = 7.80)	100
2’	2.97 (1H, *m*)	73.5		74.7
3’	3.05 (1H, *m*)	77.1		78.0
4’	3.07 (1H, *m*)	70.5		71.7
5’	3.14 (1H, *m*)	77.7		78.5
6’	3.70 (1H, *m*) and 3.56 (1H, *m*)	61.6	3.80 (1H, *m*) and 3.55 (1H, *m*)	62.9

Assignments made on the basis of COSY, HSQC and HMBC correlations; δ in ppm; Coupling constants are in Hz

The evidences presented above suggest that compound **73** is ixoroside.

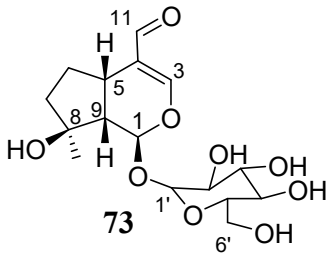

73

Ixoroside (**73**) was previously reported from the aerial parts of *Euphrasia pectinata* [61] and *Nepeta heliotropifolia* [76]

Fatty acids

Repeated column chromatographic fractionations of the acetone extract of the leaves of *C. myricoides* (eluted using hexane:EtOAc (1:1)) afforded a white powder (30 mg) identified to be a mixture of saturated and unsaturated fatty acids using NMR spectroscopic techniques. The fatty acid mixture was dissolved in boiling hexane:$CHCl_3$(1:1) and left standing overnight. The white solid obtained after filtration was analyzed using NMR and FT-MS. The ^{1}H-NMR spectrum displayed a triplet signal at δ 2.33 and a quintet at δ 1.67 corresponding to methylene protons on α- and β-carbon to a carboxyl group, respectively. The intense signal at observed at δ 1.27 is typical of protons on methylenes in an aliphatic compound. This was also evident from the appearance of an intense signal at δ 29.4 in the ^{13}C-NMR spectrum ascribed to methylene groups. The presence of terminal methyl group was evident from the appearance of a triplet signal at δ 0.90 in the ^{1}H-NMR spectrum. The corresponding carbon signal in the ^{13}C-NMR was observed at δ 14.1. The signal observed at δ 178.9 confirmed the presence of a carboxyl group in the compound.

Although the NMR spectral data is in close agreement with stearic acid, the FT-MS spectral analysis showed this white solid is a mixture of saturated fatty acids. This was particularly evident from the appearance of different peaks at different *m/z* corresponding to different saturated fatty acids (Table 6). Hence the FT-MS (Appendix 1) in combination with the NMR data demonstrated the presence of five saturated fatty acids identified as tetracosanoic acid (24:0), behenic acid (22:0), icosanoic acid (20:0), stearic acid (18:0), and palmitic acid (16:0) as depicted in Table 7.

Table 7: Fatty acids from the leaves of *C. myricoides*

m/z	Molecular formula	Name of fatty acid	Chemical Structure	No
367	$C_{24}H_{47}O_2$	Tetracosanoic acid (24:0)	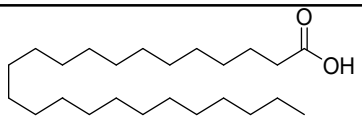	**74**
339	$C_{22}H_{43}O_2$	Behenic acid (22:0)	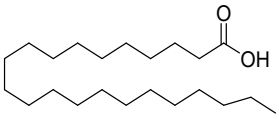	**75**
311	$C_{20}H_{39}O_2$	Icosanoic acid (20:0)	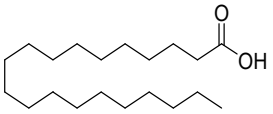	**76**
283	$C_{18}H_{35}O_2$	Stearic acid (18:0)	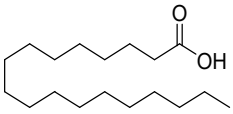	**77**
255	$C_{16}H_{31}O_2$	Palmitic acid (16:0)	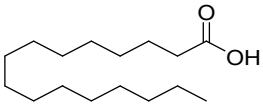	**78**

No: structure number

1.3.2. **Bioassay**

1.3.2.1. Antiplasmodial Assay

The leaves of *C. myricoides* were extracted using ethanol to afford a greenish semisolid material (18%). This was subjected to antiplasmodial test against *Plasmodium berghei* infected mice using Peter's four day suppressive assay [77]. The extract showed significant suppression of parasitaemia (74% at 300 mg/kg) in all mice as compared to the negative control groups which were administered DMSO. The percent parasitaemia of the test groups were found to be 7% at 300 mg/kg while the corresponding value of the negative control group was 26%. On the other hand those mice treated with chloroquine (CQ) as positive control were found free from the parasites on day four.

The ethanol extract was successively fractionated using hexane, EtOAc and methanol to give 0.6%, 1% and 15%, respectively. The ethyl acetate and methanol soluble fractions of the ethanol extract showed significant parasitaemia suppression of about 71 and 75% at 300 mg/kg dose, respectively, as compared to DMSO which was administered as a negative control. The mean parasitaemia of the ethyl acetate and the methanol fraction were found to be 7% and 6%, respectively, in contrast to the negative control group which exhibited parasitaemia of about 35%. The hexane fraction reduced the parasitaemia only to a limited extent (%supp = 23) and hence found inactive. The parasitaemia of the mice administered with the hexane fraction were 24% at 300 mg/kg oral dose, whereas the corresponding figure in the negative control group was 28% indicating that there is no significant difference in parasitaemia between the two groups. This observation indicated that the antimalarial active components of the extract and fractions might reside either in the medium or highly polar fractions of the plant extract.

Fractionation of the active ethyl acetate soluble portion of the ethanol extract of *C. myricoides* successively using hexane, $CHCl_3$ and *n*-butanol afford 3.6, 1 and 0.3 g, respectively. Among the three subfractions obtained from ethyl acetate soluble phase of ethanol extract of *C. myricoides*, the hexane soluble phase induced suppression of parasitaemia by 50% at 100 mg/kg while the corresponding percentage parasitaemia was found to be 14%. However, the chloroform and *n*-buthanol subfractions of the ethyl acetate soluble phase did not show significant reduction in parasitaemia with percent suppression of 8 and 28%, respectively. Column chromatographic fractionations of the active hexane subfraction afforded two compounds, namely, *α*-spinasterol (**63**) and sitosteryl-3-*O*-*ß*-D-glucopyranoside (**64**). The compounds were characterized using physical

and spectroscopic methods. The percent parasitaemia suppression of compound **63** and **64** were 51% and 44% at 40 mg/kg, respectively. Hence the activities displayed by *α*-spinasterol (**63**) and sitosteryl-3-*O*-*ß*-D-glucopyranoside (**64**) lend support to the traditional use of the leaves of *C. myricoides* against malaria.

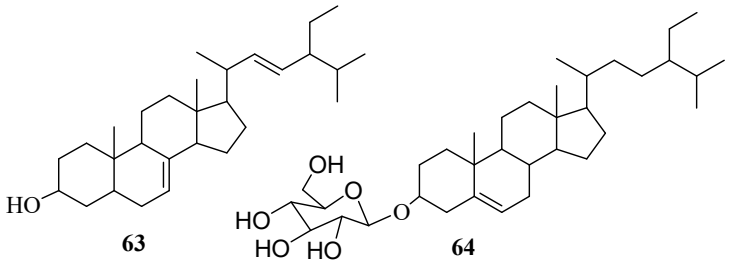

63 **64**

Mean survival time (MST) was an additional parameter used to evaluate the efficacy of antiplasmodial activities of the plant extracts and pure compounds [78]. In this study all tested mice were dead between 7-12 days except those groups of mice treated with CQ. This conclusion is consistent with the literature report [79]. It was also noted that those mice treated with extracts and constituents of the leaves of *C. myricoides* showed prolonged MST in contrast to the negative control groups treated with DMSO. The overall reduction of the pathogenic effect of the parasites on the treated mice is ascribed to the suppressing effect of the tested samples.

1.3.2.2. Radical Scavenging Assay

Antioxidants are substances that possess the ability to protect the body from the damage caused by free radicals [80]. These radicals are the cause of many deleterious diseases including Alzheimer's, Parkinson's, atherosclerosis, hypertension, cancer, diabetes, and aging [81]. Antioxidants exert their activity by suppressing the production of active species, reducing hydroperoxides, sequestering metal ions and terminating chain reactions [82]. In doing so, antioxidants can significantly delay or prevent the oxidation of cellular organelles and thereby prevent some of the damage caused by free radicals [83]. Diverse methods are currently in use to assess the antioxidant potential of plant extracts. An assay based on the use of 2,2-diphenyl-1-picrylhydrazyl radical (DPPH) is among the most popular spectrophotometric methods for determination of the antioxidant capacity of food, beverages and plant extracts [84].

DPPH radical scavenging assay is a simple method for finding antioxidants by measuring absorbance at 517 nm due to the stable 2,2-diphenyl-1-picrylhydrazyl (DPPH) radical [84]. When the radical is scavenged by antioxidants to produce neutral hydrazine, the absorbance at 517 nm is reduced. Moreover the color turns from purple to yellow as soon as the odd electron of DPPH radical becomes paired with hydrogen from a free radical scavenging antioxidant to form the reduced DPPH-H (Scheme 1) [85].

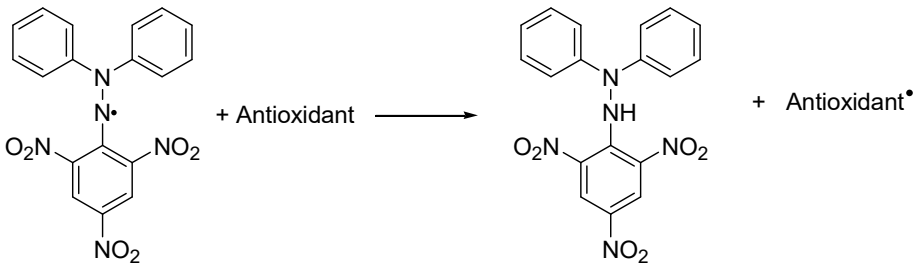

DPPH radical (Purple in color, λ_{max} = 517 nm) DPPH-H (Yellow)

Scheme 1: The structure of DPPH radical and its product (DPPH-H)

The antioxidant activity of the acetone extract and the constituents of the leaves of *C. myricoide*s were measured by bleaching of the purple-colored solution of 1,1-diphenyl-2-picrylhydrazyl radical (DPPH). The DPPH assay indicated that the acetone extract of *C. myricoide* leaves displayed pronounceable free radical scavenging activity with percent inhibition and IC_{50} value of 50% and 10 µg mL^{-1}, respectively (Table 8). Among the constituents isolated from acetone extract of *C. myricoides*, verbascoside had the highest (84%) radical scavenging activity which turned out to be comparable with ascorbic acid (90%), the most popular natural antioxidant used as a positive control. Furthermore, the lower IC_{50} value of verbascoside (Appendix 2) in contrast to the other constituents of the leaves of *C. myricoides* corresponds to the higher antioxidant activity of the compound. This is most likely due to its strong ability of donating an electron and phenolic hydrogen to DPPH radical, which was visualized by immediate discoloration of the purple DPPH solution to yellow. It also seems that the *trans*-caffeoyl moiety is an important part for enhancing the antioxidant activities of the compound. On the other hand, the other compounds showed antioxidant activities even lower than the crude extract suggesting that the antioxidant potential of the leaves of *C. myricoides* is ascribed to verbascoside.

Table 8: DPPH radical scavenging activities of acetone extract and constituents of *C. myricoides*

Tested samples	DPPH radical scavenging assay	
	% inhibition at 10 µg/mL	IC_{50} values
Acetone extract	50	10
α-spinasterol	6	124
Sitosterol-O-*β*-D-glucoside	36	16
Ixoroside	13	65
Compound **71**	15	50
Verbascoside	84	0.69
Ascorbic acid	90	0.45

Ascorbic acid was used as positive control

1.4. Conclusion

The extracts and two compounds isolated from the leaves of *C. myricoides* showed significant suppression of plasmodium parasites in infected mice. The results further corroborate the traditional use of this plant to treat malaria and indicate the potential the plant has for its use as herbal antimalarial remedy. Column chromatographic fractionation of the acetone extract of the leaves of *C. myricoides* afforded five compounds: *α*-spinasterol (**63**), sitosterol-3-O-*β*-D-glucoside (**64**), verbascoside (**12**), ixoroside (**73**) and compound **71**. Compound **71** has not been reported in the literature. The leaves of *C. myricoides* were found to be rich in fatty acids. Verbascoside isolated from the leaves of *C. myricoides* displayed strong radical scavenging activity comparable to ascorbic acid.

1.5. Experimental

General

Solvents used were obtained from Riedel-de-Haen, CARLO ERBA, Fisher Chemicals, and Neolab. Reagents used were of analytical grade. Chloroquine (CQ) and ascorbic acid were products of ETHIOPHARM, Ethiopia and Sigma-Aldrich, respectively. A special reagent known as Diaion HP-20 (SUPELCO, 595 North Harrison Road, Bellefonte, PA, USA) was used to trap organic compounds while letting very polar compounds such as simple sugars to elute on washing the column with water. The organic compounds were then eluted by washing the column with organic solvents.

Melting point was determined in capillary tube with a digital electrothermal melting point apparatus. HPTLC plates, Merck 60 F_{254} 20x20 cm, 0.2 mm thickness, were obtained from Sigma (Switzerland). Analytical TLC was run on a 0.25 mm thick layer of silica gel GF254 (Merck) on aluminum plate. Spots were detected by observation under UV light (254 nm). Spraying agents used were vanillin, fast blue B salt, and anisaldehyde. Column chromatography was performed using silica gel (230-400 mesh) Merck. Samples were applied on column by either adsorbing on silica gel or dissolving in appropriate solvent. Solvent was removed using rotavapor BUCHI, RE 121.

Optical rotations were measured using Autopol®IV Automatic polarimeter. The UV-Vis spectral measurements were done using UV-Vis on T 60 U spectrophotometer (PG instruments, UK) equipped with deuterium and tungsten lamps. NMR spectra were recorded using Bruker Avance 400 spectrometer operating at 400 MHz. The ^{1}H-^{1}H correlations were determined by COSY spectrum. The one bond ^{1}H-^{13}C chemical shift correlations were established by the HSQC

experiment, while long range ^{1}H-^{13}C correlations were determined by using HMBC experiment. The IR spectra of compounds were recorded using a Perkin-Elmer BX Spectrometer (400-4000 cm^{-1}) as KBr pellets.

FT-MS: The high resolution positive and negative ion electrospray (ESI) mass spectra were obtained from a Bruker Apex III Fourier transform ion cyclotron resonance (FTICR) mass spectrometer (Bruker Daltonics, Billerica, USA) equipped with an Infinity™ cell, a 7.0 Tesla superconducting magnet (Bruker, Karlsruhe, Germany), an RF-only hexapole ion guide and an external electrospray ion source. Nitrogen was used as drying gas at 150°C. The sample solutions were introduced continuously via a syringe pump with a flow rate of 120 µL h^{-1}. All data were acquired with 512 k data points and zero filled to 2048 k by averaging 32 scans. The data were evaluated by the Bruker XMASS 7.0.8 software.

UHPLC/ESI-MS

The positive and negative ion ESI mass spectra of the samples and the collision-induced dissociation (CID) mass spectra were obtained from a TSQ Quantum Ultra AM system equipped with a hot ESI source (electrospray voltage 3.0 kV, sheath gas: nitrogen; vaporizer temperature: 50°C; capillary temperature: 250°C). The MS system is coupled with an Accela UHPLC system (Thermofisher Scientific), equipped with a Syncronis-C18 column (1.7 µm, 50 x 1 mm, Thermo Scientific). For the UHPLC a gradient system was used starting from H_2O:CH_3CN 90:10 (each of them containing 0.2% formic acid) to 100% CH_3CN within 30 min and then hold on 5% for further 5 min; flow rate 150 µL min^{-1}; injection volume 3 µL.

FT-MS and **UHPLC-MS** measurements were done at the Leibniz-Institute for Plant Biochemistry, Weinberg 3, 06120 Halle (Saale), Germany.

GC-MS analysis were performed using Agilent Technologies 7820A gas chromatograph system equipped with HP-5 capillary column (30mx0.25; coating thickness, 0.25µm) and Agilent technologies 5977 E mass spectroscopy ion trap detector. Analytical conditions were as follows: Injector and transfer line temperature are 220 and 260°C, respectively; oven temperature programmed from 60°C to 240°C at 3°C/min; carrier gas, helium at 1 mL/min; injection 5 µL; split

ratio, 1:30. Identification of the constituents were based on search through mass\hunter\library\NIST11.L and mass\hunter\library\W9N11.L

Plant Material

Leaves of *C. myricoides* were collected from Lideta Mariam, around Russia Embassy, to the East direction of Addis Ababa in September 2011. Identification and authentication of the plant specimen was done at the National Herbarium of Addis Ababa University by Mr. Melaku Wondafrash and voucher specimen was deposited as voucher number (GG04/2011) in the Herbarium.

Extraction and Isolation of Compounds from the Leaves of *C. myricoides*

To the ground leaves of *C. myricoides* (100 g) was added acetone (600 mL), placed on shaker for 6 h with a mechanical shaker, filtered and concentrated to afford 5 g (5%) black jelly solid. This was adsorbed and subjected to silica gel column chromatography using CH_2Cl_2 for packing. Gradient elution was done using CH_2Cl_2, CH_2Cl_2:EtOAc, and EtOAc:MeOH to furnish twenty eight fractions as shown in Table 9.

Table 9: Column chromatographic fractionation of the acetone extract of the leaves of *C. myricoides*

Fractions	Eluent (ratio)	Volume of eluent in mL	Amount in mg
Fr1	CH_2Cl_2	250	510
Fr 2	CH_2Cl_2:EtOAc (9:1)	20	50
Fr 3	CH_2Cl_2:EtOAc (9:1)	100	200
Fr 4	CH_2Cl_2:EtOAc (9:1)	50	250
Fr 5	CH_2Cl_2:EtOAc (4:1)	50	100
Fr 6	CH_2Cl_2:EtOAc (4:1)	20	30
Fr 7	CH_2Cl_2:EtOAc (4:1)	20	40
Fr8	CH_2Cl_2:EtOAc (1:1)	20	20
Fr 9	CH_2Cl_2:EtOAc (1:1)	25	60

Fr 10	CH_2Cl_2:EtOAc (1:1)	20	150
Fr 11	CH_2Cl_2:EtOAc (1:1)	100	150
Fr 12	CH_2Cl_2:EtOAc (1:1)	20	50

Table 9 continued

Fractions	Eluent (ratio)	Volume of eluent in mL	Amount in mg
Fr 13	CH_2Cl_2:EtOAc (1:1)	20	50
Fr 14	CH_2Cl_2:EtOAc (1:1)	40	80
Fr 15	CH_2Cl_2:EtOAc (2:3)	50	60
Fr 16	CH_2Cl_2:EtOAc (2:3)	25	60
Fr 17	CH_2Cl_2:EtOAc (2:3)	10	10
Fr 18	EtOAc	120	65
Fr 19	EtOAc:MeOH (9:1)	10	10
Fr 20	EtOAc:MeOH (9:1)	50	50
Fr 21	EtOAc:MeOH (9:1)	50	250
Fr 22	EtOAc:MeOH (9:1)	50	250
Fr 23	EtOAc:MeOH (4:1)	40	40
Fr 24	EtOAc:MeOH (4:1)	30	45
Fr 25	EtOAc:MeOH (4:1)	30	10
Fr 26	EtOAc:MeOH (4:1)	80	1000
Fr 27	EtOAc:MeOH (4:1)	40	150
Fr 28	EtOAc:MeOH (1:1)	20	10

Fraction 3 (180 mg) was adsorbed and chromatographed over silica gel (15 g) with CH_2Cl_2 as eluent to afford five subfractions (30 mL, 30 mg, Fr1; 20 mL, 40 mg, **Fraction 2**; 50 mL, 40 mg, Fr3; 20 mL, 30 mg, Fr4; and 50 mL, 10 mg, Fr5). **Fraction 2** was identified as ***α*-spinasterol** (40 mg).

Fraction 11 (150 mg) was dissolved in $CHCl_3$ and subjected to silica gel (15 g) column chromatography. Four fractions were collected with the first eluted using hexane (20 mL, 6 mg, Fr1). The next three fractions were collected using hexane:$CHCl_3$ (4:1, 5 mL, 50 mg, **Fraction 2**; 1:1, 20 mL, 20 mg, Fr3; 1:1, 10 mL, 20 mg, Fr4). On NMR analysis, **Fraction 2** was identified to be a mixture of saturated and unsaturated fatty acids. The fatty acid mixture was dissolved in hot hexane:$CHCl_3$ (1:1). The white powder (30 mg) produced on standing overnight was filtered, air dried and analyzed using FT-MS to furnish saturated fatty acids identified to be tetracosanoic acid (24:0), behenic acid (22:0), icosanoic acid (20:0), stearic acid (18:0), and palmitic acid (16:0)

Fraction 17 (10 mg) and **Fraction 21** (250 mg) were identified as **sitosterol-O-*β*-D-glucoside** and **verbascoside** (**64**) , respectively.

Fraction 26 (1 g) was adsorbed and chromatographed over silica gel (50 g) using $CHCl_3$:MeOH as eluent to afford six subfractions. Fr1 (100 mL, 20 mg) and Fr2 (55 mL, 150 mg) were collected using $CHCl_3$ and $CHCl_3$:MeOH (9:1), respectively. The **3rd fraction** was eluted using $CHCl_3$:MeOH (4:1, 28 mL, 50 mg). Fr4 (30 mL, 68 mg) and **Fraction 5** (50 mL, 80 mg) were collected using $CHCl_3$:MeOH (1:1). Column elution ended using MeOH (1:4, 50 mL, 150 mg, Fr6). The TLC profile of the **3rd fraction** (50 mg) was promising and hence subjected to Sephadex LH20 (eluent $CHCl_3$:MeOH (1:1)) to afford two fractions (5 mL each). The second fraction was concentrated to give **compound 71 (20 mg)**. **Fraction 5** (80 mg) was rechromatographed over silica gel (15 g) column chromatography. The first three fractions eluted using $CHCl_3$:acetone (4:1, 50 mL, 33 mg) was rechromatographed over silica gel to afford three subfractions. The first two fractions were eluted using 100%EtOAc. The third fraction eluted using EtOAc:MeOH (4:1, 6 mL, 10 mg) is identified as **ixoroside (73)**. The extraction and isolation procedure is depicted in Scheme 2.

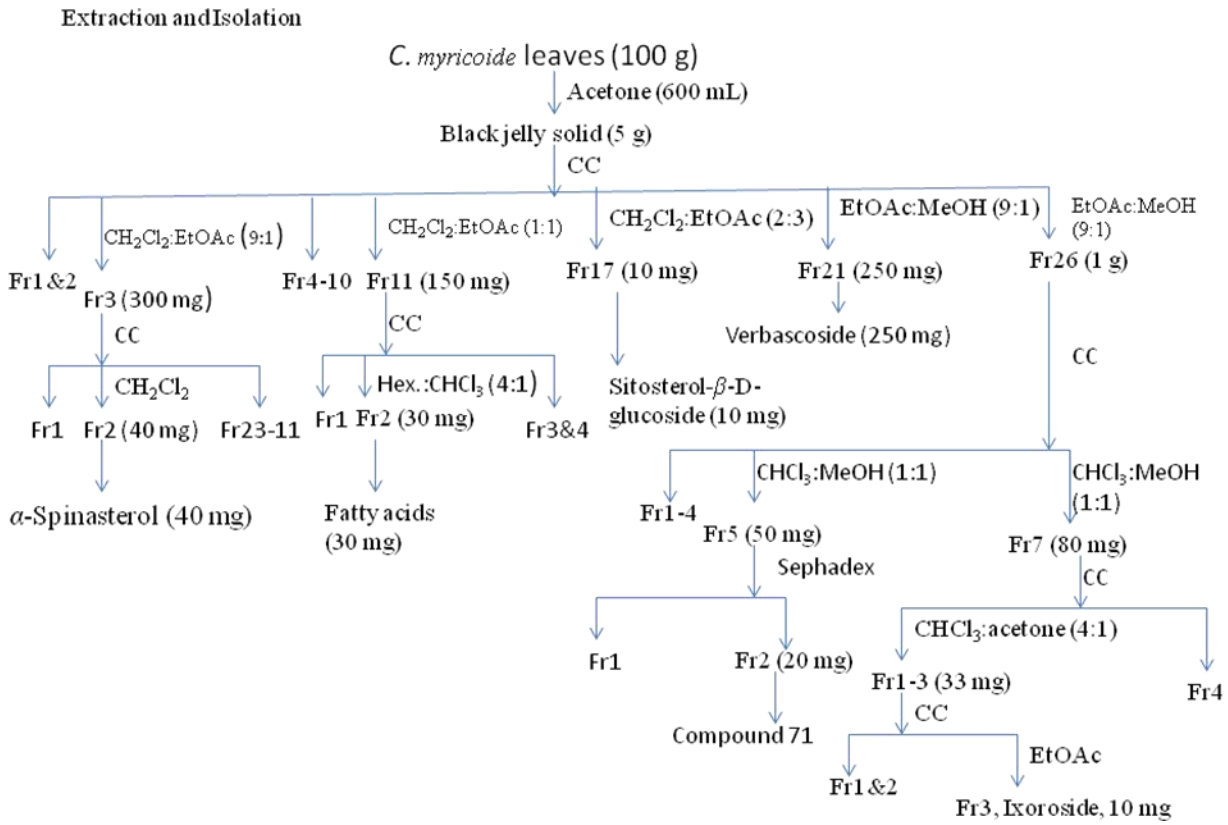

Scheme 2: Flow sheet diagram showing extraction and isolation of compounds from the leaves of *C. myricoides*

Experimental Animals: Male Swiss albino mice weighing 25-35 g, 6-8 weeks of age were obtained from Ethiopian Public Health Institute, Addis Ababa. The mice were housed in standard cages and acclimatized for duration of 10 days before using them for experiment. They were housed in plastic cages with saw dust as beddings and given a diet and tap water *ad libitum*.

Malaria Parasite and Inoculation: For *in vivo* antiplasmodial assays extracts of the plant and the mice infective CQ sensitive strain of *P. berghei* were used. The parasite was maintained by serial passage of blood obtained from infected mouse to non-infected ones on weekly basis. Each mouse used in the experiment was infected intraperitoneally with a 0.2 mL of infected blood containing about 1 x 10^6-10^7 *P. berghei* parasitized erythrocytes [86]. For each experiment about 1 mL *P. berghei* infected blood sample was used by dissecting of the donor mice with rising parasitaemia of about 25-35% in such a way that 1 mL blood contains 5 x 10^6-10^7 *P. berghei*-parasitized

erythrocytes. This was prepared by determining the percentage of parasitaemia and diluting 1 mL of blood in 4 mL of physiological saline solution of 0.9% NaCl.

Evaluating the Antiplasmodial Activity of the Extracts and Pure Compounds: The antiplasmodial activities of the constituents were evaluated using Peter's four-day suppressive method [77]. Each mouse used in the study was infected interaperitonially on D_0. The infected mice were randomly divided into two experimental groups (each group treated with plant extract) and two control groups (group treated with CQ as positive control and 20% of DMSO as a negative control). Five mice per cage as a group were assigned. Each test extract and pure compounds were prepared in two doses, CQ at 25 mg/kg in a volume of 0.2 mL/mouse and vehicles (20% DMSO) at 0.2 mL/mouse. Each extract was administered as a single dose per day. All the extracts, the drug (CQ) and DMSO were given through intragastric route by using standard intragastric tube to ensure safe ingestion of the extracts into the mouse. Treatment started after 3 hours of infection on D_0 and continued daily for the consecutive four days. On the fifth day (D_4) blood samples were collected from tail snip of each mouse. Thin smears were prepared, the smear first fix with methanol for 3-5 min and stained with 10% Geimsa solution at a p^H of 7.2 for 20 min. Then, five uniform fields from tailed region of each stained slide was examined under the microscope with an oil immersion objective of 100X magnifying lens power to evaluate the percent suppression of each extract with respect to the negative control group. The obtained parasitaemia counts were not the same from one field to another in the same slide, in different slides obtained from a mouse and in different slides obtained from different mice within one group. The average was taken to determine the percent parasitaemia. Then percent parasitaemia in each field and percent suppression for a group was calculated as follows [87].

$$\%Para = \frac{\text{Total number of PRBCs}}{\text{Total number of RBCs}} X100\%$$

Where: PRBCs = Parasitized Red Bood Cells
RBCs = Red Blood Cells

Percentage suppression for a group was calculated as:

$$\frac{\text{Parasitaemia in the negative control - Parasitaemia in treated groups}}{\text{Parasitaemia in the negative control}} X\ 100\%$$

Extraction and Bioassay Directed Fractionation

The ground leaves of *C. myricoides* (1 kg) was extracted using ethanol (6 L) by shaking for 12 h, filtered and concentrated under reduced pressure to give 18% dark semi-solid crude extract. The ethanol extract was successively fractionated using n-hexane (300 mL) followed by ethyl acetate (300 mL) to afford 6 g hexane and 11 g EtOAc soluble fractions, respectively. The marc remained was 158 g. The active EtOAc soluble phase (5 g) was dissolved in methanol (30 mL), diluted to 50% aqueous methanol solution and partitioned successively with n-hexane (3x20 mL), $CHCl_3$ (3x20 mL) and finally with *n*-butanol (3x20 mL) to afford their corresponding subfractions. Each subfractions were concentrated using rotary evaporator to yield 3.6, 1 and 0.3 g of hexane, $CHCl_3$ and *n*-butanol subfractions, respectively.

The hexane soluble fraction of the EtOAc phase which was found active was chromatographed over silica gel (70 g) using hexane for packing. The column was eluted using hexane:EtOAc and then EtOAc:MeOH of increasing polarities to afford twelve (12) combined subfractions as given in Table 10.

Table 10: Column chromatographic fractionation of the hexane fraction of the EtOAc soluble phase of the ethanol extract of the leaves of *C. myricoides*

Fractions	Eluent (ratio)	Volume of eluent in mL	Amount in mg
Fr1-5	hexane	150	290
Fr 6-7	hexane	60	90
Fr 8-10	hexane:EtOAc (9:1)	90	100
Fr 11-12	hexane:EtOAc (4:1)	60	98
Fr 13-18	hexane:EtOAc (7:3)	150	273
Fr 19-22	hexane:EtOAc (7:3)	60	113
Fr 23-25	hexane:EtOAc (1:1)	90	80
Fr26-29	hexane:EtOAc (3:7)	80	170
Fr 30-35	hexane:EtOAc (1:4)	90	76
Fr 36-37	EtOAc	80	80
Fr 38-41	EtOAc	80	890
Fr 42	EtOAc:MeOH (4:1)	90	130

Fraction 13-18 was recrystalized from isopropyl alcohol to give 112 mg white crystals identified as *α*-spinasterol (**63**). Likewise the other fraction eluted using EtOAc (**Fraction 30-35**, 80 mg) was applied on PTLC developed using hexane:EtOAc (1:4) as a mobile phase to afford two bands. The first band was scratched with a spatula, transferred to the flask and extracted with EtOAc. Silica gel was filtered and the filtrate was concentrated to afford 20 mg white solid identified as sitosterol-3-*O*-*ß*-D-glucopyranoside (**64**). **Fraction 38-41** was rechromatographed over silica gel using EtOAc as eluent to afford six subfractions (5 mL each). Upon TLC examination, the fourth subfraction (20 mg) was found similar with **64**. The extraction and isolation procedure of the antiplasmodial principles of the leaves of *C. myricoides* is displayed in Scheme 3

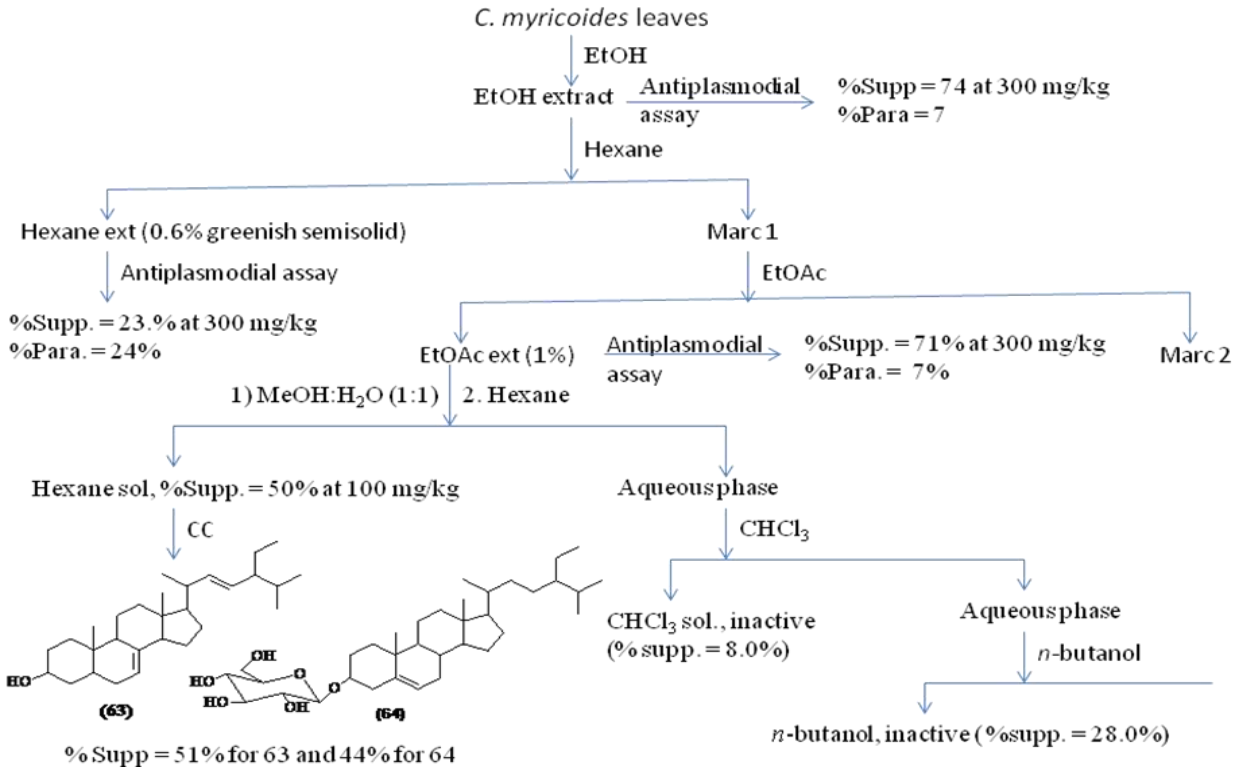

Scheme 3: Flow sheet diagram showing bioassay guided fractionation of the leaves of *C. myricoides*

DPPH assay

The radical scavenging activities of the extracts and constituents of the leaves of *C. myricoide*s were done according to [67]. Serial dilutions were carried out with the stock solutions (1 mg mL^{-1}) of the plant extract and its constituents to obtain concentrations of 50, 25, 12.5, and 6.5 µg mL^{-1}.

All of the solutions were prepared using methanol as solvent. Diluted solutions (1 mL each) were mixed with 4 mL of 2,2-diphenyl-1-picryl hydrazyl (DPPH) in a brown vials. After an incubation period of 30 min at 37°C in an oven, the absorbance was determined against a blank at 517 nm [88]. The percent of DPPH discoloration of the samples was calculated according to the formula [89]:

$$(\%)\ \text{inhibition} = \frac{(\text{A control} - \text{A sample})}{\text{A control}} \times 100$$

Where A control was the absorbance of the DPPH solution and A sample was the absorbance in the presence of plant extract [89]. The IC_{50} value, defined as the concentration of a substrate that causes 50% loss of the DPPH activity, was calculated by linear regression plots of the percentage inhibition against the concentration of the tested samples. Samples were analyzed in triplicate. Ascorbic acid was used as positive control.

***α*-Spinasterol (63):** White solid; mp 144°C-145°C; TLC: Rf 0.60, hexane:EtOAc (3:2) as a mobile phase and vanillin as spraying agent; MS: *m/z* 412, molecular formula $C_{29}H_{48}O$; IR υ_{cm-1}: 3369.0 (O-H), 2940.0 (C-H), 1609.0 (C=C) and 1062 (C-O); UV λmax ($CHCl_3$) nm: 227; ^{1}H-NMR (400 MHz, DMSO-d6): δ_H 0.60 (3H, *s*), *δ* 0.80-0.860 (9H, *m*), 0.87 (3H, *d*, *J* = 6.4 Hz), 1.13 (3H, *d*, *J* = 6.8 Hz), 2.30 to 1.00 (25H), 3.65 (1H, *m*), 5.04 (H-23, *dd*, *J* = 8.8 and 15.2 Hz), 5.17 (H-7, *m*), 5.18 (H-22, *dd*, *J* = 8.4 and 15.2 Hz); ^{13}C-NMR (100 MHz, DMSO-d6): δ_C 37.1 (C-1), 31.5 (C-2), 71.0 (C-3), 38.0 (C-4), 40.3 (C-5), 29.6 (C-6), 117.4 (C-7), 139.5 (C-8), 49.4 (C-9), 34.2 (C-10), 21.5 (C-11), 39.4 (C-12), 43.3 (C-13), 55.1 (C-14), 23.0 (C-15), 28.5 (C-16), 55.9 (C-17), 12.0 (C-18), 40.8 (C-20), 21.3 (C-21), 138.2 (C-22), 129.4 (C-23), 51.2 (C-24), 31.8 (C-25), 21.0 (C-26), 19.0 (C-27), 25.4 (C-28), 12.2 (C-29)

Sitosterol-3-O-*β*-D-glucoside (64): White powder; $[\alpha]_{589}^{21}$ = -25.0 (c 0.4, MeOH); IR υ_{cm-1}: 3429 (O-H), 2918 (C-H), 1600 (C=C), and 1063 (C-O); FT-MS: *m/z* 599.4293 (calcd 599.8100 for $C_{35}H_{60}O_6Na$) and molecular formula $C_{35}H_{60}O_6$; ^{1}H-NMR (400 MHz, DMSO-d6): δ_H 0.65 (3H, *s*),

0.95 (3H, *s*), 0.90 (3H, *t*, *J* = 6.40 Hz), 0.93 (3H, *d*, *J* = 3.20 Hz), 0.80 (6H, *m*), 4.47 (1H, *m,* H-3), 5.30 (1H, *d*, *J* = 3.20 Hz, H-6), 4.21 (1H, *d, J* = 8.00 Hz, H-1'), 3.63 (1H, *m,* H-6') and 3.45 (1H, *m*, H-6'); ^{13}C-NMR (100 MHz, DMSO-d6): δ_C 39.7 (C-1), 34.0 (C-2), 77.2 (C-3), 39.4 (C-4), 140.9 (C-5), 121.3 (C-6), 30.0 (C-7), 28.2 (C-8), 45.6 (C-9), 37.3 (C-10), 19.5 (C-11), 31.9 (C-12), 42.3 (C-13), 55.9 (C-14), 24.3 (C-15), 23.0 (C-16), 56.6 (C-17), 19.1 (C-18), 12.5 (C-19), 29.2 (C-20), 12.3 (C-21), 36.6 (C-22), 28.3 (C-23), 50.0 (C-24), 31.8 (C-25), 21.0 (C-26), 20.5 (C-27), 26.9 (C-28), 19.4 (C-29), 101.3 (C-1'), 77.3 (C-2'), 73.9 (C-3'), 70.5 (C-4'), 77.4 (C-5'), 61.5 (C-6')

Verbascoside (12): White solid; mp 147-148^{o}C (Lit. [69] 145-148^{o}C); $[\alpha]_{589}^{21}$ = -5.0 (c 0.4, MeOH); TLC: Rf 0.6 (eluent EtOAc:AcOH, 4:1) and vanillin/H_2SO_4 as spraying agent; UV λmax (MeOH) nm: 290, 329; IR υ_{cm-1}: 3398 (O-H), 1698 (*α,β*-unsaturated ester carbonyl); FT-MS: *m/z* 623.1981 (calcd 623.5794 for $C_{29}H_{35}O_{15}$) and molecular formula $C_{29}H_{36}O_{15}$; ^{1}H-NMR (400 MHz, DMSO-d6): δ_H 7.02 (1H, *d*, *J* = 1.69 Hz, H-2), 6.75 (1H, *d*, *J* = 8.14 Hz, H-5), 6.98 (1H, *dd*, *J* = 8.14, and 1.69 Hz, H-6), 7.45 (1H, *d*, *J* = 15.7 Hz, H-7), 6.20 (1H, *d*, *J* = 15.7 Hz, H-8), 6.62 (1H, *bro s,* H-2'), 6.63 (1H, *d*, *J* = 8.14 Hz, H-5'), 6.49 (1H, *dd*, *J* = 8.14 and 1.48 Hz, H-6'), 2.70 (2H, *m*, H-7'), 3.87 (1H, *m*) and 3.68 (1H, *m,* H-8'), 4.35 (1H, *d*, *J* = 7.82 Hz, H1''), 3.20 (1H, *m,* H-2''), 3.69 (1H, *m,* H-3''), 4.70 (1H, *d*, *J* = 9.60 Hz, H-4''), 3.48 (1H, *m*, 5''), 3.32/3.39 (2H, *m*, H-6''), 5.01 (1H, *d*, *J* = 1.30 Hz, H-1'''), 3.68 (1H, *m,* H-2'''), 3.28 (1H, *m,* H-4'''), 3.10 (1H, *m,* H-5'''), 0.94 (3H, *d*, *J* = 6.24 Hz, H-6'''); ^{13}C-NMR (100 MHz, DMSO-d6): δ_C 125.9 (C-1), 115.0 (C-2), 146.0 (C-3), 148.9 (C-4), 115.8 (C-5), 121.9 (C-6), 146.0 (C-7), 114.1 (C-8), 166.2 (C-9), 129.5 (C-1'), 116.7 (C-2'), 145.4 (C-3'), 143.9 (C-4'), 116.2 (C-5'), 119.9 (C-6'), 35.4 (C-7'), 70.7 (C-8'), 102.7 (C-1''), 74.9 (C-2''), 79.5 (C-3''), 69.5 (C-4''), 74.9 (C-5''), 61.1 (C-6''), 101.6 (C-1'''), 70.9 (C-2'''), 70.8 (C-3'''), 72.2 (C-4''), 69.2 (C-5'''), 18.6 (C-6''')

Compound 71: Solid; mp 178-180^{o}C; $[\alpha]_{589}^{21}$ = -147.5 (c 0.4, MeOH); TLC: Rf 0.40, EtOAc:AcOH (4:1) as eluent and vanillin/H_2SO_4 as spraying agent; UV λmax (MeOH) nm: 246 and 313; IR $\upsilon_{cm^{-1}}$: 3369 (OH), 1690 (ester carbonyl), 1674 (aldehyde carbonyl), 1631 (C=C), 1076 (C-O); ESI-FT-MS: *m/z* 551.2463 (calcd 551.7349 for $C_{26}H_{40}O_{11}Na$) and molecular formula $C_{26}H_{40}O_{11}$; ^{1}H-NMR (400 MHz, acetone-d6): δ_H 5.99 (1H, *d*, *J* = 2.40 Hz, H-1), 7.44 (1H, *s,* H-3), 3.08 (1H, *m*, H-5), 1.31 (1H, *m*, H-6) and 2.35 (1H, *m,* H-6), 2.08 (1H, *m*, H-7), 1.65 (1H, *m*, H-7), 2.70 (1H, *dd*, *J* = 1.60 and 8.40 Hz, H-9), 1.56 (3H, *s,* H-10), 9.31 (1H, *s,* H-11), 4.74 (1H, *d*, *J* = 8.00 Hz, H-1'),

3.24 (1H, *m,* H-2'), 3.46 (2H, *m,* H-3'), 3.33 (1H, *m,* H-4'), 3.46 (1H, *m,* H-5'), 3.86 (1H, *m,* H-6'), 3.92 (1H, *m,* H-6'), 6.77 (1H, *t, J* = 3.70 Hz, H-3''), 2.22 (2H, *m,* H-4''), 1.56 (1H, *m,* H-5''), 1.28 (1H, *m,* H-5''), 1.67 (1H, *m,* H-6''), 1.32 (2H, *m,* H-7''), 3.60 (1H, *m,* H-8''), 1.81 (3H, *s,* C-9''), and 0.94 (3H, *d*, *J* = 6.40 Hz, H-10''); ^{13}C-NMR (100 MHz, acetone-d6): δ_C 95.6 (C-1), 162.0 (C-3), 122.6 (C-4), 30.2 (C-5), 29.4 (C-6), 38.8 (C-7), 88.6 (C-8), 49.9 (C-9), 18.9 (C-10), 190.1 (C-11), 99.8 (C-1'), 73.5 (C-2'), 76.9 (C-3'), 70.9 (C-4'), 76.9 (C-5'), 62.4 (C-6'), 167.6 (C-1''), 128.2 (C-2''), 142.5 (C-3''), 25.9 (C-4''), 35.6 (C-5''), 29.2 (C-6''), 39.7 (C-7''), 59.9 (C-8''), 11.5 (C-9''), 20.5 (C-10'')

Ixoroside (73): White solid; mp 198-201^{o}C; TLC: Rf 0.3, EtOAc:AcOH (4:1) as eluent and vanillin/H_2SO_4 as spraying agent; $[\alpha]_{589}^{21}$ = -130.0 (c 0.4, MeOH); FT-MS: *m/z* 359.1348 (calcd 359.3484 for $C_{16}H_{23}O_9$) and molecular formula $C_{16}H_{24}O_9$; UV λmax (MeOH) nm: 246, 313; IR $\upsilon_{cm^{-1}}$: 3391 (O-H), 2922 (aldehydic C-H), 1660 (aldehydic carbonyl), 1629 (C=C) and 1075 (C-O); ^{1}H-NMR (400 MHz, DMSO-d6): δ_H 5.49 (1H, *d*, *J* = 3.97 Hz, H-1), 7.47 (1H, *s,* H-3), 2.96 (1H, m, H-5), 2.13 (2H, *m,* H-6), 1.55 (2H, *m,* H-7), 2.18 (1H, *dd*, *J* = 3.97, 9.00 Hz*,* H-9), 1.18 (3H, *s,* H-10), 9.20 (1H, *s,* H-11), 4.52 (1H, *d*, *J* = 8.00 Hz, H-1''), 3.70 (1H, m, H-6') and 3.56 (1H, m, H-6'); ^{13}C-NMR (100 MHz, DMSO-d6): δ_C 95.1 (C-1), 161.7 (C-3), 124.5 (C-4), 28.8 (C-5), 28.7 (C-6), 40.7 (C-7), 78.4 (C-8), 50.7 (C-9), 22.0 (C-10), 191.2 (C-11), 98.7 (C-1,), 73.5 (C-2'), 77.1 (C-3'), 70.5 (C-4'), 77.7 (C-5'), 61.6 (C-6')

Part 2

Bioassay Directed Chemical Study of Antimalarial Substances from *Dodonaea angustifolia*

2.1. Introduction

2.1.1. The Family Sapindaceae and the Genus *Dodonaea*

The Sapindaceae (soapberry family) is a family of flowering plants with about 150 genera and 2000 species occurring from temperate to tropical regions of the world [90]. Plants of this family are either shrubs or trees which are widely used for the treatment of various ailments [91]. Some species are reported as medication to reduce fever and stimulate metabolism. They are also reported to exhibit antioxidant, analgesic, antiviral, anti-inflammatory, antiulcer and antibacterial activities [92, 93]. About fourteen genera belonging to the family Sapindaceae (*Dodonaea*, Paullinia, Pappea, Filicium, Erythrophsa, Zanha, Cardiospermum, Allophylus, Deinbollia, Lepisanthes, Bottegoa, Lecanidiscus, Haplocoelum and Blighia) and nineteen species are registered in the Flora of Ethiopia [90]. *Dodonaea* is the largest genus containing 70 species most of which are restricted to continental Australia, one in New Guinea (*Dodonaea polyandra*), one species endemic to Madagascar (*Dodonaea madagascariensis*) and one species (*D. angustifolia*) widely distributed in all continents [94, 95].

2.1.1.1. *Dodonaea angustifolia (*synonym *Dodonaea viscosa)*

D. angustifolia, hop-bush in English and *kitkita* in Amharic (Ethiopia), is mainly found in Australia, Africa, Asia and South America [96, 97]. The greatest center of diversity appears to be the Southeast Asian region. It occurs naturally in different African countries including Ethiopia, Kenya, Somalia, Senegal, Nigeria, Mozambique, Madagascar, Democratic Republic of Congo, and South Africa. *D. angustifolia* is cultivated in Ghana, Nigeria and Cameroon. It is a hedge plant in East Africa which reproduces itself from seed very freely and grows on dry rocky slopes between 1500 and 2100 m throughout Ethiopia [98]. *D. angustifolia* is a dioecious or monoecious multi stemmed shrub or single-stemmed small tree up to 7 m tall [99]. All parts of the plant are hairless

and resinous when young. Leaves are simple and petiolate (1-5 mm long). The hard wood is used for firewood, as fencing material and also for making hut roofs in rural areas.

2.1.1.2. Brief Review on Biological Activities of the Genus *Dodonaea*

Some species in the genus *Dodonaea* are used for the treatment of a wide spectrum of diseases. The aerial parts of *D. angustifolia* are used in folk medicine against fevers, swellings and colds in Latin America, China, Africa, and India [100, 101]. The powdered leave juice is used for the treatment of trachoma and to expel roundworms [93]. Various parts of this plant are used in the traditional systems of medicine for contraceptive effect [102]. In the Tigray region of Ethiopia, the crushed fruit mixed with honey is eaten as a remedy against malaria [103]. The stems are used as fumigants to treat rheumatism [93].

The ethanol, methanol, ethyl acetate, chloroform and aqueous extracts of the leaves were found to be active against fungi [104, 105]. The leaf essential oil and extracts showed strong inhibition against bacterial pathogens such as *Staphylococcus aureus*, *Micrococcus luteus*, and *Escherichia coli* [93, 106]. The alcohol and aqueous extract of the root significantly reduced diarrhea in mice with reduction in weight of stools showing its anti-diarrheal property [107]. The leaves exhibited antidiabetic [100, 108-110], anti-inflammatory [111, 112], antioxidant [94, 113, 114], hypotensive [93], antiviral [115], analgesic [93], antipyretic [116] and wound healing activities [117]. Furthermore the crude extract of the seeds showed antimalarial activity [118]. Literature report showed that different solvent extracts of the various parts of *D. angustifolia* were capable of suppressing the germination and growth of various plants demonstrating its allelopathic potential [119].

2.1.1.3. Brief Review on Chemistry of the Genus *Dodonaea*

Phytochemical screening showed that the leaves of *D. angustifolia* contain compounds belonging to diverse groups of secondary plant metabolites such as flavonoids, terpenoids, saponins, tannins,

cardiac glycosides, steroids, etc [99]. In general, more than 40 compounds have been reported from the leaves of *D. angustifolia* and *D. polyandra*. The major secondary metabolites reported are flavonoids and terpenoids [104]. A complete list of compounds so far reported from two species of *Dodonaea* are given in Table 1.

Table 1: List of compounds isolated from *Dodonaea* organized by compound class

Compound class	Compound name	Str. No	Plant source	Ref
Flavonoids	3,5,7-Trihydroxy-4'-methoxyflavone	**79**	*D. v*	[108]
	5,7,4'-Trihydroxy-3,6-dimethoxyflavone	**80**	"	[113, 120]
	5,7-Dihydroxy-3,6,4'-trimethoxyflavone/santin	**81**	"	[113, 114]
	5-Hydroxy-3,7,4'-trimethoxyflavone	**82**	"	[93]
	5-Hydroxy-3,6,7,4'-tetramethoxyflavone	**83**	"	
	3,5-Dihydroxy-7,4',-dimethoxyflavone	**84**	"	
	3,4',5,7-Tetrahydroxyflavone	**85**	"	[113, 120]
	Pinocembrin	**86**	"	[120]
	Methylenebissantin	**87**	"	[121]
	Kaempferol 3-methyl ether	**88**	"	[121]
	5,7-Dihydroxy-3,6,4′-trimethoxy-3′-(4-hydroxy-3-methyl-but-2-enyl)flavone	**89**	"	[122]
	5,7,4'-Trihydroxy-3'(3-methylbut-2-enyl)-3-methoxy flavones (12),	**90**	*D. p*	[123]
	5,7-Dihydroxy-3'(3-methylbut-2-enyl)-3,4'-dimethoxyflavone	**91**	"	"
	5,7,4'-Trihydroxy-3',5'(3-methylbuyt-2-enyl)-3-methoxyflavone	**92**	"	"
	5,7,4'-Trihydroxy-3',5'(3-methylbuyt-2-enyl)-3-methoxy-6-metoxyflavone	**93**	"	"
	5,7,4'-Trihydroxy-3'-(3-methylbuyt-2-enyl)-3-methoxy-5'-methoxyflavone	**94**	"	"
Phenolics	Vanillic acid	**95**	*D. v*	[121]
	Nebrodenside A	**96**	"	"
	Docosyl caffeate	**97**	"	"
Terpenoids	5-(2-Furan-3-yl-ethyl)-8*α*-hydroxymethyl-5,6-dimethyl-	**98**	*D. v*	[121,

	3,4,4*α*,5,6,7,8,8*α*-octahydro-naphthalene-1-carboxylic acid			124]
	5-(2-Furan-3-yl-ethyl)-8*α*-hydroxymethyl-5,6-dimethyl-	**99**	"	"
	3,4,4*α*,5,6,7,8,8*α*-octahydro-naphthalene-1-carboxylic acid methyl			
	ester	**100**	"	

Table 1 continued

Terpenoids	5-(2-Furan-3-yl-ethyl)-8*α*-hydroxymethyl-5,6-dimethyl-			
	4*α*,5,6,7,8,8*α*-hexahydro-naphthalene-1-carboxylic acid			
	hautriwaic lactone	**101**	"	"
	6*β*-Hydroxy-15,16-epoxy-5*β*,8*β*,9*β*,10*α*-cleroda-3,13(16),14-trien-	**102**	"	"
	18-oic acid			
	Methyl dodonate C	**103**	"	"
	Methyl dodonate C	**104**		
	Methyl dodonate B	**105**	"	"
	Dodonolide	**106**	"	"
	Stictic acid	**107**	"	[125]
	Visclerodol acid	**108**	"	"
	Mkapwanin	**109**	"	[93]
	15-Methoxymkapwanin	**110**	"	"
	Ent-15,16-epoxy9*α*H-labda-13(16),14-diene-3*β*,8*α*-diol	**111**	*D. a*	[124]
	8*β*-hydroxy-3-O-*β*-D-glucopyranosyl-	**112**	"	[115]
	ent-labda-13-en-15,16-diol			
	Ent-15-ethoxy-labdan-3*α*,8*β*-dihydroxy,13(14)-en-15,16-olide	**113**	"	[115]
	ent-16-hydroxy-labdan-3*α*,8*β*-dihydroxy,13(14)-en-15,16-olide	**114**	"	[115]
	13,17-epoxy-13-methyl-15-oxo-labda-7-ene	**115**	*D. p*	[126]
	17-Hydroxy-13-methyl-labda-7,13Z-diene-15-oic acid	**116**	"	"
	13-Methyl-17-oxo-labda-7,13Z-diene-15-oic acid	**117**	"	"
	2,18-Dihydroxylabda-7,13(E)-dien-15-oic acid	**118**	*D. v*	[122]
	2,17-Dihydroxylabda-7,13(E)-dien-15-oic acid	**119**	"	"
	2-Hydroxylabda-7,13(E)-dien-15-oic acid	**120**	"	"

No: structure number; *D.v*: *D. viscosa*; *D.a*: *D. angustifolia*; *D.*p: *D. polyandra*

Chemical structures of compounds so far reported from *D. angustifolia* are given below.

Flavonoids [93, 108, 113, 114, 120-122]

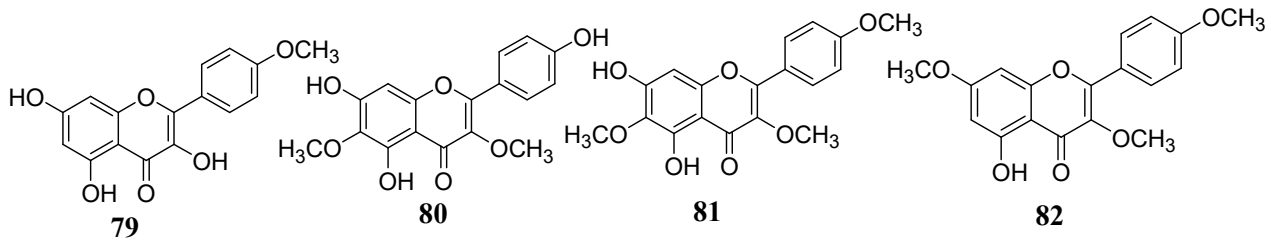

79 **80** **81** **82**

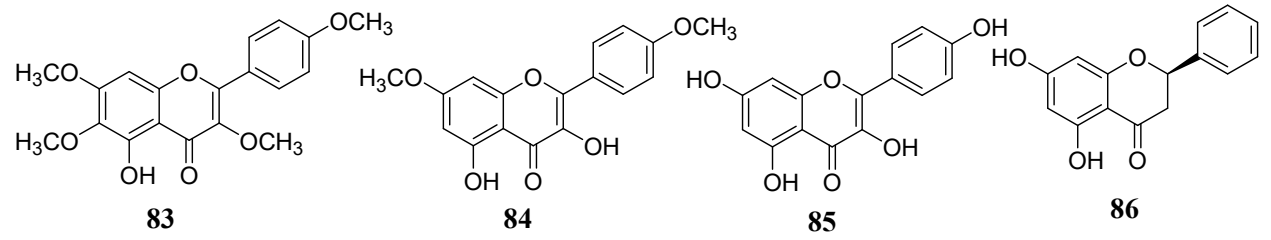

83 **84** **85** **86**

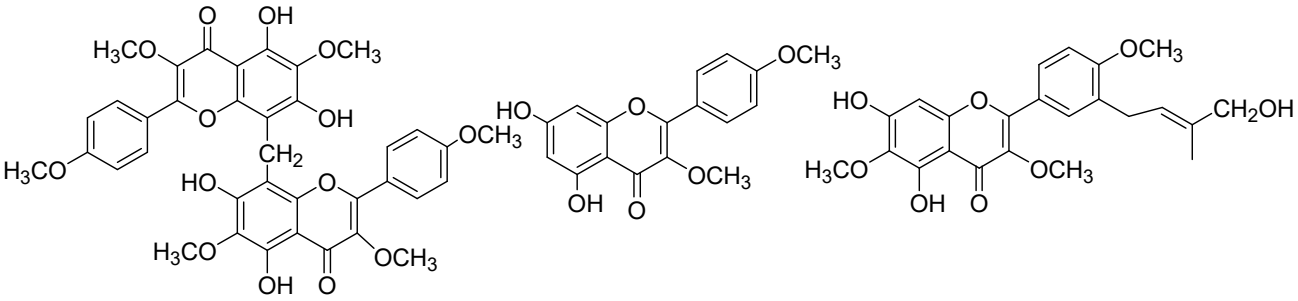

87 **88** **89**

Prenylated Flavonoids [122, 123]

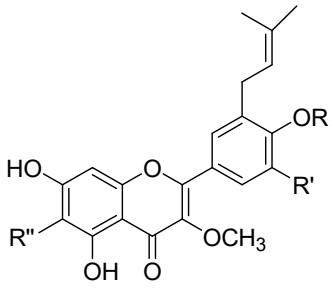

	R	R'	R''
90.	H	H	H
91.	CH_3	H	H
92.	H	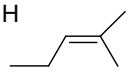	H
93.	H	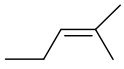	OCH_3
94.	CH_3	H	OCH_3

Phenolics [121]

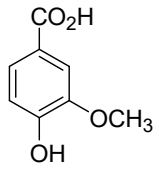

95

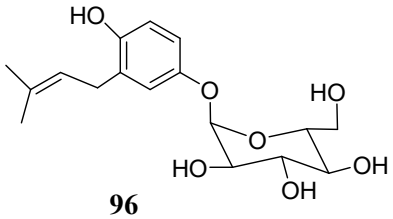

96

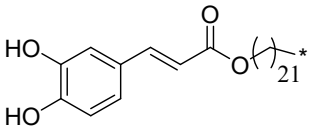

97

Terpenoids [93, 114, 121, 122-126]

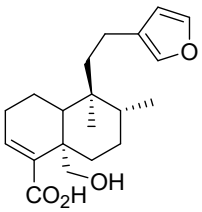

98

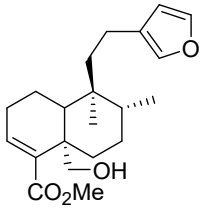

99

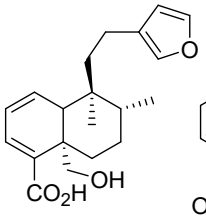

100

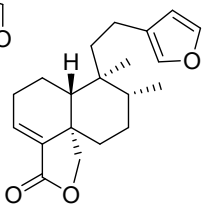

101

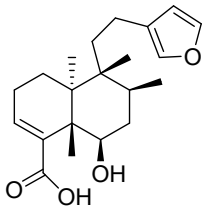

102

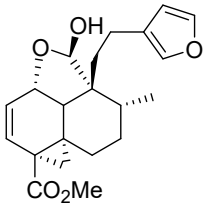

103

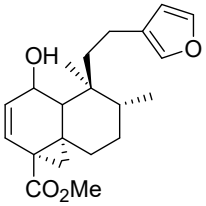

104

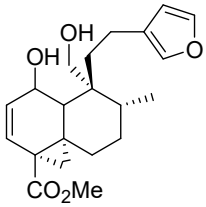

105

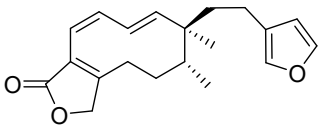

106

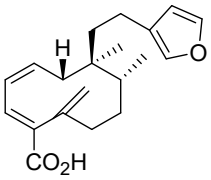

107

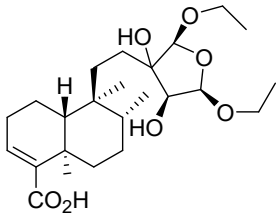

108

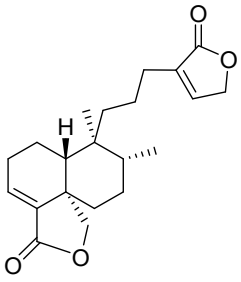

109

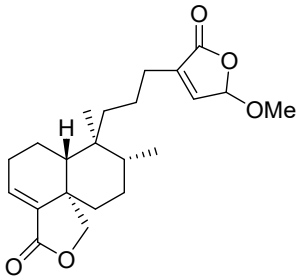

110

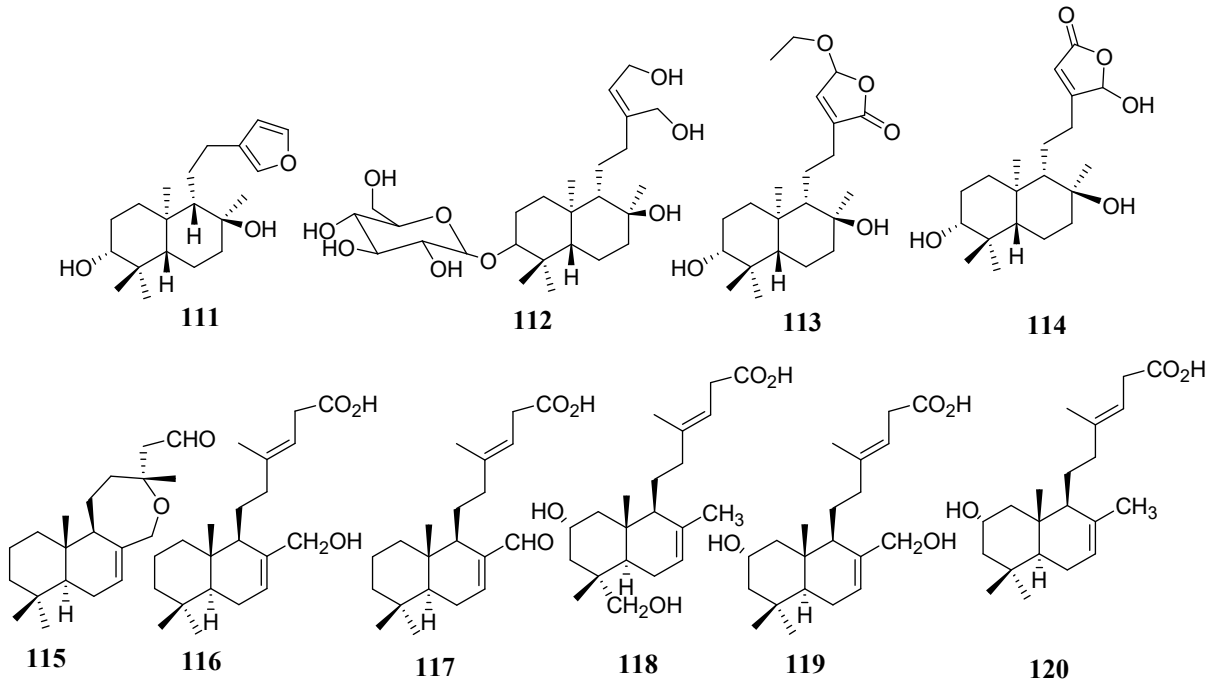

2.2. Objectives

Despite the traditional use of this plant for the treatment of malaria in some parts of Ethiopia, to our knowledge there is no published report describing the anti-malarial activities of the leaves of *D. angustifolia*. Indeed, a preliminary study conducted at the Department of Biology of Addis Ababa University [49, 127] on the crude extract of this plant for its *in vivo* antiplasmodial effect showed desirable activity. Hence this study was geared towards bioassay guided isolation of compounds responsible for the antiplasmodial activity of the extract of the leaves of *D. angustifolia*. The radical scavenging potential of the leaves of *D. angustifolia* was also explored.

2.3. Results and Discussion

Activity guided antiplasmodial study of the 80% aqueous methanol extract of the leaves of *D. angustifolia* led to the isolation of three significantly active compounds identified as pinocembrin (**86**), santin (**81**) and 15,16-epoxy-2-hydroxy-3,13(16),14-clerodtriene-18-oic acid (**128**) which suppressed the *P. berghei* by 81% at 40 mg/kg, 80% at 50 mg/kg, and 70% at 40 mg/kg, respectively. The ethanol extract and the ethyl acetate soluble portion of the ethanol extract of the leaves of *D. angustifolia* were analyzed using TLC with the results depicted in Fig. 1.

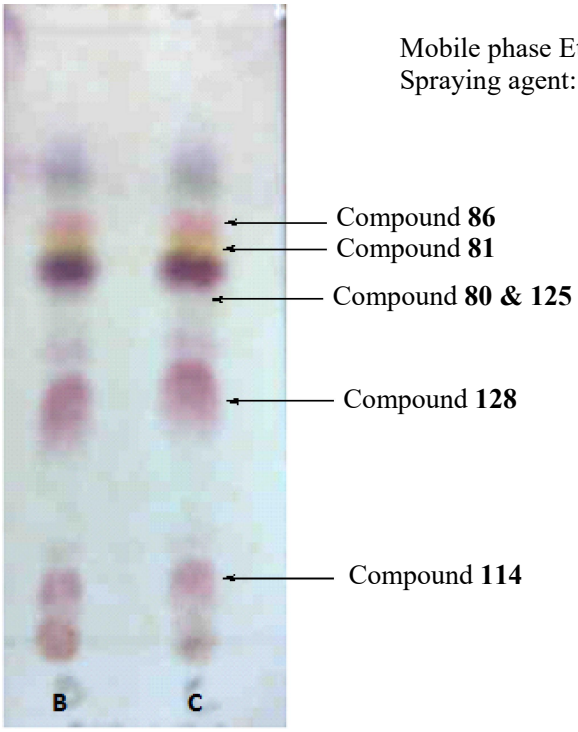

Fig. 1: TLC profile of the EtOH extract (B) and the EtOAc soluble portion of the EtOH extract (C) of the leaves of *D. angustifolia*

This section also discusses the column chromatographic fractionation of the ethyl acetate soluble portion of the ethanol extract of the leaves of *D. angustifolia* which resulted in the isolation of three other compounds in addition to **81**, **86** and **128**, identified as 5,7,4'-trihydroxy-3,6-dimethoxyflavone (**80**), 5,6,7-trihydroxy-3,4'-dimethoxyflavone (**125**), and ent-16-hydroxy-labdan-3α,8β-dihydroxy,13(14)-en-15,16-olide (**114**). Compound **125** has not been reported before as natural product. The extracts and the flavonoids isolated from the leaves of *D. angustifolia* were examined for their radical scavenging activities which furnished 5,7,4'-trihydroxy-3,6-dimethoxyflavone (**80**) as the most active compound.

2.3.1. Characterization of Compounds Isolated from the Leaves of *D. angustifolia*

Pinocembrin (86)

Compound **86** was obtained as yellow solid (mp 190-191^{o}C (Lit. 194-195^{o}C) [128]) recrystalized from ethanol. It is optically active with $[\alpha]_{589}^{21}$ = -12.5 (c 0.4, EtOH). TLC on a 0.25 mm thick layer of silica gel on aluminum plate showed a spot at Rf 0.65 using EtOAc:petrol (3:2) as eluent. It gave a pink spot after spraying with vanillin/H_2SO_4 followed by heating with hot air gun. The negative mode ESI-FT-MS of compound **86** showed molecular ion peak at *m/z* 255.0663 (calcd 255.2538 for $C_{15}H_{11}O_4$) corresponding to the molecular formula $C_{15}H_{12}O_4$ which was in agreement with the ^{13}C-NMR spectrum which showed resonances for fifteen carbon atoms. The UV-Vis spectrum (MeOH) of compound **86** showed absorption maxima at 290 and 333 nm with the latter band of lower shoulder which is characteristic feature of flavanone chromophore [130]. This is in good agreement with the literature report that flavonoids exhibited two absorption bands in their UV-Vis spectrum with the first band situated between 310-370 nm (band I) while the second band appears in the range 250-290 nm (band II) [129].Literature report also indicate that the absorption maxima involving the A-ring benzoyl system (band II) of flavanone show great bathochromic shift (above 15 nm) with respect to values for flavone analogues which occurs around 270 nm [131]. This strongly supports flavanone skeleton for compound **86**.

The ^{1}H-NMR spectrum of compound **86** (Table 2) displayed signals at δ 2.60 (1H, *dd*, *J* = 17.20 and 3.20 Hz) and 2.91 (1H, *dd*, *J* = 17.20 and 12.80 Hz) due to diastereotopic methylene protons on C-3. Another signal at δ 5.25 (1H, *dd*, *J* = 12.80 and 2.80 Hz) is due to the proton at C-2. The diastereotopic methylene proton signals at δ 2.91 and 2.61 showed COSY correlations with the proton signal at δ 5.25 (H-2). The signals at δ 5.82 (1H, *d*, *J* = 2.00 Hz) and δ 5.83 (1H, *d*, *J* = 2.00 Hz) are ascribed to aromatic protons situated *meta* to one another in the A ring of a flavonoid establishing 5,7-dihydroxy substitution patterns. These protons showed cross coupling with each other in their COSY spectrum. The absence of substitution on ring B of compound **86** is evident from the appearance of a five proton signal centered at δ 7.26.

The proton decoupled ^{13}C-NMR spectrum of compound **86** analyzed with the aid of DEPT-135 (Table 2) established the presence of six quaternary carbons. The most downfield signal at δ 195.6 is due to the ketone carbonyl (C-4). The remaining five quaternary carbon signals at δ 166.8, 163.7, 159.0, 138.8 and 102.2 were assigned to C-7, C-9, C-5, C-1' and C-10, respectively. Four well

resolved methine carbon signals appeared in the aromatic region at δ 128.6 (C-2', 6', and 4'), 125.9 (C-3', 5'), 96.3 (C-6) and 95.4 (C-8). The spectrum also exhibited a signal due to an oxygenated carbon at δ 78.9 (C-2). Furthermore the most upfield signal at δ 43.0 (C-3) is presumably due to carbon adjacent to the carbonyl.

The HMBC spectral data of compound **86** demonstrated that the methine proton signal at δ 5.23 (H-2) showed interactions with the carbon signals at δ 43.0 (C-3), 138.3 (C-1') and 195.6 (C-4). Further HMBC correlation observed was between the proton signal at δ 2.61 and the carbon signals at δ 102.2 (C-10) and 138.3 (C-1'). Additional HMBC connectivity observed was between the proton signal at δ 5.82 with the carbon signals at δ 96.3 and δ 95.4. Furthermore the signal due to H-6 (δ 5.83) correlates with the quaternary carbon signal at δ 102.2 (C-10). Some of the key correlations deduced from HMBC spectral data leading to the structure of compound **86** are depicted as in **121**.

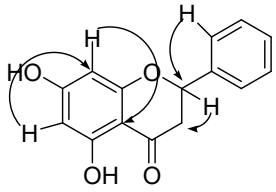

120

Compound **86** is the known flavanone pinocembrin. Table 2 compares the ^{1}H- and ^{13}C-NMR spectral data of compound **86** with those reported for pinocembrin [132].

Table 2: The ^{1}H- and ^{13}C-NMR spectral data of compound **86** and the reported spectral data for pinocembrin [132]

Posit	NMR data of compound **86** ($CDCl_3/CD_3OD$)		Data reported for pinocembrin (CD_3OD) [132]	
ion	^{1}H-NMR	^{13}C-NMR	^{1}H-NMR	^{13}C-NMR
2	5.25 (1H, *dd*, *J* = 12.80, 2.80)	78.9	5.33 (1H, *dd*, *J* = 12.8, 3.6)	80.4
3	2.60 (1H, *dd, J* = 17.20, 12.80); 2.91 (1H, *dd*, *J* = 17.20, 3.20)	43.0	2.98 (1H, *dd*, *J* = 17.4, 12.8); 2.67 (1H, *dd*, *J* = 16.9, 3.6)	44.1
4	-	195.6	-	197.3

5	-	163.7	-	165.4
6	5.83 (1H, *d*, *J* = 2.00)	95.4	5.87 (1H, *d*, *J* = 1.84)	96.2
7	-	166.8	-	168.3
8	5.82 (1H, *d*, *J* = 2.00)	96.3	5.87 (1H, *d*, *J* = 1.84)	97.2
9	-	163.0	-	164.6
10	-	102.2	-	103.3
1’	-	138.8	-	140.3
2’	7.26 (1H, *m*)	125.9	7.34 (1H, *m*)	127.3
3’	7.26 (1H, *m*)	128.6	7.34 (1H, *m*)	129.6
4’	7.26 (1H, *m*)	128.6	7.34 (1H, *m*)	129.7
5’	7.26 (1H, *m*)	128.6	7.34 (1H, *m*)	129.6
6’	7.26 (1H, *m*)	125.9	7.34 (1H, *m*)	127.3

Assignments made on the basis of COSY, HSQC and HMBC correlations; δ in ppm; Coupling constants are in Hz.

The spectroscopic data of compound **86** agreed well with the literature reported for pinocembrin (**86**) [132] which was isolated from propolis for the first time [133]. Other biological sources of pinocembrin include rhizomes of *Boesenbergia rotunda* [132] and *Boesenbergia pandurata* **[**134**]**.

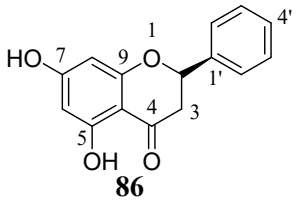

86

Pinocembrin has been reported as a non toxic flavonoid [135] with antimicrobial, anti-inflammatory, antioxidant, and anticancer activities [136]. It has a potent protective effect on neurovascular unit and is now in phase I clinical trial as a new drug to treat ischemic stroke [133]. Furthermore pinocembrin has been shown as a potent phytotoxic material for weed control which might serve as new and effective tool in organic agriculture [128].

Santin (81)

Compound **81** was isolated as a yellow solid from the ethyl acetate soluble portion of the ethanol extract of the leaves of *D. angustifolia*. It was recrystalized from ethanol, mp 160-161^{o}C. It is optically inactive ($[\alpha]_{589}^{21}$ = 0.00, c 0.4, EtOH). TLC on a 0.25 mm thick layer of silica gel on aluminum plate showed a spot at Rf 0.64 using EtOAc:petrol (3:2) as eluent. It was visualized as a yellowish spot after spraying with vanillin/ H_2SO_4 followed by heating with hot air gun. The

negative mode ESI-FT-MS of compound **81** demonstrated a peak at *m/z* 343.0858 (calcd 343.3154 for $C_{18}H_{15}O_7$) compatible with the molecular formula $C_{18}H_{16}O_7$. The peak at *m/z* 287 is due to the loss of methyl group from the parent ion. The UV-Vis spectrum (MeOH) of compound **81** showed absorption maxima at 271 and 338 nm suggesting a flavonol chromophore with 3-OH substituted. The absorption maxima of band II in the UV-Vis spectrum of a flavonoid containing 6-methoxy are reported to be below 279 nm while those with 6-hydroxy exhibit absorption maxima beyond 279 nm [137]. Hence the UV-Vis spectrum of compound **81** clearly indicated the presence of methoxy group on C-6. The IR spectrum displayed an absorption band at 1646 cm^{-1} attributable to an *α,β*-unsaturated carbonyl. The presence of C-O and C-H stretching were evident from the observed absorption bands at 1090 and 2924 cm^{-1}, respectively.

The ^{1}H-NMR spectrum of compound **81** revealed signals at *δ* 3.86 (3H, *s*), 3.91 (3H, *s*), and 4.05 (3H, *s*) suggesting the presence of three methoxy groups. The presence of five methine protons was evident from the signals in the aromatic region at *δ* 6.57 (1H, *s*), *δ* 7.03 (2H, *d*, *J* = 8.80 Hz) and *δ* 8.08 (2H, *d*, *J* = 8.80 Hz). The proton signals at *δ* 7.03 and 8.08 are due to symmetrically placed hydrogens on unsymmetrically *para* substituted B ring of flavonoid which showed mutual *ortho* coupling in their COSY spectrum as shown in **122**, whereas ring A of the flavonoid only showed a single proton singlet at *δ* 6.57 which is characteristic for H-8. The presence of a 5-hydroxy substitution on ring A of a flavonoid is evident from the appearance of a downfield signal at *δ* 12.90 (1H, *s*) corresponding to a chelated hydroxyl group in the compound.

The proton decoupled ^{13}C-NMR spectrum of compound **81**, analyzed with the aid of DEPT-135 spectrum (Table 3), showed ten quaternary carbons which are attributed to five oxygenated aromatic carbons at *δ* 130.0 (C-6), 151.8 (C-5), 152.2 (C-7), 155.0 (C-9) and 161.7 (C-4'); two oxygenated olefinic carbons at *δ* 138.4 (C-3) and 156.2 (C-2); two aromatic quaternary carbons at *δ* 106.2 (C-10) and 122.7 (C-1'); and an *α,β*-unsaturated carbonyl carbon at *δ* 179.2 (C-4). Three methine carbon signals are also observed in the aromatic region at *δ* 93.2 (C-8), 114.1 (C-3', 5') and 130.2 (C-2', 6'). Furthermore the spectrum demonstrated the presence of three methoxy groups at *δ* 55.4, 60.1 and 60.9. The HSQC showed correlation such that the methyl proton signals at *δ* 3.91, 3.86 and 4.05 correlate with the carbons at *δ* 55.4, 60.1 and 60.9, respectively. Other

HSQC correlations observed were between aromatic protons at δ 6.57, 7.03 and 8.08 with aromatic carbon signals at δ 93.2, 114.1 and 130.2, respectively.

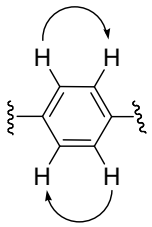

122

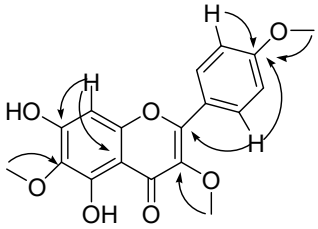

123

Close inspection of the HMBC spectral analysis revealed that the proton signal at δ 6.56 (H-8) showed long range connectivity with the carbon signals at δ 152.2 (C-7), 155.0 (C-9), 130.0 (C-6) and 106.2 (C-10) as shown in **123**. The most downfield signal in the ^{1}H-NMR at δ 12.90 (5-OH) showed HMBC cross peaks with the signals for C-5 (δ 151.8), C-6 (δ 130.0) and C-10 (δ 106.2) suggesting the position of this hydroxyl at C-5. The spectrum also showed significant correlation led to the conclusion that the methoxy groups at δ 4.05 and 3.86 are clearly attached to C-6 (δ 130.0) and C-3 (δ 138.4), respectively. The signal due to the third methoxy group at δ 3.91 correlates with the carbon signal at δ 161.2 (C-4') establishing the location of the third methoxy group at C-4' as depicted in **123**. Furthermore, the NMR spectral data of compound **81** were compared with the literature data reported for santin as shown in Table 3.

Table 3: The ^{1}H- and ^{13}C-NMR spectral data of compound **81** and the data reported in the literature for santin [138]

Position	NMR data of compound **81** ($CDCl_3/CD_3OD$)		Data reported in the literature for santin [138] ($CDCl_3$)	
	^{1}H-NMR	^{13}C-NMR	^{1}H-NMR	^{13}C-NMR
2	-	156.1	-	156.2
3	-	138.4	-	138.4
4	-	179.2	-	179.2
5	-	151.8	-	155.1

6	-	130.0	-	130.1
7	-	152.2	-	151.8
8	6.57 (1H, *s*)	93.2	6.57 (1H, *s*)	93.1
9	-	155.0	-	152.2
10	-	106.2	-	106.1
1’	-	122.7	-	122.7
2’ and 6’	7.03 (2H, *d*, *J* = 8.80)	130.2	7.02 (2H, *d*)	130.2
3’ and 5’	8.08 (2H, *d*, *J* = 8.80)	114.1	8.07 (2H, *d*)	114.1
4’	-	161.7	-	161.7
OCH_3	3.91 (3H, *s*)	55.4	3.70 (3H)	55.5
OCH_3	3.86 (3H, *s*)	60.1	3.80 (3H)	60.2
OCH_3	4.05 (3H, *s*)	60.9	3.80 (3H)	60.9

Assignments made on the basis of COSY, HSQC and HMBC correlations; δ in ppm; Coupling constants are in Hz

The above physical and spectral data of compound **81** are in close agreement with the data reported in the literature for santin [138]. Santin (5,7-dihydroxy 3,6,4’-trimethoxyflavone) was previously isolated from the leaves of *Dodonaea viscosa* [113, 114, 121], *Parthenium hysterophorus* [139] and the aerial parts of *Tanacetum microphyllum* [140].

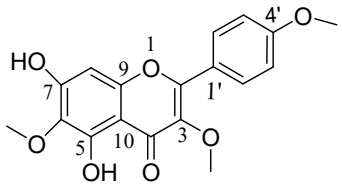

81

Santin was shown to be a non cytotoxic compound displaying trypanocidal, leishmanicidal [141] and anti-inflammatory activities [140]. It is also found to exhibit cyclo-oxygenase inhibitor, 5-lipoxygenase inhibitor, and anti-tubercular properties [139].

5,6,7-Trihydroxy-3,4’-dimethoxyflavone (125)

Compound **125** was isolated as a yellow solid (mp 226-229^{o}C) from ethyl acetate soluble portion of ethanol extract of *D. angustifolia* leaves. It is optically inactive ($[\alpha]_{589}^{21}$ = 0.00, c 0.4, EtOH). TLC on a 0.25 mm thick layer of silica gel on aluminum plate showed spot at Rf 0.50

(EtOAc:petrol, 3:2). It was visualized as a yellowish spot after spraying with vanillin/H_2SO_4 followed by heating with hot air gun. The UV-Vis spectrum (MeOH) showed absorption maxima at 285 and 346 nm which is distinctive of compounds having flavonoid skeleton with 3-OH substituted. The absorption maxima observed for band II (λ_{max} 285 nm) clearly indicated that the compound is 6-hydroxylated [137]. The (+)-ESI-FT-MS displayed a molecular ion peak at *m/z* 331.0803 (calcd 331.2968 for $C_{17}H_{15}O_7$) corresponding to the molecular formula $C_{17}H_{14}O_7$. A prominent peak was observed at *m/z* 316 accounting for the loss of methyl group from the parent ion.

The ^{1}H-NMR spectrum of compound **125** disclosed the presence of two methoxy signals at δ 3.80 (3H, *s*) and 3.90 (3H, *s*). The methine proton signal at δ 6.63 (1H, *s*) was assigned to H-8. The doublets at δ 8.02 and 7.12, showing only *ortho* coupling (each 2H, J = 8.80 Hz) were due to H-2′, 6′ and H-3′, 5′, respectively. The most downfield sharp singlet signal at δ 12.60 is characteristic of a chelated hydroxyl group establishing the presence of 5-OH.

The proton decoupled ^{13}C-NMR spectrum of compound **125** with the aid of DEPT 135 showed ten quaternary, three methine, and two methoxy carbon signals. The two methoxy carbon signals were observed at δ 54.9 and 59.3. The methine carbons at δ 113.9 (C-3', 5') and 130.0 (C-2', 6') are due to symmetrically placed aromatic carbons on unsymmetrically *para* substituted B-ring of a flavonoid. The carbon signal at δ 93.5 is due to C-8. The diagnostic signal in the ^{13}C-NMR spectrum at δ 178.7 is suggestive for the presence of α,β-unsaturated carbonyl carbon. The compound exhibited oxygenated aromatic quaternary carbon signals at δ 161.7 (C-4'), 155.8 (C-2), 152.8 (C-7), 149.7 (C-9), 146.7 (C-5), 138.2 (C-3), and 128.5 (C-6). Quaternary carbon signals were also observed at δ 123.0 and 105.2 due to C-1' and C-10, respectively. The physical and spectral data generated for compound **125** is in agreement with 5,6,7-trihydroxy-3,4'-dimethoxyflavone. This was further confirmed using 2D NMR experiments (COSY, HSQC and HMBC).

The HSQC spectrum of compound **125** showed that the proton signals at δ 8.02, 7.12, 6.63, 3.90 and 3.80 were correlated to carbon signals at δ 130.0, 113.9, 93.6, 54.9 and 59.3, respectively. The

^{1}H-^{1}H COSY spectrum showed correlation between proton signal at δ 8.02 with 7.12 and *vice versa*, confirming that these protons are symmetrically placed protons on unsymmetrically *para* substituted aromatic ring. The HMBC spectrum indicated connectivity between the proton signal at δ 12.60 with the carbon signals at δ 105.5 (C-10), 128.6 (C-6) and 146.4 (C-5) as shown in **124**. The proton signal at δ 6.63 (H-8) showed HMBC correlation with the carbons at δ 105.5 (C-10), 128.5 (C-6) and 152.8 (C-9).

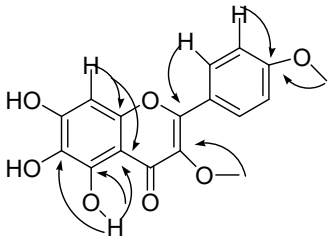

124

The positions of the two methoxy groups were established using HMBC spectral analysis. The methoxy proton signals at δ 3.80 and 3.90 showed connectivity with the olefinic carbon signals at δ 138 (C-3) and δ 161.8 (C-4'), respectively. The physical and spectroscopic findings presented above disclose that compound **125** is 5,6,7-trihydroxy-3,4'-dimethoxyflavone which has not yet been reported from any natural source.

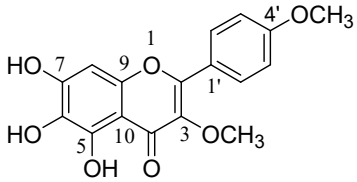

125

5,7,4'-Trihydroxy-3,6-dimethoxyflavone (80)

Compound **2** was obtained as a yellow solid from ethyl acetate soluble portion of ethanol extract of *D. angustifolia* leaves. The TLC on a 0.25 mm thick layer of silica gel on aluminum plate (EtOAc:petrol, 3:2) showed a yellow spot (Rf 0.50), which was visualized after spraying with vanillin/H_2SO_4 followed by heating with hot air gun. The ^{1}H-NMR spectrum of compound **80** suggested the presence of two methoxy groups at δ 3.60 (3H, *s*) and 3.70 (3H, *s*). A pair of doublets at δ 6.70 (2H, *d*, *J* = 8.80 Hz) and 7.74 (2H, *d*, *J* = 8.80 Hz) were characteristic of H-2'/ H-6' and H-3'/H-5', respectively, of the 1,4-disubstituted aromatic ring system. A typical signal due to H-6 was observed at δ 6.30 (1H, *s*).

The proton decoupled ^{13}C-NMR spectrum (Table 4) of compound **80** showed ten quaternary, five methine, and two methoxy carbon signals. The signals at δ 55.2 and 59.9 are evident for the presence of two methoxy groups which was found in agreement with the ^{1}H-NMR spectrum of the compound. The carbon signals at δ 94.0 (C-8), 115.2 (C-3',5') and 130.0 (C-2',6') are due to methine carbons. The latter two resonances are characteristic of symmetrically placed carbons on unsymmetrically *para* substituted aromatic ring. Other carbon signals observed were at δ 105.0 (C-10), 121.0 (C-1'), 131.0 (C-6), 138.0 (C-3), 152.0 (C-4'), 152.1 (C-9), 156.5 (C-7), 157.4 (C-5), 160.0 (C-2), and 179.0 (C-4). The presence of α,β-unsaturated carbonyl carbon is evident from the appearance of a carbon signal at δ 179.0. Table 4 gives the ^{1}H- and ^{13}C-NMR data of compound 2 and the reported spectral data for 5,7,4'-trihydroxy-3,6-dimethoxyflavone.

Table 4: The ^{1}H- and ^{13}C-NMR spectral data of compound **80** and the data reported in the literature for 5,7,4'-trihydroxy-3,6-dimethoxyflavone [120].

Position	NMR data of compound **80** ($CDCl_3/CD_3OD$)		Data reported in the literature for 5,7,4'-trihydroxy -3,6-dimethoxyflavone (CD_3OD) [120]	
	^{1}H-NMR	^{13}C-NMR	^{1}H-NMR	^{13}C-NMR
2		160.0		161.8
3		138.0		139.0
4		179.4		180.0
5		157.4		158.7
6		131.0		132.6
7		156.5		158.2

8	6.30 (1H, *s*)	94.0	6.40 (1H)	95.1
9		152.1		153.8
10		105.0		106.0
1’		121.0		122.7
2’ and 6’	6.70 (2H, *d*, *J* = 8.80)	130.0	6.8 (2H)	131.5
3’ and 5’	7.74 (2H, *d*, *J* = 8.80)	115.2	7.90 (2H)	116.0
4’		152.0		153.7
OCH_3	3.60 (3H, *s*)	59.4	3.70 (3H)	60.6
OCH_3	3.70 (3H, *s*)	59.9	3.80 (3H)	60.9

The NMR spectrum of compound **80** are in close agreement with those reported in the literature for the known compound 5,7,4’-trihydroxy-3,6-dimethoxyflavone which was isolated as a major flavonoid from *D. angustifolia* of South Africa [120].

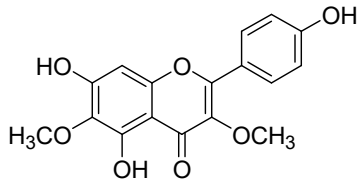

80

15,16-Epoxy-2-hydroxy-3,13 (16), 14-clerodtriene-18-oic acid (128)

Compound **128** was isolated from the leaves of *D. angustifolia* as a white solid, mp 145-147°C. It is an optically active compound with $[\alpha]_{589}^{21}$ = -17.5 (c 0.4, MeOH). The TLC Rf value was 0.35 on a 0.25 mm thick layer of silica gel on aluminum plate eluted with EtOAc:petrol (3:2). The spot visualized after spraying with vanillin/H_2SO_4 followed by heating with hot air gun. The negative mode ESI-FT-MS of compound **128** provided a peak at *m/z* 331.1990 (calcd 331.4339 for $C_{20}H_{27}O_4$) establishing the molecular formula as $C_{20}H_{28}O_4$ and this was also evident from the ^{13}C-NMR spectrum which showed resonances for 20 carbon atoms. A prominent peak at *m/z* 287 in the mass spectrum is presumably due to the loss of CO_2 from the parent ion. The UV-Vis spectrum (MeOH) showed maximum absorption bands at 270 and 333 nm indicating the presence of conjugated chromophore. The IR spectrum showed an absorption band at 1690 cm^{-1} suggesting the presence of an *α,β*-unsaturated carboxyl group. Other absorption bands appeared at 3375, 2962 and 1027 cm^{-1} due to O-H, C-H, and C-O stretching, respectively. The presence of hydroxyl group was

further confirmed by the phosphoric acid catalyzed dehydration of compound **128** which gave a compound with a greater Rf value than that of compound **128** in its TLC profile.

The ^{1}H-NMR spectrum of compound **128** (Table 5) revealed the presence of three methyl groups at δ 0.73 (3H, *s*), 0.80 (3H, *d*, *J* = 6.4 Hz) and 1.26 (3H, *s*) with the signals at δ 0.75 (H-20) and 1.26 (H-19) corresponding to methyl groups on quaternary carbons while the signal at δ 0.80 (H-17) is due to methyl group on tertiary carbon. The methylene proton at δ 1.12 (1H, *m*) and 2.30 (1H, *m*) are due to diastereotopic protons on carbon at δ 35.5 (C-6) as observed from one bond ^{1}H/^{13}C NMR spectrum of the compound. The proton signal at δ 1.98 (1H, *m*) and δ 1.39 (1H, *m*) are diastereotopic methylene protons on C-1 (δ 27.4). The diastereotopic methylene protons at δ 1.62 (1H, *m*) and δ 1.51 (1H, *m*) were situated on carbon at δ 38.5 (C-11). The compound also exhibited diastereotopic methylene proton signals at δ 2.10 (1H, *m*) and 2.30 (1H, *m*) due to protons on C-12. The proton signals at δ 4.30 (1H, *m*) and 6.60 (1H) are due to H-2 and H-3, respectively. The former signal is accounted for the methine proton on carbon bearing hydroxyl group. The proton signals in the aromatic region at δ 6.25 (1H, *s*), 7.20 (1H, *s*) and 7.30 (1H, *t, J* = 1.80 Hz) are evident for the presence of furan ring. Literature reports showed that the coupling constant for the proton signal at δ 7.30 is 1.80 Hz [142]. This strongly supports the presence of furan ring for compound **128**.

The ^{13}C-NMR and DEPT-135 spectra of compound **128** (Table 5) demonstrated the presence of 20 well resolved signals attributable to five quaternary (δ 37.9, 38.4, 125.3, 143.3 and 169.9); five methylene (δ 18.1, 26.9, 27.4, 35.5, and 38.5); three methyl (δ 15.9, 18.3 and 20.4) and seven methine carbon signals (δ 35.9, 45.1, 68.5, 110.9, 138.3, 138.9 and 142.7). The presence of an α, β-unsaturated carboxyl carbon was evident from the carbon signal at δ 169.6 (C-18). The carbon resonances at δ 138.9 (C-3) and 143.2 (C-4) are due to two olefinic carbon atoms. The presence of an aliphatic oxygenated carbon is evident from the appearance of a carbon signal at δ 68.5 (C-2). Moreover the signals at δ 110.9 (C-14), 138.3 (C-16), and 142.7 (C-15) are characteristic carbon signals of the furan ring. The ^{1}H and ^{13}C-NMR spectral data of compound **128** are given in Table 5.

Table 5: The ^{1}H- and ^{13}C-NMR spectral data ($CDCl_3/CD_3OD$) of compound **128** (δ in ppm)

Position	^{1}H-NMR (400 MHz)	^{13}C-NMR (100 MHz)	Multiplicity
1	1.98 (1H, *m*) and 1.39 (1H, m)	27.4	CH_2
2	4.30 (1H, *m*)	68.5	CH
3	6.60 (1H, *m*)	138.9	CH
4	-	143.3	C
5	-	37.9	C
6	1.12 (1H, *m*) and 2.30 (1H, *m*)	35.5	CH_2
7	1.46 (1H, *m*) and 1.39 (1H, *m*)	26.9	CH_2
8	1.51 (1H, *m*)	35.9	CH
9		38.4	C
10	1.37 (1H, *m*)	45.1	CH
11	1.51 (1H, *m*) and 1.62 (1H, *m*)	38.5	CH_2
12	2.10 (1H, *m*) and 2.30 (*m*, H)	18.1	CH_2
13	-	125.3	C
14	6.25 (1H, *bro s*)	110.9	CH
15	7.30 (1H, *t, J* = 1.80 Hz)	142.7	CH
16	7.20 (1H, *s*)	138.3	CH
17	0.80 (3H, *d*, *J* = 6.40 Hz)	15.9	CH_3
18	-	169.9	C
19	1.26 (3H, *s*)	20.4	CH_3
20	0.73 (3H, *s*)	18.3	CH_3

Assignments made on the basis of COSY, HSQC and HMBC correlations; δ in ppm; Coupling constants are in Hz

The structure of compound **128** was further deduced using 2D NMR experiments. The proton signal at δ 6.25 (H-14) showed COSY interactions with the proton signal at δ 7.30 (H-15) and 7.10 (H-16) suggesting that these protons are part of the furan ring. The olefinic proton signal at δ 6.60 (H-3) showed cross peaks, in its COSY spectrum, with the proton at δ 4.30 (H-2) and 1.98 (H-1). Another COSY coupling was displayed between methine proton signal at δ 4.30 with the proton signals at δ 1.39 (H-1), 1.98 (H-1) and 6.60 (H-3) which established the position of hydroxyl group on C-2. From ^{1}H, ^{13}C, DEPT-135 and COSY, the following fragment shown as **126** can be suggested.

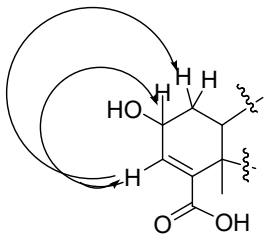

126

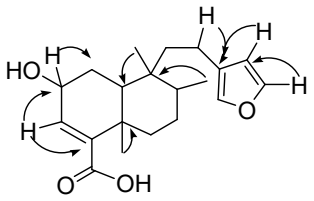

127

In the HMBC spectral analysis, the proton at δ 7.30 (H-15) showed correlation with the carbon at 110.9 (C-14) and δ 138.3 (C-16) while the proton at δ 6.25 (H-14) correlates with a carbon at δ 142.7, 138.3 and 110.9. The above HMBC correlations indicated that C-13, C-14, C-15 and C-16 constitute the furan ring. H-12 (δ 2.30) displayed long range $^{1}H/^{13}C$-NMR coupling with the carbon at δ 125.3 (C-13) and δ 38.5 (C-11) establishing the attachment of C-12 to C-13. The olefinic proton signal at δ 6.60 displayed correlation with the carbon at δ 169.8 (C-18), 143.2 (C-4), 37.9 (C-5) and 27.5 (C-1). The methine proton signal at δ 4.30 (H-2) showed long range correlations with C-3 (δ 138.9) and C-4 (δ 143.2) locating the hydroxyl group at C-2 which agreed well with the COSY spectrum of compound **128**.

The methyl proton signals at δ 0.80 (H-17) and 0.73 (H-20) showed HMBC correlations with C-8 (δ 35.9) and C-9 (δ 38.4), respectively, ascertaining the attachment of C-17 to C-8 and C-20 to C-9. The other methyl group was connected to C-5 (δ 37.9) as long range correlation was observed between H-19 and C-5. The HMBC correlations observed leading to the structure of compound **128** is displayed in **127**. Literature report showed that the C-20 of *trans*-clerodanes resonates at higher field (δ 17–19) than its *cis*-counterpart (δ 21–29) [93]. In the ^{13}C-NMR spectrum of compound **128**, the C-20 resonated at δ 18.3, supporting the *trans* geometry. From the foregoing considerations it is quite evident that compound **128** is identified as 15,16-epoxy-2-hydroxy-3,13(16),14-clerodtriene-18-oic acid.

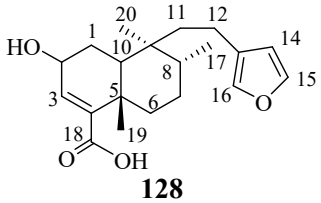

128

Ent-16-hydroxy-labdan-3α,8β-dihydroxy,13(14)-en-15,16-olide (114)

Compound **114** was isolated from the EtOAc soluble portion of the ethanol extract of the leaves of *D. angustifolia*. The TLC Rf value was 0.20 on a 0.25 mm thick layer of silica gel on aluminum plate eluted with EtOAc:petrol (3:2). It was visualized after spraying with vanillin/H_2SO_4 followed by heating with hot air gun. The ^{1}H-NMR spectrum (DMSO-d6) of compound **114** displayed signals at δ 7.60 (1H), 4.30 (1H) and 3.90 (1H) which are attributed to protons on heteroatoms as these signals did not show any correlations to carbon atoms in its HSQC spectrum. The signal due to olefinic proton adjacent to a carbonyl was observed at δ 7.00 (1H, *bro. s)* confirming the presence of only one double bond. The compound also exhibited signal at δ 6.00 (1H, *d, J* = 8.26 Hz) due to methine proton on acetal carbon. Other methine proton signals were at δ 3.00 (1H, H-3), 0.81 (1H, *dd*, *J* = 8.20 and 1.92 Hz, H-5) and δ 1.01 (1H, H-9). Signals due to diastereotopic methylene protons are evident at δ 1.69 (1H, *m*, H-7) and 1.33 (1H, *m*, H-7); δ 1.58 (1H, *m,* H-1) and 0.96 (1H, *m,* H-1); and 1.29 (1H, *m*, H-11) and 0.86 (1H, *m*, H-11). Also observed methylene proton signals are at δ 0.89 (2H, H-12), 1.46 (2H, *m*, H-2), 1.55 (2H, *m*, H-6). The proton signals at δ 1.00 (3H, *s*, H-17), 0.89 (3H, *s*, H-18), 0.72 (3H, *s*, H-20) and 0.65 (3H, *s*, H-19) are attributed to four methyl groups on quaternary carbons.

Analysis of the proton decoupled ^{13}C-NMR spectrum (DMSO-d6) of compound **114** together with DEPT-135 disclosed the presence of well resolved carbon resonances of twenty carbon atoms which are accounted to five quaternary, five methine, six methylene and four methyl groups. The most deshielded signal in the ^{13}C-NMR spectrum at δ 172.2 is evident for the presence of a carbonyl group. Two olefinic carbon signals were observed at δ 145.7 and 136.8 due to C-14 and C-13, respectively. Further inspection of the ^{13}C-NMR spectrum of compound **114** showed the presence of three oxygenated carbons at δ 72.5, 77.2 and 97.6 due to C-8, C-3 and C-16, respectively. The latter oxygenated carbon signal justifies the presence of methine carbon of the acetal group, which is consistent with the ^{1}H-NMR spectrum. The signals at δ 60.8 and 55.1 are ascribed to C-9 and C-5, respectively. Two quaternary carbon signals were observed at δ 38.9 (C-4) and 38.6 (C-10). The spectrum also displayed the presence of six methylene carbon signals at δ 44.4, 37.9, 28.3, 27.3, 23.2, and 20.2 due to C-7, C-1, C-12, C-2, C-11, and C-6, respectively. The ^{13}C-NMR spectrum also revealed signals due to four methyl groups at δ 28.7 (C-18), 24.0 (C-17),

16.1 (C-19) and 15.7 (C-20). The ^{1}H-, ^{13}C- and DEPT-135 NMR spectral analysis likely established the frame work for compound **114** as a diterepenoid, with its full structure further worked out using 2D NMR.

The COSY spectral analysis showed connectivity between the proton signal at δ 7.60 (OH) with the methine proton signal of the acetal group at δ 6.00 (H-16). This phenomenon in combination with the multiplicity observed for H-16 established the hydroxy at δ 7.60 on C-16. The hydroxy proton signal at δ 4.30 correlates with the methine proton signal at δ 3.00 (H-3) which enables the attachment of the hydroxy at δ 4.30 on C-3. The methine proton signal at δ 3.00 (H-3) showed COSY correlation with the methylene proton signal at δ 1.46 (H-2) establishing the connectivity of C-3 with C-2. Other COSY connectivities observed were between the diastereotopic methylene protons at δ 1.69 (1H, *m*, H-7) with the proton signal at δ 1.33 (1H, *m*, H-7); the proton signal at δ 1.58 (1H, *m,* H-1) with the proton signal at δ 0.96 (1H, *m*, H-1).

The HMBC spectral analysis revealed that the proton signal at δ 7.60 showed correlations with the carbon signals at δ 97.6 (C-16) and 145.7 (C-14). The olefinic proton signal at δ 7.00 displayed HMBC correlations with the carbons whose signals appeared at δ 97.6 (C-16), 136.8 (C-13), and 172.2 (C-15). The methine proton signal of the acetal group at δ 6.00 correlates with the carbonyl carbon signal at δ 172.2 (C-15). The HMBC spectral analysis leading to a five membered α,β-unsaturated lactone moiety is as depicted in **129**.

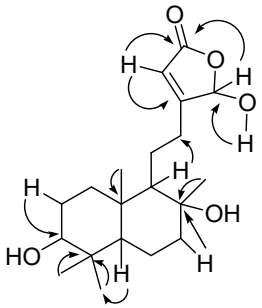

129

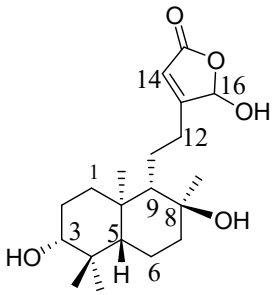

114

The methylene proton signals at δ 1.46 (H-2) and 1.33 (H-7) exhibited HMBC connectivity with C-3 (δ 77.2) and C-8 (δ 72.5), respectively. The methyl group at δ 1.00 (H-17) was placed on the oxidized quaternary carbon C-8 (δ 72.2) due to the observed HMBC correlations of this proton with the carbons at δ 44.4 (C-7), 72.5 (C-8) and 60.8 (C-9). The presence of gem-dimethyl on C-4 (δ 38.9) was evident from the observed HMBC correlations between the methyl proton signals at δ

0.89 (H-18) and 0.65 (H-19) with the carbon signal at δ 38.9 (C-4). The gem-dimethyl on C-4 along with the ^{1}H, ^{13}C and DEPT-135 spectral analysis established the presence of labdane diterpenoid core structure for compound **114**. The methine signal at δ 1.01 (H-9) showed HMBC correlation with C-12 (δ 28.3) indicating that the labdane diterpene core structure was connected to α,β-unsaturated lactone by one of the two methylenes whose signal was observed at δ 28.3 (C-12). The proton signal at δ 0.82 (H-5) correlates with the carbon signal at δ 16.1 (C-19). The key HMBC spectral analysis leading to structure **114** is shown as in **129**. In addition the HMBC correlations observed between the proton signal at δ 0.72 and the carbon signals at δ 37.9, 55.1 and 60.8 allowed theplacement of the methyl group on C-10. Hence, based on the above NMR spectral analysis compound **114** was identified as ent-16-hydroxy-labdan-3α,8β-dihydroxy,13(14)-en-15,16-olide (**114**) which was previously reported from the aerial parts of *D. viscosa* [115].

2.3.2. TLC Profiles of the Ethyl acetate Extract of Dried Leaves and the Acetone Extract of the Leaf Exudates of *D. angustifolia*

In the course of this work, the extract from the leaf surface exudates obtained by simple dipping of the fresh leaves of *D. angustifolia* in acetone was compared with the ethyl acetate extract of the dried leaves of *D. angustifolia* using silica gel TLC. The purpose of this study was to find out if those compounds isolated from column chromatographic fractionation of the EtOAc extract are present in the extracts of the leaf surface exudates. The spots on the respective TLC (eluent EtOAc:petrol, 4:1) were visualized after spraying with vanillin/H_2SO_4 followed by heating with hot air gun (Fig. 2). As shown in Fig. 2, the TLC profiles of the two extracts displayed comparable number of spots. This indicated that the TLC profile of the solvent extract of the leaves and the leaf exudates are similar.

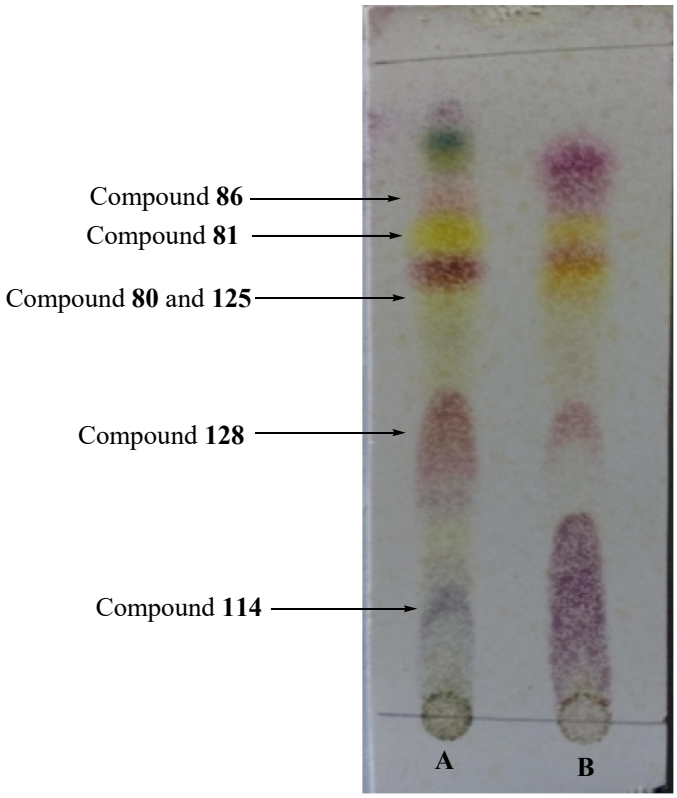

Fig. 2: TLC of the EtOAc extract of dried leaves (**A**) and the acetone extract of the leaf surface exudates (**B**) of *D. angustifolia*

It is interesting to compare the TLC profiles of the extracts obtained by the two methods of extraction. The extract obtained from the leaf surface exudates by simple dipping technique is chlorophyll free. Furthermore the yield of the extract obtained by dipping the leaves in acetone is 10% while the extraction of the dried leaves with EtOAc is 6%. This experiment clearly demonstrates that simple dipping is a quick and convenient method for the isolation of terpenoids and flavonoids from the leaves of *D. angustifolia*. The above results are in agreement with literature report for leaf exudate extraction of *Salvia divinorum* [143]. Comparison of the secondary metabolites profile of the acetone extract of the leaf surface exudates obtained by simple dipping technique with those secondary metabolites reported in the literature for surface leaf extract of *D. angustifolia* by Omosa *et al*., exhibits a gross difference [7].

2.3.3. Bioassay

2.3.3.1. Antiplasmodial Assay

The antiplasmodial activity of the ethanol extract of the leaves of *D. angustifolia* was screened at higher dose (300 mg/kg) against *Plasmodium berghei* infected mice. The extract inhibited parasitaemia significantly (%para 77) which can be attributed to the presence of secondary metabolites. The ethanol extract was sequentially extracted using hexane and ethyl acetate and the resulting hexane, ethyl acetate and the marc (the material left after extraction with ethyl acetate) were subsequently tested for their antiplasmodial activities. The ethyl acetate soluble portion of the ethanol extract was found active; however, the hexane extract and the marc were inactive.

Inspired by the antiplasmodial result of the ethyl acetate soluble portion of the ethanol extract, the plant material was extracted with 80% aqueous methanol and partitioned using EtOAc. The organic phase showed inhibition of parasitaemia by 80% at 150 mg/kg; however, the freeze dried aqueous phase was found inactive exhibiting low percent inhibition of parasitaemia (19%) as compared to the negative control mice treated with DMSO. On the other hand the percent parasitaemia for the ethyl acetate soluble phase was found to be low (7.0%) in contrast to those mice administered DMSO as the negative control which exhibited 34.0%. In order to clearly identify the active ingredients responsible for the antiplasmodial activity of the plant material, the active portion was subjected to column chromatographic separation using column chromatographic separation using silica gel and Sephadex LH20 to afford compound **86** (10 mg), **81** (40 mg), and **128** (30 mg**)**. The structures of these compounds were established using physical and spectroscopic methods with compound **86**, **81**, and **128** identified to be pinocembrin, santin and 15,16-epoxy-2-hydroxy-3,13(16),14-clerodtriene-18-oic acid, respectively.

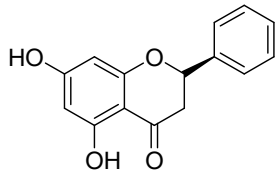

86

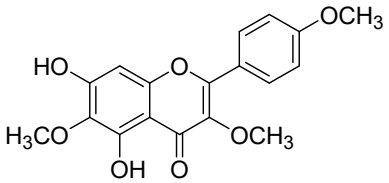

81

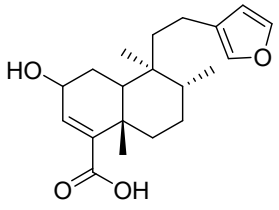

128

Compounds **86**, **81** and **128** were assayed for their antiplasmodial activities. The percent parasitaemia inhibition observed on administration of santin (**81**) at a dose of 100 mg/kg and 50 mg/kg were 85% and 80%, respectively. On the other hand pinocembrin (**86**) was found to induce

inhibition of parasitaemia by 77% and 81% at doses of 20 mg/kg and 40 mg/kg, respectively, where as 15,16-epoxy-2-hydroxy-3,13(16),14-clerodtriene-18-oic acid (**128**) inhibited the parasite by 60% and 70% at doses of 20 mg/kg and 40 mg/kg, respectively. CQ suppressed the parasites by 100% at 25 mg/kg. The percent parasitaemia of pinocembrin (**86**), santin (**81**) and 15,16-epoxy-2-hydroxy-3,13(16),14-clerodtriene-18-oic acid (**128**) were found to be 6.0 at 40 mg/kg, 4.0 at 100 mg/kg and 11.0 at 40 mg/kg of body weight, respectively. Furthermore, there was no significant difference on mean body weight between D_0 and D_4 in all groups of mice treated with the three compounds isolated from the leaves of *D. angustifolia* compared to mice treated with the standard drug (CQ). It was also found out that those mice treated with the extract and pure constituents showed prolonged MST as compared to their negative control groups treated with DMSO. The high percent suppression and low percent parasitaemia exhibited by compound **81**, **86** and **128** presumably account for the traditional use of the leaves of *D. angustifolia* against malaria.

2.3.3.2. Radical Scavenging Assay

The DPPH radical scavenging activities of the hexane and the ethyl acetate soluble portions of the ethanol extract of the leaves of *D. angustifolia* were examined by comparison with ascorbic acid. The EtOAc and hexane soluble fractions exhibited percent inhibition of DPPH by 90% and 7% at100 µg/mL, respectively. In contrast to the hexane fraction, the EtOAc soluble portion showed immediate discoloration of methanolic solution of DPPH from purple to yellow. Furthermore, the EtOAc soluble fraction exhibited the lowest IC_{50} value as compared to the hexane fraction indicating its high scavenging potential.

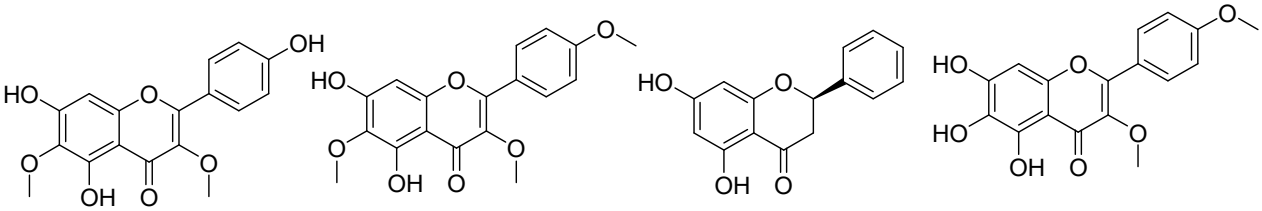

As a follow up to the antioxidant activities shown by the EtOAc soluble portion of the ethanol extract of the leaves of *D. angustifolia*, the radical scavenging tests were done for all flavonoids (pinocembrin, santin, 5,7,4'-trihydroxy-3,6-dimethoxyflavone, and 5,6,7-trihydroxy-3,4'-dimethoxyflavone) isolated from the leaves of *D. angustifolia*.

Table 6: Radical scavenging activities of flavonoids from the leaves of *D. angustifolia*

Tested samples	% Scavenging of DPPH at 10 µg/mL	IC_{50}
Pinocembrin	57	5.4
Santin	58	4.08
5,6,7-Trihydroxy-3,4'-dimethoxyflavone	70	4.37
5,7,4'-Trihydroxy-3,6-dimethoxyflavone	84	0.87
Ascorbic acid	90	0.45

Analysis were done in triplicates and the %scavenging of DPPH were reported as an average

The best radical scavenging activity was displayed by 5,7,4'-trihydroxy-3,6-dimethoxyflavone (**2**) in comparison with the others (Appendix 3) with its radical scavenging property comparable with ascorbic acid. This is most likely because of the fact that this compound has the right structural feature (hydroxyl at C-4') for free radical scavenging activity. Methylation and absence of hydroxy group in flavonoids at 4' position substantially reduce the antioxidant activity as observed in santin, pinocembrin and 5,6,7-trihydroxy-3,4'-dimethoxyflavone (Table 6, Appendix 3). The IC_{50} values of compounds isolated from *D. angustifolia* exhibited good correlation coefficients.

2.4. Conclusion

Six compounds, namely, pinocembrin (**86**), santin (**81**), 5,6,7-trihydroxy-3,4'-dimethoxyflavone (**125**), 5,7,4'-trihydroxy-3,6-dimetoxyflavone (**80**), 15,16-epoxy-2-hydroxy-3,13(16),14-clerodtriene-18-oic acid (**128**) and ent-16-hydroxy-labdan-3α,8β-dihydroxy,13(14)-en-15,16-olide (**114**) were isolated and characterized from the EtOAc soluble portion of the ethanol extract of the leaves of *D. angustifolia*. 5,6,7-Trihydroxy-3,4'-dimethoxyflavone (**125**) has not been reported before as a natural product. Activity guided antiplasmodial activity of the leaves of *D. angustifolia* led to the isolation and characterization of three active compounds: pinocembrin, santin, and

15,16-epoxy-2-hydroxy-3,13(16),14-clerodtriene-18-oic acid (**128**). The antiplasmodial activities of these compounds were significant compared to chloroquine hence accounting for the traditional use of this plant against malaria. All flavonoids isolated from the leaves of *D. angustifolia* exhibited pronounced radical scavenging activities with 5,7,4'-trihydroxy-3,6-dimetoxyflavone (**80**) identified to be the most active compound

2.5. Experimental

Plant material: *D. angustifolia* leaves were collected from Lideta Mariam, in November 2012, near the Russian Embassy, Addis Ababa. The plant specimen was identified by Mr. Melaku Wondafrash and a voucher specimen (TW001/2012) of the plant was deposited at the National Herbarium of Addis Ababa University, Addis Ababa, Ethiopia.

Reagents and Instruments: See section 1.5 (page 37)

Extraction and Isolation for Chemical Study

The ground leaves of *D. angustifolia* (150 g) were extracted with ethanol (750 mL) by shaking for 6 h with a mechanical shaker, filtered and concentrated using rotary evaporator at 40ºC to afford 25 g (16 %). The ethanol free semi solid material was defatted with n-hexane (150 mL) and the marc was extracted with EtOAc (150 mL) by shaking for 6 h, filtered and concentrated to afford 10 g (6%). The EtOAc soluble phase (6 g) was adsorbed on silica gel and subjected to silica gel (80 g) column chromatography. The column was eluted using petrol:EtOAc of increasing polarities to afford 30 fractions which were pooled together according to their TLC profile to eleven combined fractions as depicted in Table 7.

Table 7: Column chromatographic fractionation of the EtOAc extract of the leaves of *D. angustifolia*

Fractions	Eluent (ratio)	Volume of eluent in mL	Amount in mg
Fr1&2	100% petrol	100	450
Fr 3-5	petrol:EtOAc (9:1)	100	1000

Fr 6-10	petrol:EtOAc (9:1)	150	1000
Fr 11-13	petrol:EtOAc (4:1)	100	200
Fr 14	petrol:EtOAc (4:1)	50	80
Fr 15-18	petrol:EtOAc (7:3)	160	700
Fr 19-21	petrol:EtOAc (1:1)	160	250
Fr22-24	petrol:EtOAc (1:2)	100	100
Fr 25-26	petrol:EtOAc (1:3)	80	300
Fr 27&28	petrol:EtOAc (1:4)	80	150
Fr 29&30	100% EtOAc	80	150

Fraction 3-5 (700 mg) was adsorbed and applied on a silica gel (13 g) column. Elution was done first with petrol (10 mL, 20 mg, Fr1) and then petrol:EtOAc (9:1, 30 mL, 80 mg, Fr2&3; 4:1, 20 mL, 35 mg, Fr4; 1:1, 20 mL, 30 mg, Fr5; 2:3, 40 mL, 109 mg, Fr6&7; and 1:4, 10 mL, 80 mg, Fr8) of increasing polarities to afford eight subfractions. **Fraction 8** was identified to be **santin** (80 mg).

Fraction 6-10 (700 mg) was adsorbed and chromatographed over silica gel (17 g). Elution was done using petrol (10 mL, 10 mg, Fr1) first followed by gradient elution of petrol:EtOAc (9:1, 20 mL, 25 mg, Fr2; 4:1, 120 mL, 200 mg, Fr3; 3:2, 60 mL, 80 mg, Fr4; 3:2, 20 mL, 60 mg, Fr5; 1:1, 40 mL, 120 mg, **Fraction 6**) and ended with 100% EtOAc (40 mL, 68 mg, **Fraction 7**). The TLC (0.25 mm thick layer of silica gel on aluminum plate) profiles of Fraction 6 and Fraction 7 showed one similar spot identified as **santin** (188 mg).

Fraction 11-13 (100 mg) were dissolved in MeOH:$CHCl_3$ (1:1) and applied on Sephadex LH20 using MeOH:$CHCl_3$ (1:1) as eluent to afford seven fractions (each 5 mL). The sixth and seventh fractions showed one spot each on TLC (0.25 mm thick layer of silica gel on aluminum plate) and found to be **santin** (25 mg) and **pinocembrin** (12 mg), respectively.

Fraction 15-18 (500 mg) was adsorbed and applied on a silica gel (15 g) column. Gradient elution was conducted using petrol:EtOAc (9:1, 35 mL, 80 mg, Fr1; 4:1, 20 mL, 50 mg, Fr2; 3:2, 30 mL, 50 mg, Fr3; 1:1, 20 mL, 60 mg, **Fraction 4**; 2:3, 20 mL, 80 mg, Fr5; and 1:4, 20 mL, 80 mg,

Fraction 6) and ended using 100% EtOAc (20 mL, 112 mg, Fr7) to afford seven subfractions. On TLC examination, Fr4 and Fr6 showed one spot each on TLC(0.25 mm thick layer of silica gel on aluminum plate) which were identified as **santin (80 mg) and 15,16-epoxy-2-hydroxy-3,13(16),14-clerodtriene-18-oic acid (80 mg),** respectively. On the other hand, Fraction7 was suspended in $CHCl_3$ and filtered. The filtrate was concentrated to afford yellowish solid identified to be **3,5,7-trihydoxy-6,4'-dimethoxyflavone (18 mg)**.

Fraction 19-21 (250 mg) was adsorbed on silica gel and chromatographed over silica gel (12 g). Elution was done using petrol (20 mL, 20 mg, Fr1) first followed by petrol:EtOAc (9:1, 20 mL, 30 mg, Fr2; 4:1, 30 mL, 188 mg, **Fraction 3**; and 1:1, 60 mL, 68 mg, Fr4) to afford four subfractions. On eluting the fourth fraction a solid formed which was separated by decantation to afford **5,6,7-trihydroxy-3,4'-dimethoxyflavone** (**12 mg**). The third fraction was applied on Sephadex LH20 and eluted using MeOH:$CHCl_3$ (1:1, 10 mL each) to afford seven subfractions. The third and fourth subfractions were identified as **15,16-epoxy-2-hydroxy-3,13(16),14-clerodtriene-18-oic acid** (160 mg).

Fraction 25-26 (100 mg) was dissolved in $CHCl_3$:MeOH (1:1) and applied on Sephadex LH-20 and eluted with $CHCl_3$:MeOH (1:1) to afford seven fractions (each 10 mL). Fractions 2 and 3 were combined (30 mg) to afford **ent-16-hydroxy-labdan-3α,8β-dihydroxy,13(14)-en-15,16-olide** (**114)**. The flow sheet diagram showing the extraction and isolation of compounds from the leaves of *D. angustifolia* is depicted in Scheme 1.

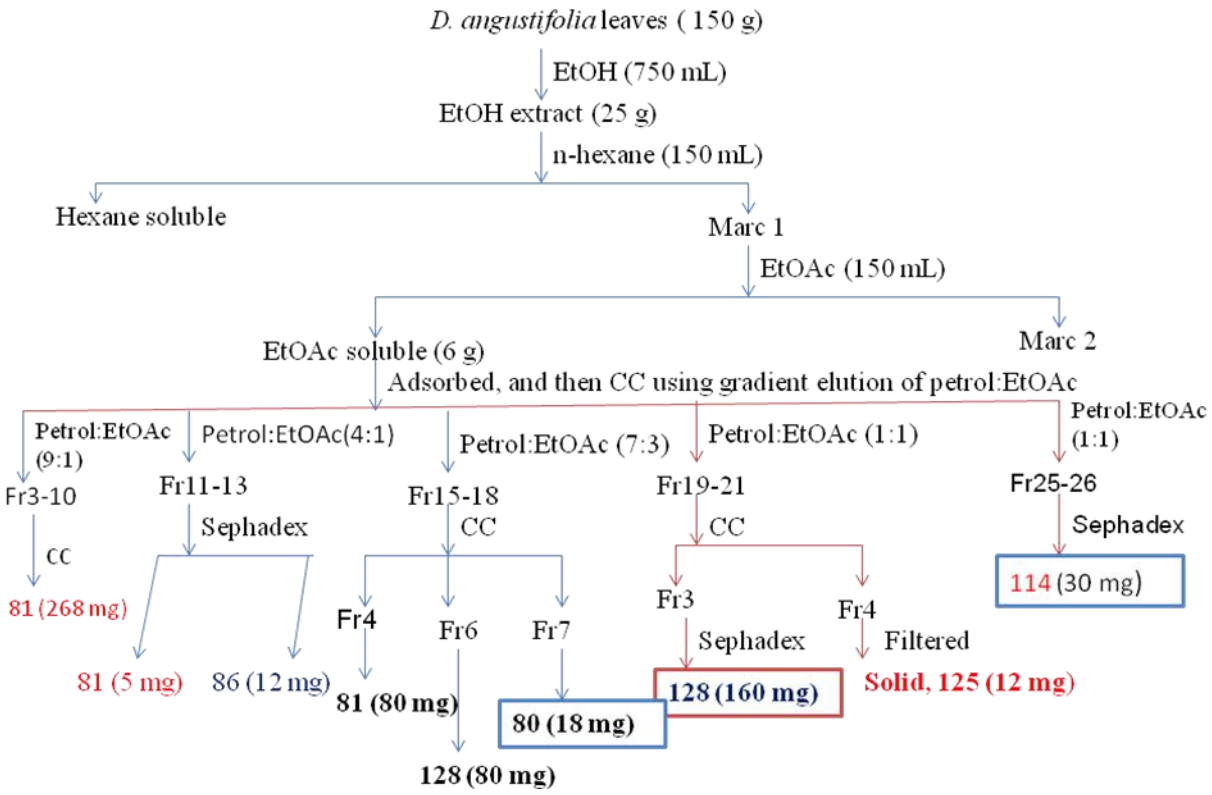

Scheme 1: Flow sheet diagram showing fractionation of EtOAc soluble portion of *D. angustifolia* leaves

Leaf Surface Extraction of *D. angustifolia*: Freshly cut *D. angustifolia* leaves (5 g) were individually dipped into a 100 mL beaker filled with acetone (40 mL) for 30 seconds with gentle swirling. Evaporation of the solvent using rotary evaporator gave a yellowish resin-like material (500 mg, 10%). The dried extract was re-dissolved in acetone and analyzed using silica gel TLC.

Extraction and Bioassay Guided Fractionation of the Leaves of *D. angustifolia*: The powdered leaves (100 g) of *D. angustifolia* were extracted with 80% aqueous MeOH by shaking for 6 h using mechanical shaker. The greenish filtrate obtained after filtration was diluted to 50% aqueous methanol solution and partitioned with ethyl acetate. The ethyl acetate soluble phase was dried over anhydrous Na_2SO_4, filtered and concentrated under reduced pressure to afford 4.5 g (4.5% with respect to dried plant material) dark green solid. It was adsorbed on silica gel and chromatographed over a silica gel (80 g) column packed with n-hexane. The column was eluted with hexane:EtOAc of increasing polarities to afford twenty seven fractions as shown in Table 8.

Table 8: Column chromatographic fractionation of the EtOAc soluble portion of the 70% aqueous EtOH extract of the leaves of *D. angustifolia*

Fractions	Eluent (ratio)	Volume of eluent in mL	Amount in mg
Fr1	100% hexane	20	30
Fr 2-4	hexane:EtOAc (4:1)	90	180
Fr 5-6	hexane:EtOAc (3:2)	60	400
Fr 7-8	hexane:EtOAc (3:2)	60	120
Fr 9-10	hexane:EtOAc (1:1)	60	80
Fr 11	hexane:EtOAc (2:3)	40	120
Fr 12-14	hexane:EtOAc (1:4)	90	120
Fr15	EtOAc	40	20
Fr 16-18	EtOAc	120	150
Fr 19-21	EtOAc	90	200
Fr 22-25	EtOAc	120	300
Fr 26-27	EtOAc	60	2

Bioassay result conducted traces the activities into four combined fractions (Fr7&8, Fr9&10, Fr11-15 and Fr19-21). Hence, Fr7&8 was suspended in petrol. Upon washing the petrol insoluble fraction with diethyl ether gave santin (40 mg) as yellow crystals. The diethyl ether soluble phase was concentrated and applied on Sephadex LH20 using MeOH:$CHCl_3$ (1:1) as eluent to afford pinocembrin (10 mg). The other active fraction, F9&10, was concentrated and dissolved in hot EtOAc:MeOH (1:1). The solid formed on addition of hexane was filtered to give 15,16-epoxy-2-hydroxy-3,13(16),14-clerodtriene-18-oic acid (30 mg). Likewise washing Fr11-15 and Fr19-21 with EtOAc:ether (1:1) gave 15,16-epoxy-2-hydroxy-3,13(16),14-clerodtriene-18-oic acid as a white solid. The extraction and isolation procedure is schematically shown in Scheme 2

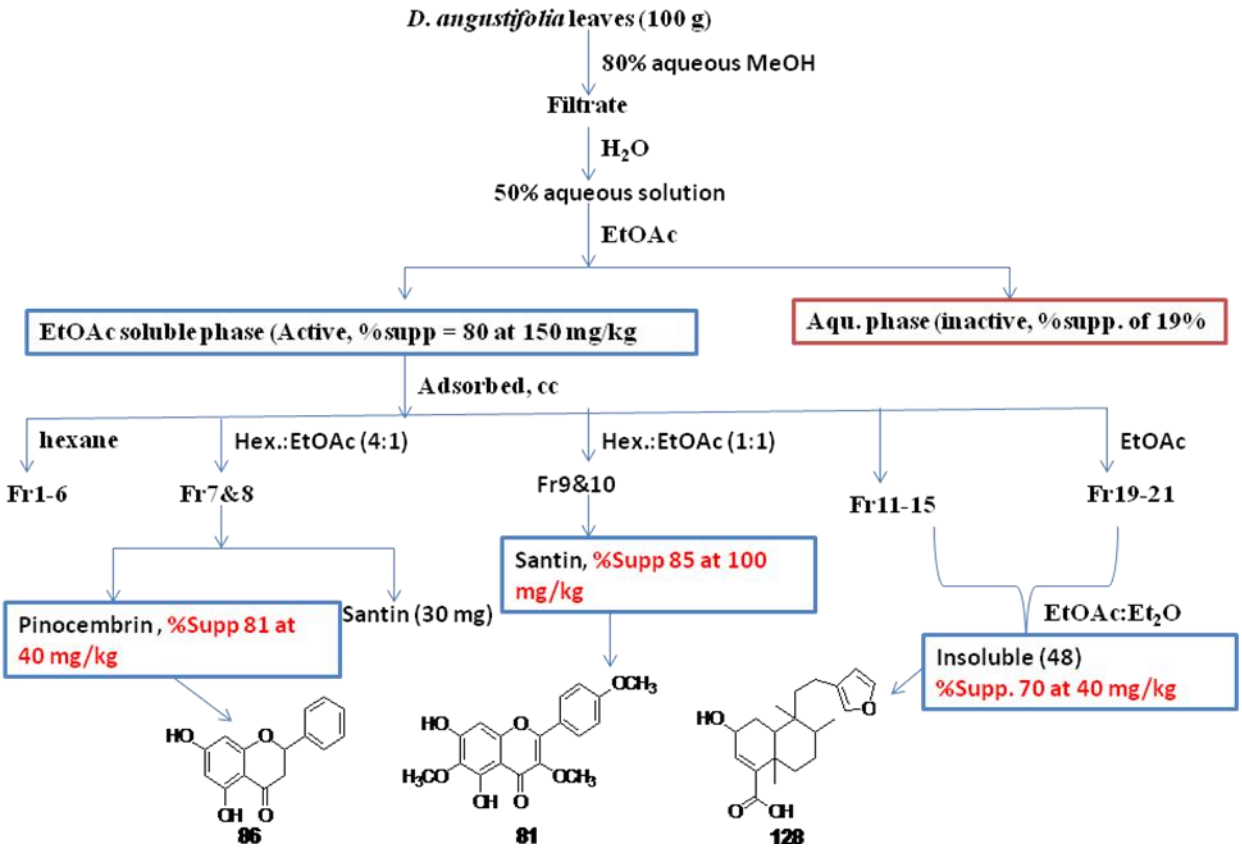

Scheme 2: Flow sheet diagram showing bioassay guided fractionation of the leaves of *D. angustifolia*

DPPH Radical Scavenging Assay: Performed in accordance with the procedure on page 45 and 46

Pinocembrin (86): yellow solid; soluble in $CHCl_3$, mp 190-191°C; $[\alpha]_{589}^{21}$ = -12.5 (c 0.4, EtOH); UV(MeOH) λ_{max} nm: 290, 333; TLC: Rf 0.65 (eluent EtOAc:petrol, 3:2); (-)-ESI-FT-MS: *m/z* 255.0663 (calcd 255.2538 for $C_{15}H_{11}O_4$), molecular formula $C_{15}H_{12}O_4$; ^{1}H NMR (400 MHz, $CDCl_3$): δ_H 2.6 (1H, *dd, J* = 17.20, 3.20, H-3), 2.91 (1H, *dd*, *J* = 17.20, 12.80, H-3), 5.25 (1H, *dd*, *J* = 12.8, 2.80, H-2), 5.82 (1H, *d*, *J* = 2.00, H-8), 5.83 (1H, *d*, *J* = 2.00, H-6), 7.26 (5H, *m*, H-2'-6'); ^{13}C NMR (100 MHz, $CDCl_3$): δ_C 195.6 (C-4), 166.8 (C-7), 163.7 (C-5), 163.0 (C-9), 138.8 (C-1'), δ 128.6 (C-2', 4' and 6'), 125.9 (C-3' and 5'), 102.2 (C-10), 96.3 (C-6), 95.4 (C-8), 78.9 (C-2) and 43.0 (C-3)

Santin (81): Yellow solid; soluble in methanol; mp 160-161°C; TLC: Rf 0.64 (mobile phase EtOAc:petrol, 3:2); UV (MeOH) λ_{max} nm: 271, 338; optically inactive; IR υ_{cm-1}: 1646 (C=O), C-O (1090), C-H (2924); (-)-ESI-FT-MS: *m/z* at 343.0858 (calcd 343.3154 for $C_{18}H_{15}O_7$), molecular formula $C_{18}H_{16}O_7$; ^{1}H NMR (400 MHz, $CDCl_3$): δ_H 3.86 (3H, *s,* OCH_3), 3.91 (3H, *s,* OCH_3), 4.05 (3H, *s,* OCH_3), 6.57 (1H, *s,* H-8), 7.03 (2H, *d*, *J* = 8.80, H-2' and 6'), 8.08 (2H, *d*, *J* = 8.80, H-3' and 5') and 12.9 (1H, *s,* 5-OH); ^{13}C NMR (100 MHz, $CDCl_3$) δ in ppm: δ_C 179.2 (C-4), 161.7 (C-4'), 156.1 (C-2), 155.0 (C-9), 152.2 (C-7), 151.8, 138.4 (C-3), 130.2 (C-2', 6'), 130.0 (C-6), 122.7 (C-1'), 114.1 (C-3', 5'), 106.2 (C-10), 93.2 (C-8), 60.1 (OCH_3), 60.9 (OCH_3) and 55.4 (OCH_3)

5,6,7-Trihydroxy-3,4'-dimethoxyflavone (125): Yellow solid; optically inactive; mp 226-229°C; TLC: Rf 0.50 (mobile phase EtOAc:petrol (3:2)); UV (MeOH) λ_{max} nm: 285, 348; (+)-ESI-FT-MS: *m/z* 331.0803 (calcd 331.2968 for $C_{17}H_{15}O_7$), the molecular formula $C_{17}H_{14}O_7$; ^{1}H NMR (400 MHz, CD_3COCD_3): δ_H 3.80 (3H, *s,* OCH_3), 3.90 (3H, *s,* OCH_3), 6.42 (1H, *s,* H-8), 7.12 (2H, *d*, *J* = 8.80, H-2' and 6'), 8.02 (2H, *d*, *J* = 8.80, H-3' and 5'), and 12.60 (1H, *s,* 5-OH); ^{13}C NMR (100 MHz, CD_3COCD_3) δ in ppm: δ_C 178.7 (C-4), 161.7 (C-4'), 155.8 (C-2), 152.8 (C-7), 149.7 (C-9), 146.7 (C-5), 138.2 (C-3), 130.0 (C-2', 6'), 128.5 (C-6), δ 123.0 (C-1'), 113.9 (C-3', 5'), 105.2 (C-10), δ 93.5 (C-8), 54.9 (OCH_3), 59.3 (OCH_3)

5,7,4'-Trihydroxy-3,6-dimethoxyflavone (80): Yellow solid; TLC: Rf 0.45 (mobile phase EtOAc:petrol (3:2)); ^{1}H NMR (400 MHz, $CDCl_3/CD_3OD$): δ_H 3.60 (3H, *s,* OCH_3), 3.70 (3H, *s,* OCH_3), 6.30 (1H, *s,* H-8), 6.70 (2H, *d*, *J* = 8.80, H-2' and 6') and δ 7.74 (2H, *d*, *J* = 8.80, H-3' and 5'); ^{13}C NMR (100 MHz, $CDCl_3/CD_3OD$) δ in ppm: δ_C 179.0 (C-4), 160.0 (C-2), 157.4 (C-5), 156.5 (C-7), 152.0 (C-4'), 138.0 (C-3), 131.0 (C-6), 130.0 (C-2', 6'), 115.2 (C-3', 5'), 105.0 (C-10), 94.0 (C-8), 59.9 (OCH_3) and 59.4 (OCH_3).

15,16-Epoxy-2-hydroxy-3,13(16),14-clerodtriene-18-oic acid (128): White solid; mp 145-147°C; TLC: Rf 0.35 (mobile phase EtOAc:petrol (3:2)); $[\alpha]_{589}^{21}$ = -17.5 (c 0.4, MeOH); (-)-ESI-FT-MS: *m/z* 331.1990 (calcd 331.4339 for $C_{20}H_{27}O_4$), molecular formula $C_{20}H_{28}O_4$; UV λ_{max} nm: 270, 333; IR $\upsilon_{cm-1:}$ 1690 (carboxyl), 3375 (O-H), 2962 (C-H) and 1027 (C-O); ^{1}H NMR (400 MHz, $CDCl_3/CD_3OD$): δ_H 1.98 (1H, *m*, H-1), 1.39 (1H, *m*, H-1), 4.30 (1H, *m*, H-2), 6.60 (1H, *m*, H-3), 1.12 (1H, *m*, H-6), 2.30 (1H, *m*, H-6), 1.46 (1H, *m*, H-7), 1.39 (1H, *m*, H-7), 1.51 (1H, *m*, H-8),

1.37 (1H, *m*, H-10), 1.51 (1H, *m*, H-11), 1.62 (1H, *m*, H-11), 2.10 (1H, *m*, H-12), 2.30 (1H, *m*, H-12), 6.25 (1H, *br s*, H-14), 7.30 (1H, *t*, *J* = 1.80, H-15), 7.20 (1H, *s*, H-16), 0.80 (3H, *d*, *J* = 6.40, H-17), 1.26 (3H, *s,* H-19), and 0.73 (3H, *s*, H-20); ^{13}C NMR (100 MHz, $CDCl_3/CD_3OD$) δ in ppm: δ_C 18.3 (C-20), 18.1 (C-12), 15.9 (C-17), 20.4 (C-19), 26.9 (C-7), 27.4 (C-1), 35.5 (C-6), 35.9 (C-8), 37.9 (C-5), 38.4 (C-9), 38.5 (C-11), 45.2 (C-10), 68.5 (C-3), 110.9 (C-14), 125.3 (C-13), 138.3 (C-16), 138.9 (-C-3), 142.7 (C-15), 143.3 (C-4) and 169.9 (C-18)

Ent-16-hydroxy-labdan-3*α*,8*β*-dihydroxy,13(14)-en-15,16-olide (114): TLC: Rf 0.20 (mobile phase EtOAc:petrol (3:2)); ^{1}H-NMR (400 MHz, DMSO-d6): δ_H 7.60 (1H, 16-OH), 7.00 (1H, *bro. s*, H-14), 6.00 (1H, *d, J* = 8.26 Hz, H-16), 3.00 (1H, H-3), 4.30 (1H, 3-OH), 3.90 (1H, 8-OH), 0.81 (1H, *dd*, *J* = 8.20 Hz and 1.92 Hz, H-5), 1.01 (1H, H-9), 1.69 (1H, *m*, H-7), 1.33 (1H, *m*, H-7), 1.58 (1H, *m,* H-1), 0.96 (1H, *m,* H-1), 1.29 (1H, *m*, H-11), 0.86 (1H, *m*, H-11), 0.89 (2H, H-12), 1.46 (2H, *m*, H-2), 1.55 (2H, *m*, H-6), 1.00 (3H, *s*, H-17), 0.89 (3H, *s*, H-18), 0.72 (3H, *s*, H-20) and 0.65 (3H, *s*, H-19); ^{13}C-NMR (100 MHz, DMSO-d6) δ in ppm: δ_C 172.2 (C-15), 145.7 (C-14), 136.8 (C-13), 97.6 (C-16), 77.2 (C-3), 72.5 (C-8), 60.8 (C-9), 55.1 (C-5), 44.4 (C-7), 38.9 (C-4), 38.6 (C-10), 37.9 (C-1), 28.7 (C-18), 28.3 (C-12), 27.3 (C-2), 24.0 (C-17), 23.2 (C-11), 20.2 (C-6), 16.1 (C-19) and 15.7 (C-20).

Part 3

Comparative Chemical Studies of *Moringa stenopetala* and *Moringa oleifera*

3.1. Introduction

3.1.1. The family Moringaceae and the genus *Moringa*

The family Moringaceae is a monotypic family that contains only one genus known as *Moringa* [144]. The genus *Moringa* comprises 14 species confined to Asia and Africa. These are *M. pterygosperma*, *M. oleifera*, *M. arborea*, *M. borziana*, *M. concanensis*, *M. drouhadii*, *M. hildebrandtii*, *M. longituba*, *M. ovalifolia*, *M. peregrina*, *M. pygmaea*, *M. rivae*, *M. ruspoliana* and *M. stenopetala* [145]. Two of the fourteen *Moringa* species occur in Asia including the widely cultivated *M. oleifera* [146]. Twelve species of *Moringa* are known to occur in Africa [146], of which six are found in Ethiopia, namely, *M. arborea*, *M. borziana*, *M. longituba*, *M. rivae*, *M. ruspoliana* and *M. stenopetala* [146].

The Asian *M. oleifera* is the most well known and widely distributed species. *M. stenopetala*, originating from Ethiopia, is the second most prominent *Moringa* species in terms of its economic and medicinal uses. Although there is huge body of scientific and other information on *M. oleifera*, there is only one report [147] to our knowledge that dwells on the comparison of these two species with respect to their main chemical constituents. Our work reported here is a further contribution that compares the nature and level of the main chemical constituents present in the two *Moringa* species.

3.1.1.1. *Moringa oleifera*

M. oleifera is the best known species of the genus which is widely cultivated in India [148]. It has also been introduced throughout the tropics and subtropics including in many African countries. The plant is commonly named as Drumstick Tree (from the appearance of the seedpods), Ben Oil Tree (from its pressed seed oil), and Horseradish Tree (from the taste of the roots which resembles horseradish and because its roots are used as horseradish substitute). *M. oleifera* is a small or medium sized tree, about 10 m high [148]. The bark is white, grey or pale brown. The branches bear two or three pinnate leaves. It is drought tolerant and grows best in the hot, semi-arid tropics with rainfalls of 250-1500 mm and altitude of less than 1000 m

Every part of *M. oleifera* tree is said to have beneficial properties. It has long been known in folk medicine as having extraordinary properties [149] including treatment of heart complaints, eye diseases, tumors, and earache [150]. There is ample evidence in the literature showing the plant to have a wide array of biological activities including anti-tumor [151-155], anti-hyperglycemic [156-159], antimalarial [160], antioxidant [153-155], anti-inflammatory [161-163], antifungal [164], and antibacterial [149].

M. oleifera is among the most nutritious trees in the world with all parts except the wood are edible [165-167]. Nutritional analyses showed that the leaves offer great varieties of nutrients including proteins [165, 168-170] with all standard twenty amino acids [166]. The leaves of *M. oleifera* are outstanding as a source of vitamin A and vitamin C [169, 171]. It provides considerable quantities of macro nutrients (Ca, P, Na, K, and Mg) and micronutrients (Mn, Cu, Fe, and Zn) [167, 172]. The seeds are good water clarifying agents [173]. The active agents playing a role in the water purifying properties of *Moringa* species are reported to be basic cationic polypeptides [174] which attract predominantly negatively charged particles such as clay, silk, and other toxic particles in water. Flocculation process occurs when peptides bind the negative charges forming flocs through the aggregation of particles in the water.

3.1.1.2 *Moringa stenopetala*

M. stenopetala, a tree growing to 12 m high, is endemic to East Africa mainly southern Ethiopia, Somalia and northern Kenya. It is the second most important domesticated *Moringa* species after *M. oleifera* which is known by different names including Cabbage Tree (English), Shiferaw (Amharic), Aleko (Gamo Gofa), Shalkayda (Konso), Haleko (Burji, Derashe), and Halakwa (Wollayta) [175]. The species occurs in southern Ethiopia between 500 and 1600 m. The leaves, seeds and pods of *M. stenopetala* are larger in contrast to *M. oleifera*. On the other hand pods of *M. stenopetala* have twisted shape while those of *M. oleifera* are straight.

M. stenopetala is a highly valued plant cultivated in home gardens in southern Ethiopia where the leaves are eaten as vegetables [176]. The flowers of *M. stenopetala* can be eaten or used to make tea [169]. Beside the nutritional aspect of *M. stenopetala*, the plant is traditionally used for the treatment of different ailments such as malaria, hypertension, and some other problems like asthma

and diabetes. It is also used to heal stomach-ache and expel retaining placenta in women [177]. Pharmacological reports showed that the leaves of *M. stenopetala* showed anti-leishmanial [178], antispasmodic [177], anti-hyperglycemic [157-159], antibacterial [149], and blood pressure lowering properties [179]. Nutritionally, different parts of *M. stenopetala* have been shown to have a wealth of essential and disease-preventing nutrients comparable with *M. oleifera* [167, 168, 172]. The seedcake powder is recommended for water treatment through coagulation [168]. Its water clarifying property is more effective than *M. oleifera* [168]. Furthermore *Moringa* seedcake can also be used to reduce the incidence of water borne diseases such as diarrheal diseases, and its effectiveness is related to the glucosinolate profile [180].

3.1.1.3. Review of the Chemistry of the Genus *Moringa*

Literature survey of the previous phytochemical studies on the genus *Moringa* shows that the plant is rich in alkaloids, flavonoids, glycosides, phenolics, glucosinolates, isothiocyanate, steroids, triglycerides and fatty acids. So far, over 60 compounds have been reported from *M. oleifera* and *M. stenopetala*. The most structurally unique compounds reported from the genus are carbamates/thiocarbamates and glucosinolate with the latter producing isothiocyanates on hydrolysis (mustard oils). A complete list of compounds reported so far from the genus *Moringa* is given in Table 1

Table 1: List of compounds from *Moringa* organized by compound class

Cpd class	Cpd name	Str. No	Plant source	Plant part	Ref
Alkaloids	Moringine	**130**	*M.o*	RB	[157]
	Pyrrolemarumine 4-O-*α*-L-rhamnopyranoside	**131**	*M.o*	RT	[181]
Amide	Marumoside A	**132**	"	LF	[162]
	Marumoside B	**133**	"	LF	[162]
	Aurantiamide acetate	**134**	"	"	[162]
Carbamate/thiocarbamate	*E*)-*O*-cyano 4-(R-L-rhamnosyloxy)-benzenethiocarbamate	**135**	"	Pod	[181]
	E)-*O*-cyano-4-(O-acethyl-R-L-rhamnosyloxy)benzenethiocarbamate	**136**	"	"	[181]
	Benzyl thiocarbamate	**137**	"	"	[181]
	4-(*α*-L-rhamnopyranosyloxy) benzylcarbamate	**138**	"	LF	[181]
	O-Methyl-4-(4'-O-acethyl-*α*-L-rha mnosyloxy)benzyl thiocarbamate	**139**	"	SD	[182]
	Benzylcarbamothioethionate	**140**	"	RB	[182]
	O-ethyl-4-(α-L-rhamnosyloxy)benzyl carbamate	**141**	"	SD	[151]
	4 (α-L-rhamnosyloxy) benzyl isothiocyanate	**142**	"	"	[151]
	Niazimicin	**143**	"	"	[151]
	Niazirin	**144**	"	"	[151]
	Niazinin	**145**	"	"	[151]
Esters	*n*-Heptacosanyl n-octadec-9, 12,15-trieneonate	**146**	"	SB	[182]
	n-Docas-4-en-11-one-1-yl-n-decanoate	**147**	"	"	[182]
	1,3-Dilinoleoyl-2-olein	**148**	*M.s*	RT	[183]
	1,3-Dioleoyl-2-linolein	**149**	"	"	[183]
Fatty acids	Palmitic acid	**78**	"	RW	[184]
	Oleic acid	**150**	"	"	[184]
	Octacosanoic acid	**151**	*M.o*	SD	[184]
	Stearic acid	**77**	*Mo/M.s*	"	[185,186]
	Linoleic acid	**152**	"	"	"
	Arachidic acid	**76**	"	"	"
	Gadoleic acid	**153**	"	"	"
	Behenic acid	**75**	"	"	"
Flavonoids	Kaempferol	**154**	*M.o*	LF	[187]
	Rhamnetin	**155**	"	"	[187]
	3-Hydroxy-4-phenylchromenone	**156**	"	"	[187]
	Quercetin	**157**	"	"	[157]
Fla. Gly.	Kaempferitrin	**158**	"	"	[187]
	Isoquercitrin	**159**	"	"	[187]
	D-(6''-O-malonyl)-glucoside	**160**	"	"	[187]
	Astragalin	**161**	"	"	[187]

Table 1 continued

	Kaempferol 3-O-*β*-D-(6’’-O-malonyl)-glucoside	**162**	“	“	[187]
	Rutin	**163**	*M.s*	LF	[188]
Glucosinolate	4-(*α*-L-rhamnopyranosyloxy) benzyl glucosinolate	**164**	*M.o/M.s*	“	[179]
Hydrocarbon	*n*-Octacosane	**165**	*M.o*	“	[184]
Isothiocyanate	Isothiocyanatomethylbenzene	**166**	*M.o*	“	[182, 189]
	4-(4’-O-acethyl-α-L-rhamno- syloxy)-benzylisothiocyanate	**167**	“	“	[182]
	4-(*α*-L-rhamnopyranosyloxy)-benzylisothiocyanate	**168**	*M.o/M.s*	SD/LF	[182, 189]
	4-(*β*-D-glucopyranosyl-1→4-*α*-L-rhamnopyranosyloxy)-benzyl isothiocyanate	**169**	*M.o*	“	[182]
	4-(4’-O-acethyl-*α*-L-rhamnosyloxy)-benzaldehyde	**170**	*M.s*	LF	[188]
Nitrile	Niazirin	**171**	*M.o*	Pod	[190]
	Niaziridin	**172**	“	“	[190]
	15-Cyano-pentadecanoic acid methyl ester	**173**	“	“	[191]
Phenolics	4-Hydroxyphenyl acetic acid	**174**	*M.o*	SD	[182]
	4-O-(4-O-*α*-D-glucopyranosyl) caffeoyl quinic acids	**175**	“	LF	[187]
	4-O-(3-O-*α*-D-glucopyranosyl) caffeoyl quinic acids	**176**	“	“	[187]
	Chlorogenic acid	**177**	“	“	[187]
	4-O-Caffeoyl quinic acid	**178**	“	“	[187]
	5-O-Caffeoyl quinic acid	**179**	“	“	[187]
Steroids	*β*-Sitosterol	**180**	*M.s*	RW	[184]
	3-*O*-(6’-*O*-oleoyl-*β*-D-glucopyranosyl)-*β*-sitosterol	**181**	*M.o*	SD	[192]
	Sitosterol-3-*O*-*β*-D-glucopyranoside	**64**	*M.o/M.p*	“	[192, 193]
Miscellaneous	Nitrile	**182**	*M.o*		[157]
	Thiocyante	**183**	“		[157]
	Isothiocyanate	**184**	“		[157]

M.s: *M. stenopetala*; *M.o*: *M. oleifera*; *M.p*: *M. peregrina*; LF: leaf; SD: seeds; RT: root; RW: root wood; RB: root bark; SB: stem bark; Cpd: compound; Fla. Gly.: Flavonoid Glycosides

The chemical structures of compounds so far reported from *M. oleifera* (53 compounds) and *M. stenopetala* (13 compounds) are given as follows

Alkaloids and amides [157, 162]

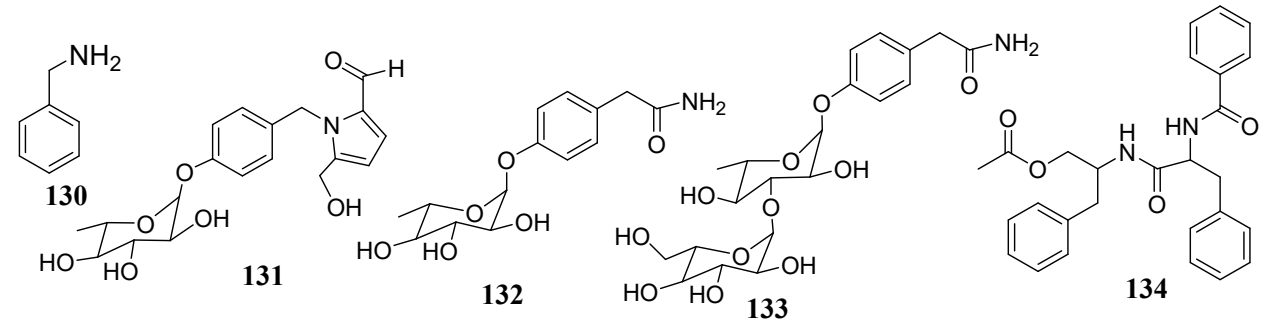

Carbamates and thiocarbamate glycosides [151, 182, 183]

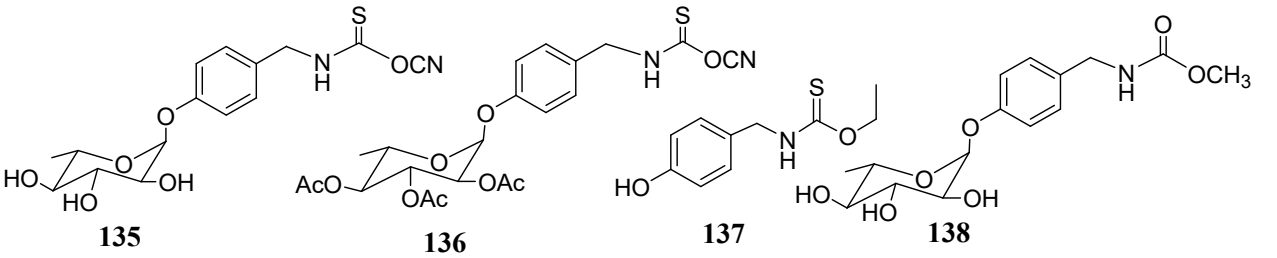

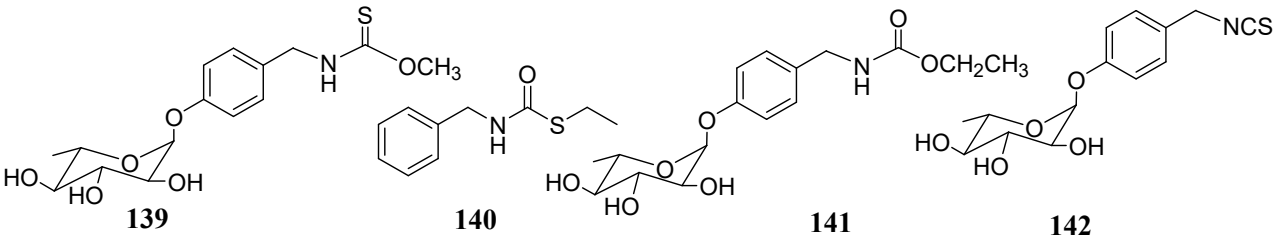

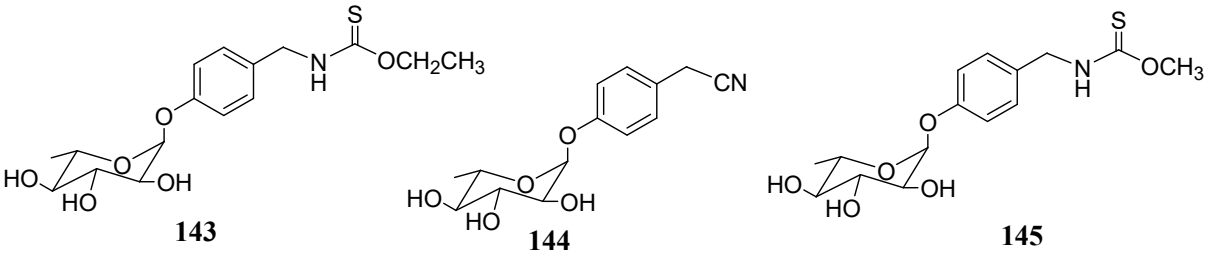

Esters/triglycerides [182, 183]

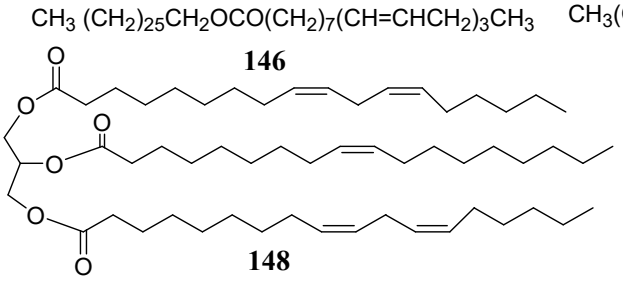

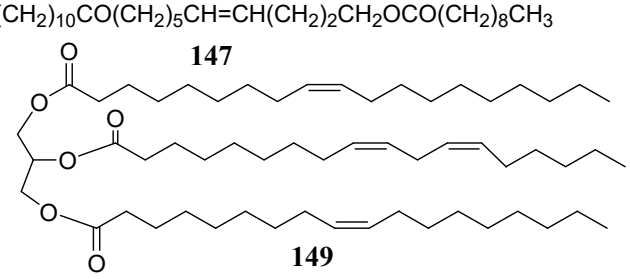

Fatty acids [184-186]

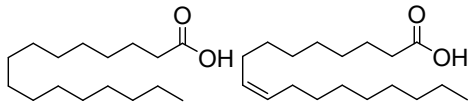

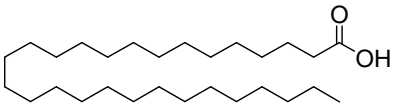

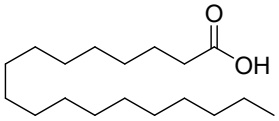

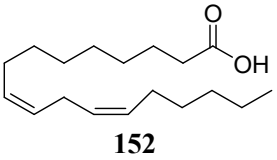

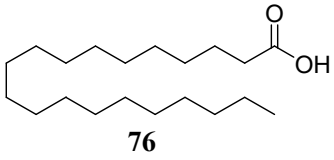

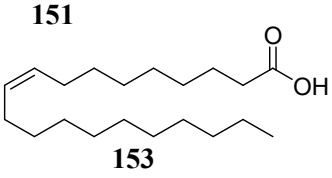

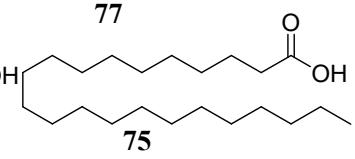

Flavonoids and flavonoid glycosides [187, 188]

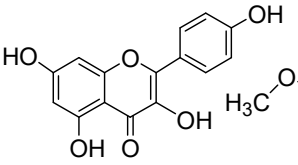

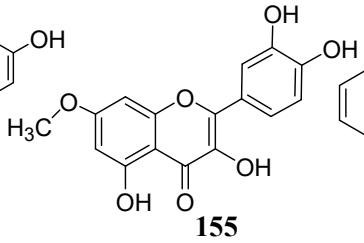

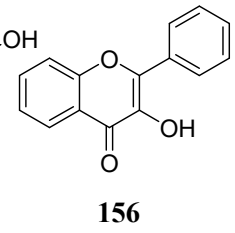

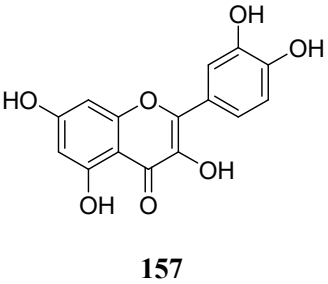

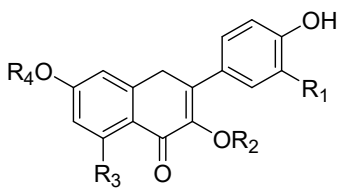

158 R_1 = OH, R_2 = rham, R_3 = H, R_4 = rham
159 R_1 = OH, R_2 = Glu, R_3 = OH, R_4 = H
160 R_1 = OH, R_2= Glu-malonyl, R_3 = OH, R_4 = H
161. R_1 = H, R_2 = Glu, R_3 = OH, R_4 = H
162. R_1 = H, R_2 = Glu-malonyl, R_3 = OH, R_4 = H
163. R_1 = OH, R_2 = Glu-rham, R_3 = OH, R_4 = H

Glucosinolate and Hydrocarbon [179, 184]

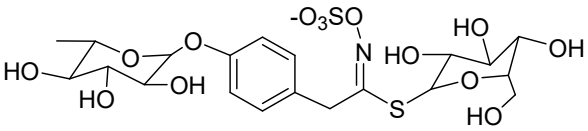

164

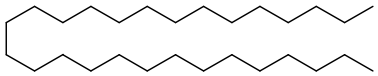

165

Isothiocyanates [182, 188, 189]

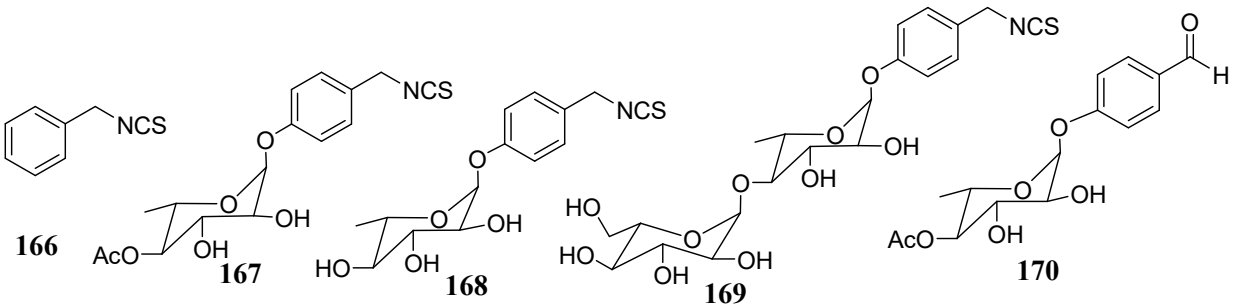

166 **167** **168** **169** **170**

Nitriles and Phenolics [180, 182, 187, 190, 191]

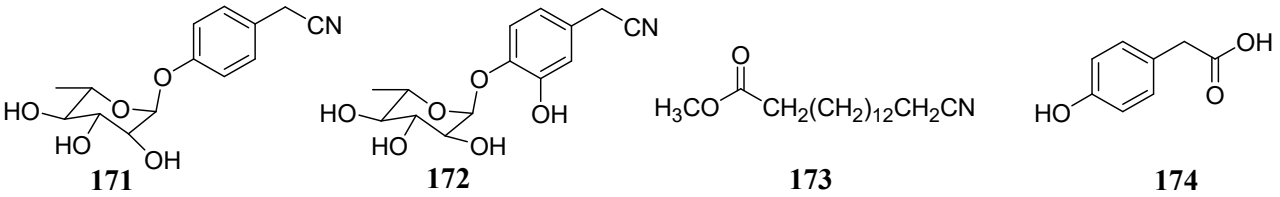

171 **172** **173** **174**

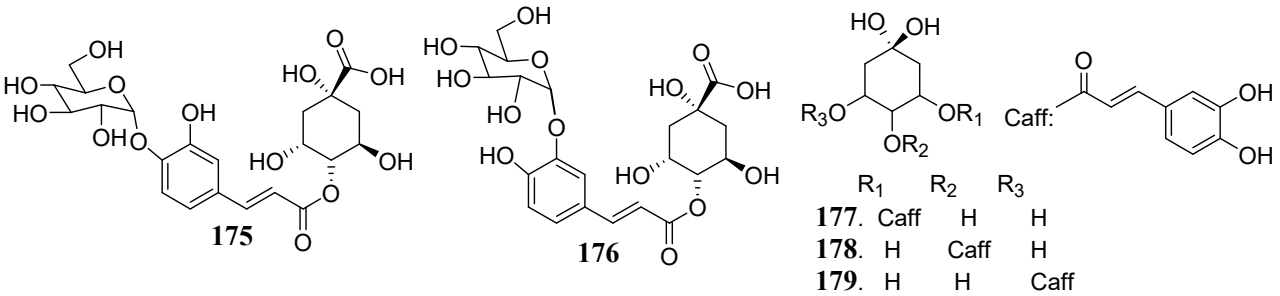

175 **176**

	R_1	R_2	R_3
177.	Caff	H	H
178.	H	Caff	H
179.	H	H	Caff

Steroids and other miscellaneous compounds [157, 184, 192, 193]

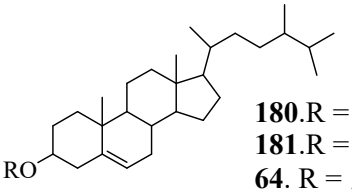

180.R = H
181.R = 6'-O-oleoyl-β-D-glucopyranosyl
64. R = β-D-glucopyranosyl

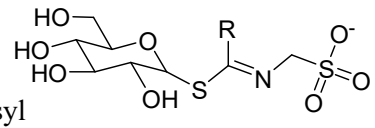

182 R= $-C\equiv N$
183 R= $-S-C\equiv N$
184 R= $-N=C=S$

The demand for the leaves and seeds of the two *Moringa* species is increasing because of the outstanding nutritional and medicinal applications. There is considerable interest among the public who also demand to know if there are scientific bases on the increasing popularity of the two species. In spite of the fact that *M. stenopetala* is known for its pharmacological, nutritional and water clarification properties, little work has been done on its chemistry. The main aim of this work was to contribute to the chemical study of the leaves and seeds of *M. stenopetala*. This has then led us to embark on the comparison of the chemical constituents of *M. stenopetala* with the better known *M. oleifera.* Our results not only help to distinguish the two species by relying on their respective diagnostic markers but could also aid in quality control of both species. Furthermore, while the antioxidant activities of *M. oleifera* are well documented in the literature [152, 153], there is no report describing the antioxidant potential of the leaves of *M. stenopetala*. Hence, the radical scavenging and anti-lipid per-oxidation potential of the extracts of *M. stenopetala* are reported here for the first time.

3.2. Objectives

The main objectives of this work are to

1. isolate and characterize marker compounds from the leaves of the two *Moringa* species
2. develop TLC, UV and HPLC-MS profiles of the leaves of *M. stenopetala* and *M. oleifera*
3. determine the level of rutin in the leaves of *M. stenopetala*
4. isolate and characterize compounds from the leaves and seeds of *M. stenopetala*
5. evaluate the radical scavenging and anti-lipid per-oxidation potential of the extract and constituents of the leaves of *M. stenopetala*

3.3. Results and Discussion

The extracts of the leaves of the two *Moringa* species, *M. stenopetala* and *M. oleifera*, were compared using TLC, HPLC-MS, and UV-Vis spectrophotometry. The results obtained in this work showed significant differences in the chemical profiles of the extracts of the leaves of the two species. Three flavonoid glycosides, one from *M. stenopetala* and two from *M. oleifera*, were isolated and characterized. Analysis of the extract of *M. stenopetala* leaves revealed the presence of rutin (**163**), which however was not observed in the extracts of *M. oleifera* leaves in consistence with previous literature report [147]. On the other hand quercetin-3-O-*β*-D-glucoside (**159**) and kaempferol-3-O-*β*-D-glucoside (**161**) were identified from the leaves of *M. oleifera* but not in the leaves of *M. stenopetala*. Furthermore the leaves of the two *Moringa* species were found to have one common compound, namely, sitosterol-3-O-*β*-D-glucoside (**64**)

High performance thin layer chromatographic (HPTLC) method for the quantitative determination of rutin in *M. stenopetala* leaves was developed and validated. Results showed that the amount of rutin in the 70% aqueous ethanol extracts of the leaves of *M. stenopetala* was found to be 1.9±0.08%. The level of rutin obtained using UV-Vis spectrophotometry (1.8%) and isolation (1.9%) were found in close agreement with the results obtained using HPTLC. The complete structure elucidations of flavonoid glycosides, fingerprint analysis of the leaves of *M. stenopetala* and *M. oleifera*, and quantification of rutin in the leaves of *M. stenopetala* are described below.

3.3.1. Isolation and Characterization of Marker Compounds from the Leaves of *M. stenopetala* and *M. oleifera*

Column chromatographic fractionation of the 70% aqueous ethanol extract of the leaves of *M. oleifera* over Diaion HP-20 followed by silica gel column chromatography afforded three glycosides: quercetin-3-O-*β*-D-glucoside (**159**), kaempferol-3-O-*β*-D-glucoside (**161**) and sitosterol-3-O-*β*-D-glucoside (**64**). Diaion HP-20 is composed of styrene-divinyl benzene copolymers used as traps for organic compounds containing double bond(s) and/or aromatic groups [194] on washing the column with water while those without such groups are eluted through the column. On the other hand the 70% aqueous ethanol extract of the leaves of *M. stenopetala* furnished rutin (**163**) as the major constituent.

Rutin (163)

Compound **163** was obtained as yellow solid and was recrystalized from methanol, mp 189-191^{o}C (Lit. 187-190^{o}C) [188]. The TLC Rf value was 0.50 on a 0.25 mm thick layer of silica gel on aluminum plate eluted with EtOAc:MeOH (3:2) as eluent. It was visualized after spraying with fast blue B salt. The compound was optically active with $[\alpha]_{589}^{21}$ = +3.50 (c 0.4, EtOH). The UV-Vis spectrum (MeOH) showed absorption maxima at 260 and 357 nm which are features of flavonols with the 3-OH substituted. The IR spectrum of compound **163** showed an absorption band at 3428 cm^{-1} due to the presence of hydroxyl group. The absorption band at 1653 cm^{-1} is attributed to chelated α,β-unsaturated carbonyl demonstrating the presence of 5-OH group. The negative mode ESI-FT-MS displayed molecular ion peak at *m/z* 609.1451 (calcd 609.5095 for $C_{27}H_{29}O_{16}$) compatible with the molecular formula $C_{27}H_{30}O_{16}$ which is in agreement with the ^{13}C-NMR which showed carbon resonances of twenty seven carbon atoms. Other prominent peaks observed in the mass spectrum of compound **163** were at *m/z* 465 and 302 presumably due to the sequential losses of two hexose sugars from the parent ion establishing the aglycone as quercetin.

With the aim to confirm the identity of the aglycone, compound **163** was subjected to acid hydrolysis which gave a yellowish solid (20%) identified to be compound **157**. The TLC Rf value was 0.7 on a 0.25 mm thick layer of silica gel on aluminum plate using EtOAc as eluent. It was visualized as yellow spot after spraying with vanillin/H_2SO_4. The UV-Vis spectrum (MeOH) of compound **157** demonstrated absorption maxima at 255 and 372 nm suggesting flavonoid chromophore with the 3-OH unsubstituted. The $[\alpha]_{589}^{21}$ = 0.00 (c 0.4, EtOH) suggesting **157** is achiral. The IR spectral analysis of compound **157** showed the presence of a hydroxyl stretching band at 3391 cm^{-1}. The (+)-ESI-FT-MS of compound **157** displayed *m/z* at 303.0510 (calcd 303.2436 for $C_{15}H_{11}O_7$) corresponding to the molecular formula $C_{15}H_{10}O_7$.

The ^{1}H-NMR spectrum of compound **157** showed a signal at δ 12.20 (1H, *s*) due to chelated hydroxy group which is in agreement with the presence of 5-OH. The three aromatic proton signals at δ 7.84 (1H, *d*, *J* = 2.00 Hz, H-2'), 7.71 (1H, *dd*, *J* = 8.80 Hz and 2.00 Hz, H-6'), and 7.00 (1H, *d*, *J* = 9.2 Hz, H-5') are typical of a flavonoid with 3',4'-disubstituted B ring. The other

aromatic proton signals at δ 6.53 (1H, *d*, *J* = 1.60 Hz, H-8) and 6.27 (1H, *d*, *J* = 1.60 Hz, H-6) are apparently due to *meta* coupled protons on the A-ring of flavonoid.

The proton decoupled ^{13}C-NMR spectrum combined with DEPT-135 of compound **157** revealed the presence of only five methine and ten quaternary carbons (Table 2). The presence of an α,β-unsaturated ketone is evident from the appearance of the carbonyl carbon signal at δ 175.6. The NMR spectral data of compound **157** was compared with that reported in the literature for quercetin (Table 2).

Table 2: The ^{1}H- and^{13}C-NMR spectral data of **157** and the reported data for quercetin (δ in ppm, *J* in Hz) [195]

NMR spectral data of compound **157** (CD_3COCD_3)			Data reported for quercetin (DMSO-d6) [195]	
Position	^{13}C-NMR	^{1}H-NMR	^{13}C-NMR	^{1}H-NMR
2	146.1	-	147.9	-
3	135.8	-	137.2	-
4	175.7	-	177.3	-
5	161.1	-	162.5	-
6	98.2	6.27 (1H, *d*, *J* = 1.60)	99.3	6.17 (1H, *d*, *J* = 2.00)
7	165.1	-	165.7	-
8	93.5	6.53 (1H, *d*, *J* = 1.60)	94.4	6.37 (1H, *d*, *J* = 2.00)
9	156.9		158.0	
10	103.2		104.4	
1’	122.8		124.1	
2’	114.8	7.84 (1H, *d*, *J* = 2.00)	116.0	7.73 (1H, *d*, *J* = 2.00)
3’	144.9		146.2	
4’	147.4		148.7	
5’	115.3	7.00 (1H, *d*, *J* = 9.20)	116.2	6.87 (1H, *d*, *J* = 8.00)
6’	120.5	7.71 (1H, *dd*, *J* = 8.8, 2.00)	121.0	7.62 (1H, *dd*, *J* = 2.0, 7.50)

The physical and spectral data of compound **157** are in close agreement with the data reported in the literature for quercetin [195]. The above NMR spectral results substantiate the mass spectral analysis of compound **157** indicating that the aglycone of compound **163** is quercetin.

The ^{1}H-NMR spectrum of compound **163** showed a singlet at 12.60 (1H) due to chelated hydroxy group. The proton signals observed in the aromatic region at δ 7.54 (1H, *dd, J* = 8.24, 2.40 Hz), 7.50 (1H, *d*, 2.40 Hz) and 6.84 (1H, *d*, *J* = 8.24 Hz) are ascribed to H-6', H-2', and H-5', respectively. The two doublets observed at δ 6.30 (1H, *d*, *J* = 2.10 Hz, H-8) and 6.20 (1H, *d*, *J* = 2.10 Hz, H-6) are characteristic of a phloroglucinol-type A-ring in a flavonoid. The two doublets at δ 5.35 (1H, *d*, *J* = 7.83 Hz) and 4.38 (1H, *bro. s*) are assigned for the anomeric protons of the glucose, H-1''and rhamnose H-1''' moieties, respectively. The latter signal along with the doublet observed at δ 0.97 (3H, *J* = 6.09 Hz) for a secondary methyl group were evident for the presence of rhamnopyranose moiety. On the basis of its coupling constant, the configuration of the glucose moiety was established as β [196, 197]. The spectrum also exhibited a series of peaks in the region between 4.00-3.00 accounting for the presence of sugar moieties. The signal at δ 5.14, 4.60 and 4.45 are due to protons on the oxygen atoms of hydroxyl groups in the structure of the compound.

The proton decoupled ^{13}C-NMR together with the DEPT-135 spectrum of compound **163** displayed ten quaternary, one methyl, one methylene and fifteen methine carbons. The downfield signal at δ 177.7 (C-4) suggested the presence of an α,β-unsaturated carbonyl group in agreement with the FT-IR spectrum of the compound. Other signals in the ^{13}C-NMR spectrum were observed at δ 156.8 (C-5), 161.6 (C-7), 157.0 (C-2), 164.4 (C-9), 148.8 (C-4'), 145.1 (C-3'), 133.7 (C-3), 122.0 (C-6'), 121.5 (C-1'), 116.6 (C-2'), 115.6 (C-5'), 104.3 (C-10), 99.1 (C-6) and 94.0 (C-8). A series of signals in the region between δ 80.0 to 67.4 combined with the signals at δ 101.5 (C-1''), 101.1 (C-1''') and 18.2 (C-6''') are evident for the presence of two sugar units. The methyl signal at δ 18.2 further supports the presence of a rhamnose group in compound **163**.

A long range ^{1}H/^{13}C-NMR correlation was observed between the proton signal at δ 6.20 (H-6) with the carbon signal at δ 156.8 (C-5), 161.6 (C-7), 94.0 (C-8) and 104.3 (C-10) justifying the location of these carbons on ring A of a flavonoid. H-8 showed HMBC correlations with C-7 (δ 161.6), C-9

(*δ* 164.4), C-6 (*δ* 99.1) and C-10 (*δ* 104.3). H-2' correlates with C-2 indicating that ring C is connected to ring B of the flavonoid skeleton through C-2 (*δ* 157.0). H-5' showed HMBC cross peaks with C-6', C-3' and C-1' while H-6' correlates with C-1', C-2', C-4' and C-5' which confirm the presence of these carbons on the same ring of the flavonoid. The NMR spectral data of compound **163** were compared with that reported in the literature for rutin (Table 3) [188].

Table 3: The ^{1}H- and^{13}C-NMR spectral data of compound **163** and that reported in the literature for rutin [188, 198]

Position	NMR data of compound **163** (DMSO-d6)		Data reported for rutin (DMSO-d6)	
	^{1}H-NMR	^{13}C-NMR	^{1}H-NMR	^{13}C-NMR
2	-	157.0		157.3
3	-	133.7		134.1
4	-	177.4		178.2
5	12.60 (1H, *s*, 5-OH)	156.8	12.60 (1H, *s*, 5-OH)	157.5
6	6.20 (1H, *d*, *J* = 2.10)	99.1	6.18 (1H, *d*)	99.5
7	-	161.6		164.9
8	6.30 (1H, *d*, *J* = 2.10)	94.8	6.38 (1H, *d*)	94.5
9	-	164.4		162.1
10	-	104.3		104.8
1'	-	121.5		122.5
2'	7.50 (1H, *d*, *J* = 2.40)	116.6	7.56 (1H, *d*)	116.1
3'	-	145.1		145.6
4'	-	148.8		149.3
5'	6.84 (1H, *d*, *J* = 8.24)	115.6	6.84 (1H, *d*)	117.1
6'	7.54 (1H, *dd, J* = 8.24, 2.40)	122.0	7.56 (1H, *d*)	122.0
1''	5.35 (1H, *d*, *J* = 7.83)	101.5	5.34 (1H, *d*)	101.6

Table 3 continued

Position	NMR data of compound **163** (DMSO-d6)		Data reported for rutin **(**DMSO-d6)	
	^{1}H-NMR	^{13}C-NMR	^{1}H-NMR	^{13}C-NMR
2''	3.22 (1H, *m*)	74.5		74.9
3''	3.28 (1H, *m*)	76.3		77.3
4''	3.39 (1H, *m*)	70.4		72.7
5''	3.21 (1H, *m*)	76.8		76.7
6''	3.69 (1H, *d*) & 3.25 (1H, *m*)	67.4		67.9
1'''	4.38 (1H, *bro. s*)	101.1	4.38 (1H, *s*)	102.2
2'''	3.26 (1H, *m*)	70.8		70.8
3'''	3.05 (1H, *m*)	71.0		71.2
4'''	3.06 (1H, *m*)	72.3		71.4
5'''	3.26 (1H, *m*)	68.7		69.1
6'''	0.97 (3H, *J* = 6.09)	18.6	0.95 (1H, *d*)	18.6
2''	3.22 (1H, *m*)	74.5		74.9
3''	3.28 (1H, *m*)	76.3		77.3
4''	3.39 (1H, *m*)	70.4		72.7
5''	3.21 (1H, *m*)	76.8		76.7
6''	3.69 (1H, *d*) & 3.25 (1H, *m*)	67.4		67.9

Assignments made on the basis of COSY, HSQC and HMBC correlations; δ in ppm; Coupling constants are in Hz.

The above spectral facts in combination with the literature report [188, 198] indicated that compound **163** is quercetin-3-O-rutinoside commonly named as rutin (**163**).

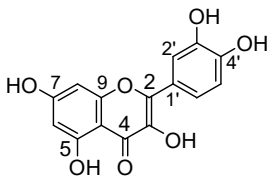

157

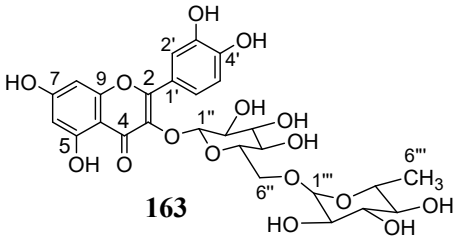

163

Rutin was reported from the leaves of *M. stenopetala* [188], *Teucrium polium* [198], *Morus atropurpurea* [199], *Delphinium staphisagria* [200] and *Astragalus hamosus* [201]. It has been shown to have remarkable pharmacological activities including antioxidant [202], antidiabetic [203], anti-cancer [204], anti-inflammatory [205], and hepatoprotective [206]. The anti-inflammatory, anti-allergic, antiviral, as well as anti-carcinogenic properties of rutin were reported as partly due to its antioxidant activity [207]. The antiglycation and insulinotropic properties of rutin were documented in the literature, demonstrating its significance in preventing glycation associated complications in diabetes [198]. Furthermore, rutin was shown to inhibit *α*-glucosidase activities demonstrating its hypoglycemic activities [199]. Rutin enhances the antibacterial activities of flavonoids such as quercetin and quercitrin [208]. Food and Drug Administration (FDA) declared rutin as a safe drug that reduces recurrent clots indicating its thrombolytic properties [209, 210].

Kaempferol-3-O-*β*-D-glucoside (161)

Compound **161** was obtained as yellow solid from the leaves of *M. oleifera*, mp 189-191^{o}C (Lit. 192-194^{o}C) [211]. The UV-Vis (MeOH) spectral analysis of compound **161** demonstrated λ_{max} at 265 and 350 nm indicating flavonoid chromophore with the 3-OH substituted. The negative mode FT mass spectrum of compound **161** revealed molecular ion at *m/z* 447.0924 (calcd 447.3689 for $C_{21}H_{19}O_{11}$) compatible with the molecular formula $C_{21}H_{20}O_{11}$. The diagnostic fragment at *m/z* 284 is due to the loss of hexose sugar establishing the aglycone as kaempferol.

The ^{1}H-NMR spectrum of compound **161** revealed the presence of six methine proton signals in the aromatic region at *δ* 8.16 (2H, *d*, *J* = 9.20 Hz) and *δ* 7.00 (2H, *d*, *J* = 9.20 Hz) which are characteristics of symmetrically placed protons on unsymmetrically *para* substituted aromatic ring. The signals due to *meta* located protons in the compound were observed at *δ* 6.54 (1H, *d*, *J* = 2.00 Hz) and *δ* 6.30 (1H, *d*, *J* = 2.00 Hz). The spectrum also showed a signal at *δ* 5.20 (1H, *d*, *J* = 7.20 Hz) which is ascribed to an anomeric proton of glucose possessing *β*-configuration [196, 197]. The other methine proton signals of the glucose moiety were observed in the oxygenated region centered at *δ* 3.59 and integrated for a total of six hydrogens.

The ^{13}C-NMR spectrum (Table 4) of **161** analyzed with the aid of DEPT-135 showed nine quaternary, eight methine and one methylene carbon signals. The presence an α,β-unsaturated carbonyl is evident from the appearance of carbon signal at δ 178.3. The five carbon signals in the region between δ 80.0 to 60.0 along with the signal at δ 103.9 clearly indicated the presence of only one hexose sugar. The carbon signal at δ 103.9 and 62.4 are ascribed to the anomeric and methylene carbons of the glucose moiety, respectively. The position of glucose moiety on C-3 was evident from the UV-Vis spectral analysis which showed the substitution of the hydroxy on C-3

Table 4: The ^{1}H- and ^{13}C-NMR spectral data of compound **161** and that reported in the literature for kaempferol-3-O-β-D-glucoside [212]

Position	NMR spectral data of **161**		Data reported for kaempferol-3-O-β-D-glucoside [212]	
	^{1}H-NMR	^{13}C-NMR	^{1}H-NMR	^{13}C-NMR
2	-	158.8	-	159.2
3	-	135.3	-	135.5
4	-	178.3	-	179.5
5	-	162.9	-	163.0
6	6.30 (1H, *d*, *J* = 2.00)	99.7	6.20 (1H, s)	100.0
7	-	165.8	-	166.2
8	6.54 (1H, *d*, *J* = 2.00)	94.6	6.40 (1H, s)	94.8
9	-	158.2	-	158.5
10	-	104.2	-	105.8
1’	-	123.0	-	122.3
2’ & 6’	8.16 (2H, *d*, *J* = 9.2)	131.2	8.02 (2H, *d*, *J* = 8.6)	132.2
3’ & 5’	7.00 (2H, *d*, *J* = 9.2)	115.9	6.87 (2H, *d*, *J* = 8.6)	116.1
4’	-	161.4	-	161.6
1’’	5.20 (1H, *d*, *J* = 7.20)	103.9	5.10 (1H, *s*)	104.2
2’’	3.59 (6H, H-2’’- H-6’’)	75.5	3.70 – 3.20 (6H, H-2’’ - H-6’’)	75.6
3’’		78.2		78.3
4’’		71.2		71.3
5’’		77.9		78.1
6’’		62.4		62.5

The aforementioned spectral data of compound **161** are in agreement with the data reported in the literature for kaempferol-3-O-*β*-D-glucoside commonly named as astragalin [212]. Kaempferol-3-O-*β*-D-glucoside was previously reported from the leaves of *M. oleifera* [187].

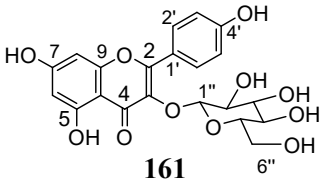

161

Other biological sources of kaempferol-3-O-*β*-D-glucoside (**161**) include aerial parts of *Cressa cretica* [212] and *Delphinium staphisagria* [200], flowers of *Asclepias syriaca* [211], leaves of *Phytolacca americana* [197], *Morus atropurpurea* [199], *Pyrus communis* [213], *Diospyros cathayensis*, *Diospyros rhombifolia* [214] and *Astragalus hamosus* [201]. Kaempferol-3-O-*β*-D-glucoside was reported to have antioxidant [214], anti-inflammatory [215], anti-hyperglycemic and *α*-glucosidase inhibitory activities [199].

Quercetin-3-O-*β*-D-glucoside (159)

Compound **159** was obtained as a yellow solid from the leaves of *M. oleifera*, mp 192-194ºC (Lit. 186-189ºC) [216]. The negative mode FT-MS showed molecular ion peak at *m/z* 463.0882 (calcd 463.3683 for $C_{21}H_{19}O_{12}$) establishing the molecular formula as $C_{21}H_{20}O_{12}$. This was in agreement with the ^{13}C-NMR spectrum of compound **159** which disclosed the presence of carbon resonances of twenty one carbon atoms. A major fragment ion was observed at *m/z* 301 in the mass spectrum of compound **159** due to the loss of hexose sugar from the parent ion establishing the aglycone as quercetin. The absorption maxima at 265 and 354 nm in its UV-Vis spectrum revealed the presence of flavonoid skeleton with the 3-OH substituted. The IR spectrum demonstrated absorption bands at 3368, 1665, 1609, and 1062 cm^{-1} due to stretching of hydroxyl, *α*,*β*-unsaturated carbonyl, C=C (aromatic), and C-O, respectively.

The ^{1}H-NMR spectrum of compound **159** demonstrated signals at *δ* 7.72 (1H, *d*, *J* = 2.40 Hz, H-2'), *δ* 7.60 (1H, *dd*, *J* = 2.40 and 8.80 Hz, H-6') and *δ* 6.80 (1H, *d, J* = 8.80 Hz*,* H-5') due to methine protons on the B-ring of a flavonoid. On the other hand the proton signals at *δ* 6.41 (1H, *d*, *J* = 2.00

Hz) and δ 6.23 (1H, *d*, *J* = 2.00 Hz) are *meta* situated protons, H-6 and H-8, of the A-ring of a flavonoid with the 5,7-dihydroxy substitution pattern. The presence of only one sugar moiety having a β-configuration was evident from the appearance of methine proton signal at δ 5.27 (1H, *d*, *J* = 7.60 Hz [196, 197]. The remaining proton signals of the glucose moiety were observed at δ 3.52 (1H, H-2''), 3.36 (1H, H-3''), 3.44 (1H, H-4''), 3.24 (1H, H-5''), 3.70 (1H, H-6'') and 3.61 (1H, H-6'').

The proton decoupled ^{13}C-NMR of compound **159** (Table 5) together with the DEPT-135 spectrum showed ten quaternary, ten methine and one methylene carbon signals. The presence an α,β-unsaturated carbonyl carbon was quite evident from the appearance of a signal at δ 178.1. The compound showed the presence of an anomeric carbon signal at δ 102.8. A series of carbon signals at δ 74.3, 76.7, 69.8, 77.0 and 61.1 are due to C-2'', C-3'', C-4'', C-5'' and C-6'' of the hexose moiety in the structure of the compound, respectively. The only methylene signal in the spectrum of compound **159** was observed at δ 61.1 (C-6''). The location of glucose on C-3 (δ 134.2) was established on the basis of HMBC spectral analysis which showed connectivity between the anomeric proton signal at δ 5.27 with the signal for C-3. This complements the results of UV-Vis spectral analysis which showed that the 3-OH is substituted. The identity of this compound as quercetin-3-O-β-D-glucopyranoside was further substantiated by comparison of its spectral data with those previously reported in the literature (Table 5).

Table 5: The ^{1}H- and^{13}C-NMR data of compound **159** and the data reported in the literature for quercetin3-O-β-D-glucoside (δ in ppm, J in Hz) [196]

Position	NMR spectral data of compound **159**		Data reported for quercetin-3-O-β-D-glucoside [196]	
	^{1}H-NMR	^{13}C-NMR	^{1}H-NMR	^{13}C-NMR
2	-	157.6	-	158.4
3	-	134.2	-	135.6
4	-	178.1	-	179.4
5	-	161.6	-	162.9
6	6.41 (1H, *d*, *J* = 2.00)	98.4	6.19 (*d*, *J* = 2.00)	99.8
7	-	164.6	-	165.9
8	6.23 (1H, *d*, *J* = 2.00)	93.2	6.38(*d*, *J* = 2.00)	94.7
9	-	157.0	-	158.4
10	-	104.9	-	105.6
1’	-	121.6	-	123.0
2’	7.72 (1H, *d*, *J* = 2.40)	116.1	7.71 (*d*, *J* = 2.00)	117.5
3’	-	144.5	-	145.8
4’	-	148.4	-	149.8
5’	6.80 (1H, *d, J* = 8.80)	114.5	6.87 (*d*, *J* = 8.40)	116.0
6’	7.60 (1H, *dd*, *J* = 2.40, 8.80)	121.7	7.58 (*dd*, *J* = 2.00, 8.40)	123.2
1’’	5.27 (1H, *d*, *J* = 7.60)	102.8	5.23 (*d*, *J* =7.60)	104.3
2’’	3.52 (1H, *m*)	74.3	3.48 (*t*, *J* = 9.20)	75.7
3’’	3.36 (1H, *m*)	76.7	3.35 (*t*, *J* = 8.80)	78.1
4’’	3.44 (1H, *m*)	69.8	3.43 (*t*, *J* = 9.60)	71.2
5’’	3.24 (1H, *m*)	77.0	3.24 (*m*)	78.3
6’’	3.70 (1H, *m*) & 3.61 (1H, *m*)	61.1	3.73 (*m*) and 3.56 (*m*)	62.5

Assignments made on the basis of COSY, HSQC and HMBC correlations; δ in ppm; Coupling constants are in Hz.

The physical and spectral data discussed above for characterization of compound **159** agreed with those reported in the literature for quercetin-3-O-β-D-glucoside [196].

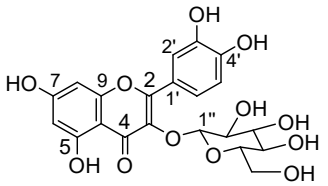

159

Quercetin-3-O-*β*-D-glucoside (isoquercitrin) was reported as constituent of apple, tea, onions [217], *M. oleifera* [187], *Azadirachta indica* [196], *Byrsocarpus coccineus* [218], *Diospyros cathayensis*, *Diospyros rhombifolia* [214], *Pyrus communis* [213], *Delphinium staphisagria* [200], *Asperula arvensis* [219] and *Cressa cretica* [112]. Quercetin-3-O-*β*-D-glucoside was shown to possess a wide range of biological activities including antimicrobial [196], antioxidant [214, 218], anti-carcinogenic [217] and anti-inflammatory [220]. Mounting evidence showed that quercetin-3-O-*β*-D-glucoside can reduce symptoms like fatigue, depression, anxiety, and coronary heart diseases [217]. It has also been reported to exhibit high phytotoxic effect demonstrating its allelopathic potential [217].

Sitosterol-3-O-*β*-D-glucoside (64): Sitosterol-3-O-*β*-D-glucoside was isolated as a white powder after Diaion-LH20 column chromatography of the 70% aqueous ethanol extract of the leaves of *M. oleifera* using acetone as eluent. The structure elucidations are discussed in pages 16-19

3.3.2. Comparison of Extracts of the Leaves of *M. stenopetala* and *M. oleifera*

Thin Layer Chromatography (TLC)

Planar chromatography is among the most versatile option for the quality control of herbal products. In spite of other available analytical techniques, such as liquid chromatography (LC), gas chromatography (GC) and high performance liquid chromatography-mass spectrometry (HPLC-MS), TLC still remains a useful, quick, effective, and low-cost method for the separation and identification of complex mixtures of plant constituents [221].

In this work, the leaves of *M. stenopetala* from Ethiopia and *M. oleifera* from Rwanda were compared using TLC. After the respective ethanol extracts of the two *Moringa* species were

defatted with dichloromethane, same amount were dissolved in ethanol and spotted on a 0.25 mm thick layer of silica gel on aluminum plate using a Camag Linomat 5 sample applicator. The TLC plate was developed using EtOAc:AcOH:HCOOH:H_2O (7:1:1:1) as a mobile phase which gave high resolution of the spots. The spots were visualized after spraying with fast blue B salt followed by heating with hot air gun.

As seen in Fig. 1, there is a clear cut difference in the chromatograms of the two *Moringa* species. The intense spot observed at an Rf value 0.49 in the thin layer chromatogram of *M. stenopetala* was not detected in the chromatogram of *M. oleifera* indicating that there is a distinct compound which can aid in distinguishing *M. stenopetala* from the other species. The spot at Rf 0.49 in the TLC profile of *M. stenopetala* was identified as rutin (**163**). The identity of this compound was confirmed by comparing its Rf value with reference rutin. The two intense spots in the thin layer chromatogram of *M. oleifera* leaves extract at an Rf value of 0.65 and 0.67 were not observed in the ethanol extract of the leaves of *M. stenopetala*. These two spots were identified as kaempferol-3-O-*β*-D-glucoside (**161**) (Rf 0.67) and quercetin-3-O-*β*-D-glucoside (**159**) (Rf 0.65). Hence TLC can distinguish these two species rapidly. Furthermore this method has the potential to detect the presence of adulterants in either of the two samples.

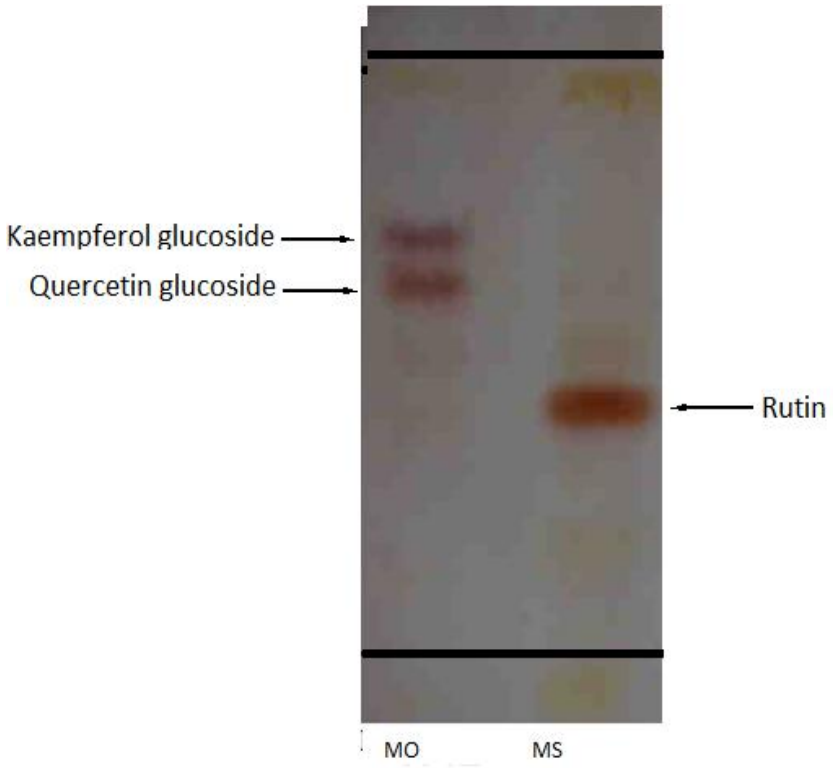

Fig. 1: TLC profile of defatted ethanol extract of *Moringa* leaves (*MO*: *M. oleifera* and *MS*: *M. stenopetala*); Spraying agent: fast blue B salt

UV-Vis spectrophotometry

The $CHCl_3$:MeOH (1:1) extract of the leaves of *M. stenopetala* and *M. oleifera* were analyzed using UV-Vis spectrophotometry (Fig. 2) and the spectrum revealed that there is clear difference between the extracts of the two species. The intensity of the bands at λ_{max} 260 and 410 nm were comparable in the UV-Vis spectrum of the leaves of *M. stenopetala*. However the band at λ_{max} 260 nm in the UV-Vis spectrum of *M. oleifera* was found more intense than the band at λ_{max} 410 nm. This aids to distinguish the two *Moringa* species.

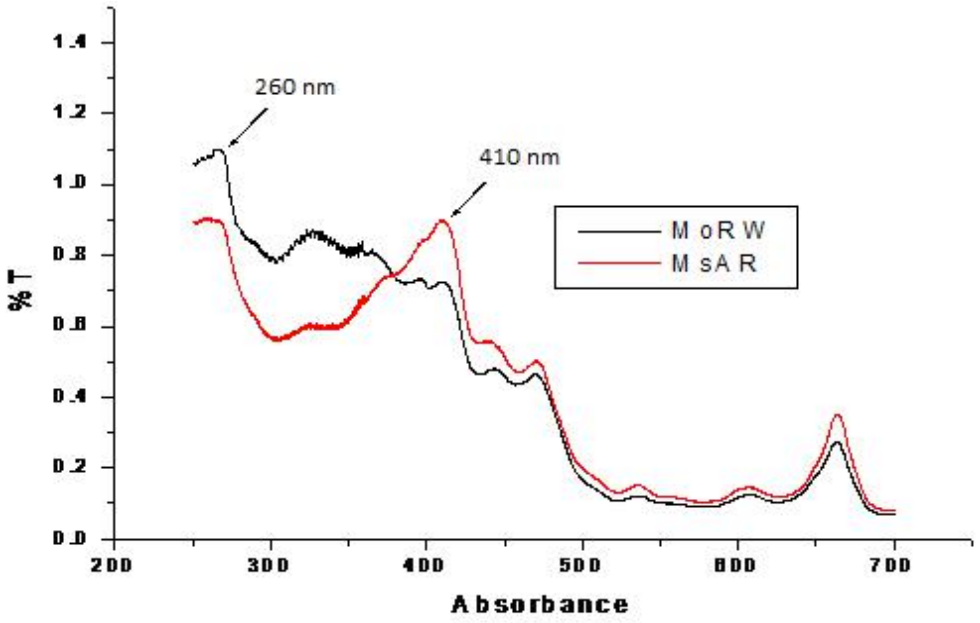

Fig. 2: Overlayed UV-Vis spectra of *M. oleifera* (black) and *M. stenopetala* (red)

High Performance Liquid Chromatography-Mass Spectrometry (HPLC-MS)

The hyphenation of chromatography with spectroscopy could provide additional spectral information, which will be helpful not only for the qualitative analysis of herbal drugs but also for the structural elucidations of the constituents [222]. The fingerprint obtained by hyphenated chromatography, can be used as the main tool for quality control of herbal medicines. In this work, HPLC-MS was employed to distinguish the two highly demanded *Moringa* species: *M. oleifera* and *M. stenopetala*. The HPLC-MS obtained for the water extract (the water extract described herein is the extract of the marc after the leaves of the plant material were extracted with $CHCl_3$:MeOH (1:1)) of the two *Moringa* species were compared. The results showed conclusively that there is clear difference between the chromatograms of the water extracts of the leaves of the two species.

Six peaks were observed in the chromatogram of the water extract of *M. stenopetala*. Especially significant in the chromatogram of the extract of the leaves of *M. stenopetala* is the intense peak eluted at retention time of 12.959 min (Fig. 3) which exhibited molecular ion peak at *m/z* 611 (Appendix 4) in its mass spectrum. The loss of hexose moiety from the molecular ion afforded a significant ion at *m/z* 465. The diagnostic fragment in the spectrum at *m/z* 303 is presumably due to

the loss of two sugar moieties from the parent ion establishing the aglycone as quercetin. Hence the mass fragmentation pattern observed indicated that the peak eluted at retention time of 12.959 min is rutin (**163**). This was confirmed through isolation and characterization of rutin from the leaves of *M. stenopetala*. It is quite clear from Fig. 3 that the flavonoid glycoside rutin is the major constituent in the chromatogram of the water extract of the leaves of *M. stenopetala* which however was not detected in the extracts of the leaves of *M. oleifera*.

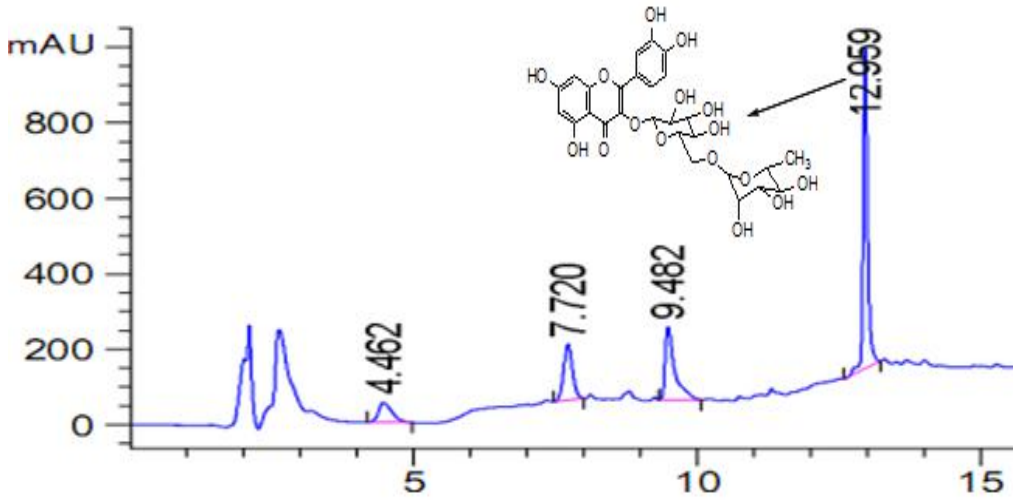

Fig. 3: HPLC fingerprint profile of water extract of *M. stenopetala* leaves

The water extract of the leaves of *M. oleifera* showed the presence of seven major peaks (Fig. 4) which however were not observed in the chromatogram of the extract of the leaves of *M. stenopetala*. The compound which eluted at retention time of 13.653 min (Fig. 4) in the chromatogram of the extract of the leaves of *M. oleifera* showed molecular ion peak at *m/z* 465 in its mass spectrum (Appendix 5). The fragment ion observed at *m/z* 303 is apparently due to the loss of hexose from the parent ion establishing the aglycone as quercetin. Hence the compound eluted at retention time of 13.653 min was found to be quercetin-3-O-*β*-D-glycoside (**159**). The peak eluted at retention time of 14.099 min (Fig. 4) in the chromatogram of *M. oleifera* leaves displayed molecular ion peak at *m/z* 449 (Appendix 6), which upon loss of hexose sugar afforded prominent peak at *m/z* 287. The latter peak is evident for kaempferol as the aglycone. Hence the mass fragmentation pattern observed showed that the peak eluted at retention time of 14.099 min is kaempferol-3-O-*β*-D-glucoside (**161**).

The two peaks eluted at retention time of 13.653 and 14.099 min in the chromatogram of the extract of the leaves *M. oleifera* corresponding to quercetin-3-O-*β*-D-glucoside and kaempferol-3-O-*β*-D-glucoside, respectively, were not observed in the chromatogram of the extract of the leaves of *M. stenopetala*. Therefore, these compounds can distinguish the extracts of the leaves of *M. oleifera* from *M. stenopetala*. The identities of these compounds were further confirmed through isolation and characterization. The results obtained from HPLC-MS were in agreement with the TLC results.

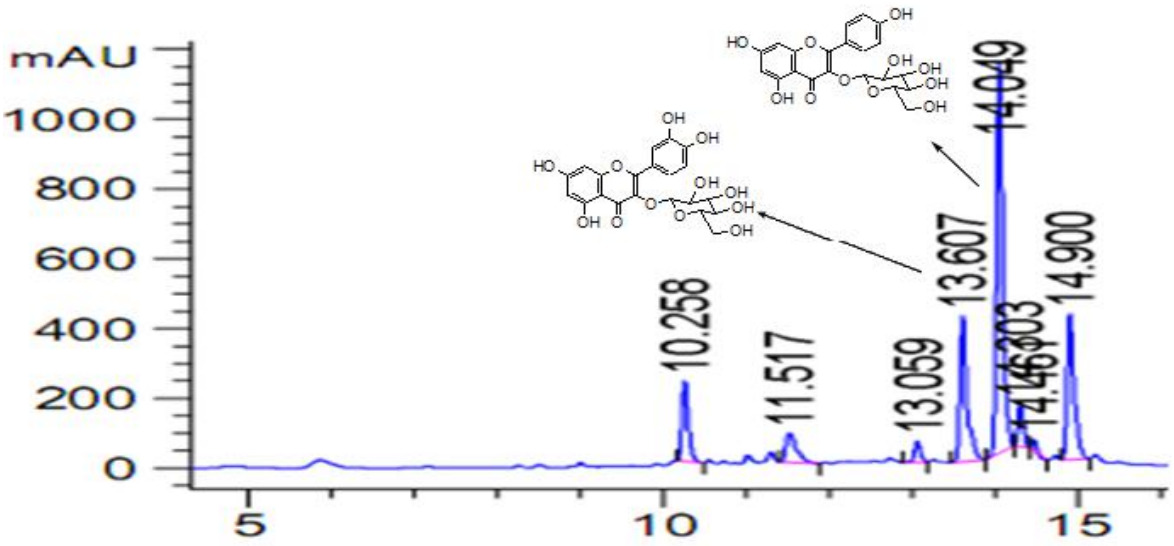

Fig. 4: HPLC fingerprint profile of water extract of *M. oleifera* leaves

3.3.3. Quantification of Rutin in the Leaves of *M. stenopetala*

High Performance Thin Layer Chromatography (HPTLC)

Fingerprint analysis shows the similarities or differences among samples, and may not display the quantity of marker compounds [223]. Nevertheless the concentrations of chemical constituents can be used as an indicator of the quality of herbal medicine [224]. In the course of this work, it was found that the leaves of *M. stenopetala* proved to be rich in the flavonoid glycoside rutin which was reported to have remarkable biological activities as described on page 101 [202-208]. Furthermore, this compound may be taken as the bioactive principle of *M. stenopetala* for which

the leaves are used in traditional medicine. Hence the quantitative evaluation of the marker compound, rutin, in the leaves of *M. stenopetala* is necessary to undertake.

The level of rutin in the 70% aqueous ethanol extract of the leaves of *M. stenopetala* collected from Arba Minch was performed using HPTLC. From the stock sample solution (1 mg/mL), 20 µL and 40 µL were applied on HPTLC plate in the form of bands with a Camag 100 µL sample syringe on tracks 2 and 4 while on tracks 1, 3 and 5 standard rutin solutions of 2, 6, and 10 µL were applied, respectively. The TLC was developed using EtOAc:HCOOH:AcOH:H_2O (7:1:1:1, v/v) as a mobile phase which showed good resolution of the spots. After development, the plate was scanned at 260 nm and eight spots were detected in the chromatogram with Rf values in the range of 0.1 to 0.9 (Fig. 5). The spot of rutin in the plant material was observed at an Rf value of 0.49 which was verified by comparing with reference rutin (Fig. 5).

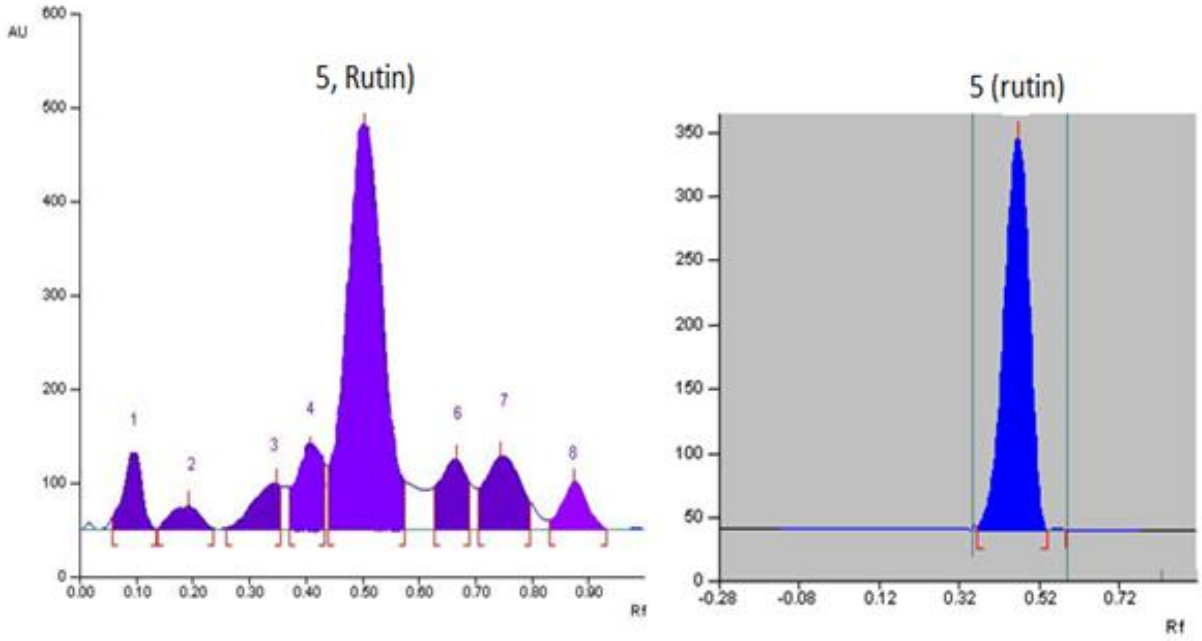

Fig. 5: Typical chromatogram of the 70% aqueous EtOH extract (left) of *M. stenopetala* leaves and standard rutin (right).

The calibration plot obtained from this result via peak area exhibited a correlation coefficient of 0.996 and standard deviation of 8.66. The peak area of rutin on track 4 of the plate was found to be

24.23 µg. Hence the level of rutin in 70% aqueous EtOH extract of *M. stenopetala* leaves collected from Arba Minch, calculated via peak area, was 2.1±0.04% w/w (Table 6).

The level of chemical constituents in herbal products may vary depending on the geographic and climatic conditions under which the plant is grown. To see if there is a potential variation in the content of rutin due to geographical location, three samples of *M. stenopetala* leaves obtained from northern (Gondar), eastern (Dire Dawa) and southern (Arba Minch) parts of Ethiopia were examined using HPTLC and UV-Vis spectrophotometry. The analysis was done following similar procedure used for the determination of rutin in the leaves of *M. stenopetala* collected from Arba Minch. Results showed that the amount of rutin in the 70% aqueous ethanol extract (1 mg/mL) of the leaves of *M. stenopetala* obtained from Gondar and Dire Dawa were found to be 1.8 and 1.9%w/w, respectively. Hence, the level of rutin in *M. stenopetala* leaves quantified using HPTLC vary between 1.8% to 2.1% w/w. As shown in Table 6, the level of rutin is slightly higher for samples collected from Arba Minch (2.1%) and lower for samples collected from Gondar (1.8%). The summary of the whole results displaying extract yield, amount of rutin obtained after 40 µL of the extracts were applied on track 4 and the percent of rutin in the leaves of *M. stenopetala* obtained from Arba Minch, Gondar and Dire Dawa are shown in Table 6.

Table 6: Level of rutin in the leaves of *M. stenopetala* using HPTLC

Sample source	Extract yield in mg from 2 g *M. stenopetala*	Amount of sample applied in µL (µg)	Peak area from Camag in µg	%Rutin (M±SD)
Arba Minch	70	40	24.23	2.1±0.04% w/w
Gondar	66	"	20.30	1.8
Dire Dawa	68	"	22.24	1.9

M±SD: mean plus or minus standard deviation; three samples of *M. stenopetala* leaves obtained from Arba Minch and each one sample of *Moringa* from Gondar and Dire Dawa were analyzed

An attempt was also made to determine the amount of rutin in the ethanol extract of *M. stenopetala* leaves collected from Arba Minch using HPTLC following similar procedure as above. The level

of rutin was found to be 1.8% w/w. This indicated that the 70% aqueous ethanol extracted slightly higher level of rutin than ethanol.

The HPTLC method was validated by assessing its linearity, limit of detection, limit of quantification, accuracy, repeatability and reproducibility. The peak areas for different concentrations of rutin were found to be linearly dependent on the concentrations in the range of 2-10 µL. This was done three times which exhibited a correlation coefficient of 0.999 indicating a high degree of correlation and a good linearity of the method. Furthermore the limit of detection and limit of quantification of rutin in *M. stenopetala* leaves were found to be 0.02 and 0.07 µg, respectively. Results for repeatability expressed as %RSD done using HPTLC were found to be 0.14% and 0.13% for intraday and interday study (Appendix 8), respectively. The low values of %RSD obtained from HPTLC reflect the high precision of the methods. Reproducibility was further checked by analyzing the samples by another analyst using same instrument and same laboratory. There was no significant difference between the %RSD values, which indicates that the proposed method is reproducible. Moreover the recovery (Appendix 9) of the method conducted using HPTLC was 99.5% which indicates excellent reproducibility of the methods.

UV-Vis spectrophotometry

The level of rutin in *M. stenopetala* leaves were evaluated using UV-Vis spectrophotometry. In this regard, the absorbance at 260 nm of the 70% aqueous ethanol extract (0.1 mg/mL) of *M. stenopetala* leaves collected from Arba Minch, Gondar and Dire Dawa were recorded using UV-Vis spectrophotometer. On the other hand, the absorbance of reference rutin at 260 nm (MeOH) was generated using various concentrations of rutin (0.15, 0.1, 0.05, 0.025 and 0.007 mg). On the basis of the results, a calibration curve with the different concentrations of reference rutin against the corresponding absorbances at 260 nm which gave a linear equation $y = 18.3x-0.108$, and $R^2 = 0.995$ (Fig. 6) was obtained using Origin software. The level of rutin in *M. stenopetala* leaves collected from the three sources (Arba Minch, Gondar and Dire Dawa) were calculated based on the linear calibration curve, with the results presented in Table 7.

Table 7: Level of rutin in *M. stenopetala* leaves using UV-Vis spectrophotometry

Sample source	Absorbance at 260 nm	Amount of rutin in 0.1 mg/mL extract sample	% Rutin
Arba Minch	0.84	0.052	1.8
Gondar	0.78	0.048	1.7
Dire Dawa	0.80	0.049	1.7

Amount of plant extracted and extract yield were shown in Table 5; %rutin was calculated with respect to dry weight basis, samples were analyzed in triplicates

The overlayed UV-Vis spectra at different concentrations of reference rutin together with the spectra of 70% aqueous ethanol extracts of the leaves of *M. stenopetala* collected from Arba Minch (MsAM), Gondar (MsG) and Dire Dawa (MsDD) aredepicted in Fig. 6. Simple inspection of the overlayed UV-Vis spectra of the leaves of *M. stenopetala* samples at λ_{max} 260 nm indicated that there is a slightly higher level of absorbance for samples collected from Arba Minch.

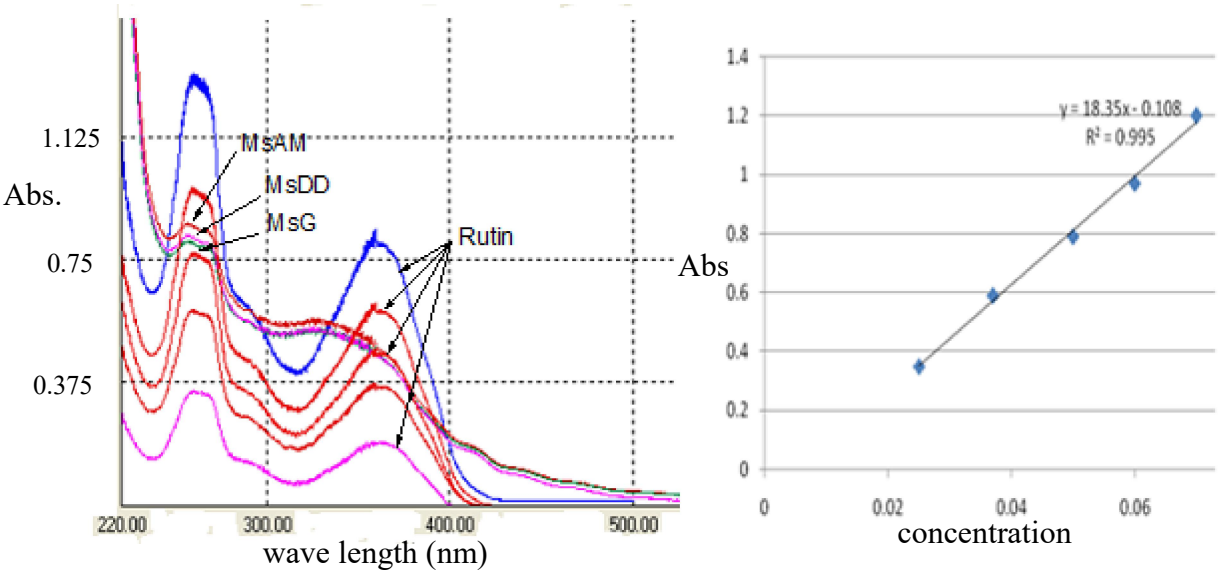

Fig. 6: Overlayed UV-Vis spectra of various concentrations of rutin along with 70% aqueous EtOH extracts of *M. stenopetala* leaves (left) and calibration curve of reference rutin (right)

For confirmation purpose, rutin was isolated from the 70% aqueous EtOH extract of *M. stenopetala* leaves and found to be 1.9% w/w. Therefore, the amount of rutin determined using HPTLC, UV-Vis spectrophotometry and isolation were in close agreement.

3.3.4. Contributions to the Chemical Studies of the Leaves and Seeds of *M. stenopetala*

The ground leaves of *M. stenopetala* were extracted with $CHCl_3$:MeOH (1:1) to afford a black semisolid material (8%) which after silica gel column chromatography furnished four compounds: 1-heptacosaol (**185**), sitosterol-3-O-*β*-D-glucoside (**64**), rutin (**163**) and inositol dimer (**186**). Soxhlet extraction of the kernel of *M. stenopetala* with petrol gave 36% yellowish oil. The marc after Soxhlet extraction was extracted with ethanol and subsequently chromatographed over silica gel to afford three compounds identified as stearic acid (**77**), 4-(*α*-L-rhamnopyranosyloxy) benzyl glucosinolate (**164**) and sucrose (**187**). FT-MS analysis of fatty acid mixtures obtained after hydrolysis of *M. stenopetala* oil afforded palmitic acid (**78**), oleic acid (**150**), icosanoic acid (**76**) and behenic acid (**75**). In addition to these fatty acids, GC-MS analysis of the fatty acid methyl esters (FAME) obtained from the oil of *M. stenopetala* furnished stearic acid (**77**), linoleic acid (**152**), myristic acid (**188**) and palmitoleic (**189**). Furthermore stearic acid (**77**), compound **190** and allantoin (**191**) were isolated by silica gel column chromatographic fractionation of the ethanol extract of the husk of *M. stenopetala* for which no prior report is available in the literature. The complete spectral assignments of the isolated compounds were carried out using spectroscopic and physical methods as discussed below.

3.3.4.1. Characterization of Compounds from the Leaves of *M. stenopetala*

Heptacosanol (185)

Compound **185** was isolated as a white powder from the leaves of *M. stenopetala* which melted at 82-83^{o}C (Lit. 81-82^{o}C) [225]. It is optically inactive. The UV-Vis spectrum ($CHCl_3$) showed absorption maxima neither in the ultra-violet nor in the visible region indicating the absence of conjugated chromophore. The IR spectrum displayed absorption bands at 3400 and 2950 cm^{-1} due to hydroxy and aliphatic C-H stretching, respectively.

The ^{1}H-NMR spectrum ($CDCl_3$) of compound **185** demonstrated a triplet signal at δ 3.66 (J = 6.60 Hz) assigned to methylene protons on oxygenated carbon. The quintet at δ 1.59 integrating for two protons is due to methylene protons on carbon flanked between two methylene groups. A broad singlet at δ 1.27 (48H) is characteristic signal for many methylene protons in the compound which was supported by appearance of an intense carbon signal at δ 29.6 in the ^{13}C-NMR spectrum. An upfield triplet signal at δ 0.90 (3H, J = 6.70 Hz) is evident for the presence of terminal methyl group in the compound. In the ^{13}C-NMR spectrum, the downfield signal at δ 63.1 corresponds to an oxygenated aliphatic carbon. Furthermore, the carbon resonance at δ 14.1 is characteristic signal for terminal methyl group.

Table 8: ^{1}H- and ^{13}C-NMR spectral data of compound **185** with those reported in the literature for heptacosanol, δ in ppm and J in Hz

NMR spectral data of compound **185**		Data reported for 1-heptacosanol [225]	
^{1}H-NMR	^{13}C-NMR	^{1}H-NMR	^{13}C-NMR
3.66 (2H, *t*, *J* = 6.60, H-1)	63.1 (C-1)	3.64 (2H, *t*, *J* = 6.30, H-1)	63.1 (C-1)
1.59 (2H, *m*, H-2)	32.8 (C-2)	1.57 (2H, *m*, H-2)	32.8 (C-2)
1.27(48H, *bro s*, H-3 to H-26)	31.9 (C-3)	1.25(48H, *br s*, H-3 to H-26)	31.9 (C-3)
	29.7-29.3(C4-24)		29.7-29.3(C4-24)
	25.7 (C-25)		25.7 (C-25)
	22.6 (C-26)		22.6 (C-26)
0.90 (3H, t, *J* = 6.70, H-27)	14.1 (C-27)	0.88 (3H, *t*, *J* = 6.60, H-27)	14.1(C-27)

Comparison of the NMR spectral data of compound **185** with those reported in the the literature for 1-heptacosal [225] was in close agreement (Table 7). This compound was previously reported from the leaves of *Strobilanthes crispus* [225] but has not been reported from any species of *Moringa.*

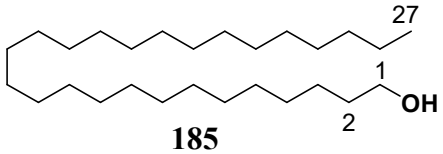

185

Sitosterol-3-O-*β*-D-glucopyranoside (64): Compound **64** was isolated as white powder from $CHCl_3$:MeOH (1:1) extract of *M. stenopetala* leaves. The physical and spectral data of compound **64** were in agreement with sitosterol-3-O-*β*-D-glucopyranoside. This compound has not been reported before from *M. stenopetala*. The full structural elucidation of sitosterol-3-O-*β*-D-glucopyranoside was presented on pages 16-19.

Rutin (163): Compound **163** was obtained as yellowish solid from column chromatographic fractionation of $CHCl_3$:MeOH (1:1) extract of *M. stenopetala* leaves. The spectral data of **163** is in close agreement with that of rutin discussed on pages 98-102.

Inositol dimer (186)

This white solid compound was obtained from silica gel column chromatographic fractionation of the $CHCl_3$:MeOH (1:1) extract of *M. stenopetala* leaves using ethanol as eluent. It was found optically active with $[\alpha]_{589}^{21}$ = -75.0 (c 0.2, MeOH). The ^{1}H-NMR spectrum (D_2O) of compound **186** displayed signals in the oxygenated region only. The triplet signal at *δ* 3.11 (2H, *J* = 9.20 Hz) is due to H-1. The other methine proton signal was observed at *δ* 3.36 (4H, *dd*, *J* = 9.60, 2.80 Hz). The compound also exhibited two methine proton signals centered at *δ* 3.49 (4H, *t*, *J* = 9.60 Hz) and *δ* 3.93 (2H, *bro t*).

The proton decoupled ^{13}C-NMR spectrum (D_2O) of compound **186** with the aid of DEPT-135 demonstrated the presence of well resolved carbon resonances of four methine carbons all of which resonated in the oxygenated region at *δ* 74.3 (C-1), 72.4 (C-2 and 6), 72.1 (C-4), and 71.1 (C-3 and 5). The carbon signals at *δ* 71.1 and 72. 4 were intense relative to the other carbon signals at *δ* 74.1 and 72.1, justifying the presence of symmetry in the compound. Key HMBC correlations observed are depicted in **192**. With the data generated, compound **186** was identified as inositol dimer. This compound has not been reported from the genus *Moringa*.

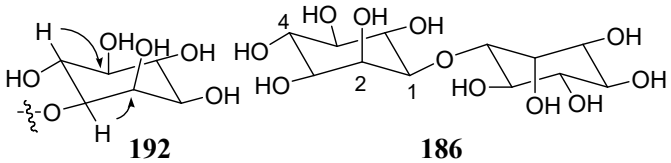

192 **186**

Inositol is a naturally occurring isomer of glucose. It was reported as a member of the B vitamins [226] and a primary component of cellular membrane phospholipids. Numerous bioactive properties have been attributed to inositol and its derivatives. The mixture of inositol and its hexaphosphate (IP6) is sold as a dietary supplement for cancer patients [226]. Research findings showed that patients suffering from clinical depression generally have decreased levels of inositol in their cerebrospinal fluid showing its antidepressant properties [227].

3.3.4.2. Chemical Constituents of *M. stenopetala* Seeds Kernel

Analysis of *M. stenopetala* Oil

The oil content of *M. stenopetala* seeds was determined by employing two methods of extraction, *viz*., solvent extraction using hexane and Soxhlet extraction. The oil content obtained using Soxhlet extraction with petrol was found to be 36% which turned out to be almost similar with the solvent extraction procedure utilizing hexane. The oil was analyzed using UV-Vis and NMR spectrometry. The UV-Vis result of *M. stenopetala* oil demonstrated absorption maxima neither in the ultra-violet nor in the visible region indicating the absence of compounds possessing conjugated chromophores. On the other hand the NMR spectrum of the oil obtained from *M. stenopetala* was compared with some edible oils used in Ethiopia such as sesame, linseed, niger seed, palm, soybean, olive and peanut. Results showed that *M. stenopetala* oil displayed similar NMR spectral profile with olive oil (Appendix 10).

An attempt was made to determine the fatty acid profiles of *M. stenopetala* oil. In this regard, fatty acid mixtures obtained on hydrolysis of *M. stenopetala* oil were analyzed using FT-MS. The negative ion ESI-FT-MS showed four major peaks at *m/z* 339.3269 (calcd 339.5786 for $C_{22}H_{43}O_2$), 311.2952 (calcd 311.5224 for $C_{20}H_{39}O_2$), 281.2481 (calcd 281.4534 for $C_{18}H_{33}O_2$), and 225.2328 (calcd 255.4151 for $C_{16}H_{31}O_2$) compatible with the molecular composition of $C_{22}H_{44}O_2$ for behenic acid (**75**), $C_{20}H_{40}O_2$ for icosanoic acid/archidic acid (**76**), $C_{18}H_{34}O_2$ for oleic acid (**150**) and $C_{16}H_{32}O_2$ for palmitic acid (**78**), respectively (Appendix 11). The presence of behenic acid (**28**) in *M. stenopetala* oil shows the close resemblance of the seeds of this plant with its sister species *M. oleifera* which is commonly called Ben Oil Tree owing to the presence of this acid.

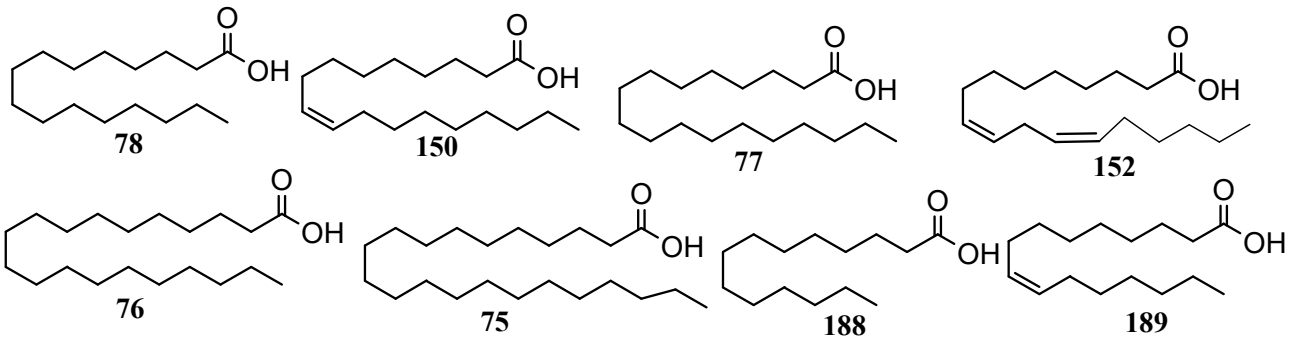

The fatty acid compositions of *M. stenopetala* oil were also determined using gas chromatography-mass spectrometry (GC-MS). This was done after the oil was converted to fatty acid methyl esters using BF_3-MeOH. The fatty acid identifications were made by comparing the spectra of the components with the database of the spectrum of known components stored in the GC-MS library. The results obtained from GC-MS (Table 8, Appendix 12) showed that *M. stenopetala* oil contains a large proportion of double bond containing fatty acids. The dominant unsaturated fatty acid was found to be oleic acid (63%) demonstrating the close resemblance of this oil with olive oil which contains large proportion of this acid. The GC-MS result was consistent with the proton NMR spectral analysis, since *M. stenopetala* oil and olive oil exhibited similar ^{1}H-NMR patterns. The fatty acid profile of the oil of *M. stenopetala* is given in Table 9

Table 9: Fatty acid composition of the oil of *M. stenopetala* seeds

Fatty acids	Structure No	Relative percent
Tetradecanoic acid/ Myristic acid (14:0)	**188**	0.2
Hexadecenoic acid/Palmitoleic acid (16:1)	**189**	1.2
Hexadecanoic acid/Palmitic acid (16:0)	**78**	11
Octadecenoic acid/Oleic acid (18:1)	**150**	63
Octadecanoic acid/Stearic acid (18:0)	**77**	11
9,12-Octadecadienoic acid/Linoleic acid (18:2)	**152**	1.2
Eicosanoic acid/archidic acid (20:0)	**76**	6
Docosanoic acid/Behenic acid (22:0)	**75**	6

Stearic acid (77)

Compound **77** was obtained from the hexane extract of *M. stenopetala* kernel as a white powder, mp 70-71^{o}C. The optical rotation was found to be zero. The UV-Vis spectrum of **77** showed no absorption maxima. The IR spectral analysis displayed the presence of carboxyl and aliphatic C-H stretching at 1707 cm^{-1} and 2917 cm^{-1}, respectively. The negative ion mode mass spectrum of compound **77** disclosed *m/z* at 284 compatible with the molecular composition of $C_{18}H_{36}O_2$.

The ^{1}H-NMR spectrum of compound **77** showed signals only in the aliphatic region. The triplet signal at δ 2.36 (2H) and quintet at δ 1.65 (2H) are distinctive of hydrogens α and β to a carboxyl group, respectively. The signal due to many overlapping methylene protons was observed at δ 1.31 (28H, *bro. s*) which was supported by the appearance of an intense carbon signal at δ 29.7 in the ^{13}C-NMR spectrum. The presence of a terminal methyl group was evident from the appearance of proton signal at δ 0.90 (3H, *t, J* = 6.70 Hz) with the corresponding carbon signal at δ 14.2. In the ^{13}C-NMR spectrum of compound **77**, the downfield signal at δ 180.6 is attributed to the carboxyl group in the compound. The remaining carbon signals observed at δ 33.8, 31.9, 29.5, 29.4, 29.3, 29.2, 29.0, 24.6, and 22.6 were due to methylene carbons in the compound. The data generated were in agreement with stearic acid (**77**).

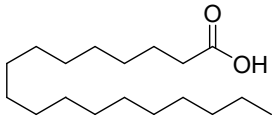

77

Oleic acid (150)

Compound **150** was obtained from the oil of *M. stenopetala*. The **(-)-**ESI-FT-MS showed a peak at *m/z* 281.24816 establishing the molecular formula as $C_{18}H_{34}O_2$. The ^{13}C-NMR spectrum of compound **150** demonstrated carbon resonances of 18 carbon atoms. The signal at δ 179.0 is evident for the presence of a carboxyl group. The compound exhibited two carbon signals in the olefinic region at δ 130.0 and 129.0 evident for the presence of one double bond in the structure of the compound. The carbon signal at δ 34.0 is typical of methylene carbon adjacent to carboxyl group. This was supported by the appearance of triplet signal at δ 2.30 (2H) in the ^{1}H-NMR spectrum of the compound. The most upfield carbon signal at δ 14.0 in the ^{13}C-NMR spectrum of

compound **150** accounts for the presence of a terminal methyl group. The remaining thirteen methylene carbon signals were observed in the range between δ 32.0 to 23.0. The NMR spectral analysis described above allowed the identification of compound **150** as oleic acid (**150**).

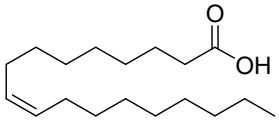

150

4-(α-L-rhamnopyranosyloxy) benzyl glucosinolate (164)

Compound **164** was isolated as a yellowish jelly solid from *M. stenopetala* kernel. It is soluble in polar solvents such as water and methanol. The TLC (Rf 0.5) developed using EtOAc:MeOH (3:2) as a mobile phase gave a yellowish spot which was detected after spraying with vanillin in H_2SO_4 followed by heating with hot air gun. The UV-Vis spectrum of this compound showed absorption maxima at 245 and 273 nm demonstrating the presence of conjugation in the compound. The IR spectral analysis displayed bands at 3400, 2924, and 1613 cm^{-1} due to hydroxyl, C-H, and aromatic C=C stretching, respectively. The molecular formula $C_{20}H_{29}NO_{14}S_2$ was established from (-)-ESI-FT-MS, which displayed a quasi-molecular ion peak at *m/z* at 570.0960 (calcd 570.5666 for $C_{20}H_{28}NO_{14}S_2^-$). A prominent fragment ion peak was observed at *m/z* 97 corresponding to bisulphate ion. The peaks at *m/z* 570 and 97 are characteristic of 4-(α-L-rhamnopyranosyloxy) benzyl glucosinolate [147].

The ^{1}H-NMR spectrum of compound **164** displayed signals at δ 7.25 (2H, *d*, *J* = 8.40 Hz) and 7.04 (2H, *d*, *J* = 8.40 Hz) which are due to *ortho* coupled protons symmetrically placed on unsymmetrically *para* substituted aromatic ring. These protons showed connectivity in their COSY spectrum. The compound exhibited anomeric proton signal at δ 5.30 (1H, *d*, *J* = 1.36 Hz) characteristic of a rhamnopyranosyl group with an α-configuration [187]. The presence of a rhamnosyl group was further supported by the appearance of terminal methyl signal at δ 1.13 (3H, *d*, *J* = 5.60 Hz). The proton signal observed at δ 4.60 (1H, *d*, *J* = 3.2 Hz) is due to H-1' which showed HSQC correlation with the carbon signal at δ 81.3 (C-1'). The methylene proton signal at δ 4.00 (2H, *bro. s*) is due to H-7. A series of proton signals between δ 4.00 to 3.00 are accounted for the methine protons of the sugar moieties.

The proton decoupled ^{13}C-NMR spectrum of compound **164** showed well resolved carbon resonances of 18 carbon atoms which agreed with the result obtained from FT-MS. The ^{13}C-NMR spectrum along with DEPT-135 displayed signals due to three quaternary carbons at δ 162.5 (C-8), 154.6 (C-1) and 130.6 (C-4); four methine carbon signals at δ 129.4 (C-3, 5), 117.5 (C-2, 6), 98.8 (C-1'') and 81.3 (C-1'); two methylene carbon signals at δ 37.4 (C-7) and 60.2 (C-6'); one methyl resonance at δ 16.5 (C-6'') and the remaining 8 carbon resonances observed in the region between δ 80.0 to 68.0 are attributed to methine carbon signals of the sugar moieties.

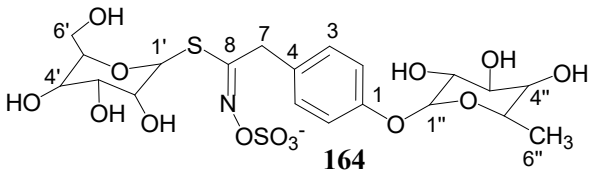

164

The HSQC spectrum showed correlations such that the proton signals at δ 7.04 (H-2, 6) and 7.25 (H-3, 5) correlates with the carbon signals at δ 117.5 and δ 129.4, respectively. The two methylene proton signals at δ 3.70 (H-6') and 4.00 (H-7) were found to correlate with the carbon signals at δ 60.0 (C-6'') and δ 37.4 (C-7), respectively. The connectivity between C-7 and C-8 was evident from the observed HMBC correlation between the carbon signal at δ 162.6 (C-8) with the methylene proton signal at δ 4.00 (H-7). Another key HMBC correlation was observed between the H-1'' signals and the quaternary carbon signal at δ 154.6 (C-1) which established the location of the rhamnopyranose group on C-1. On the basis of the above physical and spectral evidence, compound **164** was identified to be 4-(α-L-rhamnopyranosyloxy) benzyl glucosinolate (**164**).

Sucrose (187)

This water soluble compound was isolated as a white solid from the kernel of *M. stenopetala*. Compound **187** is optically active with $[\alpha]_{589}^{25}$ = +56 (c 10, H_2O). The molecular formula $C_{12}H_{22}O_{11}$ (molecular weight 342) was established from the mass spectrum of the compound. The ^{1}H-NMR spectrum of compound **187** displayed signals in the oxygenated region only. The spectrum showed signal for one anomeric proton at δ 5.30 (1H, *d*, *J* = 3.60 Hz). The remaining proton signals of this compound appeared in the region between 3.00 to 4.00. The ^{13}C-NMR spectrum together with DEPT-135 revealed the presence of one quaternary, three methylene and eight methine carbons. All were found in the oxygenated region which was found in agreement

with the result obtained from the proton NMR spectrum. The compound exhibited anomeric carbon signal at δ 103.0. The physical and spectral data above are in agreement with the structure depicted in **187**.

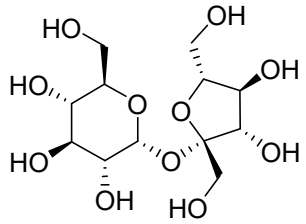

187

The identity of this compound was further confirmed using TLC, polarimetry and NMR spectrometry against standard sucrose. Compound **187** displayed similar optical rotation with reference sucrose. The TLC of compound **187** and reference sucrose, developed using EtOAc:Isopropanol:MeOH:AcOH (6:3:0.5:0.5) as eluent after same amount of each sample were spotted on the same TLC plate (0.50 on a 0.25 mm thick layer of silica gel on aluminum plate) showed that the two compounds had the same Rf values. The spots were visualized after spraying with anisaldehyde followed by heating with hot air gun. Confirmation was made using NMR after equal amount of compound **187** and reference sucrose were mixed, dissolved in D_2O and subjected to NMR studies. The NMR spectrum obtained indicated that both compounds were identical. Therefore the above spectral and physical data indicated that compound **187** is sucrose.

3.3.4.3. Characterization of Compounds from the Husk of *M. stenopetala* Seeds

Compound 190

Compound **190** was obtained as a white solid from column chromatographic fractionation of the ethanol extract of the husk of *M. stenopetala* seeds, mp 153-155ºC. The compound was optically active with an $[\alpha]_{589}^{21}$ = -15 (c 0.4, MeOH). The UV-Vis spectrum (MeOH) of compound **190** displayed absorption maxima at 271 nm due to π→π* transition. No bathochromic shift was observed on addition of sodium hydroxide to the cuvette containing methanolic solution of compound **190** suggesting the absence of free phenolic hydroxy group. The IR spectral analysis

showed the presence of hydroxyl, C=C, and C-O due to the absorption bands at 3387, 1612 and 1064 cm^{-1}, respectively. The FT-MS spectral analysis showed a peak at *m/z* 269.1028 (calcd 269.2704 for $C_{13}H_{17}O_6$) compatible with the molecular formula $C_{13}H_{18}O_6$.

The proton NMR spectrum of **190** displayed signals at δ 7.22 (2H, *d*, *J* = 8.20 Hz, H-3) and δ 6.96 (2H, *d*, *J* = 8.20 Hz, H-2) due to the presence symmetrically placed protons on unsymmetrically *para* substituted aromatic ring. These protons showed cross coupling with one another in their COSY spectrum supporting their *ortho* placement as depicted in **193**. Further analysis of the ^{1}H-NMR spectrum indicated the presence of one sugar unit, suggested to be rhamnose from the anomeric proton signal at δ 5.32 (1H, *d*, *J* = 1.32 Hz, H-1') and a secondary methyl group resonance at δ 1.07 (3H, *d*, *J* = 6.14 Hz, H-6'). The coupling constant (*J* = 1.32 Hz) established that the rhamnose has an α-configuration [187]. The two hydrogen doublet at δ 4.40 (2H, *d*, *J* = 4.73 Hz, H-7) is due to benzylic methylene protons on oxygenated carbon. The signals at δ 5.18 (1H, *d*, *J* = 4.23 Hz), 5.92 (1H, *d*, *J* = 5.92 Hz), and 4.81 (1H, *d*, *J* = 5.92 Hz) are attributed to protons on hydroxyl groups of sugar moiety as established by its HSQC spectrum. The series of signals at δ 3.25 (1H, *m*, H-5'), 3.43 (1H, *m*, H-3'), 3.61(1H, *m*, H-2') and 3.62 (1H, *m*, H-4') are due to methine protons of the rhamnose moiety.

The proton decoupled ^{13}C-NMR spectrum with the aid of DEPT 135 of compound **190** showed the presence of two quaternary, eight methine, one methylene and one methyl carbon signals. The quaternary carbons resonating at δ 155.3 and 136.2 are due to C-1 and C-4 of the aromatic ring, respectively. The other two signals in the aromatic region at δ 128.4 and 116.6 are due to C-3, 5 and C-2, 6, respectively. The spectrum further disclosed that the sugar unit is a rhamnopyranosyl moiety from the set of the chemical shifts at δ 98.8 (C-1'), 70.8 (C-2'), 70.6 (C-3'), 72.2 (C-4'), 69.7 (C-5') and 18.3 (C-6') in agreement with the proton NMR spectrum. The benzylic methylene carbon signal was observed at δ 62.9 (C-7).

The complete structure of compound **190** was deduced from the results of COSY, HSQC and HMBC spectral data. The one bond ^{1}H/^{13}C NMR spectrum showed that the proton signals at δ 1.07, 4.40, 3.25, 3.43, 3.61, 3.62, 6.96 and 7.22 were found attached on carbon atoms whose signals

appeared at δ 18.2, 62.9, 69.7, 70.6, 70.8, 72.5, 116.6, and 128.4, respectively. The HMBC spectrum showed correlation between methylene proton at δ 4.40 (H-7) with the carbon at 128.4 (C-3) and 136.2 (C-4) establishing the site of attachment of C-7 to C-4 of the benzene ring as shown in **194**

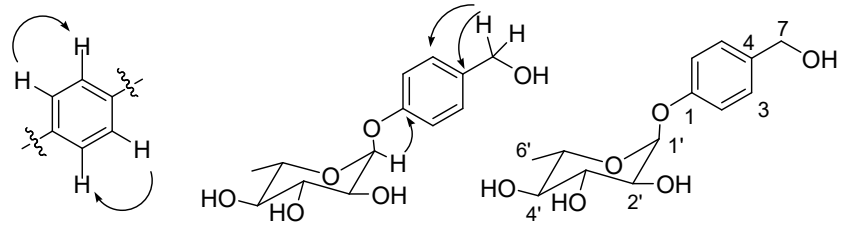

193 **194** **190**

Another key correlation observed was between anomeric proton signal at δ 5.32 (H-1') with the oxygenated aromatic carbon signal at δ 155.2 (C-1) which established the site of attachment of rhamnose to the aromatic ring as depicted in **194**. This was in agreement with the UV-Vis spectral analysis which showed the absence of phenolic hydroxy. The spectral and physical data are in agreement with structure **190** for this compound. There is no prior report of compound **190** in the literature.

Allantoin (191)

Compound **191** was isolated as a white solid from the husk of *M. stenopetala* seeds, mp 220-222^{o}C. The asymmetric and symmetric stretching of primary amide were observed in the IR spectrum at 3438 and 3343 cm^{-1}, respectively. This was substantiated by the appearance of C-N stretching of primary amide at 1385 cm^{-1}. The intense band at 1715 cm^{-1} is characteristic of five membered cyclic lactams [228]. The UV-Vis (MeOH) spectral analysis showed absorption maxima at 266 nm indicating the presence of a chromophore in the structure of the compound. The FT-MS showed molecular ion at *m/z* 181.0332 (calcd 181.10537 for $C_4H_6O_3N_4Na$) compatible with the molecular composition of $C_4H_6O_3N_4$.

The ^{1}H-NMR spectrum of compound **191** displayed signals at δ 5.21 (1H, *d*, *J* = 8.00 Hz, H-3) and 6.97 (1H, *d*, *J* = 8.00 Hz, H-3'). The latter is due to a proton on heteroatom as observed from the

absence correlation to a carbon signal in its HSQC spectrum. Other signals in the proton NMR spectrum were observed at δ 10.70 (1H, *bro. s,* H-1'), 8.10 (1H, *s,* H-2') and 5.85 (2H, *s,* H-4'). The downfield signal at δ 10.70 is due to H-1'. The singlet signal integrating for two protons at δ 5.85 is assigned to H-4'.

The proton decoupled ^{13}C-NMR with the aid of DEPT-135 spectrum of compound **191** showed the presence of well resolved resonances of four carbon atoms, three of which turned out to be quaternary (δ 174.0 (C-1), 157.9 (C-2) and 157.3 (C-4)) and one was a methine carbon signal (δ 62.8 (C-3)). The structure of compound **191** was further analyzed using 2D NMR. The proton signal at δ 5.21 showed COSY connectivity with the proton signals at δ 8.10 and 6.96. The proton signal at δ 8.10 showed HMBC correlation with the carbon signals at δ 62.8, 157.3 and 174.0. Other key correlation was established between the proton signal at δ 6.96 with the carbon signals at δ 62.8, 157.9 and 174.0. Furthermore the only methine proton signal at δ 5.21 showed HMBC correlation with the carbon signals at δ 174.0, and 157.3. The key correlation observed from COSY and HMBC leading to the structure of compound **191** are depicted as **195** and **196**, respectively. Compound **191** is the known compound allantoin.

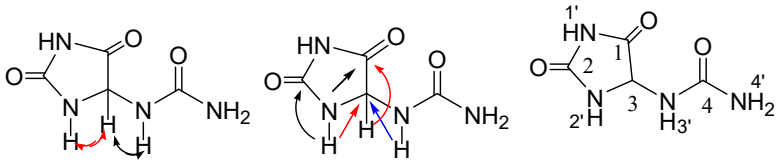

195 **196** **191**

The ^{13}C-NMR data reported for allantoin [229] are in close agreement with the ^{13}C-NMR spectral data generated for compound **191**.

Allantoin was previously reported from the root of *Symphytum asperum* [230] and *Umbilicaria esculenta* [229]. It has long been known to enhance the efficacy and desirability of cosmetic creams and lotions through its actions as a skin protectant [230]. Allantoin has been shown to promote cell division and the growth of connective tissue, bone, and cartilage and accelerate the healing of wounds [230]. The utility of allantoin as a protective agent against asthma was also reported [231].

Stearic acid (77): Stearic acid (**77**) was isolated as a white powder from column chromatographic fractionation of the husk of *M. stenopetala*. The physical and spectral data generated for this compound were in agreement with the structure of stearic acid.

3.3.5. Antioxidant Assay

The antioxidant activities of the two *Moringa* species were assayed employing two methods: DPPH (diphenylpicrylhydrazyl) radical scavenging assay and ferric thiocyanate methods.

DPPH (diphenylpicrylhydrazyl) radical scavenging assay

The radical scavenging properties of extracts of both species of *Moringa* were evaluated using DPPH. Results demonstrated that the percent inhibition of the EtOH extract of the leaves of *M. stenopetala* and *M. oleifera* were found to be 77% and 73%, respectively, indicating their strong activities radical as inhibitors. The extracts of the two species turned out to have of almost similar radical scavenging potential.

Table 10: DPPH radical scavenging activity of the EtOH extracts and constituents of the leaves of *M. stenopetala* and *M. oleifera*

Samples tested	Scavenge (%)	IC_{50}	Remark
M. stenopetala EtOH extract	77	6.1	
M. oleifera EtOH extract	73	6.0	
Rutin	83	2.45	*From M. stenopetala*
Sitosterol- *β*-D-glucoside	36	15.6	"
1-Heptacosanol	26	14	"
Quercetin glucoside	85	2.3	*From M. oleifera*
Kaempferol glucoside	75	2.7	"
Sitosterol- *β*-D-glucoside	36	15.6	"
Ascorbic acid	90	0.45	

Three compounds isolated from *M. stenopetala* (1-heptacosanol, sitosterol-*β*-D-glucoside, and rutin) and three compounds isolated from *M. oleifera* leaves (sitosterol-3-O-*β*-D-glucoside, quercetin-3-O-*β*-D-glucoside and kaempferol-3-O-*β*-D-glucoside) were subjected to radical scavenging assay. Results demonstrated that rutin exhibited radical scavenging property and IC_{50} of 83%, and 2.45, respectively (Table 10). In contrast quercetin-3-O-*β*-D-glucoside and kaempferol-3-O-*β*-D-glucoside showed percentage inhibition of DPPH by about 85% and 75%, respectively (Table 10). The antiradical activities of rutin and quercetin-3-O-*β*-D-glucoside were found to be comparable with ascorbic acid which was used as positive control (Table 10). Hence rutin presumably accounts for the radical scavenging activity of *M. stenopetala* leaves as quercetin-3-O-*β*-D-glucoside and kaempferol-3-O-*β*-D-glucoside for *M. oleifera* leaves.

Ferric thiocyanate method

Lipids having many unsaturation sites are susceptible towards free radical chain reaction [232]. On oxidation, such lipids undergo deterioration producing a number of toxic metabolites [233] which are known to interact with biological materials thereby causing cellular damage [234]. The degree of lipid peroxidation can be used to measure the antioxidant potential of compounds or extracts. This can be done using the ferric thiocyanate method. Fatty acid peroxides change Fe^{2+} to Fe^{+3} and the generated Fe^{3+} forms red colored ferric thiocyanate, which absorbs at 500 nm [235]. In the course of this work, the extracts of the leaves of both *Moringa* species were incubated with linoleic acid at 40^{o}C and a small portion was taken from the mixture after 24 h and added to a solution containing Fe^{2+} and thiocyanate ion. The absorbance at 500 nm of this solution was measured. The percentage inhibition using ferric thiocyante method was calculated according to the following formula.

$$\text{Percentage inhibition} = 100 - \left(\frac{As}{Ab} \times 100\right)\%,$$

where As is absorbance of the sample and Ab is absorbance of the blank [236].

Table 11: Anti-lipid peroxidation activities of the EtOH extracts of *M. stenopetala* and *M. oleifera*

Sample name	Absorbance at 500 nm	%inhibition	Remark
Blank	0.56	-	
Ascorbic acid	0.11	80	
M. oleifera EtOH extract	0.12	78	
M. stenopetala EtOH extract	0.14	74	

Ascorbic acid was used as positive control

As depicted in Table 11, the EtOH extracts of the leaves of *M. oleifera* and *M. stenopetala* inhibited peroxide formation by 78 and 74%, respectively, demonstrating their potential in preventing the formation of lipid peroxides. The anti-lipid per-oxidation displayed by the extracts of the two *Moringa* species were comparable with ascorbic acid indicating the potential of the leaves of the two *Moringa* species as natural antioxidants.

3.4. Conclusion

Since the use of *Moringa species* is growing steadily, a quality control method using TLC, UV and HPLC-MS were developed to differentiate this species from various sources by chemical fingerprints. Simultaneously, markers were isolated to carry out qualitative diagnosis. The marker compound for *M. stenopetala* is rutin while the markers in *M. oleifera* leaves are quercetin-3-O-*β*-D-glucoside (**159**) and kaempferol-3-O-*β*-D-glucoside (**161**). Sitosterol-3-O-*β*-D-glucoside (**64**) is the common compound isolated from the leaves of the two *Moringa* species. These results may be useful in establishing presence or absence of adulterants, an issue that is of great concern in the use and marketing of leaves, extracts and other products of *Moringa.* Therefore, the present fingerprinting profile can be used as a diagnostic tool to identity and to determine the quality and purity of the leaves of *M. stenopetala and M. oleifera*

The level of rutin in the 70% aqueous ethanol extracts of the leaves of *M. stenopetala* was found to be 1.9±0.08% indicating that the leaves of *M. stenopetala* are rich in rutin (**163**). 1-Heptacosanol (**185**) and inositol dimer (**186**) isolated from the leaves of *M. stenopetala* are new to the genus while sitosterol-3-O-*β*-D-glucoside (**64**) has not been reported from *M. stenopetala*

The kernel of *M. stenopetala* is proved to be a rich source of oil (36%) with diversified fatty acid profile including palmitic (**78**), oleic acid (**150**), stearic (**77**), linoleic (**152**), icosanoic acid (**76**), behenic acid (**75**), palmitoleic (**189**), and myristic acid (**188**). The marc left after extraction with petrol was found to contain a glucosinolate called 4-(*α*-rhamnopyranosyloxy) benzylglucosinolate (**164**) along with sucrose (**187**). Allantoin (**191**) and compound **190** were isolated from the husk of *M. stenopetala* with the latter compound has not been reported from any natural source.

The antiradical and anti-lipid peroxidation activities displayed by the extract of *M. stenopetala* leaves were accounted to the presence of rutin (**163**). On the other hand quercetin-3-O-*β*-D-glucoside (**159**) and kaempferol-3-O-*β*-D-glucoside (**161**) were responsible for the antioxidant potential of *M. oleifera* leaves. The antioxidant property displayed by *M. stenopetala* adds one positive attribute to the nutritional and pharmacological importance of the leaves of this species.

3.5. Experimental

Reagents, Standard Solutions and Materials

Standard rutin was isolated from the leaves of *M. stenopetala* and recrystalized twice from methanol. For more information see section 1.5 (page 37)

Plant Material

Leaves of *M. stenopetala* were collected from Gondar (Feb. 2012), Dire Dawa (Feb. 2012), Arba Minch (May 2013) and Adama (Sep. 2014). Seeds of *M. stenopetala* were collected from Arba Minch (May 2013). *M. oleifera* leaves and seeds were collected from Debre Zeit Agricultural Institute in September 2014. The plant identification was done by Mr. Melaku Wondafrash of the Department of Biology, Addis Ababa University, Addis Ababa, Ethiopia. Voucher specimen YM002/2015 and YM001/2014 for *M. stenopetala* and *M. oleifera* leaves, respectively, are deposited at the National Herbarium of Addis Ababa University. *M. oleifera* leaves used in this work were obtained from Rwanda and its identity was confirmed using TLC and UV in comparison with authentic *M. oleifera* leaves collected from Debre Zeit Agricultural Institute.

Extraction of *Moringa* species for HPTLC, UV and HPLC-MS Analysis

To the dried and ground leaves of *M. stenopetala* (2 g) collected from Arba Minch was added ethanol (15 mL) and extracted by shaking using a mechanical shaker for 6 h. It was filtered and concentrated at 40^{o}C under reduced pressure using rotary evaporator to afford 70 mg (3.5%) of the crude extract. Likewise *M. oleifera* leaves (2 g) was extracted using EtOH following similar procedure as above to afford 80 mg (4.0%). Both extracts were defatted with CH_2Cl_2 and subsequently analyzed using TLC.

Each 20 g ground dried leaves of *M. stenopetala* and *M. oleifera* were extracted using $CHCl_3$:MeOH (1:1) by shaking for 6 h at room temperature using a mechanical shaker, filtered and concentrated to afford 1.8 g (9%) and 2 g (10%) of the corresponding extracts, respectively. Each 0.1 mg of the extracts was separately dissolved in 1 mL of $CHCl_3$:MeOH (1:1) and analyzed using UV-Vis spectrophotometry. The marc of each *Moringa* species was further extracted with water and analyzed using HPLC-MS.

Each 2 g of *M. stenopetala* leaves from Arba Minch, Gondar (Metema), and Dire Dawa were extracted using 70% aqueous ethanol (15 mL) by shaking for 6 h using a mechanical shaker, filtered and concentrated to afford 70 mg, 66 mg and 68 mg of their corresponding extracts, respectively. These extracts were subsequently used for quantification of rutin in the leaves of *M. stenopetala*. In the course of this work, three samples of *M. stenopetala* collected from Arba Minch and each one sample collected from Gondar and Dire Dawa were analyzed.

UV-Vis Measurement

Standard rutin solution: rutin (5 mg) was dissolved in EtOH (5 mL) to afford 1 mg/mL. From the standard solution 0.15, 0.1, 0.05, 0.025 and 0.007 mg/mL of rutin solution were sequentially subjected to UV-Vis spectrophotometery and in each case absorbances at 260 nm was recorded. The linear regression equation of the calibration curve was generated using the various concentrations of rutin against the corresponding absorbance at 260 nm.

Sample stock solution: Each 1 mg of 70% aqueous ethanol extract of *M. stenopetala* leaves from Arba Minch, Gondar and Dire Dawa were separately dissolved in EtOH (10 mL) to afford 0.1

mg/mL of the corresponding solution. The absorbance of each *Moringa* sample at 260 nm was measured using UV-Vis spectrophotometer.

HPTLC measurement

Standard and sample stock solution: Standard stock solution of rutin was prepared by dissolving rutin (10 mg) in ethanol (20 mL). Similarly sample stock solutions for *M. stenopetala* leaves collected from Arba Minch, Gondar and Dire Dawa were prepared by dissolving each *Moringa* sample (10 mg) in ethanol (10 mL) to afford 1 mg/mL solution.

Chromatographic conditions, detection and quantification of rutin using HPTLC: Chromatography was performed on pre-coated silica gel HPTLC plates using ethyl acetate:formic acid:acetic acid:water (7:1:1:1, v/v) as a mobile phase. From the stock sample solution, 20 µL and 40 µL were applied in the form of bands with a Camag 100 µL sample syringe (Hamilton, Bnaduz, Switzerland) on track 2 and 4, respectively. On track 1, 3 and 5, a standard rutin solution of 2, 6, and 10 µL were applied, respectively. All samples and standard solutions were applied to the layer as 14 mm wide bands, positioned from the bottom of the plate, using an automated Linomat V (Camag, Muttenx, Switzerland) TLC applicator with nitrogen flow providing delivery from the syringe. These critical parameters were maintained for all analysis performed. The development distance was 55 mm. Spots were detected by observing under UV light. Following the development, the TLC plate was dried with the help of an air drier at 110^{o}C for 2 min, and immediately scanned at λ_{max} 260 nm with a slit width of 5.0 x 0.45 mm, a scanning speed of 10 mm/s with a computerized Camag, TLC scanner-3 integrated with winCATS 4 software. The presence of rutin in the extract was determined by comparing with the Rf of the reference rutin.

Validation of HPTLC

Linearity of HPTLC method: A calibration curve of standard rutin was obtained by plotting peak area of rutin against various concentration of rutin in µg. Stock solution of rutin was prepared in ethanol and 2, 4, 6, 8, and 10 µL/spot of these was loaded onto a TLC plate for preparing calibration curves. There was a good linear relationship between peak area and concentration in the range 1-5 µg per zone with a correlation coefficient of 0.999 and standard deviation of 2.73. The experiments were performed in triplicate

Limit of Detection (LOD) and Quantification (LOQ): The limit of detection and limit of quantification was determined based on the linear regression equation of the calibration curve. The LOD and LOQ were calculated based on the standard deviation (SD) of the Y-intercept and the slope (s) as 3SD/s and 10SD/s, respectively [237, 238].

Precision: The precision was determined as intra-day assay precision (repeatability) and inter-day assay precision (reproducibility). Intraday precision using HPTLC was determined by analyzing the level of rutin in extract of *M. stenopetala* leaves three times for the same day. Similarly the interday precision was determined by analyzing rutin in the plant material six times on different days (Appendix 8). The precision of this method is expressed as percent relative standard deviation, %RSD

Accuracy (% Recovery) using HPTLC: Recovery study of rutin was made by using standard addition method. In line with this, to a known amount of pre-analyzed sample, certain amount of rutin was added and the amount of rutin was obtained from linear regression via peak area. The accuracy of the method is expressed as the percentage recovery of the added rutin (Appendix 9).

Extraction and Isolation of Markers from *M. stenopetala* and *M. oleifera* leaves

Ground leaves of *M. stenopetala* (100 g) was extracted with 70% aqueous ethanol (700 mL) by shaking for 6 h using a mechanical shaker, filtered, the solvent reduced to about 20% using rotary evaporator and left standing overnight. The precipitate formed was filtered and the dried solid was recrystalized from methanol to afford rutin (1.9%). Similarly, to the ground leaves of *M. oleifera* (100 g) was added 70% aqueous ethanol (700 mL) and extracted by shaking for 6 h, filtered and concentrated to afford a black jelly solid (15%). This was defatted with CH_2Cl_2 and chromatographed over Diaion LH20 (50 g). The column was eluted first with water (Fr1, 250 mL) followed by EtOH:H_2O (1:1, Fr2, 100 mL), then 100% EtOH (Fr3, 20 mL, 800 mg; **Fraction 4**, 20 mL, 300 mg); and ended with acetone (Fr6, 20 mL, 50 mg) to afford six fractions. **Fraction 5** eluted with acetone was identified to be sitosterol-3-O-*β*-D-glucoside.

Fraction 4 (300 mg) was adsorbed and chromatographed over silica gel to afford nine fractions. The first seven fractions were eluted using EtOAc (10 mL each) while the last two were eluted using MeOH (10 mL each). Among fractions eluted using EtOAc, **Fraction 2-4** (160 mg) were

combined, adsorbed and rechromatographed to afford four fractions. The first three fractions were eluted using EtOAc (5 mL each) while the fourth fraction was eluted using EtOAc:MeOH (1:1, 10 mL). The third fraction was identified to be kaempferol-3-O-*β*-D-glucoside (10 mg). The forth fraction (80 mg) was dissolved in hot ethyl acetate:MeOH (1:1). The TLC profile of the soluble portion (30 mg) was promising hence was purified using Sephadex LH 20 with MeOH:$CHCl_3$ (1:1) as eluent to afford three fractions. The third fraction was found to be quercetin-3-O-*β*-D-glucoside (4 mg). The flow sheet diagram showing the isolation of marker compounds from *M. stenopetala* and *M. oleifera* leaves are depicted in Scheme 1.

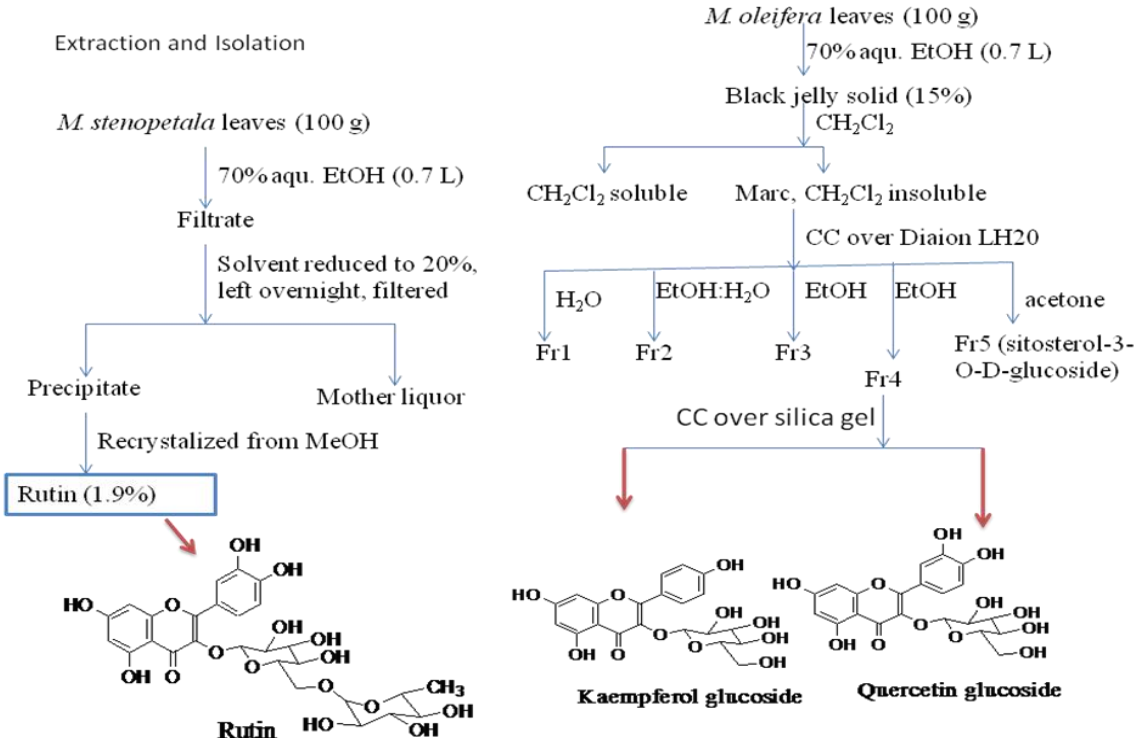

Scheme 1: Isolation of marker compounds from *M. stenopetala* and *M. oleifera* leaves

Extraction and Isolation of Compounds from *M. stenopetala* Leaves

To ground *M. stenopetala* leaves (100 g) was added $CHCl_3$:MeOH (1:1, 500 mL) and extracted by shaking for 6 h using a mechanical shaker, filtered and concentrated to afford 8 g (8%) black semisolid substance. This was adsorbed on silica gel and chromatographed over silica gel (120 g,

230-400 mesh). The column was eluted using CH_2Cl_2, CH_2Cl_2:EtOAc, 100%EtOAc, EtOAc:EtOH and ended with EtOH as depicted in Table 12.

Table 12: Column chromatographic fractionation of the $CHCl_3$:MeOH extract of the leaves of *M. stenopetala*

Fractions	Eluent (ratio)	Volume of eluent in mL	Amount in mg
Fr1	CH_2Cl_2	40	800
Fr2-4	‘’	‘’	800
Fr5	‘’	‘’	100
Fr6	‘’	‘’	80
Fr7	‘’	‘’	56
Fr8&9	‘’	‘’	30
Fr10	‘’	‘’	60
Fr 11	‘’	‘’	50
Fr12	CH_2Cl_2:EtOAc (1:1)	‘’	20
Fr13	‘’	‘’	10
Fr14-16	‘’	‘’	50
Fr17&18	‘’	‘’	40
Fr19	‘’	‘’	40
Fr20&21	‘’	‘’	60
Fr22	‘’	‘’	20
Fr23	‘’	‘’	25
Fr24	‘’	‘’	25
Fr26-30	‘’	‘’	40
Fr 32-35	EtOAc	‘’	150
Fr36	EtOAc:EtOH (4:1)	‘’	200
Fr37	‘’	‘’	150
Fr38	‘’	‘’	120

Table 12 continued

Fr39	‘’	‘’	10
Fr40	‘’	‘’	100
Fr41	EtOAc:EtOH (1:1),	‘’	200
Fr42	‘’	‘’	220
Fr43	‘’	‘’	80
Fr44	‘’	‘’	285
Fr45	‘’	‘’	30
Fr46	EtOH	‘’	20
Fr47	‘’	‘’	80
Fr48	‘’	‘’	80
Fr49	‘’	‘’	280
Fr50	‘’	‘’	150

Fraction 11 and **Fraction 39** were identified as 1-heptacosanol and sitosterol-3-O-*β*-D-glucoside **(**10 mg**),** respectively. **Fraction 43** and **Fraction 44** were combined and suspended in CH_2Cl_2 and the insoluble portion was found to be **rutin (250 mg)**. Fr49 (280 mg) was dissolved in MeOH. The insoluble portion was found to be **inositol dimer** (5 mg). The flow sheet diagram showing extraction and isolation of compounds from the leaves of *M. stenopetala* is shown in Scheme 2

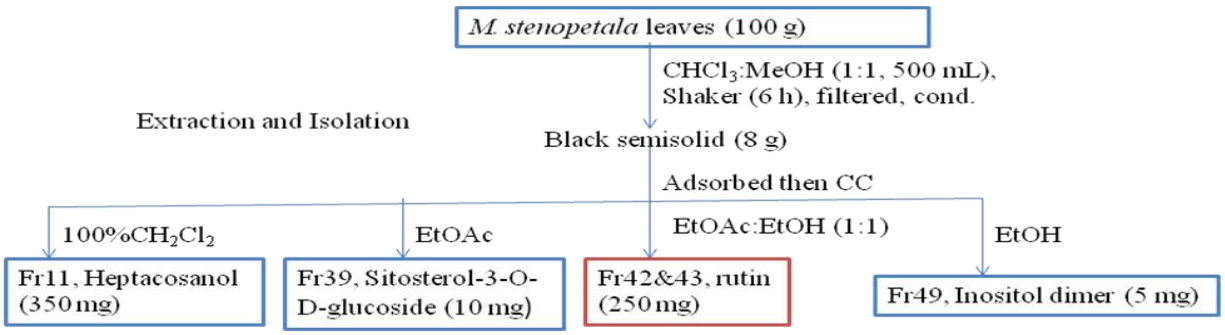

Scheme 2: Flow sheet diagram showing extraction and isolation of compounds from *M. stenopetala* leaves

Hydrolysis of Rutin: A mixture of rutin (100 mg) and H_2SO_4 (1N, 20 mL) was heated at 80ºC for 1 h. After cooling, the mixture was extracted with EtOAc (20 mLx2) and the combined organic parts were dried over anhydrous Na_2SO_4, filtered and concentrated under reduced pressure to afford a yellowish solid (20 mg). The TLC of this product showed a single spot at an Rf value of 0.7 using EtOAc as mobile phase and its structure was assigned by NMR and other spectroscopic methods.

Extraction and Fractionation of *M. stenopetala* Seeds

Ground *M. stenopetala* seeds (230 g) were Soxhlet extracted with petrol (2.3 L) for 15 h, filtered and concentrated to afford 84 g (36%) yellowish oily material. The marc (100 g) was extracted using EtOH (500 mL) by shaking for 5 h with a mechanical shaker, filtered and concentrated. The extract was defatted with petrol by heating on steam bath (30 min) and filtered. The residue (3 g, 3%) was adsorbed and chromatographed over silica gel (230-400 mesh). Gradient elution was done using $CHCl_3$:MeOH (4:1, 20 mL, 100 mg, Fr1; 3:2, 30 mL, 80 mg, Fr2; 1:1, 30 mL, 50 mg, Fr3; 2:3, 40 mL, 98 mg, **Fraction 4**; and 2:3, 40 mL, 300 mg, **Fraction 5**) to afford five fractions. The fifth fraction was identified to be **sucrose (300 mg)**. **Fraction 4** (98 mg) was applied on Sephadex LH 20 and eluted using $CHCl_3$:MeOH (1:1) to afford three fractions. The first two (14 mL, 40 mg) were combined and concentrated to afford **4-(*α*-L-rhamnopyranosyloxy) benzyl glucosinolate** while the third fraction (16 mL, 40 mg) was identified as **sucrose.**

On the other hand *M. stenopetala* oil (10 g) was mixed with MeOH (40 mL), placed on steam bath for 30 min, and on a mechanical shaker for 4 h and left overnight in a deepfreeze. The precipitate was filtered. The filtrate after concentrated was identified as **oleic acid** (200 mg).

Ground *M. stenopetala* kernels (5 g) were extracted with hexane (30 mLx2) by placing on steam bath for 5 min. and on a mechanical shaker for 6 h. It was filtered and the combined filtrate was concentrated to afford an oily material which solidifies immediately on standing (1.62 g, 32%). The solid was dissolved in hot hexane (2 mL) and left overnight. The white precipitate formed was decanted, washed with hexane to afford a white powder identified as **stearic acid** (50 mg). The schematic diagram showing the extraction procedure is depicted in Scheme 3.

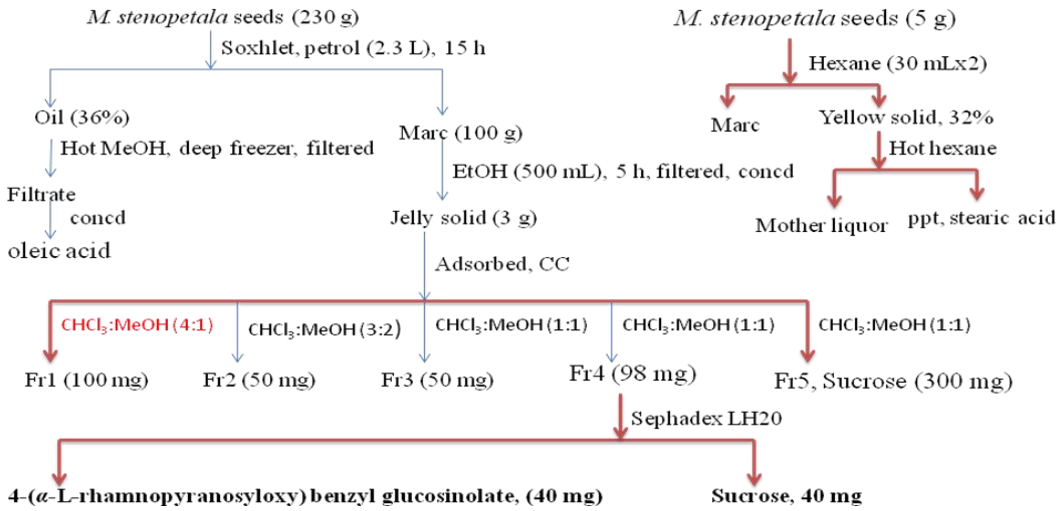

Scheme 3: Extraction and isolation of compounds from the seeds of *M. stenopetala*

Hydrolysis of *M. stenopetala* Oil: To *M. stenopetala* oil (2 g) was added EtOH (5 mL), H_2O (5 mL), 10% aqueous solution of NaOH (10 mL), and boiling chips. The mixture was refluxed over steam bath for 1 h, cooled, acidified to pH 1, filtered and the resulting white solid was washed with ice cold water, and dried to afford 1.6 g (80%). This was analyzed using FT-MS.

Preparation of fatty acid methyl esters (FAME)

M. stenopetala oil (2 g) was placed in 25 mL round bottom flask which contained 6 mL hexane to which 4 mL BF_3 in MeOH solution was added. The reaction mixture was refluxed in water bath for 30 min. Then it was cooled to room temperature. To the cooled mixture, 5 mL of water was added with vigorous shaking and two layers were formed. The upper layer was separated by using separatory funnel, dried over anhydrous sodium sulphate, filtered and concentrated to afford 500 mg (25%). A small portion of the methylated fatty acids was dissolved in hexane and analyzed using GC-MS

Extraction and fractionation of the husk of *M. stenopetala* seed: To ground *M. stenopetala* husk (100 g) was added EtOH (600 mL), placed on steam bath (20 min.), on a mechanical shaker (8 h), filtered and concentrated to afford 2 g (2%) yellowish jelly semisolid material. This was adsorbed and applied on a silica gel column packed with CH_2Cl_2. The column was eluted with CH_2Cl_2:MeOH of increasing polarities (Table 13).

Table 13: Column chromatographic fractionation of the ethanol extract of the husk of *M. stenopetala*

Fractions	Eluent (ratio)	Volume of eluent in mL	Amount in mg
Fr1	CH_2Cl_2	20	240
Fr2	‘’	30	40
Fr3	‘’	50	60
Fr4	‘’	20	10
Fr5	‘’	50	12
Fr6	‘’	50	60
Fr7	‘’	60	20
Fr 8	‘’	50	80
Fr9	‘’	40	10
Fr10	CH_2Cl_2: MeOH (9:1)	40	10
Fr11	‘’	30	20
Fr12	‘’	50	80
Fr13	‘’	10	20
Fr14	‘’	20	40
Fr15	‘’	30	40
Fr16	CH_2Cl_2: MeOH (4:1)	30	20
Fr17	‘’	30	20
Fr18	‘’	25	30
Fr19	‘’	25	20
Fr20	‘’	50	10
Fr21		25	30
Fr22	CH_2Cl_2:MeOH (1:1)	50	15
Fr23	‘’	40	20
Fr24	MeOH	30	20
Fr25	‘’	40	85
Fr26	‘’	30	50
Fr27	‘’	30	100

Fraction 8, **Fraction 19** and **Fraction 24** (20 mg) were identified to be **stearic acid** (80 mg), **compound 190** (20 mg) and **allantoin** (20 mg), respectively. The schematic diagram showing the extraction procedure is shown in Scheme 4

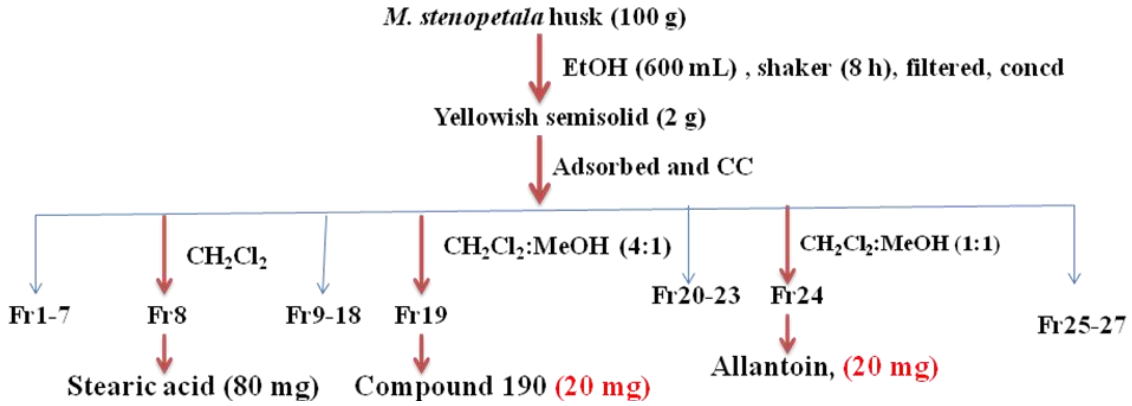

Scheme 4: Flow sheet diagram showing extraction and isolation of compounds from the husk of *M. stenopetala*

Radical Scavenging Assay: Performed according to the procedure on page 44 and 45

Thiocyanate Method: The antioxidant potential of *M. stenopetala* and *M. oleifera* leaves were done according to the method of Nagatsu, A. [235]. Each 0.1 mg EtOH extract of *M. oleifera* and *M. stenopetala*, 100 µL of linoleic acid, EtOH (5 mL) and phosphate buffer (5 mL, 0.05 M, pH = 7) in water were separately added in to a vial and incubated at 40°C in an oven. After 24 h, 0.1 mL from each were taken and added in to a vial containing 75% aqueous EtOH (7 mL), 30% of NH_4SCN (0.15 mL) and 0.15 mL of 0.02M $FeCl_2$ in 3.5% HCl. Each was then subjected to UV-Vis spectrophotometery to record the absorbance at 500 nm. Absorbance of the blank and ascorbic acid were done in the same fashion.

1-Heptacosanol (350 mg): White powder; mp 82-83°C; $[\alpha]_{589}^{21}$ = 0.00 (c 0.4, $CHCl_3$); UV λ_{max} ($CHCl_3$) nm: no absorption maxima; IR υ_{max} cm^{-1}: 3400 (OH) and 2950 (C-H); ^{1}H-NMR (400 MHz, $CDCl_3$): δ_H 3.66 (2H, *t*, *J* = 6.60 Hz, H-1), 1.59 (2H, *m*, H-2), 1.27 (48H, *br s*, H-3 to H-26) and 0.90 (3H, *t*, *J* = 6.70 Hz, H-27); ^{13}C-NMR (100 MHz, $CDCl_3$): δ_C 63.1 (C-1), 32.8 (C-2), 31.9(C-3), 29.7-29.3 (C4-24), 25.7 (C-25), 22.6 (C-26) and 14.1 (C-27)

Rutin (250 mg): Yellowish solid recrystalized from methanol; mp 189-191°C; TLC: Rf 0.50 (eluent EtOAc:MeOH, 3:2), and fast blue B salt as spraying agent; $[\alpha]_{589}^{21}$ = 3.50 (c 0.4, EtOH); UV λ_{max} (MeOH) nm: 260, 357; FTMS: molecular formula $C_{27}H_{30}O_{16}$, *m/z* 609.1451 (calcd 609.5095 for $C_{27}H_{30}O_{16}$), 465 (M-rhamnose) and 303 (M-rhamnose-glucose); IR υ_{max} cm^{-1} :3428 (O-H stretching), 2935 (C-H stretching) and 1653 (carbonyl); ^{1}H-NMR (400 MHz, DMSO-d6): δ_H 12.60 (1H, 5-OH), 7.54 (1H, *dd, J* = 8.24, 2.40 Hz, H-6'), 7.50 (1H, *d*, 2.40 Hz, H-2'), 6.84 (1H, *d*, *J* = 8.24 Hz, H-5'), 6.30 (1H, *d*, *J* = 2.10 Hz, H-8), 6.20 (1H, *d*, *J* = 2.10 Hz, H-6), 5.35 (1H, *d*, *J* = 7.83 Hz, H-1''), 3.22 (1H, *m,* H-2''), 3.28 (1H, *m*, H-3''), 3.39 (1H, *m, H-4''*), 3.21 (1H, *m, H-5''*), 3.69 (1H, *d,* H-6'') & 3.25 (1H, *m,* H-6''), 4.38 (1H, *bro. s,* H-1'''), 3.26 (1H, *m,* H-2'''), 3.05 (1H, *m,* H-3'''), 3.06 (1H, *m,* H-4'''), 3.26 (1H, *m,* H-5'''), 0.97 (3H, *J* = 6.09 Hz, H-6'''); ^{13}C-NMR (100 MHz, DMSO-d6): δ_C 177.7 (C-4), 156.8 (C-5), 161.6 (C-7), 157.0 (C-2), 164.4 (C-9), 148.8 (C-4'), 145.1 (C-3'), 133.7 (C-3), 122.0 (C-6'), 121.5 (C-1'), 116.6 (C-2'), 115.6 (C-5'), 104.3 (C-10), 101.5 (C-1''), 101.1 (C-1'''), 99.1 (C-6), 94.8 (C-8), 74.5 (C-2''), 76.3 (C-3''), 70.4 (C-4''), 76.8 (C-5''), 67.4 (C-6''), 70.8 (C-2'''), 71.0 (C-3'''), 72.3 (C-4'''), 68.7 (C-5''') and 18.6 (C-6''')

Quercetin (20 mg): Yellowish solid; TLC (Rf 0.7) using EtOAc as a mobile phase; $[\alpha]_{589}^{21}$ = 0.00 (c 0.4, EtOH); UV λ_{max} (MeOH) nm: 255, 372; FTMS: molecular formula $C_{15}H_{10}O_7$ and *m/z* 303.0510 (calcd 303.2436 for $C_{15}H_{11}O_7$); IR υ_{max} cm^{-1}: 3391 (OH), 1613 (C=C); ^{1}H-NMR (400 MHz, acetone-d6): δ_H 6.27 (1H, *d*, *J* = 1.60 Hz, H-6), 6.53 (1H, *d*, *J* = 1.60 Hz, H-8), 7.84 (1H, *d*, *J* = 2.00 Hz, H-2'), 7.00 (1H, *d*, *J* = 9.20 Hz, H-5'), and 7.71 (1H, *dd*, *J* = 8.80, and 2.00 Hz, H-6'); ^{13}C-NMR (100 MHz, acetone-d6): δ_C 146.1 (C-2), 135.8 (C-3), 175.7 (C-4), 161.1 (C-5), 98.2 (C-6), 165.1 (C-7), 93.5 (C-8), 156.9 (C-9), 103.2 (C-10), 122.8 (C-1'), 114.8 (C-2'), 144.9 (C-3'), 147.4 (C-4'), 115.3 (C-5') and 120.5 (C-6')

Kaempferol-3-O-*β*-D-glucoside (10 mg): Yellow solid; mp: 189-191°C; UV λ_{max} (MeOH) nm: 265, 354; FT-MS: molecular formula $C_{21}H_{20}O_{11,}$ *m/z* 447.0924 (calcd 447.3689 for $C_{21}H_{19}O_{11}$), and 284 (M-glucose); ^{1}H-NMR (400 MHz, acetone-d6): δ_H 8.16 (2H, *d*, *J* = 9.20 Hz, H-2', 6'), 7.00 (2H, *d*, *J* = 9.20 Hz, H-3' 5'), 6.54 (1H, *d*, *J* = 2.00 Hz, H-8), 6.30 (1H, *d*, *J* = 2.00 Hz, H-6) and 5.20 (1H, *d*, *J* = 7.20 Hz, H-1'), 3.59 (6H, H-2''– H-6''); ^{13}C-NMR (100 MHz, $CDCl_3$): δ_C 158.8 (C-2), 135.3 (C-3), 178.3 (C-4), 162.9 (C-5), 99.7 (C-6), 165.8 (C-7), 94.6 (C-8), 104.2 (C-

10), 123.0 (C-1'), 131.2 (C-2' and C-6'), 115.9 (C-3' and 5'), 161.4 (C-4'), 103.9 (C-1''), 75.5 (C-2''), 78.2 (C-3''), 71.2 (C-4''), 77.9 (C-5''), and 62.4 (C-6'')

Quercetin-3-O-*β*-D-glucoside*:* Yellow solid; mp: 192-194°C; UV λ_{max} (MeOH) nm: 265, 354; IR υ_{max} cm^{-1} = 3368 (OH stretching), 1665 (*α*,*β*-unsaturated carbonyl), 1609 (aromatic C=C), and 1062(C-O stretching); FT-MS: molecular formula $C_{21}H_{20}O_{12}$, *m/z* 463.0882 (calcd 463.3683 for $C_{21}H_{19}O_{12}$) and 301 (M-glucose); ^{1}H-NMR (400 MHz, DMSO-d6): δ_H 7.72 (1H, *d*, *J* = 2.40 Hz, H-2'), 7.60 (1H, *dd*, *J* = 2.40 and 8.80 Hz, H-6'), 6.80 (1H, *d,* H-5'), 6.41 (1H, *d*, *J* = 2.00 Hz, H-6), *δ* 6.23 (1H, *d*, *J* = 2.00 Hz, H-8), 5.27 (1H, d, *J* = 7.6 Hz, H-1'); ^{13}C-NMR (100 MHz, DMSO-d6): δ_C 178.1 (C-4), 164.6 (C-7), 161.6 (C-5), 157.6 (C-9), 157.0 (C-2), 148.4 (C-4'), 144.5 (C-3'), 134.2 (C-3), 121.8 (C-1'), 121.7 (C-6'), 116.1 (C-5'), 114.6 (C-2'), 104.2 (C-10), 102.9 (C-1''), 98.4 (C-6), 93.3 (C-8), 77.0 (C-5''), 76.7 (C-3''), 74.3 (C-2''), 69.8 (C-4''), and 61.1 (C-6'')

Inositol dimer (5 mg): White solid soluble in water; $[\alpha]_{589}^{21}$ = -75.0 (c 0.2, MeOH); ^{1}H-NMR (400 MHz, D_2O): δ_H 3.93 (2H, *br. t*), 3.49 (4H, *t*, *J* = 9.60 Hz), 3.36 (4H, *dd*, *J* = 9.60, 2.80 Hz) and 3.11 (2H, *d*, *J* = 9.20 Hz); ^{13}C-NMR (100 MHz, D_2O): δ_C 74.3 (C-1), 72.4 (C-2 and 6), 72.1 (C-4), and 71.1 (C-3 and 5).

4-(*α*-L-rhamnopyranosyloxy) benzyl glucosinolate (40 mg): Yellowish jelly solid soluble in water and methanol; TLC (Rf 0.5) using EtOAc:MeOH (3:2) as a mobile phase and vanillin as spraying reagent; UV λ_{max} (MeOH) nm: 245, 273; FTMS: molecular formula $C_{20}H_{28}NO_{14}S_2^-$ and *m/z* 570.0960 (calcd 570.5666 for $C_{20}H_{28}NO_{14}S_2^-$); IR υ_{max} cm^{-1}: 3400 (OH stretching), 2924 (C-H stretching), and 1613 (C=C stretching); ^{1}H-NMR (400 MHz, D_2O): δ_H 7.25 (2H, *d*, *J* = 8.40 Hz, H-3,5), 7.04 (2H, *d*, *J* = 8.40 Hz, H-2,6), *δ* 5.30 (1H, *d*, *J* = 1.36 Hz, H-1''), 1.13 (3H, *d*, *J* = 5.60 Hz, H-6''), 4.00 (2H, *bro. s,* H-7) and 4.00 to 3.00 (methine protons of the sugar moieties); ^{13}C-NMR (100 MHz, D_2O): δ_C 162.5 (C-8), 154.6 (C-1), 129.4, (C-3, 5), 117.5 (C-2, 6), 98.8 (C-1''), 81.3 (C-1'), 60.2 (C-6'), 37.4 (C-7), 16.5 (C-6''), 79.8, 76.6, 72.0, 71.7, 70.0, 69.9, 69.4, 68.7 and 60.2 (C-6')

Compound 190 (20 mg): White solid; mp 153-155°C; $[\alpha]_{589}^{21}$ = -15 (0.4, MeOH); UV λ_{max} (MeOH) nm: 271; IR υ_{max} cm^{-1}: 3387 (OH stretching), 2920 (C-H stretching), 1612 (aromatic C=C), and

1064 (C-O stretching); ^{1}H-NMR (400 MHz, DMSO-d6): δ_H 7.22 (2H, *d*, *J* = 8.20 Hz, H-3), 6.96 (2H, *d*, *J* = 8.20 Hz, H-2), 5.32 (1H, *d*, *J* = 1.32 Hz, H-1'), δ 4.40 (2H, *d*, *J* = 4.73 Hz, H-7), 5.18 (1H, *d*, *J* = 4.23 Hz, OH), 5.92 (1H, *d*, *J* = 5.92 Hz, OH), and 4.81 (1H, *d*, *J* = 5.92 Hz, OH), 3.25 (1H, *m*, H-5'), 3.43 (1H, *m*, H-3'), 3.61(1H, *m*, H-2') and 3.62 (1H, *m*, H-4'), δ 1.07 (3H, *d*, *J* = 6.14 Hz, H-6'); ^{13}C-NMR (100 MHz, DMSO-d6): δ_C 155.3 (C-1), 136.2 (C-4), 128.4 (C-3), 116.6 (C-2), 98.8 (C-1'), δ 72.2 (C-4'), 70.8 (C-2'), 70.6 (C-3'), 69.7 (C-5'), 62.9 (C-7), 18.2 (C-6')

Allantoin (20 mg): White solid; mp 220-222^{o}C; UV λmax (MeOH) nm: 266; FTMS: molecular formula $C_4H_6O_3N_4$ and *m/z* 181.0332 (calcd 181.10537 for $C_4H_6O_3N_4Na$); IR υ_{max} cm^{-1}: 3438 (NH stretching), 2921 (C-H stretching), and 1715 (amide carbonyl); ^{1}H-NMR (400 MHz, DMSO-d6): δ_H 10.70 (1H, *br. s,* H-1'), 8.10 (1H, *s*, H-2'), 6.97 (1H, *d*, *J* = 8.00 Hz), 5.85 (2H, *s,* H-4'), 5.21 (1H, *d*, *J* = 8.00 Hz, H-3); ^{13}C-NMR (100 MHz, $CDCl_3$): δ_C 174.0 (C-1), 157.9 (C-2), 157.3 (C-4) and 62.8 (C-3)

3.6. References

1. Mahmood, K.T., Mugal, T., Haq, I.U. **2010**. *Moringa oleifera*: A natural Gift-A review , *J. Pharm. Sci. and Res.* **2**(11), 775–781
2. Mamedov, N. **2012**. Medicinal Plants Studies: History, Challenges and Prospective, *Med Aromat Plants*, **1**, 8
3. Phillipson, J.D. **2001**. Phytochemistry and Medicinal Plants, *Phytochemistry*, **56**, 237–243
4. Gurib-Fakim, A. **2006**. Medicinal plants: Traditions of Yesterday and Drugs of Tomorrow, *Molecular Aspects of Medicine*, **27**, 1–93
5. Joy, P.P., Thomas, J., Mathew, S., Skaria, B.P. **1998**. Medicinal Plants, Aromatic and Medicinal Plants Research Station, Kerala Agricultural University, Kerala, India.
6. Chhetri, H.P., Yogol, N.S., Sherchan, J., Anupa, K.C., Mansoor, S., Thapa, P. **2008**. Phytochemical and Antimicrobial Evaluations of Some Medicinal Plants of Nepal, *Kathmandu University Journal of Science, Engineering and Technology*, **1**(5), 49–54
7. Hostettmann, K., Marston, A., Ndjoko, K., Wolfender, J. **2000**. The Potential of African Plants as a Source of Drugs, *Current Organic Chemistry*, **4**, 973–1010
8. Jamil, A., Shahid, M., Khan, M.M., Ashraf, M. **2007**. Screening of Some Medicinal Plants for Isolation of Antifungal Proteins and Peptides, *Pak. J. Bot*., **39**(1), 211–221
9. Jamil, A., Shahid, M., Khan, M.M., Ashraf, M. **2007**. Screening of Some Medicinal Plants for Antifungal Proteins and Peptides, *Pak. J. Bot*., **39**(1), 211–221
10. Bekele, E. **2007**. Actual Situation of Medicinal Plants in Ethiopia, Prepared for Japan Association for International Collaboration of Agriculture and Forestry, Addis Ababa, Ethiopia, pp 1-65
11. Yirga, G. **2010**. Assessment of Indigenous Knowledge of Medicinal Plants in Central Zone of Tigray, Northern Ethiopia, *African Journal of Plant Science*, **4**(1), 006–011
12. Birhanu, Z. **2013**. Traditional Use of Medicinal Plants By the Ethnic Groups of Gondar Zuria District, North-western Ethiopia, *Journal of Natural Remedies*, **13**(1), 47-55
13. Second Country Report on the State of Plant Genetic Resources for Food and Agriculture to FAO. **2007**. Institute of Biodiversity Conservation (IBC) , Addis Ababa, Ethiopia
14. Razavi, S.M., Zahri, S., Zarrini, G., Nazemiyeh, H., Mohammadi, S. **2009**. Biological activity of Quercetin-3-*O*-*β*-D-glucoside, a Known Plant Flavonoid, *Russian Journal of Bioorganic Chemistry*, **35**(3), 376–378

15. Dias, D.A., Urban, S., Roessner, U. **2012**. A Historical Overview of Natural Products in Drug Discovery, *Metabolites*, **2**, 303-336
16. Peteros, N.P., Mylene M.U. **2010**. Antioxidant and Cytotoxic Activities and Phytochemical Screening of Four Philippine Medicinal Plants, *Journal of Medicinal Plants Research*, **4**(5), 407-414
17. Mahesh, B., Satish, S. **2008**. Antimicrobial Activity of Some Important Medicinal Plant Against Human and Plant Pathogens. *World Journal of Agricultural Sciences*, **4**, 839-843
18. Kocabas, Y.Z., karaman, S. **2001**. Essential Oils of Lamiaceae Family from South East Mediterranean Region, *Pakistan Journal of Biological Sciences*, **4**(10), 1221–1223
19. Raja, R.R. **2012**. Medicinally Potential Plants of Lamiaceae Family: An Overview, *Research Journal of Medicinal plant*, 1–11
20. Chakraborthy, G.S., Mazumder, A., Singh, S., Verma, P. **2013.** *Clerodendrum inerme*: A Current Review, *Pharmacophore*, **4**(6), 230–232
21. Wang, P., Sun, L., Tan, J., Xu, J., Guo, F., Li, Y. **2012**. Two New Glycosidated Coumaramides from *Clerodendron cyrtophyllum*, *Fitoterapia*, **83**, 1494–1499
22. Jadeja, R.N., Thounaojam, M.C., Singh, T.B., Devkar, R.V., Ramachandran, A.V. **2012**. Traditional Uses, Phytochemistry and Pharmacology of *Clerodendron glandulosum*-A review, *Asian Pacific Journal of Tropical Medicine*, 1–6
23. Steane, D.A., Scotland, R.W., Mabberley, D.J., Olmstead, R.G. **1999**. Molecular Systematics of *Clerodendrum* (Lamiaceae): Its Sequences and Total Evidence, *American Journal of Botany*, **86**(1), 98–107
24. Kalita, J., Singh, S.S., Khan, M.L. **2012**. *Clerodendrum colebrookianum*: A Potential Folk Medicinal Plant of North East India, *Asian J Pharm Biol Res*, **2**(4), 256–262
25. Shrivastava, N., Patel, T. **2007**. *Clerodendrum* and Heath Care: An Overview, *Medicinal and Aromatic Plant Science and Biotechnology*, **1**(1), 142–150
26. Yankanchi S. R., Koli S. A. **2010**. Anti-inflammatory and Analgesic Activity of Mature Leaves Methanol Extract of *Clerodendrum inerme*, *J. Pharm. Sci. & Res.*, **2**(11), 782–785
27. Anitha, R., Kannan, P. **2006**. Antifungal Activity of *Clerodendrum inerme* (L). and *Clerodendrum phlomidis* (L)., *Turk J Biol*, **30**, 139–142

28. Oly, W.T., Islam, W., Hassan, P., Parween, S. **2011**. Antimicrobial Activity of *Clerodendrum viscosum*, *International Journal of Agriculture & Biology*, **13**, 222–226
29. Balogun, E.A., Adebayo, J.O., Zailani, A.H., Kolawole, O.M., Ademowo, O.G. **2009**. Activity of Ethanolic Extract of *Clerodendrum violaceum* Leaves Against *Plasmodium berghei* in Mice, *Agric. Biol. J. N. Am*, **1**(3), 307–312
30. Praveen, M., Radha, K., Padmaja, V., William, H., Ajithkumar, P. **2013**. *In vitro* Anthelmintic Activity of *Clerodendrum Paniculatum* Linn Leaves, *Research Journal of Pharmaceutical*, *Biological and Chemical Sciences*, **4**(2), 321–326
31. Edwards, S., Kelbessa, E., Demissew, S. **2006**. Flora of Ethiopia and Eritrea, Gentianceae to Cyclochilaceae, **5**, 525
32. Pascaline, J., Charles, M., Lukhoba, C., George, O. **2011**. Phytochemical Constituents of Some Medicinal Plants Used by the Nandis of South Nandi District, Kenya, *Journal of Animal & Plant Sciences*, **9(**3), 1201–1210
33. Wambugu, S.N., Mathiu, P.M., Gakuya, D.W., Kanui, T.I., Kabasa, J.D., Kiama, S.G. **2011**. Medicinal Plants Used in the Management of Chronic Joint Pains in Machakos and Makueni Counties, Kenya, *Journal of Ethnopharmacology*, **137**, 945– 955
34. Hayelom, K, Mekbeb, A, Eyasu, M, Wondwossen, E, Kelbesa, U. **2012**. Methanolic Effect of *Clerodendrum myricoides* Root Extract on Blood, Liver and Kidney Tissues of Mice, *African Health Sciences*, **4**(12), 489–501
35. Assefa, A., Urga, K., Guta, M., Mekonene, W., Melaku, D., Mudie, K., Kidanemariam, T. **2007**. *In vivo* Antimalarial Activities of Plants used in Ethiopian Traditional Medicine, Delomenna, Ethiopia, Department of Drug Research Ethiopia Health and Nutrition Research Institution
36. Reid, K.A., Maes, J., Maes, A., van Staden, J., Kimpec, N.D., Mulholland, D.A., Verschaeve, L. **2006**. Evaluation of the Mutagenic and Antimutagenic Effects of South African Plants, *Journal of Ethnopharmacology*, **106**, 44–50
37. Stark, T.D., Mtui, D.J., Balemba, O.B. **2013**. Ethnopharmacological Survey of Plants Used in the Traditional Treatment of Gastrointestinal Pain, Inflammation and Diarrhea in Africa: Future Perspectives for Integration into Modern Medicine, *Animals*, **3**, 158–227

38. Shrivastava, N., Patel, T. **2007**. *Clerodendrum* and Heath care: An Overview, Part II Phytochemistry and Biotechnology, *Medicinal and Aromatic Plant Science and Biotechnology*, **1**(2), 209–223
39. Ono, M., Furusawa, C., Matsumura, K., Noguchi, S., Yasuda, S., Okawa, M., Kinjo, J., Eto, M., Yamaguchi, K., Yoshimitsu, H., Nohara, T. **2013**. A New Diterpenoid from the Leaves of *Clerodendron trichotomum*, *J Nat Med*, **67**, 404–409
40. Patel, J.J., Acharya, S.R., Acharya, N.S. **2014**. *Clerodendrum serratum* (L.) Moon. A review on Traditional Uses, Phytochemistry and Pharmacological Activities, *Journal of Ethnopharmacology*, Article in press
41. Liu, Q., Hu, H., Li, P., Yang, Y., Wu, L., Chou, G., Wang, Z., **2014**. Diterpenoids and Phenylethanoid Glycosides from the Roots of *Clerodendrum bungei* and Their Inhibitory Effects Against Angiotensin Converting Enzyme and *α*-Glucosidase, *Phytochemistry* xxx, xxx–xxx, Article in press
42. Yang, H, Wang, J, Hou, A, Guo, Y, Lin, Z., Sun, H. **2000**. New Steroids from *Clerodendrum colebrookianum*, *Fitoterapia*, **71**, 641–648
43. Macabeo, A.P.G., Villafranca, M.C.G., Aguinaldo, A.M., Hussain, H., Krohn, K. **2008**. Clerosterols from *Clerodendrum quadriloculare*, *Biochemical Systematics and Ecology*, **36**, 659–660
44. Pandey, R., Verma, R.K., Gupta, M.M. **2005**. Neo-clerodane Diterpenoids from *Clerodendrum inerme*, *Phytochemistry*, **66**, 643–648
45. Goswami, P., Kotoki, J., Chen, Z., Lu, Y. **1996**. A Sterol Glycoside from the Leaves of *Clerodendron colebrookianum*, *Phytochemistry*, **41**(1), 279–281
46. Zhu, H., Huan, L., Chen, C., Yang, J., He, J., Chen, Y., Yao, G., Luo, Z., Xue, Y., Zhang, Y. **2014**. A Pair of Unprecedented Cyclohexylethanoid Enantiomers Containing Unusual Trioxabicyclo[4.2.1]nonane Ring from *Clerodendrum bungei*, *Tetrahedron Letters*, **55**, 2277–2279
47. Xu, R., Wang, R., Ha, W., Shi, Y. **2014**. New Cyclohexylethanoids from the Leaves of *Clerodendrum trichotomum*, *Phytochemistry Letters*, **7**,111–113

48. Miller, R.E., McConville, M.J., Woodrow, I.E. **2006**. Cyanogenic Glycosides from the Rare Australian Endemic Rainforest Tree *Clerodendrum grayi* (Lamiaceae), *Phytochemistry*, **67**, 43–51
49. Tadesse, Y. **2011**. Bioactivity guided study on the antimalarial activities of *Clerodendrum myricoides* and *Dodonaea angustifolia*, MSc. Thesis, Biology Department, Addis Ababa University, Addis Ababa, Ethiopia
50. Gebretsadik, G. **2012.** Bioactivity guided fractionation and antimalarial activity of fractions of ethanol extract of *Clerodendrum myricoides* leaves in mice model, MSc Thesis, Biology Department, Addis Ababa University, Addis Ababa, Ethiopia.
51. Ragasa, Y., Galian, R.F., Arenal, M., Tan, V., Shen, C. **2014**. Triterpenes and Sterols from *Samanea saman*, *Research Journal of Pharmaceutical, Biological and Chemical Sciences*, **5**(4), 1501–1508
52. Tareq, S.M., Apu, A.S., Basak, D., Islam, M.S. **2010**. Isolation and Identification of Compounds from the Leaf Extract of *Dillencia indica* linn, *Bangladesh Pharmaceutical Journal*, **13**(1), 49–54
53. Billah, A.H., Hussain, M.M., Dastagir, M.G., Ismail, M., Quader, A. **2013**. Isolation of α-Spinasterol from *Amaranthus spinosus* Stems, *Bol Latinoam Caribe Plant Med Aromat*, **12**(1), 15–17
54. Ismail, M., Hussain, M.M., Dastagir, M.G., Billah, M., Quader, A. **2010**. Phytochemical and Antimicrobial Investigation of *Luffa cylindrical*, *Bol Latinoam Caribe Plant Med Aromat*, **9**(5), 327–332
55. Kim, H.M., Ahn, M., Lee, S. **2012**. Isolation and Identification of Phytochemical Constituents from *Scrophularia takesimensis*, *Journal of Medicinal Plants Research*, **6**(22), 3923–3930
56. Proksa, B., Uhrín, D., Fuska, J. **1991**. Secondary Metabolites of *Stenactis annua* L., *Chem. Papers*, **45**(6), 837–844
57. Kumar, S., Siddhu, S.K., Mehta, B.K. **2014**. New Triterpene Compound (Lup-20(29)-en-3β-3,27-diol) Isolated from Extract of *Nigella sativa* (seeds), *Journal of Natural Products*, **7**, 113–115

58. Gook-Che, J., Myoung-Soon, P., Do-Young, Y., Chul-Ho, S., Hong-Sig, S., Soo-Jong U. **2005**. Antitumor Activity of α-Spinasterol Isolated from Pueraria Roots, *Experimental and Molecular Medicine*, **37**(2), 111–120
59. Jeong, G., Li, B., Lee, D., Kim, K., Lee, I.K., Lee, K.R., Kim, Y. **2010**. Cytoprotective and Antiinflammatory Effects of Spinasterol via Induction of Hemeoxygenase in Murine Hippocampal and Microglial Cells, *International Immunopharmacology*, **10**, 1587–1594
60. Islam, M., Al-Amin, M., Siddiqi, M.M.A., Akter, S., Haque, M.M., Sultana, N., Chowdhury, A.M.S. **2012**. Isolation of Quercetin-3-O-β-D-glucopyranoside from the Leaves of *Azadirachta indica* and Antimicrobial and Cytotoxic Screening of the Crude Extracts, *Dhaka Univ. J. Sci.* **60**(1), 11–14
61. Ersoz, T., Berkman, M.Z., Tasdemir, D., Calis, I. **2002**. Iridoid and Phenylethanoid Glycosides from *Euphrasia pectinata*, *Turk J Chem*, **26**, 179–188.
62. Yayli, N, Yildirim, N., Usta, A., Ozkurt, S., Akgun, V. **2003**. Chemical Constituents of *Campanula lactiflora, Turk J Chem*, **27**, 749–755
63. Shabana, M.M., Salama, M.M., Ezzat, S.M., Ismail, L.R. **2013**. *In vitro* and *In vivo* Anticancer Activity of the Fruit Peels of *Solanum melongena* Against Hepatocellular Carcinoma, *J Carcinogene Mutagene*, **4**(3), 149–155
64. Hegazy, A. K., Tahany, M.A.A., Sayed, A.M., Kabiel, H.F., El-Alfy, T., El-Komy, S.M., **2010**. Study on Combined Antimicrobial Activity of Some Biologically Active Constituents from Wild *Moringa peregrina* Forssk, *Journal of Yeast and Fungal Research*, **1**(1), 015–024
65. Sajad, T, Zargar, A. Ahmad, T., Bader, G. N., Naime, M., Ali, S. **2010**. Antibacterial and Anti-inflammatory Potential of *Bergenia ligulata*, *Am. J. Biomed. Sci*., **2**(4), 313–321
66. El-Kashoury, E.A., El-Askary, H.I., Kandil, Z.A., Ezzat, S.M., Salem, M.A., Sleem, A.A. **2014**. Chemical and Biological Study of *Mentha suaveolens* Cultivated in Egypt, *J. Med. Plants Res*, **8**(20), 747–755
67. El-Sharabasy, F., Mohamed, N.Z. **2013**. Chemical Constituents and Biological Activity from Chloroform Extract of *Zilla spinosa*, *International Journal of Pharmacy and Pharmaceutical Sciences*, **5**(1), 422–427

68. Motawe, H.M., Wahba, H.E., Ibrahim, A.Y., El-Nakkady, A.N. **2013**. Steryl Glycosides, Lipoidal Matter and Volatile Constituents of *Urtica pilulifera*, *Global Journal of Pharmacology*, **7**(4), 377–382
69. Brandão, G.C., Kroon, E.G., Souza, D.E.R., Filho, J.D.S., Oliveira, A.B. **2013**. Chemistry and Antiviral Activity of *Arrabidaea pulchra* (Bignoniaceae), *Molecules*, **18**, 9919–9932
70. Micol, V., Caturla, N., Perez-Fons, L., Mas, V., Perez, L., Estepa, A. **2005**. The Olive Leaf Extract Exhibits Antiviral Activity Against Viral Haemorrhagic Septicaemia Rhabdovirus (VHSV), *Antiviral Research*, **66**, 129–136
71. Mahato SB, Sahu NP, Roy SK, Sharm OP. **1994**. Potential Antitumor Agents from *Lantana camara*: Structures of Flavonoid and Phenylpropanoid Glycosides, *Tetrahedron*, **50**(31), 9439–9446
72. Abougazar H, Bedir E, Khan IA, Cails I. **2003**. Wiedemanniosides A-E: New Phenylethanoid Glycosides from the Roots of *Verbascum wiedemonnianum, Planta Med*., **69**(9), 814–819
73. Carrillo-Ocampo, D., Bazaldúa-Gómez, S., Bonilla-Barbosa, J.R., Aburto-Amar, R., Rodríguez-López, V. **2013.** Anti-inflammatory Activity of Iridoids and Verbascoside Isolated from *Castilleja tenuiflora*, *Molecules*, **18**, 12109–12118
74. Dellaquila, M.E., Bogliolo, L., Russo, R., Martino, N.A., Uranio, M.F., Ariu, F., Amati, F., Sardanelli, A.M., Linsalata, V., Ferruzzi, M.G., Cardinali, A., Minervini, F. **2014**. Prooxidant Effects of Verbascoside, a Bioactive Compound from Olive Oil Mill Wastewater, on *In vitro* Developmental Potential of Ovine Prepubertal Oocytes and Bioenergetic/Oxidative Stress Parameters of Fresh and Vitrified Oocytes, *BioMed Research International*, 1–14
75. Tong-fei, Z., Ke, J., Zhi-hui, Y., Juan-juan, H., Lian-chun, Z., Da-cheng, W., Xu-ming, D. **2013**. A New Secoiridoid Glycoside from Roots of *Picrorhiza scrophulariiflora*, *Chinese Herbal Medicines*, **5**(3), 237–239
76. Guvenalp, Z., Ozbek, H., Kuruuzumuz, A., Kazaz, C., DemIrezer, L. **2009**. Secondary Metabolites from *Nepeta heliotropifolia, Turk J Chem*, **33**, 667–675
77. Peters W, Portus H, Robinson L. **1975**. The Four Day Suppressive *In vivo* Antimalarial Test, *Ann. Trop. Med. Parasitol.*, **69**, 155–171

78. David, F., Philip, R., Simon, C., Reto, B., Solomon, N. **2005**. Antimalarial Drug Discovery: Efficacy Models for Compound Screening, *Nature Rev.*, **3**, 509–520
79. Piguet, P.F., Da Kan, C., Vesin, C., Rochat, A., Donati, Y., Barazzone, C. **2011**. Role of CD_{40}-$CD_{40}L$ in Mouse Sever Malaria, *American J. Pathol*., **159**(2), 733–742
80. Hamid, A.A., Aiyelaagbe, O.O., Usman, L.A., Ameen, O.M., Lawal, A. **2010**. Antioxidants: Its Medicinal and Pharmacological Applications, *African Journal of Pure and Applied Chemistry*, **4**(8), 142–151
81. Sen, S., Chakraborty, R., Sridhar, C., Reddy, Y.S.R., De, B. **2010**. Free Radicals, Antioxidants, Diseases and Phytomedicines: Current Status and Future Prospect, *International Journal of Pharmaceutical Sciences Review and Research*, **3**(1), 91–101
82. Oyedemi, S.O., Afolayan, A.J. **2011**. *In vitro* and *In vivo* Antioxidant Activity of Aqueous Leaves Extract of *Leonotis leonurus*, *International Journal of Pharmacology*, **7**(2), 248–256
83. Priyadarsini, K.I. **2005**. Molecular Mechanisms Involving Free Radical Reactions of Antioxidants and Radioprotectors, Founder's Day Special Issue, 1–6
84. Gulcin, I., Huyut, Z., Elmastas, M., Aboul-Enein, H.Y. **2010**. Radical Scavenging and Antioxidant Activity of Tannic Acid, *Arabian Journal of Chemistry*, **3**, 43–53
85. Luqman, S., Srivastava, S., Kumar, R., Maurya, A.K., Chanda, D. **2012**. Experimental Assessment of *Moringa oleifera* Leaf and Fruit for Its Antistress, Antioxidant, and Scavenging Potential Using *In vitro* and *In vivo* Assays, *Evidence-Based Complementary and Alternative Medicine*, 1–12
86. Shittu, I., Emmanuel, A., Nok, J.A. **2011**. Antimalarial Effect of the Ethanolic Stem Bark Extracts of *Ficus platyphylla. J. Parasitol. Res.*, 1–5.
87. Chen Y, Li S, Sun F, Han H, Zhang X, Fan Y, Tai G, Zhou Y. **2010**. *In vivo* Antimalarial Activities of Glycoalkaloids Isolated from Solanaceae Plants, *Pharm. Biol.* **48**, 1018–1024
88. Ghasemi, K., Ghasemi, Y., Ebrahimzadeh, M.A. **2009**. Antioxidant Activity, Phenol and Flavonoid Contents of 13 Citrus Species Peels and Tissues, *Pak. J. Pharm. Sci*. **22**(3), 277–281
89. Qusti, S.Y., Abo-Khatwa, A.N., Lahwa, M.A.B. **2010**. Screening of Antioxidant Activity and Phenolic Content of Selected Food Items Cited in the Holly Quran, *EJBS*, **2**(1), 40–52

90. Hedgerg, I., Edwards, S. **1989**. Pittosporaceae to Araliaceae, Flora of Ethiopia, **3**, 490–503
91. Cook, A., Turner, S.R., Baskin, J.M., Baskin, C.C., Steadman, K.J., Dioxon, K.W. **2008**. Occurrence of Physical Dormancy in Seeds of Australian Sapindaceae: A Survey of 14 Species in Nine Genera, *Annals of Botany*, **101**, 1349–1362
92. Hamerski, L., Somner, G.V., Tamaio, N. **2013**. *Paullinia cupana* (Sapindaceae): A Review of Its Ethnopharmacology, Phytochemistry, and Pharmacology, *Journal of Medicinal Plants Research*, **7**(30), 2221–2229
93. Rani, M.S., Pippalla, R.S., Mohan, P.K. **2009**. *Dodonaea viscosa* Linn.-An Overview, *JPRHC*, **1**(1), 97–112
94. Shepherd, K.A., Rye, B.L., Meissner, R.A., West, J.G. **2007**. Two New Western Australian Species of *Dodonaea* (Sapindaceae) from Northern Yilgarn Ironstones, *Nuytsia*, **17**, 375–384
95. Harrington, M.G., Gadek, P.A. **2009**. A species Well Travelled- The *Dodonaea viscosa* (Sapindaceae) Complex Based on Phylogenetic Analysis of Nuclear Ribosomal ITS and TSF Sequences, *Journal of Biogeography*, **36**, 2313-2323
96. Omosa, L.K., Midiwo, J.O., Derese, S., Yenesew, A., Peter, M.J., Heydenreich M. **2010**. neo-15,16-Epoxy-2-hydroxy-3,13(16),14-clerodtriene-18-oic acids from the Leaf Exudate of *Dodonaea angustifolia*, *Phytochem. Lett*., **3**, 217–220
97. Liu, J., Noshiro, S. **2003**. Lack of Latitudinal Trends in Wood Anatomy of *D. viscosa* (Sapindaceae), A Species with World Wide Distribution, *American Journal of Botany*, **94**(4), 532-539
98. Cunningham, P.L., Joubert, D.F., Adank, W. **2004**. *Dodonaea angustifolia* – an Alien Invasive to the Auas Mountains in Namibia?, *Dinteria*, **29**, 11–18
99. Al-Asmari, A.K., Al Otaibi, K.E., Al-Omani, S., Athar, M.T. **2013**. An Updated Phyto-pharmacological Review on Medicinal Plant of Saudi Arabia-*Dodonaea viscosa* Linn, *American Journal of Research Communication*, **1**(12), 519–531
100. Meenu, J., Sunil, S., Manoj, K. **2011**. Evaluation of Antihyperglycemic Activity of *Dodonaea Viscosa* Leaves in Normal and Stzdiabetic Rats, *International Journal of Pharmacy and Pharmaceutical Sciences*, **3**(3), 69–74

101. Naidoo, R., Patel, M., Gulube, Z., Fenyvesi, F. **2012**. Inhibitory Activity of *Dodonaea viscosa* var. *angustifolia* Extract Against *Streptococcus mutans* and its Biofilm, *Journal of Ethnopharmacology*, **144**, 171–174

102. Ramya, R., Sivasakthi, R., Senthilkumar, S., Anudeepa, J., Santhi, N., Narayanan, R.V. **2011**. Preliminary Phytochemical and Anti-fertility Studies on *Dodonea viscosa*, *Asian J. Res. Pharm. Sci.*, **1**(3), 77–79

103. Yirga, G. **2010**. Assessment of Indigenous Knowledge of Medicinal Plants in Central Zone of *Tigray*, Northern Ethiopia, *African Journal of Plant Science*, **4**(1), 006–011

104. Pirzada, A., Shaikh, W., Usmanghani, K., Mohiuddin, E. **2010**. Antifungal Activity of *Dodonaea viscosa* Jacq Extract on Pathogenic Fungi Isolated from Super Facial Skin Infection, *Pak. J. Pharm. Sci*., **23** (3), 337–340

105. Prakash, N.K.U., Selvi, C.R., Sasikala, V., Dhanalakshmi, S., Prakash, S.B.U. **2012**. Phytochemistry and Bio-Efficacy of a Weed, *Dodonaea viscosa*, *Int J Pharm Pharm Sci*, **4**(2), 509–512

106. Khurram, M., Khan, M.A., Hameed, A., Abbas, A., Qayum, A., Inayat, H. **2009**. Antibacterial Activities of *Dodonaea viscosa* using Contact Bioautography Technique, *Molecules*, **14**, 1332–1341

107. Rajamanickam, V., Rajasekaran, A., Anandarajagopal, K., Sridharan, D., Selvakumar, K., Rathinaraj, B.S. **2010**. Antidiarreal Activity of *Dodonaea viscosa* Root, *IJPBS*, **2**(4), 182–185

108. Muthukumran, P., Begumand, V.H., Kalaiarasan, P. **2011**. Anti-diabetic Activity of *Dodonaea viscosa* (L) Leaf Extracts, *Int.J. PharmTech Res*. **3**(1), 136–140

109. Veerapar, V.P., Prabhakar, K.R., Thippeswamy, B.S., Pansal, P., Sirinvasan, K.K., Unikrshanan, M.K. **2010**. Antidiabetic Effect of *D. viscosa* Aerial Parts in High Fructose-Fedinsulin Resistant Rats: A mechanism Based Study, *Indian J Exp Biol*. **48**, 800–810

110. Akhtar, M.S., Ahmed, M., Gulzar, K., Adnan, H. **2011**. Hypoglycemic Activity of *Dodonaea viscosa* Leaves in Normal and Alloxan-Induced Diabetic Rabbits, *Diabetologia Croatica*, **40**(3), 71–80

111. Khalil, N.M., Sperotto, J.S., Manfron, M.P. **2006**. Anti-inflammatory Activity and Acute Toxicity of *Dodonaea viscosa*, *Fitoterapia*, **77**, 478–480

112. Getie, A., Gebre-Mariam, T., Rietz, R., Huschka, C., Schmidtke, M., Abate, A., Neubert, R.H.H. **2003**. Evaluation of the Anti-microbial and Anti-inflammatory Activities of the Medicinal Plants *Dodonaea viscosa*, *Rumex nervosus* and *Rumex abyssinicus, Fitoterapia*, **74**, 139–143

113. Teffo, L.S., Aderogba, M.A., Eloff, G.N. **2009**. Antibacterial and Antioxidant Activities of Four Kaempferol methyl ethers Isolated from *Dodonaea viscosa* var. *angustifolia* leaf extracts, *South African Journal of Botany*, 1–5

114. Riaz, T., Abbasi, M.A., Rehman, A.A., Shahzadi, T., Ajaib, M., Khan, K.M. **2012**. Phytochemical Screening, Free Radical Scavenging, Antioxidant Activity and Phenolic Content of *Dodonaea viscosa* Jacq., *J. Serb. Chem. Soc.*, **77**(4), 423–435

115. Oliveira, S.Q., de Almeida, M.T.R., Maraslis, F., Silva, I.T., Sincero, T.C.M., Palermo, J.A., Cabrera, C.M., Caro, M.S.B., Simoes, C.M.O., Schenkel, E.P. **2012**. Isolation of Three New ent-Labdane Diterpenes from *Dodonaea viscosa* (Sapindaceae): Preliminary evaluation of antiherpes activity, *Phytochemistry Letters*, **5**, 500–505

116. Anilreddy, B. **2009**. Preparation, Characterization and Biological Evaluation of Some Overview of *Dodonaea viscosa*, *Journal of Pharmaceutical Science and Technology*, **1**(1), 1–9

117. Ramya, R., Anudeepa, J., Senthilkumar, C., Rajendran, S.S., Sivasakthi, R, Moorthy , C., Venkatnarayanan, D.R. **2011**. Wound Healing Activity of *Dodonea viscosa* Linn Ointment In Rats, *International Journal of Research in Pharmacy and Chemistry*, **1**(3), 481–484

118. Mengiste, B., Makonnen, E., Urga, K. **2012**. *In vivo* Antimalarial Activity of *Dodonaea angustifolia* Seed Extracts Against *Plasmodium berghei* in Mice Model*, MEJS.*, **4**(1), 47–63

119. Rajeswari, D.T., Gajalakshmi, S., Jayanthi, P., Vijayalakshmi. S. **2011**. Pharmacological Activities of *Dodonaea viscosa, Journal of Pharmacy Research,* **4**(10), 3331–3333

120. van Heerden, F.R., Viljoen, A.M., van Wyk, B.E. **2000**. The Major Flavonoid of *Dodonaea angustifolia, Fitoterapia*, **71**, 602–604

121. Muhammad, A., Anis, I., Ali, Z., Awadelkarim, S., Khan, A., Khalid, A., Shah, M.R., Galal, M., Khan, I.A., Choudhary, M.H. **2012**. Methylenebissantin: A rare Methylene-Bridged Bisflavonoid from *Dodonaea viscosa* which Inhibits *Plasmodium falciparum* enoyl-ACP reductase, *Bioorganic & Medicinal Chemistry Letters*, **22**, 610–612

122. Wabo, H.K., Chabert, P., Tane, P., Noté, O., Tala, M.F., Peluso, J., Muller, C., Kikuchi, H., Oshima, Y., Lobstein, A. **2012**. Labdane-type Diterpenes and Flavones from *Dodonaea viscosa*, *Fitoterapia*, **83**, 859–863

123. Simpson, B.S., Claudie, D.J., Smith, M.N., Gerber, J.P., McKinnon, R.A., Semple, S.J. **2011**. Flavonoids from the Leaves and Stems of *Dodonaea polyandra*: A Northern Kaanju Medicinal Plant, *Phytochemistry*, **72**, 1883–1888

124. Ortega A, Garcia EP, Cardenas C, Marquina S, Garduno LD, Maldonado E. **2001**. Methyl dodonates, a New Type of Diterpenes with Modified Clerodane Skeleton from *Dodonaea viscosa*, *Tetrahedron*, **57**, 2981–2989

125. Huang, Z.,Jiang, M., Zhou, Z., Xu, D. **2009**. Two New Clerodane Diterpenes from *Dodonaea viscosa, Z. Naturforsch*, **65**, 83–86

126. Simpson, B.S., Claudie, D.J., Smith, N.M., McKinnon, R.A., Semple, S.J. **2012**. Rare, Seven-membered Cyclic Ether Labdane Diterpenoid from *Dodonaea polyandra*, *Phytochemistry*, **84**, 141–146

127. Worku, T. **2013**. *In vivo* anti plasmodial activity of active fraction/s of *Dodonaea angustifolia* in *Plasmodium berghei* infected mice, MSc Thesis, Biology Department, Addis Ababa University, Ethiopia

128. Napal, G.N.D., Palacios, S.M. **2013**. Phytotoxicity of Secondary Metabolites Isolated from *Flourensia oolepis*, *Chemistry & Biodiversity*, **10**, 1295–1305

129. Tsimogiannis, D., Samiotaki, M., Panayotou, G., Oreopoulou, V. **2007**. Characterization of Flavonoid Subgroups and Hydroxy Substitution by HPLC-MS/MS, *Molecules*, **12**, 593–606

130. Bloor, S.J. **2001**. Overview of Methods for Analysis and Identification of Flavonoids, Methods in Enzymology, vol. 335, Academic Printing Press, London, pp 13–15

131. Liu, G., Ma, J., Chen, Y., Tian, Q., Shen, Y., Wang, X., Chen, B., Yao, S. **2009**. Investigation of Flavonoid Profile of *Scutellaria bacalensis* Georgi by High Performance Liquid Chromatography with Diode Array Detection and Electrospray Ion Trap Mass Spectrometry, *Journal of Chromatography*, **1216**, 4809–4814

132. Ching, A.Y.L., Wah, T.S., Sukari, M.A., Lian, G.E.C., Rahmani, M., Khalid, K. **2007**. Characterization of Flavonoid Derivatives from *Boesenbergia Rotunda* (L.), *The Malaysian Journal of Analytical Sciences*, **11**(1), 154–159

133. Qingyun, Y., Yuanfeng, Y., Feng, C., Yan, Q., Wei, L., Song, W. **2012**. Identification and Synthesis of Impurities in Pinocembrin-A new Drug for the Treatment of Ischemic Stroke, *Chin. J. Chem.* **30**, 1315–1319

134. Punvittayagul, C., Pompimon, W., Wanibuchi, H., Fukushima, S., Wongpoomchai, R. **2012**. Effects of Pinocembrin on the Initiation and Promotion Stages of Rat Hepatocarcinogenesis, *Asian Pacific Journal of Cancer Prevention*, **13**, 2257–2262

135. Charoensin, S., Punvittayagul, C., Pompimon, W., Mevatee, U., Wongpoomchai, R. **2010**. Toxicological and Clastogenic Evaluation of Pinocembrin and Pinostrobin Isolated from *Boesenbergia pandurata* in Wistar Rats, *Thai. J. Toxicology*, **25**(1), 29–40

136. Rasul, A., Millimouno, F.M., Eltay, W.A., Ali, M., Li, J., Li, X. **2013**. Pinocembrin: A Novel Natural Compound with Versatile Pharmacological and Biological Activities, *BioMed Research International*, 1–9

137. Elema, E.T., Schripsema, J., Malingre, T.M. **1989**. The Falvones and Falvanol Glycosides from *Eupatorium carrabinum*, *Pharmaceutisch Weekblad Scientific Edition*, **11**(15), 161–164

138. Bekele, D. **2009**. Phytochemical Investigation on the Leaves of *Dodonaea viscosa* var. *angustifolia*, Thesis, Chemistry Department, Addis Ababa University, Addis Ababa, Ethiopia

139. Roy, D.C., Shaik, M.M. **2013**. Toxicology, Phytochemistry, Bioactive Compounds and Pharmacology of *Parthenium hysterophorus, Journal of Medicinal Plants Studies*, **1**(3), 126–141

140. Martinez, J., Silvan, A.M., Abad, M.J., Bermejo, P., Villar, A. 1997. Isolation of Two Flavonoids from *Tanacetum microphyllum* as PMA-Induced Ear Edema Inhibitor, *J. Nat. Prod.* **60**, 142–144

141. Sülsen, V.P., Cazorla, S.I., Frank, F.M., Redko, F.C., Anesini, C.A., Coussio, J.D., Malchiodi, E.L., Martino, V.S., Muschietti, L.V. **2007**. Trypanocidal and Leishmanicidal

Activities of Flavonoids from Argentine Medicinal Plants, *Am. J. Trop. Med. Hyg.,* **77**(4), 654–659

142. Kasal, A., Budesinsky, M., Griffiths, W.J. **2010**. Spectroscopic Methods of Steroid Analysis, Institute of Organic Chemistry and Biochemistry, Academy of Sciences of the Czech Republic, Czech Republic, pp 27–136
143. Kutrzeba, L.M., Ferreira, D., Zjawiony, J.K. **2009**. Salvinorins J from *Salvia divinorum*: Mutarotation in the Neoclerodane System, *J. Nat. Prod.* **72**, 1361–1363
144. Arora, D.S., Onsare, J.G., Kaur, H. **2013**. Bioprospecting of *Moringa*: Microbiological Perspective, *Journal of Pharmacognosy and Phytochemistry*, **1**(6), 193–216
145. Usman, M.R.M., Barhate, S.D., Usman, M.A.M. **2012**. A Review on Drumstick Tree (*Moringa pterygosperma*): Multiuse Tree with Higher Economical Values, *International Journal of Current Pharmaceutical Review and Research*, **3**(1), 15–22
146. Edwards, S., Tadesse, M., Demissew, S., Hedberg, I. **2000**. Flora of Ethiopia and Eritrea, Magnoliaceae to Flacourtiaceae, **2**(1), 155–162
147. Bennett, R.N., Mellon, F.A., Foidl, N., Pratt, J.H., Dupont, M.S., Perkins, L., Kroon, P.A. **2003**. Profiling Glucosinolates and Phenolics in Vegetative and Reproductive Tissues of the Multi-Purpose Trees *Moringa oleifera* L. (Horseradish Tree) and *Moringa stenopetala* L., *J. Agric. Food Chem.* **51**, 3546–3553
148. Goyal, B.K., Agrawal, B.B., Goyal, R.K., Mehta, A.A. **2007**. Phyto-pharmacology of *Moringa oleifera* lam, *Natural Product Radiance*, **6**(4), 347–353
149. Walter, A., Samuel, W., Peter, A., Joseph, O. **2011**. Antibacterial Activity of *Moringa oleifera* and *Moringa stenopetala* Methanol and n-Hexane Seed Extracts on Bacteria Implicated in Water Borne Diseases, *African Journal of Microbiology Research*, **5**(2), 153–157
150. Nikkon, F., Saud, Z.A., Rahman, H., Haque, M.E. **2003**. *In vitro* Antimicrobial Activity of the Compound Isolated from Chloroform Extract of *Moringa oleifera* Lam., *Pakistan Journal of Biological Sciences*, **6**(22), 1888–1890
151. Guevara, A.P., Vargas, C., Sakurai, H., Fujiwara, Y., Hashimoto, K., Maoka, T., Kozuka, M., Ito, Y., Tokuda, H., Nishino, H. **1999**. An Antitumor Promoter from *Moringa oleifera* Lam, *Mutation Research*, **44**, 181–188

152. Luqman, S., Srivastava, S., Kumar, R., Maurya, A.K., Chanda, D. **2012**. Experimental Assessment of *Moringa oleifera* Leaf and Fruit for Its Antistress, Antioxidant, and Scavenging Potential Using *In vitro* and *In vivo* Assays, *Evidence-Based Complementary and Alternative Medicine*, 1–12

153. Sreelatha, S., Padma, P.R. **2009**. Antioxidant Activity and Total Phenolic Content of *Moringa oleifera* Leaves in Two Stages of Maturity, *Plant Foods Hum Nutr*, **64**, 303–311

154. Kumbhare, M.R., Guleha, V., Sivakumar, T. **2012**. Estimation of Total Phenolic Content, Cytotoxicity and *In vitro* Antioxidant Activity of Stem Bark of *Moringa oleifera*, *Asian Pacific Journal of Tropical Disease*, 144–150

155. Shih, M., Chang, C., Kang, S., Tsai, M. **2011**. Effect of Different Parts (Leaf, Stem and Stalk) and Seasons (Summer and Winter) on the Chemical Compositions and Antioxidant Activity of *Moringa oleifera, Int. J. Mol. Sci.* **12**, 6077–6088

156. Dubey, D.K., Dora, J., Kumar, A., Gulsan, R.K. **2013**. A Multipurpose Tree- *Moringa oleifera, International Journal of Pharmaceutical and Chemical Sciences*, **2**(1), 415–423

157. Mbikay, M. **2012**. Therapeutic Potential of *Moringa oleifera* Leaves in Chronic Hyperglycemia and Dyslipidemia: A Review, *Ethnopharmacology*, **3**(4), 1–12

158. Jaiswal, D., Rai, P.K., Kumar, A., Mehta, S., Watal, G. **2009**. Effect of *Moringa oleifera* Lam. Leaves Aqueous Extract Therapy on Hyperglycemic Rats, *Journal of Ethnopharmacology***, 123**, 392–396

159. Nardos, A., Makonnen, E., Debella, A. **2011**. Effects of Crude Extracts and Fractions of *Moringa stenopetala* (Baker F) Cufodontis Leaves in Normoglycemic and Alloxan-Induced Diabetic Mice, *African Journal of Pharmacy and Pharmacology*, **5**(20), 2220–2225

160. Ugwu, O. P.C., Nwodo, O.F.C, Joshua, P.E., Odo, C.E., Bawa, A., Ossai, E.C., Adonu C.C. **2013**. Anti-Malaria and Hematological Analyses of Ethanol Leaf Extract of *Moringa oleifera* on Malaria Infected Mice, *IJPBS*, **3**(1), 360–371

161. Singh, J.P., Garg, R., Bhardwaj, S., Sharma, S.K. **2012**. Anti-inflammatory Evaluation of Leaf Extract of *Moringa* Flower, *Journal of Pharmaceutical and Scientific Innovation*, **1**(1), 22–24

162. Sashidhara, K.V., Rosaiah, J.N., Tyagi, E., Shukla, R., Raghubir, R., Rajendran, S.M. **2009**. Rare Dipeptide and Urea Derivatives from Roots of *Moringa oleifera* as Potential Anti-

inflammatory and Antinociceptive Agents, *European Journal of Medicinal Chemistry*, **44**, 432–436

163. Chandrashekar, K.S., Thakur, A., Prasanna, K.S. **2010**. Anti-Inflammatory Activity of *Moringa oleifera* Stem Bark Extracts Against Carrageenen Induced Rat Paw Edema, *J. Chem. Pharm. Res.* **2**(3), 179–181
164. Chuang, P., Lee, C., Chou, J., Murugan, M., Shieh, B., Chen, H. **2007**. Anti-Fungal Activity of Crude Extracts and Essential Oil of *Moringa oleifera* Lam, *Bioresource Technology*, **98**, 232–236
165. Urga, A.K., Knapp, H., Selmar, D., Omwega, A.M., Imungi, J.K., Winterhalter, P. **2003**. Compositional Study of *Moringa stenopetala* Leaves, *East African Medical Journal*, 51-56
166. Johnson, B.C. **2005**. Clinical Perspectives on The Health Effects of *Moringa oleifera*: A Promising Adjunct for Balanced Nutrition and Better Health, *KOS Health Publications,* **1**, 1–5
167. Melesse, A., Berihun, K. **2013**. Chemical and Mineral Compositions of Pods of *Moringa stenopetala* and *Moringa oleifera* Cultivated in the Lowland of Gamo Gofa Zone, *J Environ Occup Sci*, **2**(1), 33–38
168. Yang, R., Chang, L., Hsu, J., Weng, B.B.C., Palada, M.C., Chadha, M.L., Levasseur, V. **2006**. *Moringa* and Other Highly Nutritious Plant Resources: Strategies, Standards and Markets for a Better Impact on Nutrition in Africa. Accra, Ghana, pp 1–9
169. Mensah, J.K., Ikhajiagbe, B., Edema, N.E., Emokhor, E. **2012**. Phytochemical, Nutritional and Antibacterial Properties of Dried Leaf Powder of *Moringa oleifera* (Lam) from Edo Central Province, Nigeria, *J. Nat. Prod. Plant Resour*., **2**(1), 107–112
170. Omotesho, K.F., Sola-Ojo, F.E., Fayeye, T.R., Babatunde, R.O., Otunola, G.A., Aliyu, T.H. **2013**. The Potential of *Moringa* Tree for Poverty Alleviation and Rural Development: Review of Evidences on Usage and Efficacy, *International Journal of Development and Sustainability*, **2**(2), 799–813
171. Babu, S.C. **2000**. Rural Nutrition Interventions with Indigenous Plant Foods –A Case Study of Vitamin A Deficiency in Malawi, *Biotechnol. Agron. Soc. Environ.* **4**(3), 169–179

172. Debela, E., Tolera, A. **2013**. Nutritive Value of Botanical Fractions of *M. oleifera* and *M. Stenopetala* Grown in The Mid-Rift Valley of Southern Ethiopia, *Agroforest Syst*, **87**, 1147–1155
173. Mataka, L.M., Sajidu, S. M. I., Masamba, W. R. L., Mwatseteza, J. F. **2010**. Cadmium sorption by *Moringa stenopetala* and *Moringa oleifera* seed powders: Batch, time, temperature, pH and adsorption isotherm studies, *International Journal of Water Resources and Environmental Engineering,* **2**(3), 50 –59
174. Gassenschmidt, U., Jany, K.D., Tauscher, B., Niebergall, H. **1995**. Isolation and Characterization of a Flocculating Protein from *Moringa oleifera* Lam, *Biochimica et Biophysics Acta*, **12**(43), 477–481
175. Mengistu, M. **2007**. Hypotensive Effects of Aqueous Extract of *Moringa stenopetala in* Both *In vivo* and *In vitro* Animal Models, MSc Thesis, Medical Physiology, Addis Ababa University, Addis Ababa, Ethiopia
176. Padayachee, B., Baijnath, H. **2012**. An Overview of the Medicinal Importance of *Moringa*ceae, *Journal of Medicinal Plants Research*, **6**(48), 5831–-5839
177. Mekonnen, Y. **1999**. Effects of Ethanol Extract of *Moringa stenopetala* Leaves on Guinea-Pig and Mouse Smooth Muscle, *Phytother Res*, **13**(5), 442–444
178. Bekele, B., Adane, L., Tariku, Y., Hailu, A. **2013**. Evaluation of Antileishmanial Activities of Triglycerides Isolated from Roots of *Moringa stenopetala*, *Med Chem Res*, 1–8
179. Mengistu M, Abebe Y, Mekonnen Y, Tolessa, T. **2012**. *In vivo* and *In vitro* Hypotensive Effect of Aqueous Extract of *Moringa stenopetala*, *African Health Sciences*, **12**(4), 545–562
180. Mekonnen, Y., Drager, B. **2003**. Glucosinolate in *Moringa stenopetala, Planta Med*, **69**, 380–382
181. Sahakitpichan, P., Mahidol, C., Disadee, W., Ruchirawat, S., Kanchanapoom, T. **2011**. Unusual Glycosides of Pyrrole Alkaloid and 4'-Hydroxyphenylethanamide from Leaves of *Moringa oleifera*, *Phytochemistry*, **72**, 791–795
182. Oluduro, O.A., Idowu, T.O., Aderiye, B.I., Famurewa, O., Omoboye, O.O. **2012**. Evaluation of Antibacterial Potential of Crude Extract of *Moringa oleifera* seed on

Orthopaedics Wound Isolates and Characterization of Phenylmethylamine and Beznzyl Isothiocyanate Derivatives, *Research Journal of Medicinal Plant*, **6**(5), 383–394

183. Maria, K., Mohammad, A. **2011**. Phytochemical Investigation of the Stem Bark of *Moringa oleifera*, *IJARAP*, **2**(5), 1577–1579
184. Tesemma, M., Adane, L., Tariku, Y., Muleta, D., Demise, S. **2013**. Isolation of Compounds from Acetone Extract of Root Wood of *Moringa stenopetala* and Evaluation and Their Antibacterial Activities, *Research Journal of Medicinal Plant*, **7**(1), 32–47
185. Lalas, S., Tsaknis, J., Sflomos, K. **2003**. Characterization of *Moringa stenopetala* seed oil variety "Marigat" from island Kokwa **,** *Eur. J. Lipid Sci. Technol.* **105**, 23–31
186. Anwar, F., Rashid, U. **2007**. Physico-Chemical Characteristics of *Moringa oleifera* Seeds and Seed oil from Wild Provenance of Pakistan, *Pak. J. Bot*. **39**(5), 1443–1453
187. Kashiwada, Y., Ahmed, F.A., Kurimoto, S., Kim, S., Shibata, H., Fujioka, T., Takaishi, Y. **2012**. New *α*-Glucosides of Caffeoyl Quinic acid from the Leaves of *Moringa oleifera* Lam. *J Nat Med*, **66**, 217–221
188. Mekonen, A., Gebreyesus, T. **2000**. Chemical Investigation of the Leaves of *Moringa stenopetala*, *Bull. Chem. Soc. Ethiop*. **14**(1), 51–55
189. Eilert, U., Wolters, B., Nahrstedt, A. **1981**. The Antibiotic Principle of Seeds of *Moringa oleifera* and *Moringa stenopetala*, *Planta Medica*, **42**(5), 55–61.
190. Shanker, K., Gupta, M.M., Srivastava, S.K., Bawankule, D.U., Pal, A., Khanuja, S.P.S. **2007**. Determination of Bioactive Nitrile Glycoside(s) in Drumstick (*Moringa oleifera*) by Reverse Phase HPLC, *Food Chemistry*, **105**, 376–382
191. Faizi, S., Siddiqui, B.S., Saleem, R., Noor, F., Husnain, S. **1997**. Isolation and Structure Elucidation of a Novel Glycoside Niazidin from the Pods of *Moringa oleifera*, *J. Nat. Prod.*, **60**, 1317–1321
192. Guevara, A.P., Vargas, C., Sakurai, H., Fujiwara, Y., Hashimoto, K., Maoka, T., Kozuka, M., Ito, Y., Tokuda, H., Nishino, H. **1999**. An Antitumor Promoter from *Moringa oleifera* Lam., *Mutation Research*, **44**, 181–188
193. Tahany, M.A.A., Hegazy, A. K., Sayed, A.M., Kabiel, H.F., El-Alfy, T., El-Komy, S.M. **2010**. Study on Combined Antimicrobial Activity of some Biologically Active Constituents from Wild *Moringa peregrina*, *Journal of Yeast and Fungal Research*, **1**(1), 015–024

194. Synthetic Adsorbents Diaion HP Series, available on: Http//WWW.m Kagaku.co.jp>Home>products and services>departments, Accessed on March 2014
195. Guvenalp, Z., Demirezer, L.O. **2005**. Flavonol Glycosides from *Asperula arvensis* L., *Turk J Chem*, **29**, 163–169
196. Islam, M., Al-Amin, M., Siddiqi, M.M.A., Akter, S., Haque, M.M., Sultana, N., Chowdhury, A.M.S. **2012**. Isolation of Quercetin-3-O-*β*-D-glucopyranoside from The Leaves of *Azadirachta indica* and Antimicrobial and Cytotoxic Screening of The Crude Extracts, *Dhaka Univ. J. Sci.* **60**(1), 11–14
197. Bylka, W., Matlawska, I. **2001**. Flavonoids, and Free Phenolic Acids from *Phytolacca americana* Leaves, *Polish Pharmaceutical Society*, **58**(1), 69–72
198. Esmaeili, M.A., Sad, H. **2009**. Pancreatic B-Cell Protective Effect of Rutin and Apigenin Isolated from *Teucrium polium, Pharmacologyonline*, **2**, 341–353
199. Hong, H., Li, S., Zhang, X., Ye, W., Zhang, Q. **2013**. Flavonoids with *α*-Glucosidase Inhibitory Activities and Their Contents in The Leaves of *Morus atropurpurea*, *Chinese Medicine*, **8**(19), 1–7
200. Dıaz, J.G., Carmona, A.J., de Paz, P.P., Herz, W. **2008**. Acylated Flavonol Glycosides from *Delphinium staphisagria*, *Phytochemistry Letters*, **1**, 125–129
201. Krasteva, I.K. **2013**. Phenolic Compounds in Four Astragalus Species, *European Journal of Medicinal Plants*, **3**(4), 616–623
202. Patil, S.L., Somashekarappa, H.M., Rajashekhar, K. P. **2012**. Evaluation of The Radioprotective Action of Rutin in Mice Exposed to *γ*-Radiation, *International Journal of Biological & Pharmaceutical Research*, **3**(1), 12–18
203. Kamalakkannan, N., Prince, P.S.M. **2006**. Antihyperglycaemic and Antioxidant Effect of Rutin, a Polyphenolic Flavonoid, in Streptozotocin-Induced Diabetic Wistar Rats, *Basic & Clinical Pharmacology & Toxicology*, **98**, 97–103
204. Khan, R.A., Khan, M.R., Sahreen, S. **2012**. CCl_4-Induced Hepatotoxicity: Protective Effect of Rutin on p53, CYP2E1 and the Antioxidative Status in Rat, *BMC Complementary and Alternative Medicine*, **12**, 178–182
205. Eo, S., Kim, S. **2013**. Rutin Induces Cyclooxygenase-2 (COX-2) and Matrix Metalloproteinase (MMP)-9 Expression via the ERK and PI3K/Akt Pathways in A549

Human Lung Cancer Cells, *Journal of Convergence Information Technology(JCIT*), **8**,(13), 414–422

206. Cruz, T., Galvez, .J, Ocete, M.A., Crespo, M.E., Sanchez de Medina, L.H.F., Zarzuelo, A. **1998**. Oral Administration of Rutoside Can Ameliorate Inflammatory Bowel Disease in Rats, *Life Sci*, **62**, 687–695
207. Tapas, A.R., Sakarkar, D.M., Kakde, R.B. **2008**. Flavonoids as Nutraceuticals: A Review, *Tropical Journal of Pharmaceutical Research*, **7**(3), 1089–1099
208. Arima, H., Ashida, H., Danno, G. **2002**. Rutin Enhanced the Antibacterial Activities of Flavonoids Against *Bacillus cereus* and *Salmonella enteritidis*, *Biosci. Biotechnol. Biochem*., **66**(5), 1009–1014
209. Esmaeili, M., Sadeghi, H. **2009**. Pancreatic B-Cell Protective Effect of Rutin and Apigenin Isolated from *Teucrium polium*, *Pharmacologyonline,* **2**, 341–353
210. Dar, M.A., Tabassum, N. **2012**. Rutin-Potent Natural Thrombolytic Agent, *International Current Pharmaceutical Journal*, **1**(12), 431–435
211. Sikorkska, M., Matlawska, I. **2001**. Kaempferol, Isorhamentin, and Their Glycosides in the Flowers of *Asclepias syriaca*, *Acta Poloniae pharmaceutica-Drug Research*, **58**(4), 269–272
212. Shahat, A.A., Nazif, N.M., Andel-Azim, N.S., Pieters, L., Vlietinck, A.J. **2005**. Flavonoids from *Cressa cretica*, *Qatar Univ Sci. J*., **25**, 72–77
213. Kaur, R., Arya, V. **2012**. Ethnomedicinal and Phytochemical Perspectives of *Pyrus communis* Linn. *Journal of Pharmacognosy and Phytochemistry*, **1**(2), 14–20
214. Furusawa, *M.,* Tanaka, M., Ito, *T.,* Nakaya, *K.,* Iliya,*I.,* Ohyama, *M.,* Iinuma, *M.,* Murata, *H.,* Inatomi, *Y.,* Akira, I., Nakanishi, *T.,* Matsushita, *S.,* Kubota, *Y.,* Sawa, *R.,* Takahashi, Y. **2005**. Flavonol Glycosides in Leaves of Two Diospyros Species**,** *Chem. Pharm. Bull.* **53**(5) 591–593
215. Parveen, Z., Deng, Y., Saeed, M.K., Dai, R., Ahmed, W., Yu, Y., Yasmeen, T. **2006**. Optimizations of Conditions for Maximum Recovery of Astragalin from *Thesium chinese* , *Journal of Applied Sciences*, **6**(13), 2829–2832
216. Gudej, J. **2003**. Kaempferol and Quercetin Glycosides from *Rubus idaeus* Leaves, *Acta Poloniae Pharmaceutica-Drug Research*, **60**(4), 313–316

217. Razavi, S.M., Zahri, S., Zarrini, G., Nazemiyeh, H., Mohammadi, S. **2009**. Biological Activity of Quercetin-3-*O*-Glucoside, a Known Plant Flavonoid, *Russian Journal of Bioorganic Chemistry*, **35**(3), 376–378

218. Ahmadu, A.A., Hassan, H.S., Abubakar, M.U., Akpulu, I.N. **2007**. Flavonoid Glycosides from *Byrsocarpus coccineus* Leaves (Connaraceae), *Afr. J. Trad. CAM* **, 4**(3), 257–260

219. Guvenalp, Z., Demirezer, L.O. **2005**. Flavonol Glycosides from *Asperula arvensis* L. *Turk J Chem*, **29**, 163–169

220. Wang, J., Zhao, L., Sun, G., Liang, Y., Wu, F., Chen, Z., Cui, S. **2011**. A Comparison of Acidic and Enzymatic Hydrolysis of Rutin, *African Journal of Biotechnology*, **10**(8), 1460–1466

221. Wagner, H., Bladt, S. **1996**. Plant Drug Analysis: A thin Layer Chromatography Atlas, 2nd edition, Munchcn, Germany

222. Li, M., HOlI, X., Zhang, J., Wang, S., Fu, Q., He, L. **2011**. Applications of HPLC/MS in the Analysis of Traditional Chinese Medicines, *J Pharm Anal,* **1**(2), 81–91

223. Sirikatitham, A., Chuchom, T., Itharat, A. **2007**. Development of the Chromatographic Fingerprint Analysis of Dioscorealides and Dioscoreanone from *Dioscorea membranacea* Pierre, *J. Sci. Technol*, **29**, 101–108

224. Li, S., Han, Q., Qiao, C., Song, J., Cheng, C.L., Xu, H. **2008**. Chemical Markers for the Quality Control of Herbal Medicines: an overview, *Chinese Medicine*, **3**(7), 1–16

225. Koay, C.Y., Wong, C.K., Osman, H., Eldeen, I.; Asmawi, Z.M. **2013**. Chemical Constituents and Biological Activities of *Strobilanthes crispus* L., *Rec. Nat. Prod*. **7**(1), 59–64

226. Shamsuddin, A.M., Vucenik, I. **2005**. IP6 and Inositol in Cancer Prevention and Therapy, *Current cancer Therapy Reviews*, **1**, 259–269

227. Pazourek, J. **2014**. Fast Separation and Determination of Free Inositol by Hydrophilic Liquid Chromatography, *Carbohydrate Research*, **391**, 55–60

228. Silverstein, R.M., Webster, F.X. **1998**. Spectrometric Identification of Organic Compounds, 6th Ed, John Wiley and Sons, Inc. New York, USA, pp 1–324

229. Xu, B., Sung, C., Han, B. **2011**. Crystal Structure Characterization of Natural Allantoin from Edible Lichen *Umbilicaria esculenta, Crystals*, **1**, 128–135

230. Barbakadze, V., Mulkijanyan, K., Gogilashvili, L., Amiranashvili, L., Merlani, M., Novikova, Z., Sulakvelidze, M. **2009**. Allantoin- and Pyrrolizidine Alkaloids-Free Wound Healing Compositions from *Symphytum asperum, Bulletin of the Georgian National Academy of Sciences*, **3**(1), 159–165
231. Lee, M., Lee,N., Jung, D., Lee, J., Seo, C., Lee, H., Kim, J., Shin, H. **2010**. Protective Effects of Allantoin Against Ovalbumin (OVA)-Induced Lung Inflammation in A Murine Model of Asthma, *International Immunopharmacology*, **10**, 474–480
232. Antolovich, M., Prenzler, P.D., Patsalides, E., McDonald, S., Robards, K. **2002**. Methods for Testing Antioxidant Activity, *Analyst*, **127**, 183–198
233. Fang, Y., Yang, S., Wu, G. **2002**. Free Radicals, Antioxidants, and Nutrition, *Nutrition* **18**, 872– 879
234. Frankel, E.N. **1984**. Lipid Oxidation: Mechanisms, Products and Biological Significance**,** *JAOCS*, **61**(12), 1908–2008
235. Nagatsu, A. **2004**. Investigation of Anti-oxidative Compounds from Oil Plant Seed, *FABAD J. Pharm. Sci.*, **29**, 203–210
236. Gulcin, I., Huyut, Z., Elmastas, M., Aboul-Enein, H.Y. **2010**. Radical Scavenging and Antioxidant Activity of Tannic Acid, *Arabian Journal of Chemistry*, **3**, 43–53
237. Raja, T., Rao, A.L. **2012**. Validated HPTLC Method for Simultaneous Quantitation of Paracetamol and Lornoxicam in Bulk Drug and Pharmaceutical Formulation, *Int J Pharm Biomed Res*, **3**(3), 162–166
238. Abou-Donia, A.H., Toaima, S.M., Hammoda, H.M., Shawky, E. **2008**. New Rapid Validated HPTLC Method for the Determination of Galanthamine in Amaryllidaceae Plant Extracts, *Phytochem. Anal,* **19**, 353–358

Appendices

Appendix 1: Mass spectrum of fatty acid mixtures of the leaves of *C. myricoides*

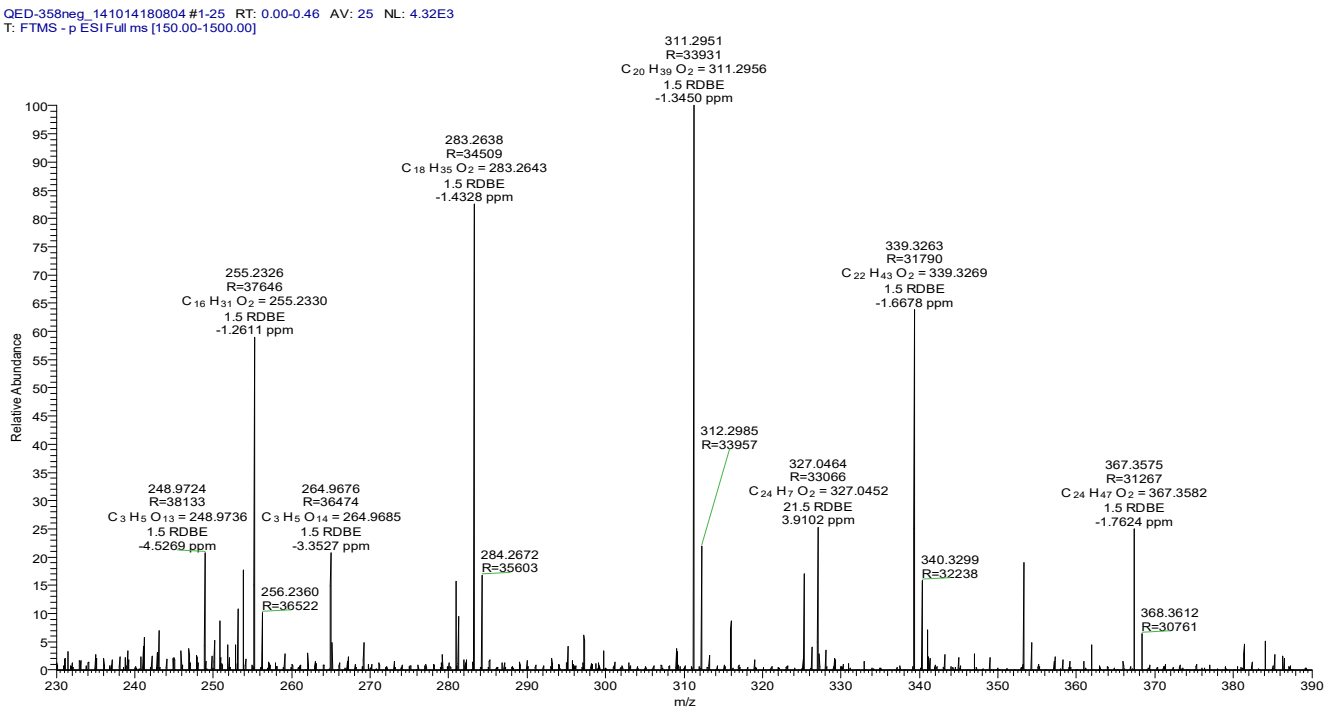

Appendix 2: DPPH inhibition and IC_{50} values of compounds isolated from *C. myricoides* leaves

Sample tested	Concentration in µg/mL	% Scavenging of DPPH	IC_{50}
α-spinasterol	10	6	124
	5	5	
	2.5	4.8	
	1.25	1.7	
Verbascoside	10	84	0.69
	5	63	
	2.5	58	
	1.25	52	
Ixoroside	10	13	65
	5	9.2	
	2.5	7.8	
	1.25	7	
Compound **72**	10	15	50

	5	11
	2.5	9
	1.25	7

Appendix 3: DPPH inhibition, IC_{50} and ARP of compounds isolated from *D. angustifolia* leaves

Tested Samples	Concentration in µg/mL	% Scavenging of DPPH	IC_{50}	Anti-radical activity
Pinocembrin	10	57	5.4	0.185
	5	52		
	2.5	47		
	1.25	38		
Santin	10	58	4.08	0.245
	5	53		
	2.5	49		
	1.25	44		
5,6,7-Trihydroxy-3,4'-dimethoxyflavone	10	70	4.37	0.23
	5	53		
	2.5	47		
	1.25	38		
5,7,4'-Trihydroxy-3,6-dimethoxyflavone	10	84	0.87	0.31
	5	67		
	2.5	57		
	1.25	50		

Appendix 4: Mass spectrum of compound at retention time of 12.959 min

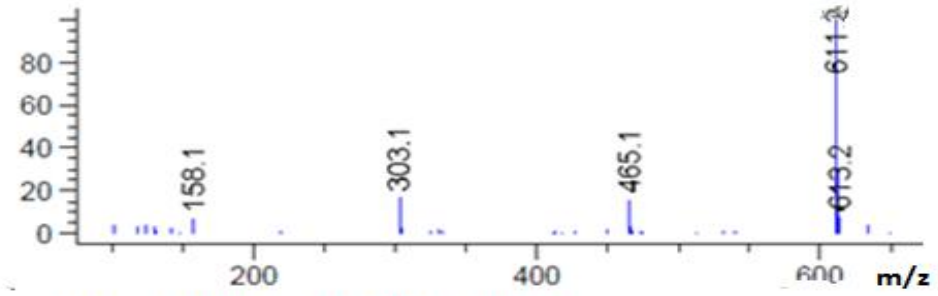

Peak at 12.959 min (12.684 to 13.464 min)
The analysis found only one component, indicating a pure peak

Appendix 5: Mass spectrum of compound at retention time of 13.653 min

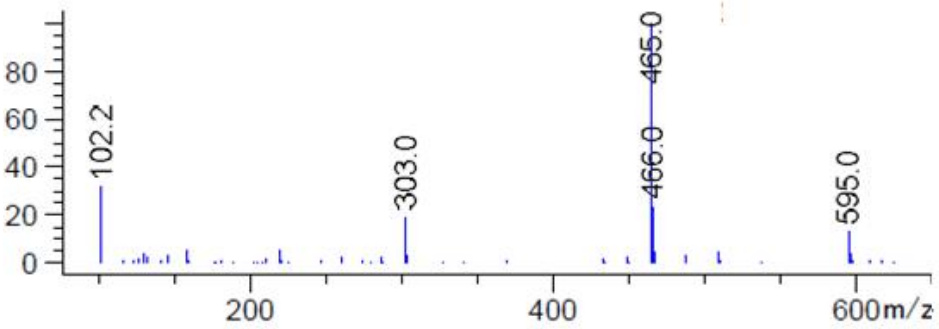

Peak at 13.653 min (13.485 to 13.917 min)
-> The analysis found 2 components, indicating an impure peak.

Appendix 6: Mass spectrum of compound at retention time of 14.099 min

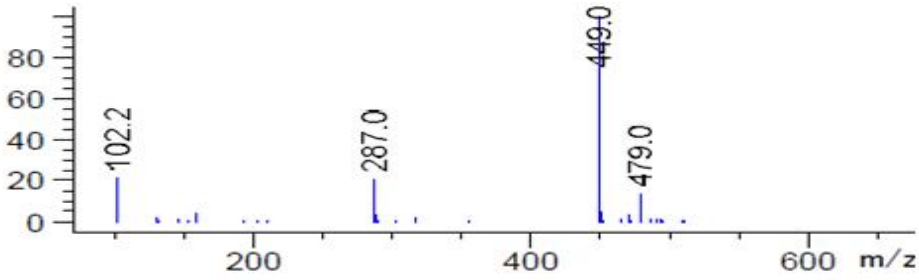

Peak at 14.099 min (13.917 to 14.683 min)
-> The analysis found 2 components, indicating an impure peak
Component 1: Peak at Scan 847.3. Top ions are 551 552
Component 2: Peak at Scan 862.3. Top ions are 449

Appendix 8: Intra- and Inter-day precision of HPTLC method

Amount	Intraday precision (n = 3)		Interday precision (n = 6)	
(µg spot^{-1})	Mean area from Camag	%RSD	Mean area from Camag	%RSD
20	6458	0.14	6397	0.13

Appendix 9: HPTLC results of the recovery study

Rutin in pre-analyzed sample (µg)	Spiked amount(µg)	Theoretical value(µg)	Experimental value(µg)	Recovery (%)
3.923	1.00	4.923	4.944	100
4.000	1.00	5	4.944	99
10.19	0.50	10.69	10.46	98
10.46	0.50	10.98	11.00	100

Appendix 10: Overlayed ^{1}H-NMR spectra of *M. stenopetala* oil and olive oil

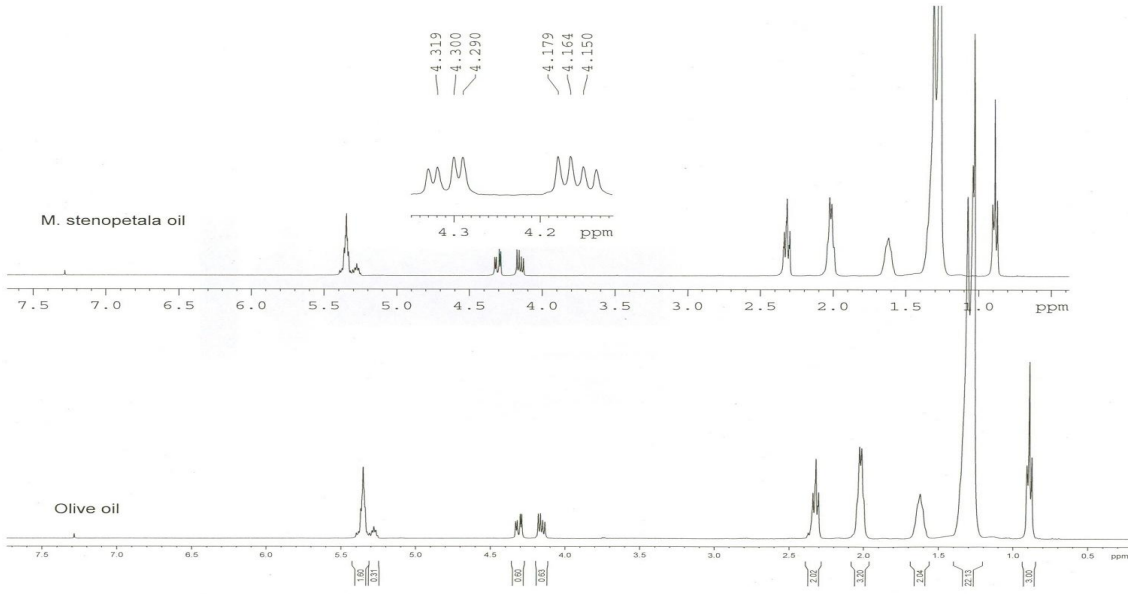

Appendix 11: FT-MS profile of fatty acid mixtures of *M. stenopetala* oil

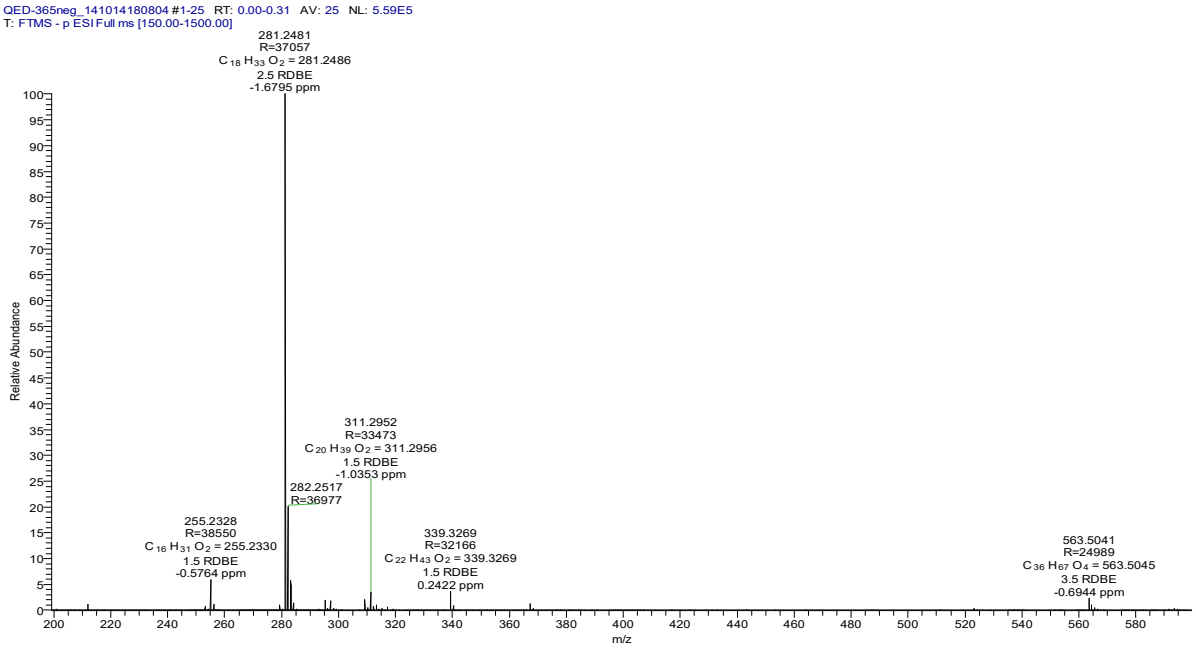

Appendix 12: GC-MS profile of fatty acids of the oil of *M. stenopetala*

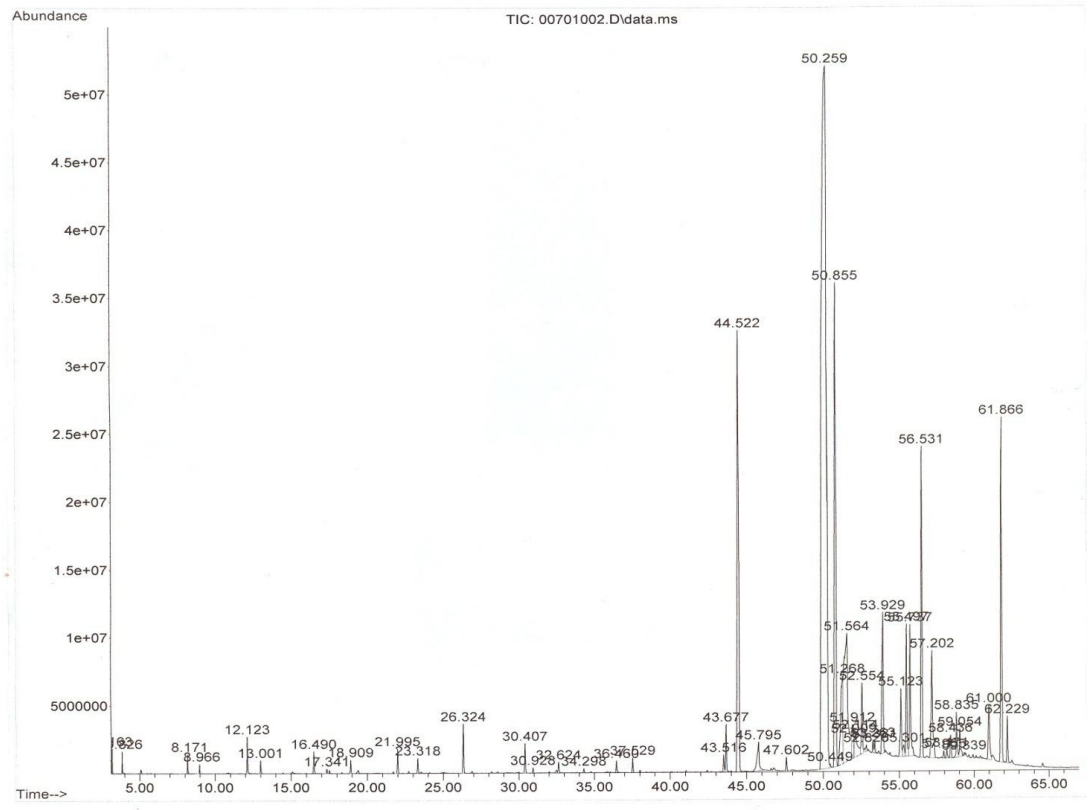

Appendix 13: List of compounds isolated in this project

Cpd No	Compound Name	Plant Source	Amt (mg)	Structures
81	Santin	*D. angustifolia*(LF)	80	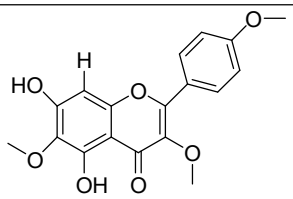
86	Pinocembrin	*D. angustifolia*(LF)	3	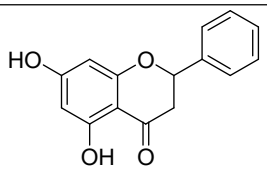
12	Verbascoside	*C. myricoides* (LF)	150	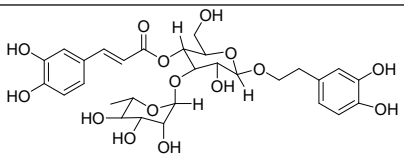
77	Stearic acid	*M. stenopetala (SD)*	70	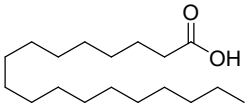
157	Quercetin	*M. stenopetala*(LF)	40	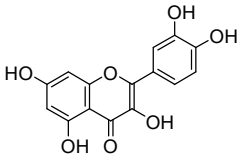
163	Rutin	*M. stenopetala*(LF)	2500	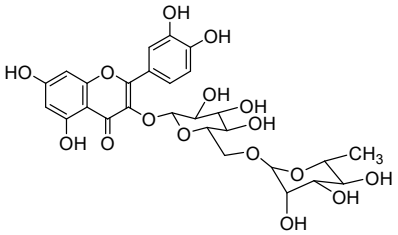

Appendix 13 continued

Cpd No	Compound Name	Plant Source	Amt (mg)	Structures

164	4-(α-L-rhamnopyranosyloxy) benzyl glucosinolate	*M.stenopetala*(SD)	-	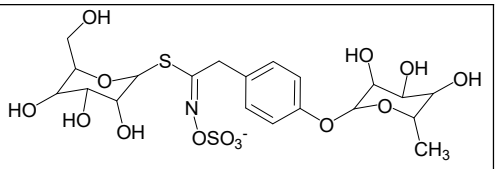
125	5,6,7-trihydroxy-3,4'-dimethoxyflavone	*D.angustifolia* (LF)	1	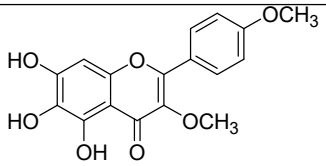
128	15, 16-Epoxy-2-hydroxy-3, 13 (16), 14-clerodtriene-18-oic acid	*D. angustifolia*(LF)	150	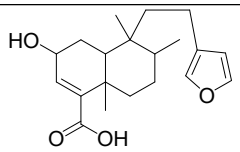
61	Heptacosanol	*M. stenopetala*	100	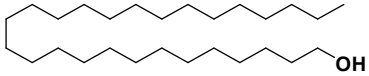
63	α-Spinasterol	*C. myricoides*(LF)	5	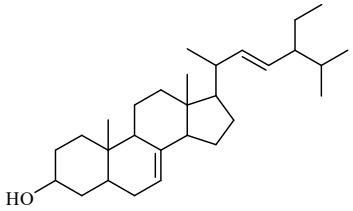
64	Sitosterol-3-O-β-D-glucoside	*C. myricoides*(LF)	2	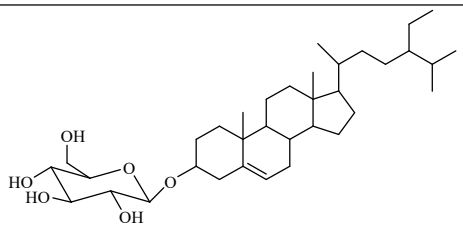
	Sesamin	sesame (SD)	20	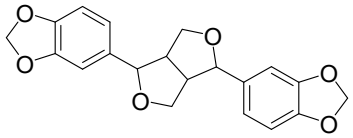

Appendix 13 continued

Cpd No	Compound Name	Plant Source	Amt (mg)	Structures

71	-	*C. myricoides* (LF)	-	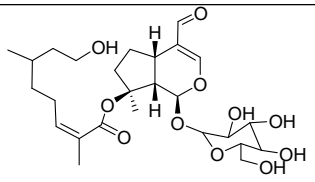
73	Ixoroside	*C. myricoides* (LF)	-	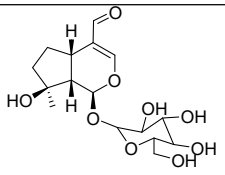
80	5,7,4'-trihydroxy-3,6-dimethoxyflavone	*D. angustifolia*(LF)	-	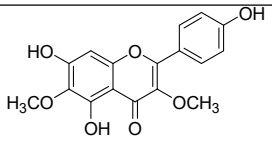
117	ent-16-hydroxy-labdan-3*α*,8*β*-dihydroxy,13(14)-en-15,16-olide	*D. angustifolia* (LF)	-	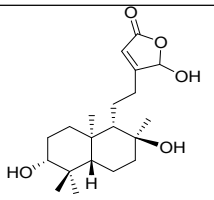
161	kaempferol-3-O-*β*-D-glucoside	*M. oleifera* (LF)	-	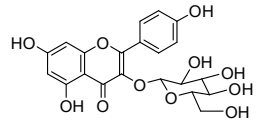
159	Quercetin-3-O-*β*-D-glucoside	*M. oleifera* (LF)		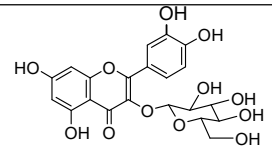
186	Inositol dimer	*M. stenopetala* (LF)		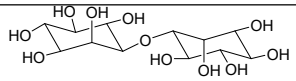
190	-	*M. stenopetala* (husk)		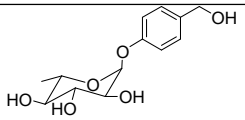
191	allantoin	*M. stenopetala* (husk)		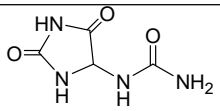

Appendix 14

Comparative Chemical Study of the Wondrous Ethiopian Plant: *Moringa stenopetala* with the Indian *Moringa oleifera*[1]

Abstract: *Moringa stenopetala* is a cultivated plant in home gardens and farms mainly in southern regions of Ethiopia. It is known as cabbage tree, indicating its use as food and also by different local names (e.g. Aleko, Shiferaw). Families depend on it as an additional source of food. In the past few years, wide interest has been generated outside of its origin areas on account of the claimed nutritional and medicinal values. The leaves of this plant are now being sold in different parts of Ethiopia including in shops and supermarkets in Addis Ababa. This means that farmers in the South now have an additional source of income from their home garden plant. However, there is misconception about this new market, as if it is a cause of new threat. How can a cabbage plant grown in home gardens be threatened by new markets? On the contrary, since there is huge potential for wider cultivation of this plant in home gardens or in farms, this plant brings a truly golden economic opportunity for the farmers.

In a pioneer chemical study conducted in the Department of Chemistry (AAU) several years ago the flavonoid glycoside rutin was found to be the major constituent of the leaves [1]. In this study [2] we compared *M. stenopetala* from Ethiopia with the well known Indian species *M. oleifera.* Several compounds were isolated from leaves of both species. Different techniques including TLC, HPLC-MS, and UV-Vis were employed. Our results unambiguously show significant differences in the chemical profiles of the leaves of the two species. Rutin (**1**) is the principal flavonoid glycoside (2%) of the leaves of *M. stenopetala*, which however was not detected in the leaves of *M. oleifera*. On the other hand *M. oleifera* contains significant amounts of two other glycosides: quercetin-3-O-*β*-D-glucoside (**2**) and kaempferol-3-O-*β*-D-glucoside (**3**). It is interesting to note that compounds **2** and **3** are not detected in *M. stenopetala.*

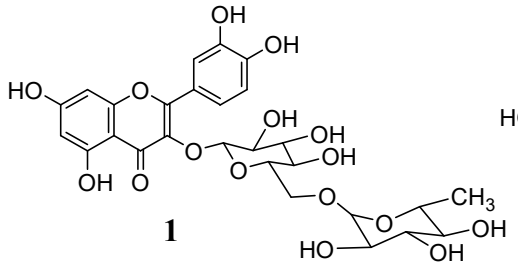

1

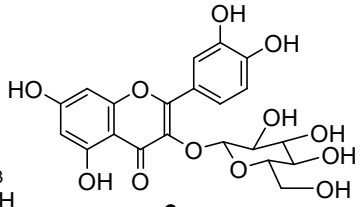

2

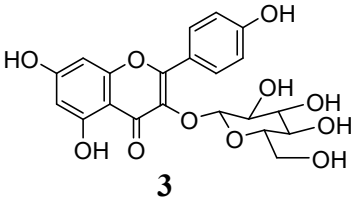

3

[1]Oral presentation by Yadessa Melaku at RiSE (Research in Science Exposition) held at the College of Natural Sciences, AAU, June 19, 2015

Appendix 15: PhD defence presentation slides

DEPARTMENT OF CHEMISTRY
COLLEGE OF NATURAL SCIENCES
ADDIS ABABA UNIVERSITY

Bioassay Directed Chemical Study of Antimalarial Substances from *Clerodendrum myricoides* and *Dodonaea angustifolia* and Comparative Chemical Studies of *Moringa stenopetala* and *Moringa oleifera*

By Yadessa Melaku
Advisor: Prof. Ermias Dagne

June 1, 2015

Part 1: Bioassay Directed Chemical Study of Antimalarial Substances from *Clerodendrum myricoides*

Picture 1: *C. myricoides* aerial part (Lideta Mariam, Addis Ababa, Picture by YM)

1.1. Introduction

- *Clerodendrum myricoides*, *Misrch* in Amharic
  - Indigenous plant in Ethiopia
  - Also occurs in Nigeria, Kenya, and South Africa
- Traditional uses of *C. myricoides*: Against malaria, diabetes, typhoid, fevers, pneumonia
- Previous biological reports:
  - Antimutagenic properties against *Salmonella typhimurium* [36]
  - Against diarrhea and dysentery
- Previous studies showed crude extract possesses antiplasmodial activities
- No prior report on chemical constituents of the plant

[36] Reid, K.A. *et al*., **2006**. *Journal of Ethnopharmacology*, **106**, 44–50

1.2. Objectives

- To conduct bioassay guided isolation and characterization of compounds responsible for the antiplasmodial activities of the extracts of the leaves of *C. myricoides*
- To identify the compounds responsible for the radical scavenging activities of the extracts

1.3. Results and Discussion

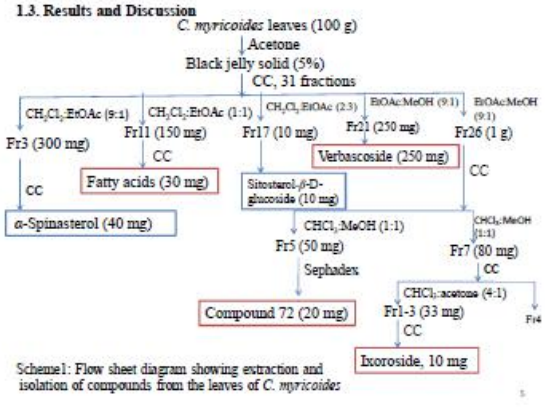

Scheme1: Flow sheet diagram showing extraction and isolation of compounds from the leaves of *C. myricoides*

1.3.1. Characterization of 5 compounds isolated in this study from leaves of *C. myricoides*

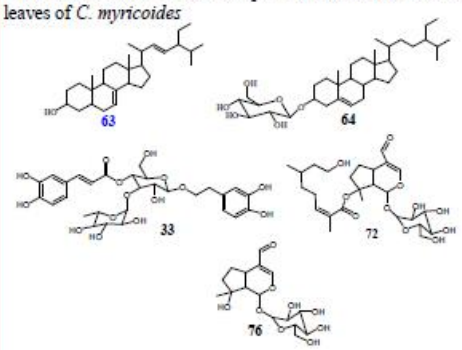

Compound 63

- White solid recrystalized from isopropyl alcohol; mp144-145°C
- MS: *m/z* 412, $C_{29}H_{48}O$
- The IR υcm^{-1}: 3369.0 (O-H), 1609.0 (C=C) and 1062 (C-O)
- ^{1}H-NMR: six methyls at *δ* 0.60 (3H, *s*), *δ* 0.80-0.860 (9H, *m*), *δ* 0.87 (3H, *d*, *J* = 6.4 Hz) and *δ* 1.13 (3H, *d*, *J* = 6.8 Hz)
- Proton signals integrating for 25H were observed in the range *δ* 2.30 to 1.00
- The signal at *δ* 3.65 (1H, *m*) along with three olefinic protons at *δ* 5.04 (H-23), 5.17 (H-7) and 5.18 (H-22)
- UV λmax: 227 nm for isolated double bonds

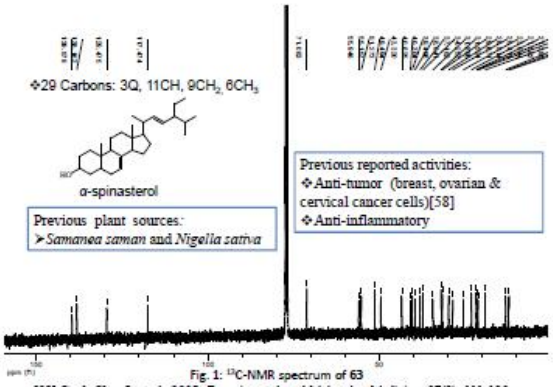

Fig. 1: ^{13}C-NMR spectrum of **63**

[58] Gook-Che, J. *et al.*, **2005**. *Experimental and Molecular Medicine*, **37**(2), 111-120

Compound 64

- White powder; TLC (Rf = 0.4), hexane:EtOAc (1:4)
- $[\alpha]_{589}^{21}$ = -25.0 (c 0.4, MeOH)
- IR: 3429 (OH), 2918 (C-H), and 1063 cm^{-1} (C-O)
- FT-MS: *m/z* 599.4293, $C_{35}H_{60}O_6$
- UV: no absorption maxima
- ^{1}H-NMR: six methyl groups at *δ* 0.65 (3H, *s*), 0.95 (3H, *s*), 0.90 (3H, *t*), 0.93 (3H, *d*), and *δ* 0.80 (6H, *m*)
- Olefinic proton: *δ* 5.30
- Proton on oxygenated carbon: *δ* 4.47 (1H, *m*)
- Anomeric proton of glucose: *δ* 4.21 (1H, *d*, *J* = 8.00 Hz)
- ^{13}C-NMR: 35 carbon signals (3Q, 14CH, 12CH$_2$, 6CH$_3$)
- Sitosterol-3-O-*β*-D-glucoside: anticancer [63] and antibacterial

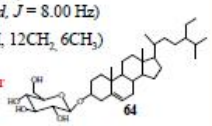

[63] Shabana, M.M. *et al.*, **2013**. *J Carcinogene Mutagene*, **4** (3), 149-155

Compound 33

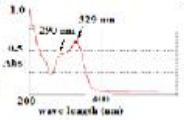

- Major constituent; mp 147-148°C
- FT-MS: m/z 623.1981, $C_{29}H_{36}O_{15}$
- IR: 3398 cm^{-1}(OH) and 1698 cm^{-1}(ester CO)
- ^{1}H-NMR: *δ* 7.45 (1H, *d*, *J* = 15.7 Hz) and 6.20 (1H, *d*, *J* = 15.7 Hz), double bond
- *δ* 7.02 (1H, *d*, *J* = 1.69 Hz), 6.98 (1H, *dd*, *J* = 8.14, 1.69 Hz), and 6.75 (1H, *d*, *J* = 8.14 Hz), caffeic acid substituent
- Phenylethyl moiety at *δ* 6.63 (1H, *d*, *J* = 8.14 Hz), 6.62 (1H, *bro s*), and 6.49 (1H, *dd*, *J* = 8.14, and 1.48 Hz)
- Rhamnose: *δ* 5.01 (1H, *d*, *J* = 1.3 Hz) and 0.94 (3H, *d*, *J* = 6.24 Hz)
- Anomeric proton of glucose at *δ* 4.35 (1H, *d*, *J* = 7.82 Hz)

- ^{13}C-NMR and DEPT-135: showed 29 carbon resonances
- HMBC

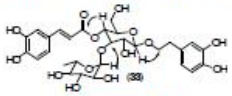

Verbascoside (**33**)

- Previous plant source: leaves of olive [43]
- Previous pharmacological reports: antiviral , antitumor and anti-inflammatory

[43] Micol, V., *et al.*, **2005**. *Antiviral Research*, **66**, 129–136

5. Compound 76

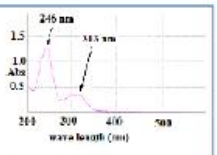

- White solid; mp 198-201°C
- $[\alpha]_{589}^{21}$ = -130.0 (c 0.4, MeOH)
- IR υcm^{-1}: 3391 (O-H),1660 (C=O),
- FT-MS: *m/z* 359.1348, $C_{16}H_{24}O_9$

^{13}C-NMR and DEPT-135 spectrum

- *δ* 191.2, 161.7 and 124.5, *δ* 95.1, *δ* 78.4 (1Q), *δ* 50.7 and 28.8 (two CH), *δ* 40.7 and 28.7 (two CH$_2$) and *δ* 22.0 (one CH$_3$): Iridoid moiety
- One sugar moiety: *δ* 98.7 (C-1'), 77.7 (C-5'), 77.1 (C-3'), 73.5 (C-2'), 70.5 (C-4') and 61.6 (C-6')
- Compound **76** is ixoroside

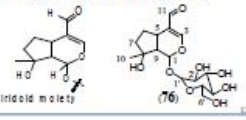

Compound 72

- Mp: 178-180°C
- TLC (Rf 0.4) using EtOAc:AcOH (4:1)
- IR: 1690 (ester CO), 1674 (Aldehyde CO)
- FT-MS: *m/z* 551.2463, $C_{26}H_{40}O_{11}$

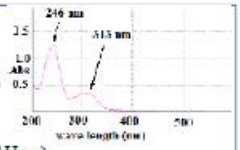

- ^{1}H-NMR: δ 6.77 (olefinic) and 1.67 (1H, *m*)
  - Four methylenes: δ 2.22, 1.56 &1.28, 1.32 and 3.60
  - Two methyls: δ 1.81 (3H, *s*) and 0.94 (3H, *d*)
- ^{13}C-NMR spectrum and DEPT-135 showed:
  - Ester carbonyl (δ 167.6),
  - Olefinic carbons (δ 128.2 & 142.5),
  - Four methylenes,
  - One methine (δ 29.2) and
  - Two methyls (δ 11.5 and 20.5)

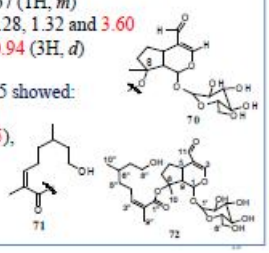

Fatty acids: white solid

- NMR result: saturated and unsaturated fatty acids

▪The fatty acid mixture was dissolved in hexane:$CHCl_3$(1:1) on boiling and left standing overnight

- NMR result: stearic acid
- FT-MS: $C_{24}H_{47}O_2$ (*m/z* 367), $C_{22}H_{43}O_2$ (*m/z* 339), $C_{20}H_{39}O_2$ (*m/z* 311), $C_{18}H_{35}O_2$ (*m/z* 383), $C_{16}H_{31}O_2$ (*m/z* 255) identified as tetracosanoic (74), behenic (75), icosanoic (76), stearic (77), and palmitic acid (78)

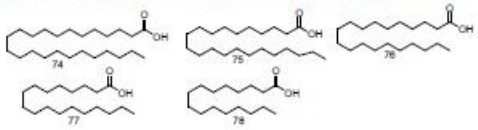

1.3.2.1. Antiplasmodial assay conducted in collaboration with research group of Professor Yalemtsehay Mekonnen

Antiplasmodial assay cont'd

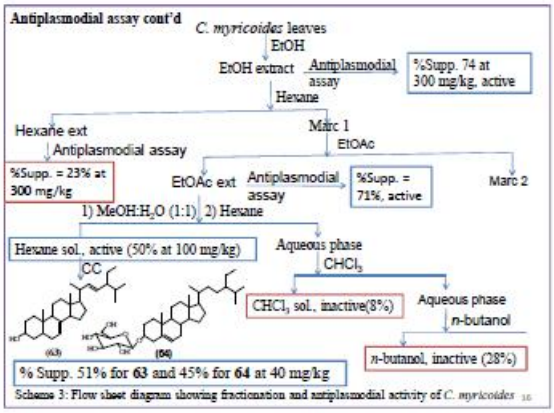

Scheme 3: Flow sheet diagram showing fractionation and antiplasmodial activity of *C. myricoides*

1.3.2.2. Radical Scavenging Assay

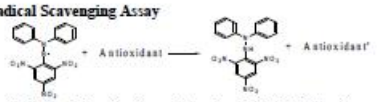

DPPH radical (Purple in color, λ_{max} = 517 nm) DPPH-H (Yellow)

Tested samples	DPPH radical scavenging assay	
	% inhibition at 10 µg/mL	IC_{50} values
Acetone extract	50	10
α-spinasterol	6	123
Sitosterol-3-O-β-D-glucoside	36	16
Ixoroside	13	65
Compound 72	15	50
Verbascoside	84	0.75
Ascorbic acid	90	0.45

Table 1: DPPH radical scavenging activities of the acetone extract and constituents of the leaves of *C. myricoides*

1.4. Summary of major findings on the leaves of *C. myricoides*

- The acetone extract afforded five compounds: α-spinasterol, sitosterol-3-O-β-D-glucoside, verbascoside, ixoroside and compound 72.
- Compound 72 has not been reported previously as a natural product
- The extracts and the tested 2 compounds exhibited significant suppression of plasmodium parasites on infected mice corroborating the traditional uses of this plant
- The acetone extract displayed high free radical scavenging activity with verbascoside as the most active compound
- The leaves were found to be rich in fatty acids

Part 2: Bioassay Directed Chemical Study of Antimalarial Substances from *Dodonaea angustifolia*

Picture 2: *D. angustifolia* aerial part (Lideta Mariam, AA, picture by Yadessa M.)

2.1. Introduction

➢*Dodonaea angustifolia* (syn. *D. viscosa)*, *kitkita* in Amharic
❖It occurs in most Ethiopian regions

Traditional Uses:
❖Against fevers, malaria, trachoma, to expel roundworms

Pharmacological reports: Antibacterial, anti-fungal, antioxidant, anti-diarrheal, antidiabetic, anti-inflammatory, hypotensive, and wound healing activity [106]

➢No information describing the antimalarial properties of *D. angustifolia*

[106] Khurram, M., *et al*., **2009**. *Molecules*, **14**, 1332–1341

2.2. Objectives

➢To conduct antiplasmodial activity guided isolation and characterization of compounds from the leaves of *D. angustifolia*

➢To examine the radical scavenging activities of the crude and the pure constituents of the leaves of *D. angustifolia*

2.3. Results and Discussion

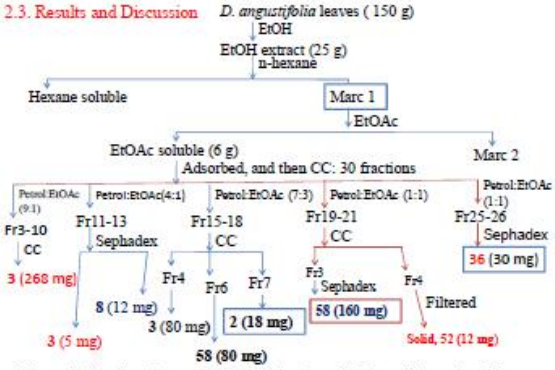

Scheme 4: Flow sheet diagram showing fractionation of EtOAc soluble portion of *D. angustifolia* leaves

2.3.1. Characterization of Compounds from the Leaves of *D. angustifolia*

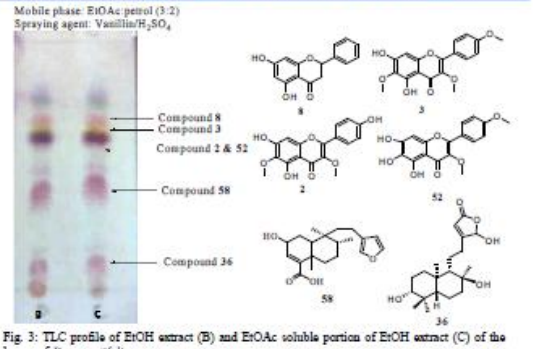

Fig. 3: TLC profile of EtOH extract (B) and EtOAc soluble portion of EtOH extract (C) of the leaves of *D. angustifolia*

Compound 8

❖Yellow solid ; mp 190-191°C
❖$[\alpha]_{589}^{25}$ = -12.5 (c 0.4, EtOH)
❖HR-FT-MS: *m/z* 255.0663, $C_{15}H_{12}O_4$

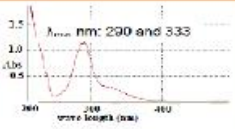

❖^{1}H-NMR spectrum:
➢δ 2.60 (1H, *dd*) and 2.91 (1H, *dd*)
➢δ 5.25 (1H, *dd*, *J* = 12.80 and 2.80 Hz)
➢δ 5.82 (1H, *d*, *J* = 2.00 Hz) and δ 5.83 (1H, *d*, *J* = 2.00 Hz)
➢δ 7.26 (5H, *m*), no substitution pattern on ring B

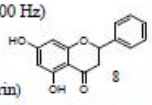

❖Compound 8 is 5,7-dihydroxyflavanone (Pinocembrin)
❖Pinocembrin: antimicrobial, anti-inflammatory, antioxidant, and anticancer
▪Has a potent protective effect on neurovascular unit [133]
▪Phytotoxic material for weed control

[133] Qingyun, Y., *et al*., **2012**. *Chin. J. Chem.* **30**, 1315-1319

Compound 3

- Yellow solid recrystalized from ethanol; mp 160-161°C
- IR υcm^{-1}: 1646 (α,β-unsaturated carbonyl), C-O (1090)
- $[\alpha]_{589}^{21}$ = 0.00 (c 0.4, EtOH)
- FT-MS: *m/z* 343.0858, $C_{18}H_{16}O_7$; *m/z* 287 (loss of methyl)

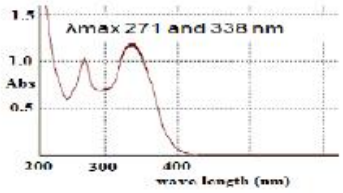

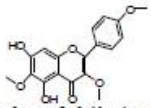

5,7-dihydroxy 3,6,4'-trimethoxy flavone (Santin)

- 2D NMR
- Reported from *D. viscosa*
- Previous biological reports: trypanocidal, leishmanicidal, anti-inflammatory and anti-tubercular [140]

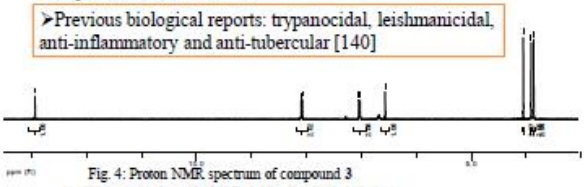

Fig. 4: Proton NMR spectrum of compound 3

[140] Martinez, J., *et al.*, **1997**. *J. Nat. Prod.* **60**, 142–144

- Compound 52
- Yellow solid; mp 226-229°C
- $[\alpha]_{589}^{21}$ = 0.00 (c 0.4, EtOH)
- TLC (Rf 0.50) using EtOAc:petrol (3:2)
- (+)-ESI-FT-MS: *m/z* 331.0803, $C_{17}H_{14}O_7$; *m/z* 316 (loss of methyl group)

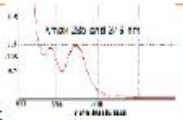

- ^{13}C-NMR and DEPT-135:10Q, 5CH and 2methoxy groups
  Two methoxy groups: δ 54.9 and 59.3
- ^{1}H-NMR: Two methoxy: δ 3.60 (3H, *s*) and 3.70 (3H, *s*)
  - A pair of doublets at δ 8.10 (2H, J = 8.8) and 7.10 (2H, J = 8.8)
  - A singlet at δ 6.50 (1H, *s*)
- **52** is 5,6,7-trihydroxy-3,4'-dimethoxyflavone

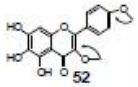

Compound 2

- Yellow solid; TLC (Rf 0.5) using EtOAc:petrol (3:2) as eluent
- ^{1}H-NMR Spectrum:
  - Two methoxy: δ 3.60 (3H, *s*) and 3.70 (3H, *s*)
  - A pair of doublets at δ 6.70 (2H, J = 8.8) and 7.74 (2H, J = 8.8 Hz)
  - A singlet at δ 6.30 (1H, *s*)
- ^{13}C-NMR and DEPT-135: 10Q, 5CH and 2methoxy groups
  Two methoxy: δ 59.4 and 59.9
- Compound **2** is 4',5,7-trihydroxy-3,6-dimethoxyflavone
- ✓Reported from *D. angustifolia* [120]

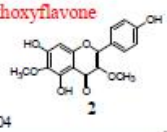

[120] van Heerden, F.R. *et al.*, **2000**. *Fitoterapia*, **71**, 602-604

Compound 58

- White solid; mp 145-147°C;
- $[\alpha]_{589}^{25}$ = -17.5 (c 0.4, MeOH)
- IR υcm^{-1}: 1690 (α,β-unsaturated carboxyl), 3375 (OH)
- On treatment with H_3PO_4, 58 gave a compound with greater Rf value
- FT-MS: *m/z* 331.1990, $C_{20}H_{28}O_4$ and *m/z* 287.2015 (M-CO_2
- ^{1}H-NMR spectrum:
  - three methyls: δ 0.73 (3H, *s*), 0.80 (3H, *d*, J = 6.4 Hz) and 1.26 (3H, *s*)
  - δ 4.30 (proton on oxygenated carbon) and 6.60 (olefinic)
  - Furan ring: δ 6.25 (1H, *s*), 7.20 (1H, *s*) and 7.30 (1H, *t*, 1.80 Hz)

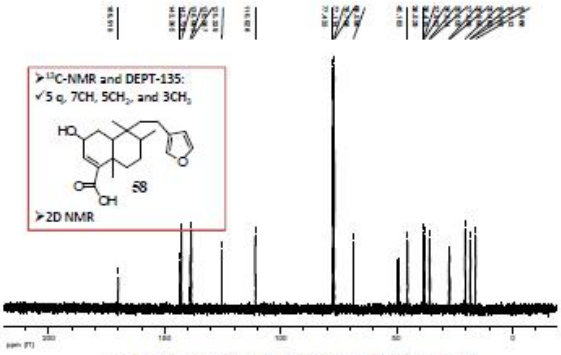

Fig. 6: Proton decoupled ^{13}C-NMR spectrum of compound **58**

Compound 36

❖TLC: Rf 0.20 (EtOAc:petrol, 3:2)

❖^{1}H-NMR and HSQC:
- ➢δ 7.60, 4.30 and 3.90 (OH)
- ➢δ 7.00 (1H, *bro. s*) olefinic proton
- ➢δ 6.00 (1H, *d*) acetal proton
- ➢Three methines
- ➢Six methylene protons
- ➢Methyl singlets at δ 1.00 , 0.89, 0.72 and 0.65

❖^{13}C-NMR and DEPT-135:
- ➢δ 172.2 (carbonyl group)
- ➢δ 145.7 and 136.8 (two olefinics)
- ➢δ 72.5, 77.2 and 97.6 (oxygenated carbons)
- ➢δ 60.8 and 55.1 (methine carbons)
- ➢Quaternary carbons: δ 38.9 and 38.6
- ➢Six methylenes: δ 44.4, 37.9, 28.3, 27.3, 23.2, and 20.2
- ➢Four methyls: δ 28.7, 24.0, 16.1 and 15.7

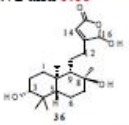

➢Compound **36** is ent-16-hydroxy-labdan-3α,8β-dihydroxy,13(14)-en-15,16-olide (**36**) which was reported from the aerial parts of *D. viscosa* [115]

[115] Oliveira, S.Q., *et al*., 2012. *Phytochemistry Letters*, **5**, 500–505

2.3.2. TLC Profiles of Ethyl acetate Extract of Dried Leaves and Acetone Extract of Leaf Exudates of *D. angustifolia*

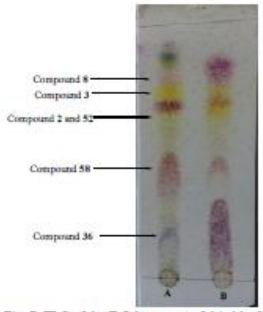

❖Simple dipping is a quick and convenient method for the isolation of terpenoids and flavonoids from the leaves

Fig. 7: TLC of the EtOAc extract of dried leaf (**A**) and acetone extract of leaf surface exudates (**B**) of *D. angustifolia*; Eluent EtOAc:petrol (3:2) and vanillin as spraying agent

2.3.3.1. Antiplasmodial Assay

D. angustifolia leaves
↓ 80% aqu. MeOH
Filtrate
↓ H_2O
50% aqu. solution
↓ EtOAc

EtOAc sol. (%supp = 80 at 150 mg/kg) → Adsorbed, CC

Aqu. phase, %supp.= 19%

Pinocembrin, %Supp 80 at 40 mg/kg

Santin, %Supp 85 at 100 mg/kg

58, %Supp. 70 at 40 mg/kg

Scheme 5: Flow sheet diagram showing antiplasmodial activity guided isolation of compounds from the leaves of *D. angustifolia*

2.3.3.2. Radical Scavenging Assay

Tested samples	Concentration (µg/mL)	% Scavenging of DPPH	IC_{50}
EtOAc ext	100	90	-
Pinocembrin	10	57	5.4
Santin	10	58	4.08
5, 6, 7-Trihydroxy-3,4'-dimethoxyflavone	10	70	4.37
5,7,4'-Trihydroxy-3,6-dimethoxyflavone	10	84	0.6

Table 2: Radical scavenging activities of flavonoids isolated from *D. angustifolia*

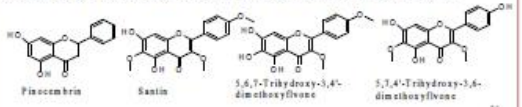

2.4. Summary of major findings on the leaves of *D. angustifolia*

➢Four flavonoids and two terpenoids were isolated and characterized

➢5,6,7-Trihydroxy-3,4'-dimethoxyflavone has not been reported as a natural product

➢Activity guided antiplasmodial activity led to the isolation of three active compounds: pinocembrin (**8**), santin (**3**), and 15,16-epoxy-2-hydroxy-3,13(16),14-clerodtriene-18-oic acid (**58**)

➢The antiplasmodial activities of these compounds were significant compared to chloroquine hence accounts for the traditional use of this plant against malaria.

➢The flavonoids isolated exhibited pronounceable antioxidant activity with 5,7,4'-trihydroxy-3,6-dimetoxyflavone identified as the most active compound

Part 3: Comparative Chemical Studies of *Moringa stenopetala* and *Moringa oleifera*

Picture 3: *M. stenopetala* from Adama

Picture 4: *M. oleifera* from DAI

3.1. Introduction

- Moringaceae: one genus and 14 species
  Two species in Asia and 12 are in Africa
- *M. oleifera* and *M. stenopetala* are highly valued plants in different parts of the world
- The demand of Moringa species is increasing
- Little work has been done on the chemical study of *M. stenopetala*
- No report dealing with the antioxidant potential of the leaves of *M. stenopetala*

3.2. Objectives

- Isolate and characterize marker compounds from the leaves of the two Moringa species
- Develop TLC, UV and HPLC-MS profile of the leaves of *M. stenopetala* and *M. oleifera*
- Determine level of rutin in the leaves of *M. stenopetala*
- Isolate and characterize compounds from the leaves and seeds of *M. stenopetala*
- Evaluate the radical scavenging and anti-lipid peroxidation potential of the extract and constituents of the leaves of *M. stenopetala*

3.3. Results and Discussion

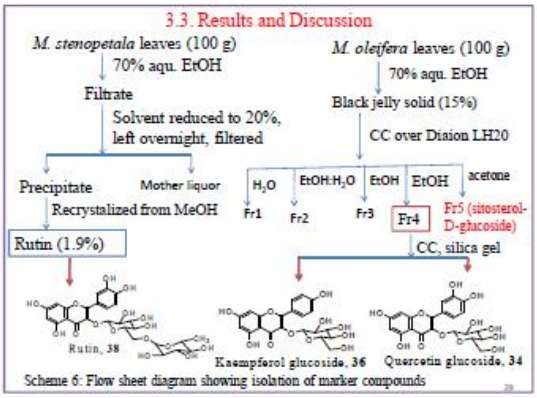

Scheme 6: Flow sheet diagram showing isolation of marker compounds

3.3.1. Characterization of Marker Compounds

Compound 38

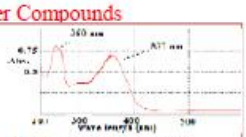

- Yellowish solid; mp 189-191°C
- IR υcm^{-1}: 3428 (OH), 1653 (carbonyl)
- FT-MS: *m/z* 609.1451, $C_{27}H_{30}O_{16}$; *m/z* 302 (quercetin)
- The hydrolysis of compound 38 confirms the aglycone as quercetin
- ^{1}H-NMR of 38: δ 5.35 (1H, J = 7.83 Hz): anomeric proton of glucose
  - δ 4.38 (1H, *bro. s*) and 0.97 (3H, *d*, J = 6.09 Hz): rhamnose moiety
- Compound 38 is rutin which was reported from the same plant [188]

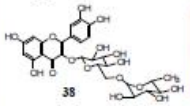
38

Previous pharmacological reports: Antioxidant, antidiabetic, anti-cancer, anti-inflammatory, hepatoprotective, thrombolytic and α-glucosidase inhibitory

[188] Mekonen, A. *et al.*, **2000**. *Bull. Chem. Soc. Ethiop.* **14**(1), 51-55

Compound 36

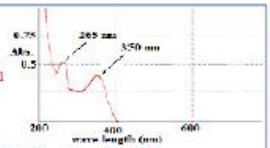

- Yellow solid; mp 189-191°C
- FT-MS: *m/z* 447.0924, $C_{21}H_{20}O_{11}$
  m/z at 284 (aglycone)
- ^{1}H-NMR spectrum
- δ 8.16 (2H, *d*, J = 9.2 Hz), δ 7.00 (2H, *d*, J = 9.2 Hz)
- δ 6.54 (1H, *d*, J = 2 Hz) and δ 6.30 (1H, *d*, J = 2 Hz)
- Anomeric proton at δ 5.20 (1H, *d*, J = 7.20 Hz)
- Compound 36 is kaempferol-3-O-β-D-glucoside [212]
- Previous biological reports:
- antioxidant, antiallergy, anti-inflammatory

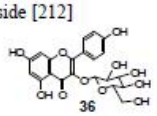
36

[212] Shahat, A.A., *et al.*, **2005**. *Qatar Univ Sci. J.*, **25**, 72–77

Compound 34

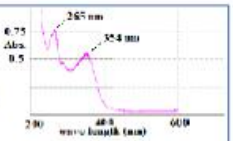

- Yellow solid, mp 192-194°C
- IR υcm^{-1} : 3368 (OH), 1665 (CO)
- HR-FT-MS: *m/z* 463.0882, $C_{21}H_{20}O_{12}$
  m/z 301 (aglycone)
- ^{1}H-NMR:
- δ 7.72 (*d*, J = 2.4 Hz), 7.60 (*dd*, J = 2.4, 8.8 Hz), 6.80 (*d*, J = 8.8 Hz)
- δ 6.41 (1H, *d*, J = 8.4 Hz) and δ 6.23 (1H, *d*, J = 2.00 Hz)
- Anomeric proton at δ 5.27 (1H, *d*, J = 7.6 Hz)
- Compound 34 is quercetin-3-O-β-D-glucoside
- Previous sources: *M. oleifera*, and *A. indica*

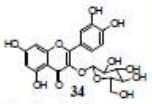
34

- Previous biological reports: antiinflammatory, antimicrobial, anticarcinogenic [217]

[217] Razavi, S.M., *et al.*, **2009**. *Russian Journal of Bioorganic Chemistry*, **35**(3), 376–378

3.3.2. Comparison of Extracts of the Leaves of *M. stenopetala* and *M. oleifera*

3.3.2.1. Thin Layer Chromatography (TLC)

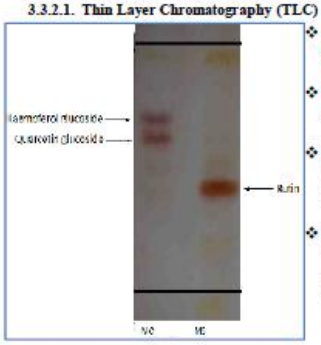

- Eluent: EtOAc:AcOH:HCOOH:H_2O (7:1:1:1)
- Spraying agent: fast blue B salt
- TLC can quickly distinguish these two species of Moringa rapidly
- TLC has the potential to detect presence of adulterants in either of the two samples

Fig. 9: TLC profile of *M. stenopetala* (MS) and *M. oleifera* (MO)

3.3.2.3. High Performance Liquid Chromatography-Mass Spectrometry

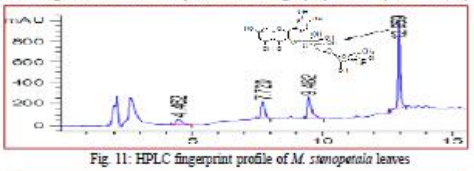

Fig. 11: HPLC fingerprint profile of *M. stenopetala* leaves

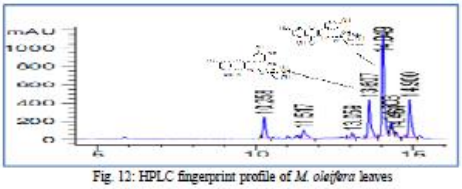

Fig. 12: HPLC fingerprint profile of *M. oleifera* leaves

3.3.3. Quantification of Rutin in *M. stenopetala* Leaves

3.3.3.1. HPTLC

Extraction

M. stenopetala leaves (2 g) → EtOH → Black jelly solid

M. stenopetala leaves → 70% aqu. EtOH → Black jelly solid

➢HPTLC measurement

✓Standard stock solution: Rutin (10 mg) in ethanol (20 mL)
✓Sample stock solution: Extract (10 mg) in ethanol (10 mL)

➢20 µL and 40 µL of the sample were applied on track 2 and 4 while on track 1, 3 and 5 a standard rutin solution of 2, 6, and 10 µL were applied on HPTLC plate, respectively

➢Good resolution of spots: EtOAc:HCOOH:AcOH:H_2O (7:1:1:1)
➢The plate was scanned at 260 nm
➢Eight spots were detected in the HPTLC chromatogram of *M. stenopetala* leaves extract
➢The spot of rutin in the plant material was detected at an Rf value of 0.49

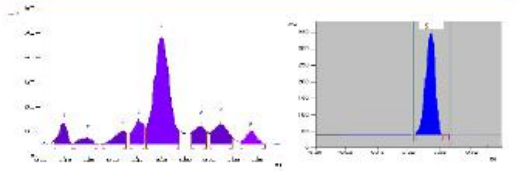

Fig 13: Typical chromatogram of *M. stenopetala* leaves extract (left) and standard rutin (right)

Sample source	Amount applied in µL (µg)	Peak area (µg)	%Rutin
Arba Minch	40	24.23	2.1
Gondar	"	20.30	1.8
Dire Dawa	"	22.24	1.9

Table 3: Level of rutin in *M. stenopetala* using HPTLC

➢This was repeated for EtOH extract and found to be 1.7%
➢Confirmed through isolation (1.9%)

Validation of HPTLC Method

➢Linearity (n = 3), r = 0.999, sdv = 2.73%
➢Limit of Detection (LOD) and Quantification (LOQ)
➢Accuracy: %recovery study of 99.5%
➢Intraday precision (repeatability): %RSD = 0.14%
➢Interday precision (reproducibility):%RSD = 0.13%

3.3.3.2. UV-Vis spectrophotometry

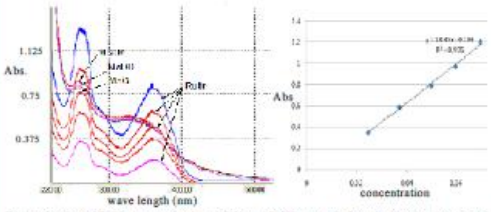

Fig. 14: Overlayed UV-Vis spectra of rutin and 70% aqu. EtOH extract (Left) and calibration curve (right)

Sample source	Absorbance at 260 nm	% Rutin
Arba Minch	0.84	1.77
Gondar	0.78	1.68
Dire Dawa	0.80	1.71

Table 4: Level of rutin in *M. stenopetala* leaves using UV-Vis spectrophotometry

Conclusion

✓Since the use of Moringa species is growing steadily, a quality control method using TLC, UV and HPLC-MS were developed to differentiate this species from various sources by chemical fingerprints

✓The marker compound for *M. stenopetala* is rutin while the markers in *M. oleifera* leaves are quercetin-3-O-β-D-glucoside and kaempferol-3-O-β-D-glucoside

✓A simple HPTLC and UV method for the determination of rutin in the extracts of *M. stenopetala* was developed and validated

✓The level of rutin in the 70% aqueous EtOH extract of the leaves of *M. stenopetala* is 1.9±0.08%

✓These fingerprinting results may be useful not only in differentiating the two species but also in establishing presence or absence of adulterants, an issue that is of great concern in the use and marketing of leaves, and other products of *Moringa*

3.3.4. Contributions to the Chemical Studies of the Leaves and Seeds of *M. stenopetala*

Isolation of Compounds from the Leaves of *Moringa stenopetala*

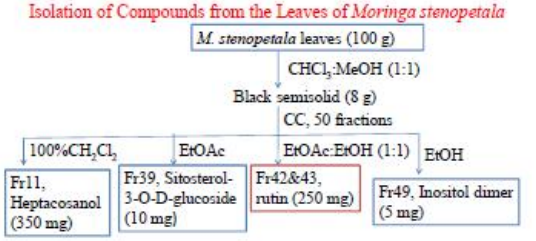

Scheme 10: Schematic diagram showing extraction and isolation of compounds from *M. stenopetala* leaves

Characterization of Compound 61 and 62

Compound 61

❖ White solid powder; mp 82-83°C
❖IR: 3400 (OH))
❖UV-Vis spectrum: no absorption maxima

❖^{1}H-NMR spectrum:
➢δ 3.66 (2H, *t*, *J* = 6.6 Hz);
➢δ 1.59 (2H, quintet);
➢δ 1.27 (48H, bro. s) and 0.90 (3H, *t*)

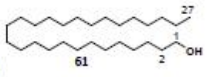

❖Compound **61** is 1-heptacosanol which was confirmed by comparison with literature reported for the same compound [225]

[225]. Kosy, C.Y., *et al*., **2013**. *Rec. Nat. Prod.* 7(1), 59-64

Compound 62

❖a white solid soluble in water
❖ $[\alpha]_{589}^{21}$ = -75.0 (c 0.2, MeOH)

^{13}C and DEPT-135 NMR:
➢δ 74.3 (C-1),
➢δ 72.4 (C-2 and 6),
➢δ 72.1 (C-4), and
➢δ 71.1 (C-3 and 5)

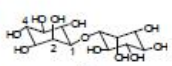

62

Inositol dimer (**62**)

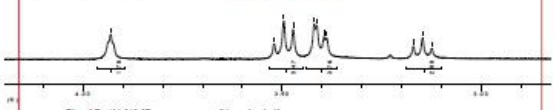

Fig. 15: ^{1}H NMR spectrum of Inositol dimer

3.3.4.2. Chemical Constituents of *M. stenopetala* Seeds Kernel

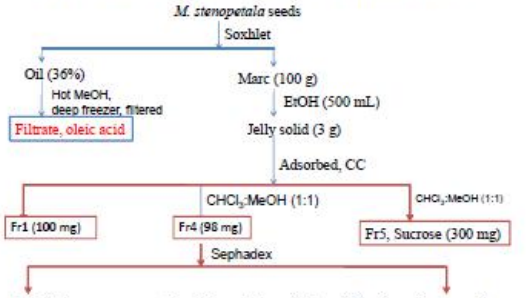

Scheme 11: Diagram showing extraction and isolation of compounds from *M. stenopetala* seeds

Analysis of *M. stenopetala* Oil

➢UV-Vis spectrum: no absorption maxima

➢The NMR spectrum was compared with some edible oils

❖Displayed similar NMR pattern with olive oil

➢FT-MS:

❖*m/z* 339.3269 ($C_{22}H_{44}O_2$), behenic acid (**28**),

❖*m/z* 311.2952 ($C_{20}H_{40}O_2$), archidic acid (**26**),

❖*m/z* 281.2481 ($C_{18}H_{34}O_2$), oleic acid (**22**) and

❖*m/z* 225.2328 ($C_{16}H_{32}O_2$), palmitic acid (**21**)

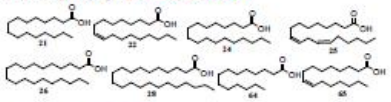

➢FAME analysis using GC-MS

Results: myristic (0.2%), palmitoleic (1%), palmitic (1%), oleic (53%), stearic (9%), linoleic (1%), archidic (4%) and behenic acid (5%)

3.3.4.3. Characterization of Compound 39

Compound 39

➢Yellowish jelly solid; UV λ max nm: 245 and 273

➢IR υcm^{-1}: 3400 (OH),1613 (C=C)

➢FT-MS: *m/z* at 570.5666, $C_{20}H_{28}NO_{14}S_2^-$

➢The peaks at *m/z* 97 and 570 are characteristic of 4-(α-L-rhamnopyranosyloxy) benzyl glucosinolate [147]

➢ ^{1}H-NMR: *δ* 7.25 (2H, *d*, *J* = 8.8) and *δ* 7.04 (2H, *d*, *J* = 8.8 Hz)

❖Rhamnose: *δ* 5.43 (1H, *d*, *J* = 1.36) and *δ* 1.13 (3H, *d*, *J* = 5.6 Hz)

❖*δ* 4.60 (1H, *d*, *J* = 3.2 Hz, H-1')

❖*δ* 4.00 (2H, *bro. s*, H-7)

❖*δ* 4.00 to 3.00: protons of sugar

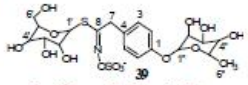

39

➢Compound **39** is 4-(α-L-rhamnopyranosyloxy) benzyl glucosinolate

[147] Bennett, R.N., *et al.*, **2003**. *J. Agric. Food Chem.* **51**, 3546–3553

Isolation of Compounds from the Husk of *M. stenopetala* Seeds

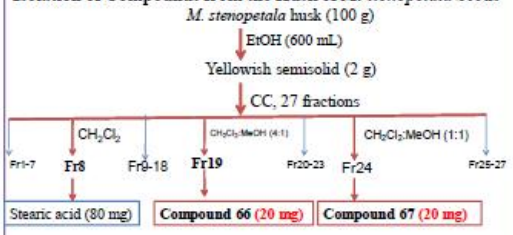

Scheme 12: Extraction and isolation of compounds from the husk of *M. stenopetala* seeds

Characterization of Compound **66** and **67**

Compound 66

➢White solid, mp 153-155°C

➢IR υcm^{-1}: hydroxyl (3387)

➢FT-MS: *m/z* at 269.1028, $C_{13}H_{18}O_6$

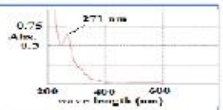

➢ ^{1}H-NMR: *δ* 7.22 (2H, *d*, *J* = 8.2 Hz) and 6.96 (2H, *d*, *J* = 8.20 Hz)

❖*δ* 4.40 (2H, *d*, *J* = 4.40 Hz), benzylic protons

❖Rhamnose: *δ* 5.32 (1H, *d*, *J* = 1.32 Hz) and *δ* 1.07 (3H, *d*, *J* = 6.14 Hz)

➢ ^{13}C-NMR and DEPT-135: *δ* 155.3, 136.2, 128.4, and 116.6

❖*δ* 98.8, 70.8, 70.6 , 72.2, 69.7 and 18.3 due to CH of rhamnose

❖*δ* 62.9 due to benzylic carbon

➢No bathochromic shift

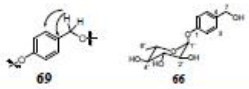

69 **66**

Compound 67

➢White solid; mp 220-222°C

➢IR υcm^{-1}: 1715 (amide), 3438 (N-H) and 3343 (N-H),

➢FT-MS : *m/z* 181.0332, $C_4H_6O_3N_4$

➢^{1}H-NMR: *δ* 5.21 (1H), 6.97 (NH), 10.70 (NH), 8.10 (NH) and 5.85 (NH_2)

➢^{13}C-NMR and DEPT-135: *δ* 174.0, 157.9, 157.3 and 62.8 (CH)

❖Compound **67** is identified as allantoin

❖COSY and HMBC

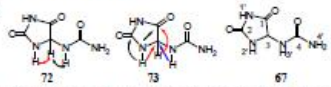

72 **73** **67**

➢Allantoin enhance the efficacy and desirability of cosmetic creams

➢Accelerate the healing of wounds

➢Against asthma

Antioxidant Activities of *M. stenopetala* and *M. oleifera* Leaves

A. DPPH radical scavenging assay

Samples tested	Scavenge (%)	IC_{50}
M. stenopetala EtOH extract	77	6.1
M. oleifera EtOH extract	73	6.0
Rutin	83	2.45
Sitosterol-3-O-*β*-D-glucoside	36	15.6
1-Heptacosanol	26	14
Quercetin-3-O-*β*-D-glucoside	85	2.3
Kaempferol-3-O-*β*-D-glucoside	75	2.7

Table 5: DPPH radical scavenging activity of extract and pure compounds from *M. stenopetala* and *M. oleifera* leaves

B. Ferric thiocyanate method

Linoleic acid + sample → incubated at 40°C, 24 h → small amount was transferred to vial containing $FeCl_2$ and NH_4SCN → Absorbance at 500 nm

Samples tested	Absorbance at 500 nm	%inhibition
Blank	0.56	-
Ascorbic acid	0.11	80
M. oleifera EtOH extract	0.12	78
M. stenopetala EtOH extract	0.14	74

Table 6: Anti-lipid peroxidation potential of *M. stenopetala* and *M. oleifera* EtOH extract

61

Conclusion

➢The leaves extract of *M. stenopetala* afforded heptacosanol, sitosterol-3-O-*β*-D-glucoside, rutin and inositol dimer

➢*M. stenopetala* seeds kernel is a rich source of oil (36%) with diversified fatty acid profile including behenic, icosanoic, linoleic, oleic, stearic, palmitoleic, palmitic and myristic acid

➢4-(*α*-rhamnopyranosyloxy) benzylglucosinolate and sucrose were isolated from the kernel of *M. stenopetala* seeds

➢The husk of *M. stenopetala* seeds furnished allantoin and compound 66

➢The antiradical and anti-lipid peroxidation activity displayed by the extract of *M. stenopetala* leaves were due to the presence of rutin

62

Acknowledgments

➢Prof. Ermias Dagne
➢Prof. Wondimagegn Mamo
➢Dr. Tarekegn G/yesus
➢Dr. Ashebir Fiseha, Dr. Nigist Asfaw and Dr. Estifanos Ele
➢Prof. Yalemtsehay Mekonnen and her co-workers (Tefera, Yemane and Gebremichael)
➢Dr. Ahmed Mustafa
➢Dr. Norbert Arnold and Dr. Juergen Schmidt

➢W/o Woineshet and Mr. Teshome
➢My co-workers (Yohannes, Hanna, Mesfin, Minbale, Sisay, Zelalem)
➢ My friends (Koster, Bedassa, Defaru)
➢My parents, sisters, brothers, wife, and my son
➢Chemistry Department of Addis Ababa University
➢Adama Science and Technology University

63

Thank YOU

64